NTNU – Trondheim
Norwegian University of
Science and Technology

Energy Efficient Drying Systems for the Dried Cured Meat Industry

Karoline Husevåg Kvalsvik

Master of Energy and Environmental Engineering	
Submission date:	June 2015
Supervisor:	Trygve Magne Eikevik, EPT
Co-supervisor:	Michael Bantle, SINTEF Energi AS Inna Petrova, EPT

Norwegian University of Science and Technology
Department of Energy and Process Engineering

NTNU

Norwegian University
of Science and Technology

Department of Energy
and Process Engineering

EPT-M-2015-46

MASTER THESIS

for

Student Karoline Husevåg Kvalsvik

Spring 2015

Energy efficient drying systems for the dried cured meat industry

Energieffektive tørkesystemer for spekematindustrien

Background and objective

In order to reach EU climate goal (20-20-20) it is necessary to reduce emission of climate gases, increase the use of renewable energy and decrease energy consumption, especially in energy intensive industry and processes.

The focus of the work will be on coupled heat- and mass transfer processes, which are applied in the production of dry-cured meat. Drying is the most important step in the dry-cured meat manufacture; during this period the meats obtain their distinctive quality. At the same time it is the most time and energy consuming step and that is why it is of a special interest for development of new energy efficient system solutions. The mass transfer will directly influence the product quality and the energy consumption (~production costs) of the process. The correct estimation of the drying rate is therefore the most important parameter for processing of dry-cured meat.

The aim of the thesis work is to develop models for calculations of energy systems for the drying process of dry-cured meat. The focus shall be on physical models which are more suitable for upscaling and variation of drying conditions. The simulations should be based on the product model developed in the project work.

The work will be connected to a larger competence research project "Sustainable production of traditional and novel cured dried meat products – DryMeat", coordinated by SINTEF Energy Research.

The following tasks are to be considered:

1. Literature review related to the scope of work of the thesis
2. Further development of systems models for the tunnel drier in Dymola
3. Investigate different systems for energy efficient drying of cured meat
4. Make a scientific paper of the main results from the work
5. Make proposal for the further work

-- " --

Within 14 days of receiving the written text on the master thesis, the candidate shall submit a research plan for his project to the department.

When the thesis is evaluated, emphasis is put on processing of the results, and that they are presented in tabular and/or graphic form in a clear manner, and that they are analyzed carefully.

The thesis should be formulated as a research report with summary both in English and Norwegian, conclusion, literature references, table of contents etc. During the preparation of the text, the candidate should make an effort to produce a well-structured and easily readable report. In order to ease the evaluation of the thesis, it is important that the cross-references are correct. In the making of the report, strong emphasis should be placed on both a thorough discussion of the results and an orderly presentation.

The candidate is requested to initiate and keep close contact with his/her academic supervisor(s) throughout the working period. The candidate must follow the rules and regulations of NTNU as well as passive directions given by the Department of Energy and Process Engineering.

Risk assessment of the candidate's work shall be carried out according to the department's procedures. The risk assessment must be documented and included as part of the final report. Events related to the candidate's work adversely affecting the health, safety or security, must be documented and included as part of the final report. If the documentation on risk assessment represents a large number of pages, the full version is to be submitted electronically to the supervisor and an excerpt is included in the report.

Pursuant to "Regulations concerning the supplementary provisions to the technology study program/Master of Science" at NTNU §20, the Department reserves the permission to utilize all the results and data for teaching and research purposes as well as in future publications.

The final report is to be submitted digitally in DAIM. An executive summary of the thesis including title, student's name, supervisor's name, year, department name, and NTNU's logo and name, shall be submitted to the department as a separate pdf file. Based on an agreement with the supervisor, the final report and other material and documents must be given to the supervisor in digital format. All relevant data collected and produced during the project shall be delivered to the supervisor on a Memory stick at the end of the project.

☐ Work to be done in lab (Water power lab, Fluids engineering lab, Thermal engineering lab)
☐ Field work

Department of Energy and Process Engineering, January 12th 2015

Olav Bolland

Prof. Olav Bolland Department Head	Prof Trygve M. Eikevik Academic Supervisor e-mail: Trygve.m.eikevik@ntnu.no
Research Advisor: Dr. Michael Bantle, SINTEF Energy PhD-student Inna Petrova, NTNU	e-mails michael.bantle@ntnu.no inna.petrova@ntnu.no

ABSTRACT

Production of dry-cured meat requires large amounts of energy. To reduce the running costs in the dry-cured meat industry, which are closely related to the energy needs, eight energy systems for drying of meat were simulated and compared. Realistic drying conditions, 13 °C and 68 % humidity, were applied. The best performing system was a system using a CO_2 heat pump, dehumidifying as little of the drying air as possible, above the freezing point. The second best was similar, except an ammonia heat pump was used, with glycol circuits for heat transfer. Heat pump drying resulted in improvements from 70 to 92 % compared to an existing solution with cooling and electrical heating. Utilization of excess heat could improve this further, and had a large impact. Dewatering as little of air as possible and avoiding extra temperature differences with glycol were other important factors. A system compressing the air to allow condensation at higher temperatures performed worse than the existing solution, but was simple and avoided the use of a heat pump. An attempt to model an adsorber was not completed, but a preliminary result, close to an estimation based on the rated power, resulted in savings of 60 %. However, if surplus heat could be utilized, the best heat pump system required about 85 % less energy than the adsorber. At the applied conditions, the adsorber seemed to be less efficient than heat pump systems.

SAMANDRAG

Å produsere spekekjøt krev store mengder energi. For å redusere driftsutgiftene i spekekjøtindustrien, som er nært knytt til energibruken, vart åtte energisystem for turking av kjøt simulert og samanlikna. Realistiske turkeforhold, 13 °C og 68 % fukt, vart nytta. Systemet som gjorde det best brukte ei CO_2-varmepumpe, og avfukta so lite av turkelufta som råd, over frysepunktet. Det nest beste var likt bortsett frå at ei ammoniakkvarmepumpe vart brukt, med glykolkrinsar for varmeoverføring. Varmepumpe-turking førte til forbetringar på 70 til 92 % samanlikna med ei eksisterande løysing med kjøling og elektrisk oppvarming. Utnytting av overskotsvarme kunne betre dette enno meir og hadde stor innverknad. Andre viktige grep var å avfukte so lite av lufta som råd og å unngå ekstra temperaturdifferansar med glykol. Eit system som komprimerte lufta for å tillate kondensering ved høgare temperaturar gjorde det dårlegare enn den eksisterande løysinga, men var enkelt og unngjekk bruken av varmepumpe. Eit forsøk å modellere ein adsorbar vart ikkje fullført, men eit førebels resultat, svært likt eit overslag basert på nominell effekt, sparte 60 % av energibruken. Likevel, dersom overskotsvarme kunne nyttast, trong det beste varmepumpesystemet om lag 85 % mindre energi enn adsorbaren. Ved dei nytta forholda, verka adsorbaren mindre effektiv enn varmepumpesystema.

PREFACE

This master thesis was performed at NTNU during the spring 2015. It was related to the DryMeat project (grant 225262/E40), supported by the Research Council of Norway, Nortura AS, BWL Maskin and Alfsen & Gunderson, Food Technology Group of NTNU and Sintef Energy Research, and I thank all of their employees who have contributed to this work. PhD. Michael Bantle, Civil engineer Erlend Indergård, and PhD. Cand. Nicolas Fidorra at Sintef Energy Research and Sales engineer Willy Bruräs at BWL Maskin and Alfsen & Gunderson have all supplied information, data, help in programming and advice. Professor Trygve Magne Eikevik has been my supervisor and shall have great thanks for many a helpful discussion and advice on the way. Thanks also to Fredrik Hildrum, for making and supplying the template for this document, and help with LaTeX in general.

It should be mentioned that this thesis uses results from [Kvalsvik, 2014], which was a pre-work for this master thesis, available at the department of energy and process engineering at NTNU. This thesis uses a meat model developed in that work, and parts of the literature study, definitions and manufacture description are taken directly from it. Because this pre-work and its resulting meat model was based on ham and results from experiments with ham, dry-cured ham has somewhat more focus than other meat products in this thesis.

The electronic version of this document contains clickable internal hyperlinks to all referred figures, tables, citations and so on. I hope the reader will find this work informative, tidy and understandable, requests can be directed to karolinehk@broadpark.no.

Trondheim, June 5, 2015

Karoline H. Kvalsvik

CONTENTS

LIST OF FIGURES

LIST OF TABLES

NOMENCLATURE

Table 1: Nomenclature: Subscripts

Subscript	Description	Subscript	Description
`1, 2, ...`	before and after, or fluid no. 1, 2, ...	`j`	counting index
`a`	air	`lm`	logarithmic mean
`c`	compressed	`min`	minimum
`C`	cold stream	`max`	maximum
`compr`	compressor	$\mathtt{NH_3}$	ammonia
`cool`	for cooling	`out`	outlet condition
`dry`	dry, drying	`pro`	for the drying process
`H`	hot stream	`sat`	saturated
`HP`	heat pump	`th`	thermal
`ham`	property of ham	`tot`	total, all effects or components together
`heat`	for heating	`w`	water, water vapour
`ideal`	ideal case	`wall`	property of pipe wall
`in`	inlet condition	`wb`	wet basis
`is`	isentropic	`wet`	wet bulb

Table 2: Nomenclature: Greek letters

Symbol	Parameter	Unit
α	heat transfer coefficient	$\frac{\mathrm{W}}{\mathrm{m^2\,K}}$
β	mass transfer coefficient	$\frac{\mathrm{m}}{\mathrm{s}}$
Δ	change in the parameter to follow	-
ϵ	highest roughness peak on pipe wall	m
η	efficiency	%
λ	volumetric efficiency	%
μ	reduction in diffusion coefficient	-
μ	dynamic viscosity	$\frac{\mathrm{kg}}{\mathrm{ms}}$
ν	kinematic viscosity	$\frac{\mathrm{m^2}}{\mathrm{s}}$
Π	pressure ratio	-
ρ	density	$\frac{\mathrm{kg}}{\mathrm{m^3}}$
ϕ	relative humidity	%

Table 3: Nomenclature: Latin letters

Symbol	Parameter	Unit
$\mathtt{a}$	activity	-
$\mathtt{A}$	area	m^2
$\mathtt{c}$	cost of energy	NOK
$\mathtt{C}$	heat transfer capacity	$\frac{\mathrm{W}}{\mathrm{K}}$
$\mathtt{COP}$	coefficient of performance	-
c_p	specific heat capacity at constant pressure	$\frac{\mathrm{J}}{\mathrm{kg\ K}}$
$\mathtt{d}$	diameter	m
$\mathtt{D}$	diffusivity	$\frac{\mathrm{m}^2}{\mathrm{s}}$
$\mathtt{E}$	energy	J or Wh
$\mathtt{f}$	fugacity	Pa
$\mathtt{f}$	friction factor	-
$\mathtt{F}$	function	-
$\mathtt{h}$	specific enthalpy	$\frac{\mathrm{J}}{\mathrm{kg}}$
$\mathtt{h}_{fg}$	enthalpy of vaporization	$\frac{\mathrm{J}}{\mathrm{kg}}$
$\mathtt{k}$	thermal conductivity	$\frac{\mathrm{W}}{\mathrm{m\ K}}$
$\mathtt{K}$	geometric value for pressure drop	-
$\mathtt{K}$	adsorber's correction factor	-
$\mathtt{L}$	length	m
$\mathtt{Le}$	Lewis number	-
$\mathtt{M}$	molecular mass	$\frac{\mathrm{kg}}{\mathrm{kmol}}$
$\mathtt{m}$	mass	kg
$\mathtt{n}$	frequency	Hz
$\mathtt{NPV}$	net present value	NOK
$\mathtt{NTU}$	number of transfer units	-
$\mathtt{Nu}$	Nusselt number	-
$\mathtt{P}$	power, effect	W
$\mathtt{p}$	total pressure	Pa
p_i	partial pressure of species i	Pa
p^o	saturation pressure	Pa
$\mathtt{Pr}$	Prandtl number	-
$\dot{Q}$	heat flow per time, effect	W
$\mathtt{r}$	discount rate	- or %
$\mathtt{R}$	universal gas constant	$\frac{\mathrm{J}}{\mathrm{kmol\ K}}$
$\mathtt{Re}$	Reynolds number	-
$\mathtt{s}$	thin layer thickness	m
$\mathtt{S}$	saving	NOK
$\mathtt{SMER}$	specific moisture extraction rate	$\frac{\mathrm{kWh}}{\mathrm{kg\ water}}$
$\mathtt{T}$	temperature	K or ^{o}C
$\mathtt{t}$	time	s (weeks, years)
$\mathtt{V}$	volume	m^3
$\mathtt{v}$	velocity	$\frac{\mathrm{m}}{\mathrm{s}}$
$\mathtt{x}$	absolute humidity	$\frac{\mathrm{kg\ vapour}}{\mathrm{kg\ dry\ air}}$
$\mathtt{y}$	molar fraction	-

Chapter 1

INTRODUCTION

Drying, and especially dry-curing of meat, is a process with large energy needs [Clemente et al., 2011]. To reduce the high costs caused by the high energy needs, more efficient energy systems should be assessed. Developed countries spend 12-25 % of their energy in drying processes [Mujumdar and Wu, 2007] and 85 % of the dryers worldwide are hot air dryers, which have low energy efficiency [Atuonwu et al., 2011a, Jon and Kiang, 2006]. The costs and energy requirements follow each other closely [Bantle and Eikevik, 2014], and use of energy also causes impacts on the environment. There is therefore much to save on choosing an energy effective system, both economically and for the sake of the environment.

Dry-curing of meat both preserves it and improves its taste, colour and texture [Toldrà, 2002, p. 27]. Curing involves adding salt and eventually other curing agents [Toldrà, 2002, p. 3], whereas drying is the most energy intensive part of the process [Atuonwu et al., 2011a, Clemente et al., 2011].

One important reason for the high energy needs is that meat requires relatively low drying temperatures to ensure high quality. Low temperature drying is slow, and results in long drying times [Strumillo et al., 2006], which leads to high energy demands. Reducing drying time by a small amount would lower the energy demand substantially [Okos et al., 2006], but this is not easy due to the low temperatures required and, in some cases, chemical reactions that must find place during drying to achieve the desired quality.

Making drying more efficient has been increasingly important [Colak and Hepbasli, 2009b]. Attempts to increase efficiency by reducing the amount of circulated air or using outdoor thermal energy for cooling or heating has shown potentials for 5-20 % energy reduction [Alcazár-Ortega et al., 2011, Bantle et al., 2015, Jon and Kiang, 2006]. Other attempts include increasing the drying temperature [Atuonwu et al., 2011a], finding techniques to speed up the drying process [Bantle and Eikevik, 2014, Bantle et al., 2013, Jon and Kiang, 2006], using heat pumps [Colak and Hepbasli, 2009b, Jon and Kiang, 2006] and drying by adsorption [Atuonwu et al., 2011a, Atuonwu et al., 2012b]. The two first could damage meat quality, and some techniques for speeding up the drying rate were also found to increase energy demand [Bantle and Eikevik, 2014, Bantle et al., 2013]. The two latter have shown promising results in terms of both energy and quality [Jon and Kiang, 2006, Colak and Hepbasli, 2009a].

Adsorbers can reach thermal efficiencies close to 100 % when heat recovery is applied [Atuonwu et al., 2011a]. The efficiency of heat pumps systems have been found to be much larger than for systems without, and can exceed 100 % [Jon and Kiang, 2006].

Testing different energy systems by experiment is very expensive due to the long drying times and the investment costs, but cheap testing of different systems can be performed by computer simulations. This however, requires a realistic model of the meat to obtain valid results. Such a model was developed by [Strømmen, 1980] and fitted to results for dry-cured ham samples in [Kvalsvik, 2014]. This model was used in this work, and ham therefore has a more prominent role in this work than other meat products.

The focus of this study was rather to optimize how efficiently the normal drying conditions could be achieved than increasing the drying rate, as the latter could damage the meat. Promising solutions are heat pump and adsorber systems, in addition to reducing the amount of circulated air. These were investigated in this study. Using free cooling from surroundings has already been considered for the same process as in this work [Bantle et al., 2015].

A drying process based on real drying conditions and energy system was modelled in DYMOLA. This was then compared to several alternative energy systems, maintaining the same drying conditions. Some important terms are explained in Chapter 2 and the dry-curing process in Chapter 3. A literature review is given Chapter 4. The chosen systems are presented in Chapter 5 and the methodology in Chapter 6. Possible potentials for energy reduction are reported in Chapter 7. A cost analysis and discussion of the changes required in converting one system into another was also provided, to assess whether the saved energy would pay for investments. This is found in Chapter 8, and conclusions in Chapter 9. The work is summarized in an article in Appendix A, and other appendices evaluate the operation of the systems.

Chapter 2

DEFINITIONS

Measures of energy efficiency are convenient in comparisons of energy systems. Some usual measures are the specific moisture extraction rate, the SMER and the drying efficiency. SMER is the amount of water evaporated divided by the energy input,

$$\mathrm{SMER} = \frac{\text{water evaporated [kg]}}{\text{energy used [kWh]}} = \frac{\Delta m_w}{E_{tot}},$$

and the drying efficiency is the fraction of the supplied energy that actually is used for evaporating liquid,

$$\eta_{dry} = \frac{\text{water evaporated [kg]} \cdot \text{enthalpy of vaporization} \left[\frac{\text{kJ}}{\text{kg}}\right]}{\text{energy used [kJ]}} = \frac{\Delta m_w h_{fg,w}}{E_{tot}}.$$

Both these will be given, to more easily compare with other studies where one of them, but not the other is used.

In order to describe drying, some parameters should be defined. The **water activity** a_w is defined at the surface of the product as

$$a_w = \frac{\overline{f_w}}{f_w^o(T)}, \tag{2.1}$$

where $\overline{f_w}$ is the fugacity of water vapour in mixture with other components, $f_w^o(T)$ is the fugacity of water vapour alone at the process temperature T and a reference pressure. In the theoretical, ideal case, the activity would be equal to the molar fraction y_w of water in the air, times the total pressure p, divided by the saturated water vapour pressure at the temperature:

$$a_{w,ideal} = \frac{y_w p}{p_w^o(T)} = \frac{p_w}{p_w^o(T)}. \tag{2.2}$$

Here p_w is the partial pressure of the water vapour. Fugacity is a way to account for that gases, like water vapour, do not behave in an ideal manner, and is therefore often described as an «effective pressure» [Moran and Shapiro, 2006]. The water activity is then described as a measure of the amount of water free to take part in reactions and thereby a measure of how easily the product will be destroyed by microorganisms [Raiser, 2014]. In many cases the ideal behaviour is assumed, as this is convenient and almost true. This was assumed in the meat model applied in this work.

The **relative humidity**, denoted by ϕ, is defined in the same way as the ideal water activity (2.2), except that it is not only defined at the product surface, but everywhere in the air and inside the pores of the product. Since the relative humidity equals the ratio of vapour pressure to the saturated vapour pressure, $\phi \in [0, 1]$, normally expressed as a percentage.

Water can be firmly bound to the product structure, more loosely bound or not bound at all. The latter is called «free water.» Water can be bound in different ways, which are further explained in Section 4.3. An example is the loose bond between a water molecule and a surface that it rests on, which is called **adsorption**. Energy is required to remove the molecule. All effects that bind water to the structure are called **sorption** effects [Strømmen, 1980, p. 15].

A **driving potential** is an imbalance that will start a process, acting as a driving force. In the case of meat drying, the driving potential is assumed to be the difference in local vapour pressures inside and outside the product [Song, 1990]. In the inner, undried region of the meat, the vapour pressure is assumed to be equal to the saturated water pressure [Bantle et al., 2014] or somewhat lower due to the sorption of the water. Sorption, binding the water more strongly to the structure, lowers the saturated pressure in the meat compared to that of pure water [Luikov, 1966, p. 192].

The meat structure and sorption effects slow down the rate of vaporization relative to that in pure water. Everything that slows down evaporation can be classified as a resistance to the mass transfer. **Internal resistance** to mass transport is what slows down the transport inside a substance, **external resistance** the resistance to transport mass from the surface to the air. In some cases, a gradient (in temperature, air velocity and/or species concentration) can develop in the air outside the product. The air layer close to the product that differs more than 1 % from the surrounding air is then called the **boundary layer**. This layer is the reason why external resistance develops, as the local differences in for example vapour pressure will be gradual and small in the boundary layer, slowing down the drying.

Osmotic dehydration is a phenomenon that occurs because hams normally are salted before drying [Petrova, 2015]. The addition of salt to the surface creates a higher salt concentration in the outer part of the product than in the inner. This creates a concentration gradient for salt, and hence, there will be a driving potential to transport salt towards the inner regions with less salt.

Meat acts as a semi-permeable membrane, and salt travels through it much faster and much more easily than the water [Costa-Corredor et al., 2010]. This affects the water activity of the product. Salt binds water. The activity of pure water is one, but lower when solutes are present. Hence, the water activity, or the effective pressure of the water, decreases in the part of the meat where salt is added. As a result, water will experience a higher pressure inside the meat than in the outer layer and due to this be transported towards the surface. This pressure difference is called osmotic pressure (or salt pressure in Greek). Both driving potentials are present until the salt and water concentrations are equal everywhere.

The outwards water transport will contribute to drying out the product, but as the process continues, more of the water in the meat contains salt, and thus, the water activity and driving potential decreases. Thus salt increases the drying rate initially, but then retards it. Higher salt contents in clip fish led to faster dehydration [Strømmen, 1980], while studies on ham imply that higher salt content slows down the overall drying so much that even with higher initial water contents, unsalted samples are faster dried than salted [Bantle et al., 2014, Raiser, 2014, Gou et al., 2003]. The longer processing time for hams might be the main reason for this difference. Salt is initially mainly in the outer layers, but the salt distribution will be quite even after four to five months. Later the core will contain more salt than the outer layers due to its higher water content [Toldrà, 2002, p. 47].

Diffusion is a transport phenomenon, described by Fick's laws, where the flux of a specimen is proportional to a gradient the concentration gradient related to it. The gradient is an expression for an imbalance or driving potential. The flux is also proportional to a coefficient, called the **diffusion coefficient,** $D_{specimen,medium}$. This phenomenon is affected by the media in which it occurs, chemical reactions and composition, temperature and pressure. There are more types of diffusion: gaseous or vapour diffusion, liquid diffusion and surface diffusion of adsorbed molecules [Okos et al., 2006, Waananena et al., 1993].

Drying is often described by three **drying steps** [Okos et al., 2006], [Song, 1990, p. 4-5], [Strømmen, 1980, p. 6-7 and 97], [Raiser, 2014]: initially the free water near the surface evaporates like pure water. Said in another way; the ham has no effect on the drying rate, which is constant, and determined solely of external conditions. This step was not observed in ham [Bantle et al., 2014, Raiser, 2014] or clip fish [Strømmen, 1980, p. 7]. [Raiser, 2014] explained this by the osmotic dehydration before the convective drying, which removes the free water close to the surface, so that this step one cannot occur.

The second step is characterized by a falling drying rate as the outer layer of the product is dried and properties in this region altered. The outer, drier layer creates a larger resistance to mass flow than a wet product, as water keeps the pores in the ham open [Okos et al., 2006]. As the dry layer grows, this internal resistance increases and drying rate falls.

Another drop in drying rate characterizes the third step, when more firmly bound water (chemically bound water and capillary water, see Section 4.3) is removed [Okos et al., 2006, sec. 10.2.0], [Song, 1990, p. 5].

Raw meat consists mainly of water [Toldrà, 2002, p. 9-10], the other main component is protein, which is mainly found in the muscle fibres, also called the myofibrils, and they are placed as parallel threads in the meat. The breakdown or degradation of these proteins is called **proteolysis** and is performed by enzymes called proteases [Toldrà, 2002, Petrova, 2015, p. 9-10]. Proteolysis leads to the formation of amino acids and improves the texture as it breaks down the muscle fibres. This process is very important for high quality meat products.

Between the different muscles there are fat tissues, which are barriers for water [Gou et al., 2004]. In fat, **lipids** are the main constituent, and the breakdown of these, by a set of reactions called **lipolysis**, is essential for flavour development in high quality products. Proteolysis and lipolysis are the most important groups of biochemical reactions occurring [Toldrà, 2002, p. 12-18]. Too much of these reactions is however not desirable [Toldrà, 2002, p. 135].

Excessive degradation of proteins (proteolysis) creates more amino acids than desirable. This affects the flavour to the worse, and can also lead to the formation of a tyrosine **crystal layer** on the ham surface. This white layer can be brushed off, but is a visual sign of an undesired reaction and a too tender product. In hams, the reason is often related to the age and breed of the pig [Toldrà, 2002, p. 116 and 122].

In the same way, excessive lipolysis, or lipid oxidation, affects the product quality to a high extent. Some oxidation elaborates the flavour, too much causes rancidity and is highly unwanted [Toldrà, 2002, p. 135-7]. These reactions are mainly active during the first five months of the ripening period, hence it extends over the whole drying stage. Therefore, fat content and the degree of lipolysis and rancidity is of major importance for the final taste and quality [Toldrà, 2002, p. 135-7]. All these chemical processes depend on water and salt content, pH and temperature, and the key to a high quality product involves low temperature and decrease of a_w [Okos et al., 2006, Marinos-Kouris and Maroulis, 2006]. Optimal pH for desired flavour development is in the range 5.4-6.2 depending on the product [Ruiz-Cabrera et al., 2004, Gou et al., 2002, Toldrà, 2002, Hayes et al., 2007, Arnau et al., 2007, p. 12 and 29]

Other concerns in dry-curing are those affecting quality. These are caused by too high temperatures or too fast or too slow dehydration, which can result in a burnt surface, microorganism or a hard dried out surface which prevents drying of the inner parts of the ham [Strømmen, 1980, Parolari, 1996, Bantle et al., 2014]. Another concern is **non-enzymatic browning** or maillard browning, which is the reduction of proteins and/or their components with sugars and ascorbic acid (vitamin C). This is desirable in some amount, but too much is bad and can be a danger to the kidneys [Friedman, 1996]. It is normally accompanied by brown colour, which gives it its name [Friedman, 1996]. It can be prevented by ensuring the temperature and water activity are not too high.

Adsorption is the process when some fluid component, in this work water vapour, is attracted and can be collected on the surface of a substance [Theodore, 2008]. The substance undergoes a process similar to, but opposite of drying. After a while, so much of the fluid component has accumulated that the substance's further removal capacity is zero. No more of the component can be attached to its surface. An adsorber must therefore alternately remove the component from one fluid stream and alternately be cleaned by another stream [Atuonwu et al., 2012b, Atuonwu et al., 2011b, Theodore, 2008]. The substance is called an adsorbent, and the removed component the adsorbate [Theodore, 2008].

The removal of the component from the substance is called regeneration of the adsorber. In the case of removing water vapour, the regeneration is ensured by blowing a very dry air stream, with low vapour pressure, through the material [Atuonwu et al., 2011a]. This then becomes some sort of drying process, which, unlike meat drying, can take place at a much higher temperature. This is advantageous because the low temperature drying is energy intensive, whereas high temperature drying is effective [Atuonwu et al., 2011a, Colak and Hepbasli, 2009a].

Chapter 3

THE PRODUCTION OF DRY-CURED MEAT

Different products are produced in different ways, and this text is based on texts about pork ham [Parolari, 1996, Raiser, 2014, Bantle et al., 2014, Toldrà, 2002], clip fish [Strømmen, 1980], mutton [Villalobos-Delgado et al., 2014], beef [Hayes et al., 2007, Hui, 2012] and sausages [Toldrà, 2002, Hui, 2012]. In addition, the same dry-cured meat products are in some cases made from other animals. [Hui, 2012, p. 515 and 517] mentions goats, ducks, camel, ostrich, horse, buffalo, deer and boar, but ham and sausages seem to be the most usual.

3.1 WHY DRY-CURE MEAT?

Dry-curing meat preserves it. This is because a wet product is easily contaminated by moulds, bacteria and mites, which today is still a problem in dry-curing of some products [Raiser, 2014, Parolari, 1996]. Removing the available water by drying, equivalent to obtain lower water activity, ensures microorganism cannot live within the meat. Curing involves addition of salts, and this binds water.

Today, the chemical changes for flavour and texture development are more important than the preservation, as refrigeration could preserve the meat equally well, and faster [Toldrà, 2002, p. 27]. However, these important chemical processes can only occur when the meat is nonfrozen, and thus, preservation must be ensured by drying and curing. In addition, the weight loss in drying is an economic loss. Therefore excessive drying is unwanted, and there is a fine balance between economic loss and safety of microorganism.

The importance of the flavour development varies between products. For high quality products, like some types of beef and ham, this is of major importance, and most of the production time is devoted to allow ripening, improving tenderness and flavour[Petrova, 2015, Hui, 2012]. In contrast, lower quality products can be salted and dried and are then ready for sale [Strømmen, 1980]. Note that, in this context, «lower quality products» are not products of low quality. They are products without a long ripening time. However, taste and texture change for these products too, as ripening also takes place during drying [Toldrà, 2002, p. 93 and 113-122], but not to such a high degree as the higher quality products.

Ripening does not only affect taste, but also texture. Degradation of the proteins by proteolysis is the main reason for the texture changes in dry-curing of ham. These are important for quality [Petrova, 2015], and so is the lipolysis (see Chapter 2). Lipolysis is highly affecting the development of desirable aromas, but excessive lipolysis can also destroy product quality [Toldrà, 2002, p. 135-7]. The type of animal, the animal feed, salt and water content, size (for fish), temperature and drying and ripening time highly determines the flavour developed and final product [Strømmen, 1980, Toldrà, 2002, p. 27].

3.2 HOW TO DRY-CURE MEAT?

When meat is supplied to the production site, it is in some cases frozen for a few months [Toldrà, 2002, p. 32-33], [Villalobos-Delgado et al., 2014]. After thawing, it can eventually be pressed. Pressing is done to bleed out any blood left in the meat and to create and/or open pores within the meat to enhance transport of water and salt in the product [Raiser, 2014, Strømmen, 1980, Toldrà, 2002, p. 30-32 and 40-41]. A water loss occurs upon thawing, and another loss due to pressing. These are only a few percent of total mass, and the main reason for these operations is to enhance later dry-curing processes [Toldrà, 2002, p. 30-32].

For products like clip fish, the initial processing involves cleaning and rinsing [Strømmen, 1980], and for sausages the first step is to mix minced meat with salts, spices and other components, which are filled into casings. Starter cultures can be added to enhance maturation. Some sausages are also cooked and smoked before drying [Hui, 2012, p. 515].

For other meat products than sausages and minced meat, some additives like nitrate, nitrite, potassium chloride or other salts are added to the surface before the meat is sent to rest, dry and ripen [Raiser, 2014, Toldrà, 2002, p. 37-38]. The salt can be added in undecided amounts by a bath in salt solution or storage in containers filled with salt for a period of two-four weeks [Strømmen, 1980, Toldrà, 2002, p. 37-39]. Eventually, the specific desired amount of salt is rubbed onto the surface before the hams are packed in plastic and stored. Osmotic dehydration occurs in this stage, see Chapter 2, and due to this, some of the water is withdrawn ($3-4$ % in hams) [Toldrà, 2002, p. 37]. Some products are salted twice, with a resting stage in between, and in many processes, the meat must be stabled over again several times during salting to obtain even salt content and dripping loss, caused by the osmotic dehydration [Strømmen, 1980, Villalobos-Delgado et al., 2014, Toldrà, 2002, p. 37-39].

After salting, surface salt is washed or brushed off and the meat is in some cases stored again to rest. Resting gives time to develop a more evenly distributed salt and water content. Another $4-6$ % of the mass is lost during these weeks [Raiser, 2014, Toldrà, 2002, p. 39]. Resting can last for some hours [Villalobos-Delgado et al., 2014] or up to nine weeks [Hui, 2012, p. 515], [Toldrà, 2002, p. 39].

During the salting and resting stages, the environment must be moist, in order to prevent dehydration of the surface and creation of a hard crust on the outside that might prevent transport of water. This can again create internal water pockets where bacteria can develop [Parolari, 1996]. The temperature must be low, typically $2-6\,°\mathrm{C}$, because the meat at this stage is wet and the salt content in its core low: Bacteria growth must be prevented [Raiser, 2014, Villalobos-Delgado et al., 2014]. Other products do not have a resting stage [Strømmen, 1980].

Some meats, like Cecina de Leon, are smoked before drying [Hui, 2012, p. 515], and in some processes more additives are used to prevent growth of microorganism before the meat is hanged in ranks or placed on shelfs to dry. Both drying chambers and drying tunnels are usual, depending on product [Raiser, 2014, Strømmen, 1980]. Ideally, the meat pieces should not touch each other to have as much surface area open to the free stream air blowing above them as possible [Toldrà, 2002, p. 40].

Air conditioning is extremely important to avoid quality problems. If the air velocity is not high enough, the surface will be wet and mould grow on the outside [Raiser, 2014]. Clip fish are stabled again several times during drying as well, to obtain even drying [Strømmen, 1980]. This is important for products placed in layers on shelves, but not for products that hang and have airflow at all sides. Production time varies between a few weeks and three years depending on product and desired quality [Petrova, 2015].

The drying step is the most energy intensive part of the process [Clemente et al., 2011]. During this time, temperature is higher than in salting and resting periods. For ham, it can be kept constant at $10-18\,°\mathrm{C}$ or varied. Some hams have one week with temperatures as high as $22-26\,°\mathrm{C}$ to enhance drying and enzymatic reactions, but this cannot be done safely for a longer period for previously mentioned reasons [Toldrà, 2002, p. 40-41]. Generally, the temperature can be increased during the process as the surface becomes drier and higher temperature safer [Strømmen, 1980, Hui, 2012, p. 515]. For clip fish, the temperature can be as high as $32\,°\mathrm{C}$. At higher temperatures the product is burnt [Strømmen, 1980]. [Hui, 2012, p. 515] also mentions that some processes can reach $35\,°\mathrm{C}$ for a short period and $40\,°\mathrm{C}$ during smoking, but microorganism might not be a problem then due to the smoke.

The humidity of the air should be low in order to dry the products, but as in the salting process, there is a danger of drying out the surface that must be avoided [Bantle et al., 2014], thus imposing a lower limit to the humidity of the drying air. This varies between products. Normally, the relative humidity is at least 60 % for hams [Toldrà, 2002, p. 36] and beef [Hui, 2012, p. 515] and 30 % for clip fish [Strømmen, 1980]. For some sausages, it is decreased from 80 % during drying [Hui, 2012, p. 516]. To obtain the highest qualities, higher humidity and lower temperatures are used. These processes are even slower and therefore require more energy, but also prevents dry surfaces and develop better aromas [Petrova, 2015].

Drying ends when the moisture content has reached a desired value. At this point, the water activity a_w defined in Chapter 2 is normally in the range $[0.87, 0.94]$, and usually the drying has then lasted for some weeks or a few months, depending on meat type, quality, salt content and size [Bantle et al., 2014, Petrova, 2015, Villalobos-Delgado et al., 2014, Hui, 2012, p. 512-516]. When $a_w < 0.9$ the hams are safe of bacteria, microbial activity and reactions that could impair the taste [Raiser, 2014, Okos et al., 2006]. However, mould and yeast could be a problem unless $a_w < 0.80$, according to [Okos et al., 2006].

After drying, some products are ready for sale, others are ripened further, and this is the main difference between expensive, high quality products and other dry-cured meats. Ripening takes place both during and after drying, and the final quality mainly depends on the length of this step. Dehydration during ripening is minimized by higher humidity (often 80-90 %) and hams are also covered with lard, which is fat with salt and pepper [Toldrà, 2002, p. 40-41]. Any additional mass loss is a purely economic loss.

The amount and type of lipids present, and the degradation of lipids and proteins are important for the flavour development and required maturation time. Enzymes carry out degradation. Some enzymatic reactions only take place in sour environments, created by the amino acids formed by proteolysis [Toldrà, 2002, p. 93 and 113-122]. One could also create artificially sour conditions by injection of acids or starter cultures [Hayes et al., 2007]. The best conditions for proteolysis involves long time and low salt content, and most of it occurs during the forth to tenth month or so. Lipolysis is most important the first five months [Toldrà, 2002, p. 93 and 113-122].

Flavour also depends on additives like nitrate, nitrite, salt, etc. [Cassens, 1995]. When added, potassium nitrate and/or sodium nitrate dissolve in the water in the meat. The nitrate ions (NO_3^-) can then be reduced to nitrite (NO_2^-) [Toldrà, 2002, p. 30]. The reduction rate of nitrate is high at pH 5.6-6.0 and ascorbic or erythorbic acid is often added simultaneously to reduce the nitrate. Nitrite can further be reduced to nitric oxide (NO). This is very important, as nitric oxide reacts with myoglobin in the meat to nitromyoglobin and this gives the meat the desired red colour typical for many cured meats [Toldrà, 2002, p. 30]. However, these components also prevent oxidation processes, and thereby they can have an unwanted effect on flavour. This is why they were forbidden in Parma ham from 1993 and limited in other products [Parolari, 1996].

Additives affect colour, texture, flavour, pH and many of them need much time to react to the desired state. An increase of some components, like certain lipids, have been found to enhance flavour development, but water removal then tends to be slower [Ruiz-Cabrera et al., 2004]. Removal of heavy metals from the added salt can prevent oxidation of fat (rancidity). Both browning and oxidation of fat are desirable to some extent in some products, but too much is detrimental [Toldrà, 2002, p. 164-168]. The reactions taking place depend on the type of breed, gender, diet and age at slaughter [Toldrà, 2002, p. 167, 196].

The total mass loss on wet basis throughout the entire process is about 33-36 % for hams [Toldrà, 2002, Raiser, 2014, p. 40-41], 30-45 % for beef [Hui, 2012, p. 515] and 60-65 % for clip fish [Bantle and Eikevik, 2014]. During the entire process, salt and water content slowly balance. Quality tests can be performed both during and at the end of production, and unacceptable meat is rejected [Strømmen, 1980, Parolari, 1996]. The outside of meat can be inspected for yeasts, mould, mites and proper colour. For hams, the quality inside is tested by a probe and sniff method. A probe (horse bone) is then inserted into the meat and trained experts smell whether the inside is acceptable or not [Parolari, 1996] before the hams are boned pressed in shapes [Toldrà, 2002, Raiser, 2014, p. 41] and ready for consumers.

3.3 ENERGY CONSIDERATIONS

For the lower quality products, those that do not require long ripening times, faster drying means higher throughput and possible energy savings. For the latter to be valid, the method of achieving the increased drying rate must not require too much energy [Bantle and Eikevik, 2014]. For high quality products, the situation is different. Unlike other dried products, both dry-cured and others, the goal is not to remove as much water as possible as quickly as possible, because the many ripening processes need time to take place. These processes require that the water content is not too low, as they will otherwise not occur [Petrova, 2015]. Therefore, the meat cannot be dried nor produced faster without an increase in the ripening processes [Toldrà, 2002, p. 58-59].

Chapter 4

LITERATURE REVIEW

In this literature review, it is useful to have in mind that shorter production time in itself lowers the energy consumption per kg meat produced. However, if the way to shorten the drying time requires much energy, the net energy consumption could increase [Bantle et al., 2013]. For high quality meat, like some beef and ham types, ripening is essential for quality, and production time cannot be reduced without accelerated maturation [Toldrà, 2002, p. 58-59]. Neither should the drying time for these products be shortened without accelerated ripening, as the water content influences the maturation processes, which are more active during the first months [Petrova, 2015]. For lower quality meat, ripening is less important, and enhancing the drying rate is desirable. Shorter production time increases the production capacity regardless of energy use.

4.1 EARLY DRYING

Preservation of food has been important for several thousand years, and when salting and drying was first used is unknown [Toldrà, 2002, p. 1]. The origin was probably around the Mediterranean sea where the access to salt from the sea and the climate that allowed for drying. From the Sumerian culture, texts from 2000 B.C. mention how meat was an important part of the diet [Toldrà, 2002, p. 2]. Northern Europe too has traditions for dry-cured meat. In this region, smoking the meat was more usual due to the cold climate, and combined smoking and drying of meat has been done for at least 1000 years [Petrova, 2015, Toldrà, 2002, p. 2]. Europeans also started dry-curing of fish around 1500 A.D. [Strømmen, 1980].

In the early drying processes, the meat was salted and hanged to dry under natural conditions. Cool climates like those in northern countries or mountain regions with natural ventilation of outdoor air were used. Preservation was the reason for drying, and the meat hang for long times after being dried, allowing several, slow ripening processes to develop special texture and aroma [Toldrà, 2002, p. 113-122 and 135]. Salting, post-salting, final drying and eventually ripening are and were the main steps in the production. Earlier, the drying and ripening conditions were badly controlled, because the regulation mainly consisted in opening and closing the windows. Today, dry-cured meat is therefore produced in drying chambers with regulated temperature and humidity of the air [Toldrà, 2002, p. 40], [Hui, 2012, p. 515-516], [Strømmen, 1980].

4.2 Early studies

The need for conservation is demonstrated by that [Milroy, 1917] wrote about attempts to transport meat safely on ships by freezing it as early as 1861. Among other products were salted and frozen ham and beef. The effect of salting has been known for very long times. The earliest detected study of this was performed in 1911 [McBryde, 1911] in [Besley, 1942], and was a study of sodium chloride and potassium nitrate distribution in food.

Additives that prevent microorganism contamination and thereby preserve the food are curing agents. These are salts, typically NaCl and a salt containing nitrate and/or nitrite [Toldrà, 2002, p. 3]. All meat contains NaCl, which gives the meat taste and makes up a few percent of its weight. This percentage is 4-9 % for dry-cured ham [Raiser, 2014], and about 11 % for Cecina de Leon, a type of dry-cured beef [Hui, 2012].

The moisture content of a product in equilibrium with the relative humidity of the air, can be described by sorption isotherms [Comaposada et al., 2000]. These are graphs with water content as the ordinate and relative humidity or water activity as the abscissa, which are equal at equilibrium. The term «water activity» was introduced early, before 1936, to describe the conditions for microorganisms [Kapsalis, 1987]. This was useful because water activity, unlike moisture content, says something about the availability of water that organisms can utilize, and hence what degree of drying that is required to preserve the food. A mathematical model for the sorption isotherms is Bradley's equation from 1936, given in [Okos et al., 2006] along with several other models.

The role of muscle structure and content has also been known for many years. Lipids and proteins have been studied since before 1937, when [Anderson and Williams, 1937] wrote about «The role of fat in diet» and mentioned lipids of different types, other chemical components in food and whether ham is good or bad for the human diet. A study of meat products, [Hankins, 1945], then reported that most people ate much meat without considering the dangers related to it, like health risks if the animals were not well. He also wrote that this problem was especially related to pork, but

> *«. . . certain procedures in freezer storage and curing are now known to kill the organism . . . Except in farm and home curing and canning, spoilage of meat does not present a serious problem . . . »* [Hankins, 1945]

> *«. . . rancidity in fat is accompanied by a change to a yellowish color. Pork is especially predisposed to such changes.»* [Hankins, 1945]

It was also mentioned that meat, especially beef, can have different shades of red, dark or light. Why was not always clear, but the content of certain components, like vitamin A, was one of the known causes. Thus, something can be said about the nutrients in meat simply by considering its colour. The first quotation also reveals a practice to cure meat at home.

Concerns were, and are still, browning, nutrient degradation, rancidity and formation of a crystal layer [Hankins, 1945, Parolari, 1996, Toldrà, 2002, p. 116], discussed in Chapter 2.

Drying by adsorption has been known since before 1960 [Dubinin, 1960]. A company which has experience with this adsorption technique from 1960, claims that it requires less energy than other drying methods, and several plants producing clip fish apply it [AG,].

Another method to lower energy use was investigated by [Rogers et al., 1965] in [Arnau et al., 2007]. They injected enzymes into high quality meat to achieve faster lipolysis, proteolysis and flavour development. Although the processes were accelerated, the quality was lower than that of untreated meat.

4.3 QUALITY AND ITS RELATION TO WATER

Quality is a major factor for studies on meat [Hankins, 1945]. It is affected by water, among other reasons because bacteria need water to live. According to [Kuprianoff, 1958] in [Okos et al., 2006], not all water in products is free to take part in reactions; some of it is bound. «Bound water» desorbs less easily than unbound water, and he defined it as water that does not freeze below the freezing point of water. Drying is affected by how water is bound to the product structure, which was described by [Luikov, 1966]. He wrote that water in different substances can be present in several ways, and these are [Strømmen, 1980, p. 15], [Luikov, 1966, p. 193-197]:

- chemically combined water
- adsorbed water (which is assumed to constitute a monomolecular layer on the inside of the ham structure, called the monolayer. [Okos et al., 2006] discuss its existence.)
- capillary bound water (which is bound by the surface tension and wetting properties of water)
- osmotically bound water (which is bound by ionic forces/polar attraction)
- free water

The first four types are bound water, and all the binding phenomena together are called sorption [Strømmen, 1980, p. 15]. Due to the sorption effects, more energy than the latent heat of evaporation is needed to release the water, and therefore, the vapour pressure in the substance will be slightly lower than the saturated vapour pressure of water at the present temperature [Luikov, 1966, p. 192 and 198]. This decreases the driving forces in drying. Solids that have water bound to it by adsorption, like meat, are called hygroscopic [Kapsalis, 1967].

Some studies in the 1960s revealed that some meat easily loses much water, and this was characterized as pale soft and exudative, or PSE, meat [Cassens, 2000, Daigle et al., 2005]. This can perhaps be partially explained by the different ways water can be bound to a meat structure. PSE meat has high drying rates and low quality, because the water is mainly dried from the surface, hence, the inside is not safe of bacteria and the outer layer was reported to be rancid [Cassens, 2000]. It was also recognized in the 60s that pigs can have PSS, porcine stress syndrome, and this was then considered as one reason for PSE [Cassens, 2000].

The colour of PSE meat is pale, but there is also a similar type of meat, that has the desired red colour, RSE (red, soft and exudative). This causes similar problems, but this is less recognizable due to the colour [Warner et al., 1997] in [Toldrà, 2002].

A third type of meat classified in the 60s is DFD meat, dark, firm and dry meat [Cassens, 2000]. This looks good, but should not be used at all, because it binds water and has a neutral pH, which allows bacterial growth. Ideally meat should have slightly lower pH, 5.6-6.2 for hams [Gou et al., 2002, Toldrà, 2002, p. 12 and 29] and 5.4-6.0 for beef and sausages [Hayes et al., 2007, Arnau et al., 2007]. DFD is more rear, but also more severe than PSE meat [Toldrà, 2002, p. 24]. In 1963, 18 % of the pork in the USA were PSE and 16 % in 1992. 16 % were of high quality, 10 % were DFD and the rest RSE [Cassens, 2000].

The bound water content in protein was studied by [Berlin et al., 1970]. 50-60 % of dry mass was bound water. Up to about 1970, studying the water content and profile was cumbersome and the methods lacked accuracy. A sample would have to be removed from the experiment and the water content measured, hence different samples would be studied at each observation [Gou et al., 2004, Okos et al., 2006]. Around 1970 however, studies using nuclear magnetic resonance spectroscopy, or NMR, were performed [Okos et al., 2006]. NMR allows the study of water content without interrupting the drying process. For dry-cured meat, no study with NMR before [Lundberg, 1983] was detected. Studying the binding and release of water in solids, or the sorption and desorption characteristics, often displays a tendency of hysteresis. This means that different equilibrium water contents are detected for sorption and desorption. The hysteresis for pork was found to be small and present for water activities between 0 and 0.85 [Wolf et al., 1972]. The isotherms for different types of meat are similar [Trujillo et al., 2003, Okos et al., 2006].

4.4 ENHANCING PRODUCTION RATE AND QUALITY

The 1970s was the time when controlled drying environments with coolers to prevent microorganisms became usual [Parolari, 1996]. Before that, more meat was destroyed because both temperature and water content could be high, and at least one of them should be low to prevent contamination. Before the conditions could be controlled, some production sites could not operate all year [Parolari, 1996].

Controlling the drying environments focused on improving meat quality, not on low power consumption. Energy was cheap, but meat of high quality expensive. Due to this, economics has prevented many energy saving techniques since the 70s [Strumillo et al., 2006]. Very few studies on energy were performed, thus the interest for this was low. Several authors writing about energy concerns, like [Strumillo et al., 2006, Chen and Hernandez, 1997], have their earliest references from the 70s. For example, thermal and mechanical vapour recompression were mentioned as means to reduce energy consumption by [Anonymous, 1977], as the earliest reference in [Chen and Hernandez, 1997]. In addition, the meat industry has been very slow to develop in the field of energy efficiency[Alcazár-Ortega et al., 2011].

Several studies on faster production of dry-cured meat were also performed in the 70s. One way to accelerate the curing is by tumbling. The first detected reference about this is [Treharne, 1971] in [Hayes et al., 2007], who reported that tumbling enhances curing, but too much tumbling can cause undesired amounts of myosin on the meat surface. It can also result in more tender, uniform and aromatic meat [Weiss, 1973] in [Hayes et al., 2007].

Vacuum treatment of meat was investigated by several references in [Hayes et al., 2007]. It enhanced salt penetration and myosin extraction, but there were disagreement between the studies on whether intermittent or continuous operation gave best results. Boning and skinning hams before they were dried and ripened enhanced salt penetration, shrinkage, moisture loss rate and proteolysis, while it did not affect the eating experience [Montgomery et al., 1976]. This result is very promising, as it can make both capacity larger and energy required per kg lower. An accelerated dry-curing process for beef was achieved by tumbling, and additional vacuum improved colour as well [Hayes et al., 2007].

Heat pumps became usual in the drying industry for clip fish from the early 1980s [Bantle and Eikevik, 2014]. A heat pump dryer and its optimal running procedure was discussed and described by [Strømmen, 1980]. Heat pump drying is more energy efficient than hot air drying [Bantle and Eikevik, 2014, Jon and Kiang, 2006], but requires an investment. What seems to have made it attractive for the industry was expanded capacity. 36 % increase in capacity could be achieved by increasing the drying temperature a few degrees [Strømmen, 1980], which requires less energy with a heat pump than with another heater. The only reason not to increase the temperature further was the risk of burning the product and/or developing of a hard crust on the outside [Strømmen, 1980, Parolari, 1996, Jon and Kiang, 2006, Bantle et al., 2014]. Many drying industries also implemented automatic control to improve their drying processes in the 1980s according to [Su et al., 2014]. Their earliest reference from the meat industry was from 2010.

4.5 CONTROLLING DRYING MECHANISM

Which mechanisms that dominate drying of different materials and how they should be modelled has been discussed for about a century [Whitaker, 1977]. The most widely used model for drying of food is probably Fick's law of diffusion [Gou et al., 2004, Ruiz-Cabrera et al., 2004, Waananena et al., 1993, Okos et al., 2006]. It makes use of a diffusion coefficient to describe the mass transport. Adolf Eugen Fick developed Fick's law of diffusion in 1855 for gases, but there are also other types of diffusion [Waananena et al., 1993].

It is and has been usual to swop the diffusion coefficient with an effective diffusion coefficient that takes hand of all the deviations from pure, true Fickean diffusion, which, if such a thing exists, would occur in pure media [Whitaker, 1977]. This means that all other effects than diffusion only were accounted for through the allowed variation of the effective diffusion coefficient. This has lead to critique of the model, since «all other effects» vary and make the coefficient hard to predict [Whitaker, 1977].

Applying the diffusion equation and let the effective diffusion coefficient be a function of moisture content gave good results in biological material [Berger and Pei, 1973] in [Whitaker, 1977]. In lean mutton Fickean diffusion was fund to be the dominating mechanism [Radford, 1976] in [Trujillo et al., 2007]. [Radford et al., 1976] were some of the first to model mass diffusivity by means of the «effective» diffusion coefficient in meat.

A model based on the analogy between heat and mass transfer gave good fits when applied to drying of clip fish [Strømmen, 1980]. Two mechanisms were included: an external convective and an internal diffusion mechanism. The latter dominated during most of the drying, and most of the moisture transport happened in vapour phase, about 75 %. Of the three different drying stages described in Chapter 2, only the two last were observed.

4.6 PROCESS MANIPULATIONS

Several researchers in the 80s found that thawed meat is dried faster than unthawed meat [16, 2003, Toldrà, 2002, p. 47]. They found that frozen and thawed hams had salt diffusion coefficient $2.9 \times 10^{-10}\,\frac{\mathrm{m}^2}{\mathrm{s}}$ and green ham had $2.2 \times 10^{-10}\,\frac{\mathrm{m}^2}{\mathrm{s}}$. Pressing the meat mechanically had the same effect as freezing and thawing, as all these processes make cracks and open up pores for mass transport [Strømmen, 1980, Toldrà, 2002, p. 203-4]. One drawback is that yeast and mould can start growing in such pores, thereby closing them and lower water transport [Toldrà, 2002, p. 47].

Making cuts in the meat to enhance diffusion gave higher salt penetration, but did not increase ripening or water loss rate [Marriott et al., 1983] in [Toldrà, 2002]. Vacuum or treatment with NO also enhances the curing [Marriott et al., 1984] in [Hayes et al., 2007] and it has also made the salt distribution more even in hams and cheese [Hayes et al., 2007]. Tumbled and vacuum tumbled beef was cured faster, and vacuum gave better colour [Ghavimi et al., 1986]. Tumbling ham before curing also resulted in higher salt content and moisture removal [Marriott et al., 1987]. [Marriott et al., 1992] concluded that

> *«Dry-curing can be accelerated through production techniques such as tumbling, blade tenderizing, microbial inoculation, use of nitric oxide and processing as skinned and/or boneless legs,»*

but more research was necessary to ensure quality was satisfactory.

Freezing accelerated lipolysis and proteolysis by three to six months in a study of [Motilva et al., 1994] in [Toldrà, 2002]. Only the salt taste was affected, but adjusting the amount of salt should not be too difficult. This finding is especially important for high quality products.

4.7 STUDIES ON QUALITY IMPROVEMENT

During the 1980s, many scientists looked into the enzymatic reactions during ripening. The focus on understanding why PSE and DFD occurred and controlling the drying environment has first started during the last decades. Problems with destroyed, contaminated meat have become fewer the last decades due to the controlled drying environments with cooled air and studies revealing necessary air circulation, salt contents and water activity levels [Parolari, 1996]. Still, this has not been enough to prevent surface problems of all products. One example of this is Parma ham, which requires high drying rates and cold air in the first resting period before the main drying[Parolari, 1996]. Although many of these requirements were met during the 80s, problems with microorganism and mould are far from over [Raiser, 2014, Parolari, 1996, Toldrà, 2002, p.40-41].

Nitrate and nitrite are added to some of the meat products in order to prevent botulism and hence quality degradation [Richard, 1981]. This and obtaining good colour are the only functions of these additives, and their activity is highest for pH between 5.6 and 6.0 [Toldrà, 2002, p. 30]. For health reasons, one should avoid too much of these components, and therefore there are maximum allowed amounts of them [Cassens, 1995, Cingi et al., 1992]. They were completely forbidden in Parma ham from 1993, as their prevention of oxidation processes also affects the flavour [Parolari, 1996].

[Arnau et al., 2007] reported many studies, mainly from the 90s and onward, trying to accelerate drying and the ripening processes for high quality ham and sausages. Both proteolysis, lipolysis and colour development could be enhanced by additives and temperature, but the desired traditional flavour and quality were not obtained. Applying vacuum reduced drying time for sausages from 18 to 12 days in 1995 [Chin et al., 1995] in [Arnau et al., 2007]. Some of the techniques mentioned could also reduce energy demands, but energy was not mentioned. Again, larger capacity seem to have been the motivation.

Problems with PSE meat could, according to [Cassens, 2000], be overcome due to research on genetics and molecules. [Schilling et al., 2004] presented a study in which PSE ham was treated with soy protein, sodium casienate and food starch and quality was improved. Similarly, quality was improved when PSE turkey meat was treated with collagen, soy protein or carrageenan [Daigle et al., 2005]. How animals were treated directly before slaughter affected the meat quality, which was reduced when the animals were stressed [Álvarez et al., 2009]. This was in accordance with the suggestion from the 60s, when stress was assumed to be a reason for PSE meat [Cassens, 2000].

4.8 Factors influencing the process

Research around 2000 A.D. seems to be mainly on which parameters affect the process and how. In addition, new methods for imaging and studying the actual processes were applied. Diffusion depended on salt content in a study of raw ham [Comaposada et al., 2000]. Effects of pH, fibre direction, temperature, salt content and muscle type on drying were investigated [Gou et al., 2003, Gou et al., 2002], and the conclusions were that pH and muscle type are unimportant, but diffusion parallel to muscle fibres is 31 % higher than when it is perpendicular. Diffusion in these studies decreased with salt content and increased with temperature. The Arrhenius equation described the temperature dependence of the effective diffusion coefficient, but this equation alone did not describe it completely, since for example salt affects diffusion and salt content was not included in the Arrhenius equation. In addition, it might be that proteolysis affects the drying process [Gou et al., 2004].

If the Arrhenius equation was coupled with a moisture dependent expression, the equation appeared to describe effective diffusion well [Ruiz-Cabrera et al., 2004, Gou et al., 2004]. The effect of fat content on diffusion was found to be unimportant by [Gou et al., 2002] and [Gou et al., 2003], whereas it is highly important for ripening and flavour development [Toldrà, 2002, p. 11-12 and 196]. Others have found that increased lipid content decreased diffusion dramatically [Ruiz-Cabrera et al., 2004], which is in accordance with many other findings mentioned by [Hayes et al., 2007].

Fibre direction showed negligible effect in the study by [Ruiz-Cabrera et al., 2004]. Neither did they find any effect of temperature, but attributed this to different compositions of the samples, and this result was regarded as unreliable. The moisture profiles in hams were found to be Fickean[Ruiz-Cabrera et al., 2004, Gou et al., 2004], just like [Radford, 1976] found in mutton. All these references used the Fickean diffusion model with good results, but obtained diffusion coefficients ten times larger than those presented in Section 4.6.

4.9 Shortening production time

[Toldrà, 2002, p. 58-59] stated that shortening production time for hams requires that conditions for ripening are optimized, so that ripening becomes faster. Eventually, extra enzymes could be rubbed onto the surface and penetrate the meat along with the curing agents to enhance ripening. The method was not fully developed, as it gave a poorer taste.

A more successful technique is quick-dry-slice drying, or QDS drying, which has reduced both ripening and drying time for fifteen products [Comaposada et al., 2004]. It involves slicing the product before drying, under reduced pressure, and then a modified atmosphere during ripening. Auxiliary energy can be supplied to the drying stage. The potential to save energy by this method is large, because about half of the hams produced are sold as sliced ham [Toldrà, 2002, p. 43] and many other products, like sausages, are also frequently sliced.

For products without long ripening times, slicing alone could save time and energy without big process changes, as one only must move the slicing stage in the production. Applying QDS to sausages, the drying time was lowered from 18 days to 30-45 minutes [Stollewerk et al., 2012, Arnau et al., 2007], and so was the required energy [Stollewerk et al., 2012].

Pulsed electrical fields have been applied to meat in order to improve its quality and speed up the production. This technique has two main functions: killing microorganisms and structural changes causing mass transfer enhancement [Jäger, 2012]. It can have some thermal side effects that can be wanted or unwanted, and [Jäger, 2012] discussed what to do with these. He wrote that local high temperature fields killed enzymes and was bad for heat sensitive products, but a new chamber design solved this, making the temperature distribution more uniform. This is in accordance with [Strumillo et al., 2006, p. 1090] who wrote that both radiofrequency and microwave heating must by uniformly distributed to be beneficial.

[Jäger et al., 2008] stated that pulsing electric fields creates pores and availability for mass flow within food, and that it improves tenderness. The technique showed many applications for minced meat, beef, pork and fish, such as improved digestibility. Results from applying an electric field to beef loin agreed with this, and concluded tenderness was improved [Bekhit et al., 2014]. In addition, cooking loss was lower, which might improve the juiciness [Bekhit et al., 2014]. The additional use of electricity increased the energy use, which was reported to vary between 3.1 and 73.2 $\frac{\text{kJ}}{\text{kg}}$. This is one of the few articles mentioning energy use and economics. Both the improvement in tenderness and required energy increased with frequency, but tenderness was unaffected by other factors, like voltage.

Ultrasound applied to drying gave improved meat structure and faster curing [McDonnell et al., 2014, Siró et al., 2009]. Other characteristics, including quality, were either not affected, or affected to a low extent [McDonnell et al., 2014]. Improvement of the salt diffusion depended on the intensity of the ultrasound, and could also be achieved by vacuum tumbling [Siró et al., 2009]. The reported optimal intensity varies between the studies, so its value is uncertain, but it must be above 640 $\frac{\text{kW}}{\text{m}^2}$ for water and 510 $\frac{\text{kW}}{\text{m}^2}$ for sodium chloride to give any effect [Cárcel et al., 2007]. Agitating the meat showed no detectable difference [Cárcel et al., 2007].

4.10 LOWER POWER CONSUMPTION

Despite many attempts to improve process efficiency, most of these are mainly related to quality and to achieve a higher throughput, not to reduce the power consumption, due to the low energy prices [Marinos-Kouris and Maroulis, 2006, Alcazár-Ortega et al., 2011, Strumillo et al., 2006, Chen and Hernandez, 1997]. Consideration of environmental aspects are even more rear, but an analysis of the environmental impacts from producing dry-cured ham and other foods was performed by [Črnivec and Marinšek-Logar, 2010]. According to [Bantle and Eikevik, 2014], it is often mentioned that new technologies increase the drying rate, but the fact that the energy demand also increases is omitted, and the drying is thereby said to be more efficient, although it might use more energy.

One of the few studies that did mention energy, tested applications of ultrasound to accelerate clip fish drying [Bantle and Eikevik, 2014]. Even though they found that this was possible and therefore perhaps economical, the required energy was many times higher per kg when ultrasound was applied. The same result was found for microwave heating, which also burnt the product at too high intensities [Bantle et al., 2013]. Then, time could be reduced by 90 % (applying 155 $\frac{\text{W}}{\text{kg}}$), and by 35 % without harming the product (applying 35 $\frac{\text{W}}{\text{kg}}$). However, the energy needs increased manifold, and it was concluded that hot air drying requires a maximum 6.2 $\frac{\text{W}}{\text{kg}}$ and heat pump drying maximum 1.6 $\frac{\text{W}}{\text{kg}}$ to be economical for a 50 % reduction of time [Bantle et al., 2013].

Ultrasound only had a high effect on drying at the start, thus it should be turned off after a while [Bantle and Eikevik, 2014]. Interrupting the air supply for short periods has also lowered energy use without slowing down the drying, and intermittent operation of air velocity, temperature or humidity can even increase the drying rate [Jon and Kiang, 2006]. Lowering the fan speed and running them for a longer time saved 1.65 % of the supplied energy, and turning off the cooling equipment in periods saved 5 % in a study by [Alcazár-Ortega et al., 2011]. They wrote about the latter method that it should be used with care as it utilizes the temperature rise to keep humidity low. There are also several other simple ways to save energy, like better insulation and minimization of air leakages [Alcazár-Ortega et al., 2011].

The amount of evaporated water decreases with time in batch drying processes [Bantle et al., 2013], and one could perhaps reduce the entire air flow towards the end of drying, when mass transfer is internally controlled [Strømmen, 1980] so the surface is dry and safe of microorganism. This could lower energy use. Another possibility for reducing energy needs by about 21 % is to dehumidify the drying air by utilizing a cold climate for free cooling [Bantle et al., 2015].

Hybrid drying techniques, like infrared heating, ultrasound and microwave heating all increase the drying rate, and all require extra energy to do so [Jon and Kiang, 2006]. Both infrared and microwave heating have been reported to burn the product surface [Bantle and Eikevik, 2014, Jon and Kiang, 2006], whereas ultrasound has the advantage that it is not thermal energy, thus, it spares the surface and can decrease the inner mass transfer resistance as well as the outer [Bantle and Eikevik, 2014].

Adsorption drying has recently been investigated to lower energy use compared to hot air drying [Atuonwu et al., 2012a, Atuonwu et al., 2013, Atuonwu et al., 2011b]. The regeneration temperature, humidity and mass flow affect the overall efficiency to a high extent, and must therefore be chosen well according to [Atuonwu et al., 2011b], who optimized these variables for drying at 25-50 °C. They found that the higher the regeneration temperature, the better when no heat recovery for the used regeneration air was included. This was because high regeneration temperature in an adsorber desorbs much water quickly. Regeneration temperatures between 200 and 400 °C were considered. When a preheating heat exchanger was included, lower regeneration temperatures also increased efficiency [Atuonwu et al., 2011b].

Smart drying technology is automatic monitoring systems supposed to optimize both quality and energy efficiency. The development of intelligent monitoring could significantly improve drying and conditions for the ripening processes, but normal dryers still have high energy consumption and low automatic control [Su et al., 2014, Strumillo et al., 2006].

4.11 PROCESSES INSIDE MEAT

Several studies on chemical development in food products were presented by [Okos et al., 2006]. These were never coupled with the mass transfer, but studied separately from the drying, even though their interaction might be important [Gou et al., 2004]. Investigation of dry-cured meat has traditionally been divided into two parts, one studying the chemistry and development of taste and structure, and another studying drying of ham alone. The coupling has, as far as the author knows, never been done, but is planned in a study of [Petrova, 2015].

Many studies on chemical components aimed to find out which components affect flavour, speed of ripening and quality and in which way, utilizing techniques like infrared spectroscopy [Prevolnik et al., 2011] and chromatography [Mora et al., 2014, Herrmann et al., 2014] to determine composition. The recent focus on lower salt for health reasons turns the production to less salted products. One drawback is that these are more easily attacked by microorganism, but a successful method to ensure safe production of sausages has been to pressurize the drying stage [Stollewerk et al., 2012].

The model developed by [Strømmen, 1980] for clip fish was applied to drying of dry-cured ham by [Raiser, 2014, Bantle et al., 2014], but performed worse than the Fickean model to which it was compared. The Fickean diffusion coefficients were ten times lower than those in Section 4.8, hundred times lower than those in Section 4.6. A modified version of the Strømmen model gave better fits than the Fickean model in [Kvalsvik, 2014], and the first was considered more realistic, partly because Fickean coefficients obtained in this and other studies vary several orders of magnitude.

4.12 SUMMING UP

Today dry-curing is done mainly to develop traditional flavours and textures, not to preserve meat as earlier. It is not simply a drying process, because additives must penetrate the product, and these often developing structural and aromatic changes. There are different goals for different products: some meat is only supposed to by salted and dried as quickly as possible, production of other types of dry-cured meat is mainly a ripening process, because the ripening stage lasts much longer than drying.

Few studies on energy have been found, and most of them are relatively new. Generally, the focus is on quality, and accelerated processes are mainly considered to get a higher throughput, not lower power consumption. Process changes must be economical, and quality is of major importance for this. To achieve a safe, high quality product, a relatively low humidity, low temperature that slows down chemical reactions and thereby bacterial growth and/or a high salt content could be utilized. The raw material is also important. DFD meat should not be used, but PSE meat can be treated.

Shorter drying time can reduce the energy needs. For the meats that do not need ripening, faster drying would lower power consumption provided the accelerated process was not achieved by higher power input. Faster drying must also involve a faster curing. Salt diffuses more easily when water content is high. Tumbling, vacuum treatment and slicing are all techniques to accelerate curing and drying. For meat that should ripen, shorter drying time must be accompanied by faster maturation. Otherwise, the use of long time is necessary to obtain high quality, and faster drying alone could rather be detrimental than beneficial. Hence, to reduce production time one must speed up lipolysis, proteolysis and salt penetration. Freezing, use of modified atmosphere and QDS seem to be the most promising techniques so far. Adding extra enzymes also has potential, but the final taste with this technique is not yet satisfactory.

Ultrasound and microwave heating both accelerate drying much, but are very energy intensive, and much research remains to make these technologies energy efficient in production. An alternative to reduce required energy by reducing production time is to set the focus on methods for dewatering air that require less energy than conventional. Adsorption, installing heat pumps or changing operation procedure for airflow or temperature are some promising ideas. Smart drying technology can optimise conditions for both quality and energy.

Chapter 5

ENERGY SYSTEMS CONSIDERED

This work only involves simulations, no experiments. This limited which energy improvements that could be considered, and a discussion of which systems could be evaluated and why some were considered and others not is given here. To compare the results, a basic system based on data for an existing plant was established, and all results were compared to this one. The work used a model for meat developed in [Kvalsvik, 2014], based on experimental data from drying dry-cured ham slices.

5.1 HOW TO CHOOSE SYSTEMS

To reduce energy one could lower production time. Lowering production time by injecting additives is possible, and applying vacuum or modified pressure or atmosphere has shown faster ripening and curing [Comaposada et al., 2004]. This enhancement of ripening is chemistry and outside the scope of this work.

Ultrasound, microwave and infrared heating have all potentials to increase drying [Bantle and Eikevik, 2014, Bantle et al., 2013, Jon and Kiang, 2006]. However, since ultrasound and microwave showed many times higher energy consumption in the listed studies than conventional systems, they were not considered. Infrared heating often scores the surface [Jon and Kiang, 2006], which could create a barrier for further drying. Because quality is of major importance and high temperatures must be avoided [Jon and Kiang, 2006, Strømmen, 1980, Parolari, 1996], this was not included here either.

Steam drying would probably give very good quality, especially the surface would not be crusty, and easy heat recovery. However, it would require an extremely low pressure in order not to destroy the product, and this method is only economical if the excess steam can be utilized somewhere else at the plant [Mujumdar, 2006]. Systems where waste heat can be used were not included, because this need might vary and it is not given that this possibility is there. Yet, the different purposes for which energy was used were reported separately, and a calculation on how much could be saved if the possibility is there was performed.

Vacuum can also enhance drying, but the pressure dependence is not verified in any model known to the author, and these alternatives were therefore considered unrealistic to make reliable models of.

Reducing the air flow and thereby velocity reduces the energy consumption [Alcazár-Ortega et al., 2011]. Air velocity also matters for the amount of evaporation from the product [Clemente et al., 2011], and must be high enough to prevent yeast. How in influences the process was an unsolved challenge in the developed model to be used, and it would thus be difficult to obtain reliable results if the velocity was allowed to vary. For this reason this parameter was not changed in the drying process, and the air flow normally used in the industry was applied.

Lowering the velocity towards the end of drying could perhaps be safe and worth trying, but as the industry reports problems with yeasts [Parolari, 1996], this is no promising idea. However, one could try to dehumidify a smaller part of the air stream In order to lower energy consumption, and this was considered in some energy systems in this work.

Higher temperature generally increases both chemical reactions and evaporation while it lowers energy use, but quality aspects often limits this, and the conditions in industry are normally chosen as a near optimal trade-off between a high temperature, low temperature for quality and safety, low relative humidity for safety and faster drying and high humidity for avoiding crusty surfaces. Experimenting with other conditions should involve experiments, not only simulations. Besides, only data for two, constant temperatures were used to develop the model at hand, and thus, results deviating much from these could be invalid. Hence, the conditions from the experiments, which are actually applied in the ham industry, were used.

Using the model at the conditions on which it was based also omitted the use of any intermittent operation of drying parameters. The model to be used was not developed for such conditions, and its validity would be uncertain.

Another consequence of the decision to apply normal drying conditions was that obtaining shorter drying time was no longer an option. The goal, therefore, became to deliver the normal drying conditions by using as little energy as possible.

Heat pump drying is reported to be better than hot air drying [Bantle and Eikevik, 2014], and even though some plants use heat pumps, many do not. The development in this area is generally slow, and thus, the savings from using a heat pump was considered. Other simple but energy effective arrangements can be achieved by inserting extra heat exchangers at strategic points [Haukås, 2010, Bantle et al., 2015] or other process modifications. Some arrangements with extra heat exchangers were therefore also evaluated.

For processes using a heater and a cooler, free cooling or heating in some cases can reduce the load [Bantle et al., 2015, Strumillo et al., 2006]. Solar heated systems have been even more efficient than heat pump systems [Jon and Kiang, 2006] but requires another climate than in Norway, and this type of system was not included due to its irrelevance to the Norwegian industry. Free cooling on the other hand, is available during the Norwegian winters. From simulations, this lowered the load on the cooler and reduced energy demand by 21 % relative to the same type of basic system as in this work [Bantle et al., 2015]. Because an evaluation was already performed for this system, this was not repeated in this work.

Dewatering by adsorption is claimed to be more energy effective than other drying methods [AG,]. The most efficient system delivered by [AG,] was therefore modelled and compared to the basic system. All systems considered in this study are briefly presented here, further detalis and theory is given in Section 6.4.

5.2 THE SYSTEMS CONSIDERED IN THIS STUDY

Basic system (BS), shown in Figure 5.1, where the drying air is cooled by a refrigerator using ammonia and glycol and heated again by electricity. The glycol circuit is required because ammonia is toxic.

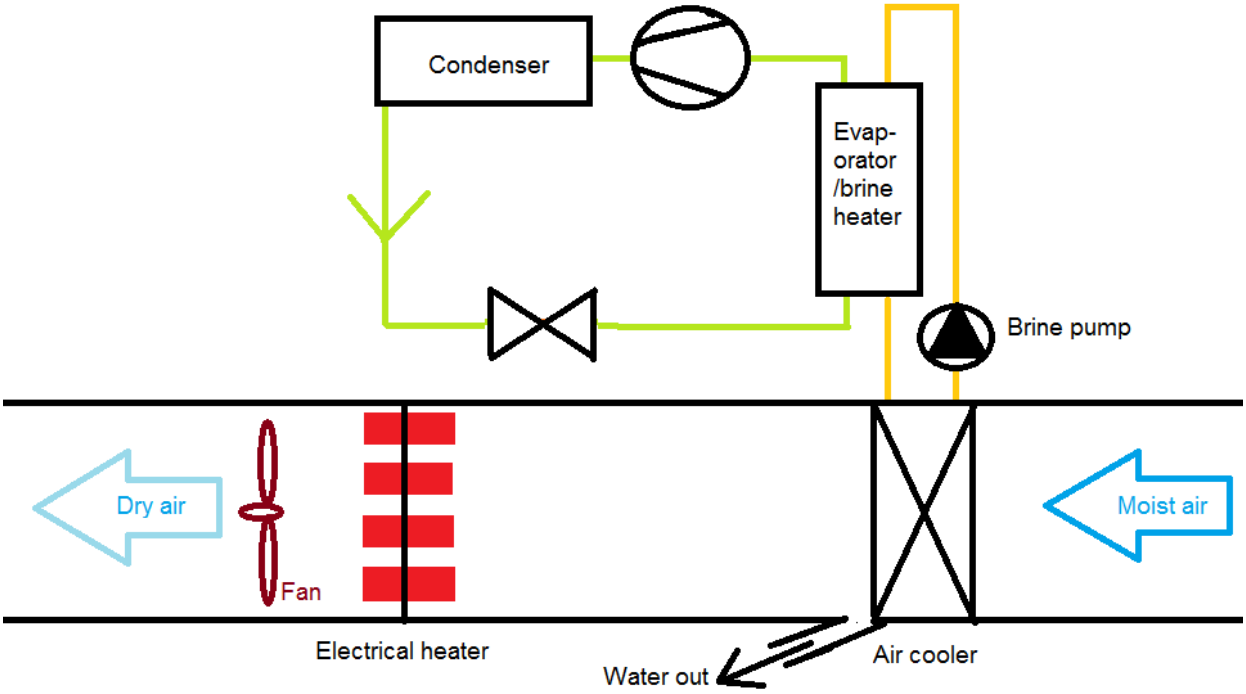

Figure 5.1: Basic system, using an ammonia (green) heat pump and glycol circuit (yellow) for cooling and heating by electricity

Heat pump system (HPS) is a system where an ammonia heat pump and two glycol circuits deliver both cooling and heating, shown in Figure 5.2. A closed system for the process air was used, to avoid polluted air, dirt and to minimize energy losses by rejecting it. This is also done in the industry. The heat pump load is then determined by the cooling load and there will be a heat surplus which an extra heat exchanger must remove.

Some heat pump systems with an extra heat exchanger (HPSX) were modelled and meant to improve HPS. The idea is shown in Figure 5.3. There are more versions of this system. One involved cooling down the entire air flow, two others versions cooled only a part of it.

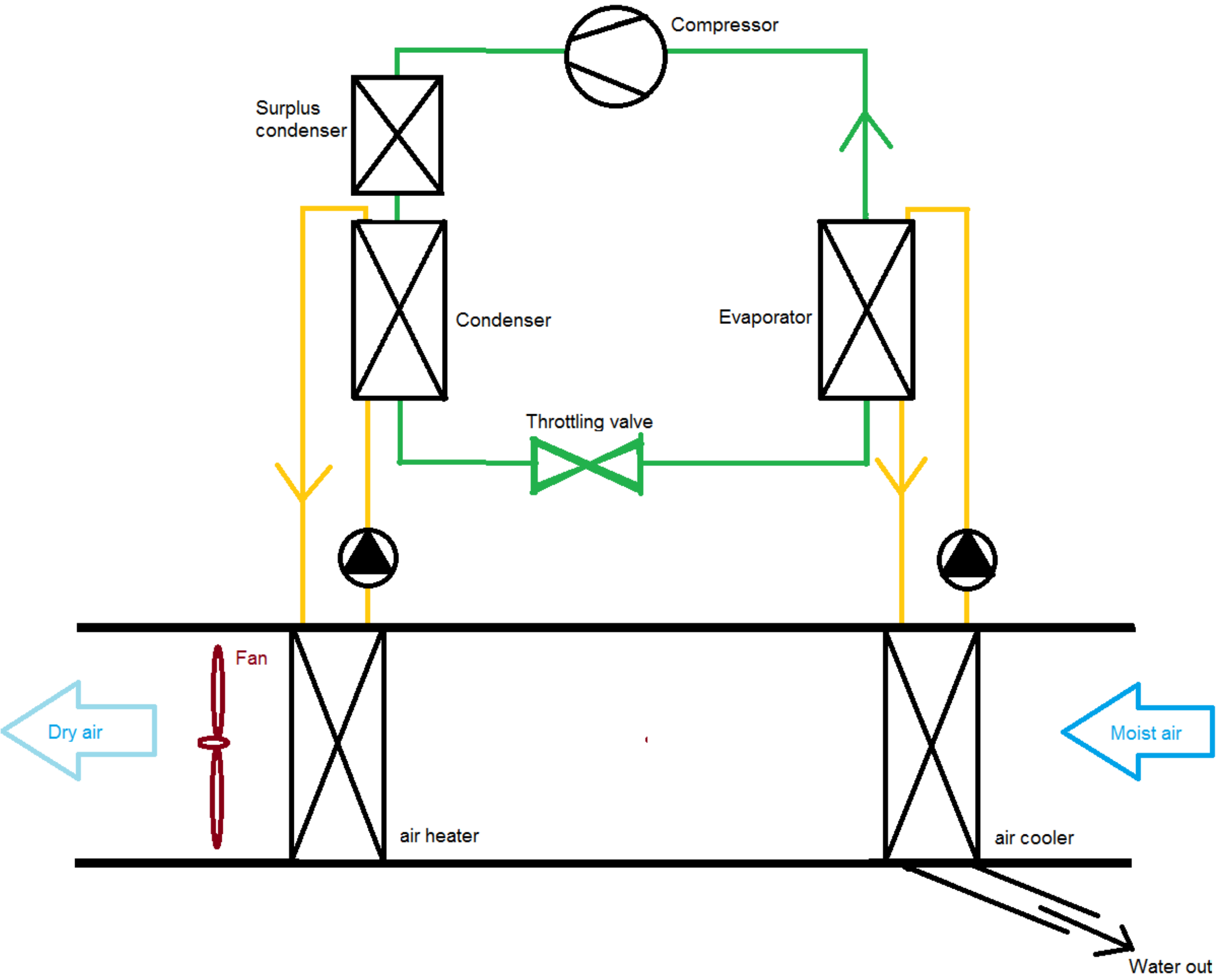

Figure 5.2: HPS, heat pump drying with ammonia

Cooling the entire flow corresponds to that the grey arrow in Figure 5.3 has 0 % flow and the blue ones 100 %. If only a part of the air was cooled, for example 20 %, the grey arrow could have 80 % air flow and the blue ones 20%. One system cooled a constant fraction of the air (37 %) and another a decreasing fraction, keeping the lowest air temperature constant. This is further explained in Section 6.4.2.

The best performing of the ammonia systems were also modelled using CO_2 instead of ammonia as working fluid. This was denoted the CO_2 system, or CO2S. The advantage with this was that it eliminated the need for the glycol circuits. Extra heat exchange with glycol means two extra temperature differences, and thereby a higher temperature lift and lower heat pump efficiency. Using a nontoxic refrigerant like CO_2 this can be avoided and efficiency might improve [Fornasieri et al., 2009]. All the above systems could be made this way, but only the best performing was considered, in order to avoid double work. Figure 5.4 shows an example with HPS performed with CO_2.

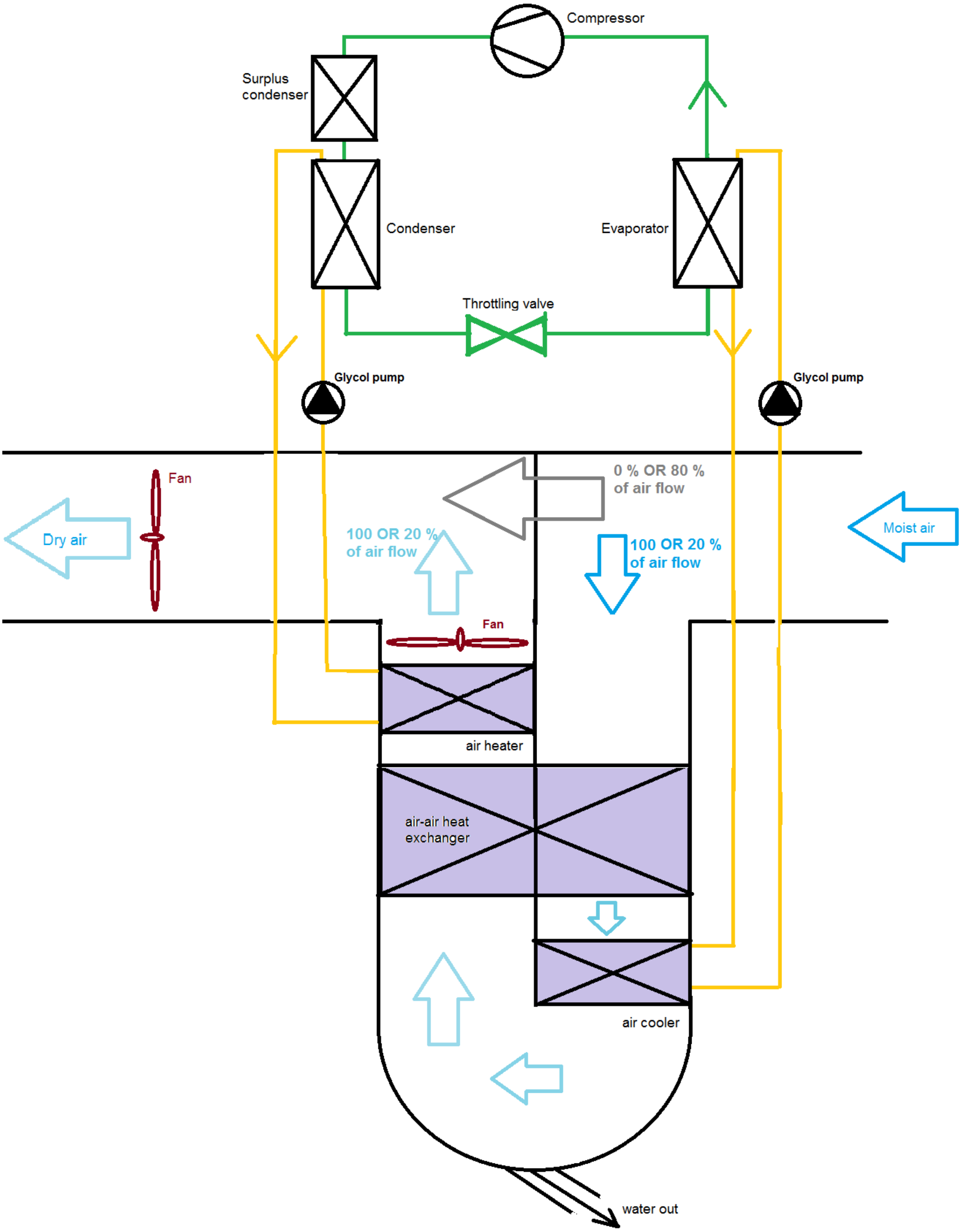

Figure 5.3: HPSX, heat pump drying with extra heat exchanger, the entire air flow could be cooled and heated, or only a part of it.

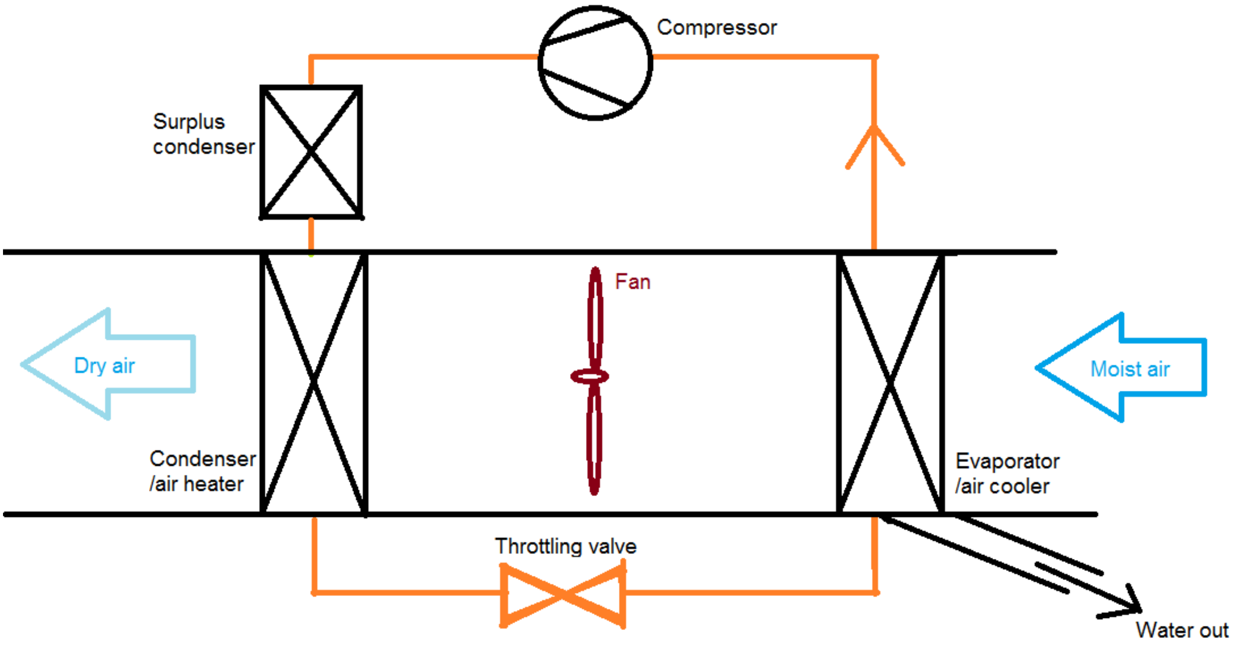

Figure 5.4: CO2S, heat pump drying with CO_2 as working fluid

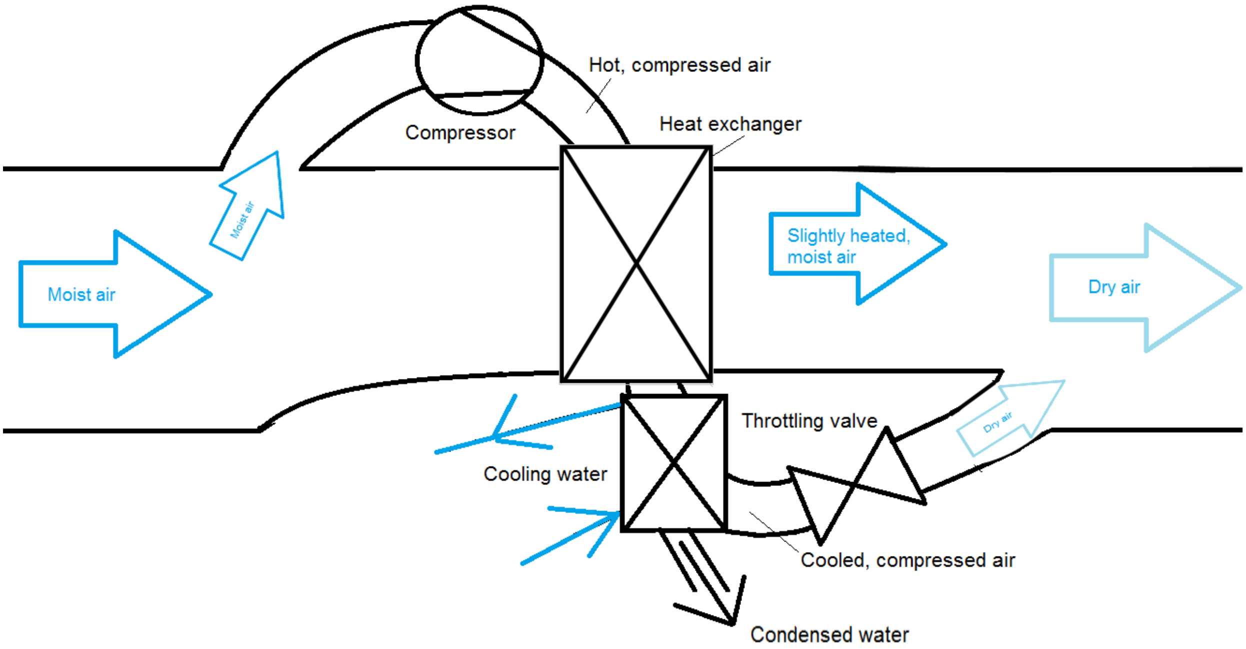

Figure 5.5: CS compressing the air to condense water and deliver heat, excess heat was removed by heat exchange with water

The compression system, CS is shown in Figure 5.5. Here a part of the process air was compressed to increase the wet bulb temperature for vapour. The higher pressure required cooling to a higher temperature than otherwise, removing the need for a heat pump. Cooling could be delivered for free by cooling water, and heating by excess heat was available from compression. This could potentially increase overall energy efficiency.

Adsorption system (ADS) displayed in Figure 5.6, is an alternative to cooling and condensing vapour from air. It is reported to be more effective than heat pump drying by the producer [AG,]. This firm supplied most of the used information on adsorbers. Their most effective unit, Econosorb, was considered in this work, because other adsorbers cannot achieve efficiencies as high as the heat pump systems, which will be further explained in Section 6.13.

Figure 5.6 shows the adsorber material, shaped as a wheel, and two air streams. The left stream is the process air, the right is regeneration air. The process air from the drying chamber is cooled in an evaporator, it then enters the wheel, where moisture is adsorbed and the air is heated. The air is then dehumidified. The other air stream is ambient air, which is preheated by the heat exchanger to the left and further heated by a heat pump condenser and eventually by an electrical heater. This hot air removes moisture from the wheel and adds heat to it.

Removing the moisture is called desorbing or regeneration of the wheel. Hence, there is a drying process for the wheel in the regeneration air (left side), and a wetting process in the process air (right side). The regeneration air leaves the wheel as moist, cooled air.

Table 5.1: This is an overview over the energy systems considered, where the adsorber system used a CO_2 heat pump and all heat pump systems except CO2S used an ammonia heat pump and glycol circuits for heat transfer.

System name	Description
BS	Basic system with refrigeration for cooling and electrical heating
HPS	Heat pump system with a heat pump for both cooling and heating
HPSX100	Heat pump system with extra heat exchanger, dehumidifying 100 % of the air
HPSX37	Heat pump system with extra heat exchanger, dehumidifying 37 % of the air
HPSX1	Heat pump system with extra heat exchanger, always cooling to 1 °C
CO2S	Best performing ammonia system made with CO_2 heat pump, without glycol
CS	Compression system where air is compressed to condense water
ADS	Adsorption system using Econosorb and recovering heat in a heat exchanger

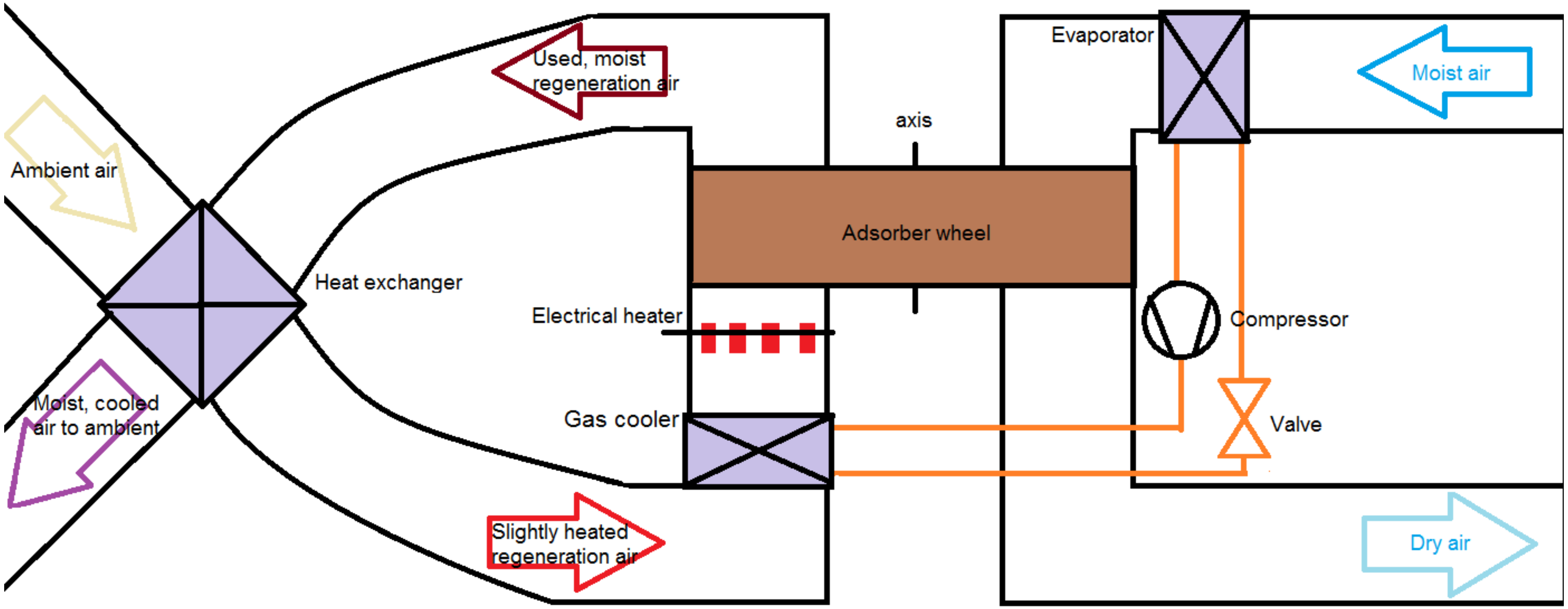

Figure 5.6: Adsorption system with heat pump: Most of the principle shown is taken from [AG,], only the heat exchanger to the left is added.

Chapter 6

THEORY

To find the energy consumption for the different system solutions, dynamic computer simulation was performed. All elements necessary to model the meat drying and energy systems are described in this chapter.

6.1 SIMULATION TOOL

For the simulations, DYMOLA 2014 (64-bit) was used. Graphical presentations and curve fitting were performed in MATLAB R2012b (32-bit) and many design calculations in Excel 2013. A program called StateViewer, version 1.3, was used to estimate enthalpies and temperatures in heat pumps.

DYMOLA is a program allowing modelling and simulation of dynamic, physical systems. The program was used with two extensional libraries called TIL and TILMedia. TILMedia contains data on many fluids, and these are categorized as liquids, gases and VLEFluids (Vapour-Liquid Equilibrium Fluids). The last group consists of typical working fluids for heat pumps. The fluids used in this work were TILMedia.MoistAir, TILMedia.Water, TILMedia.CO2, TILMedia.Ammonia and TILMediaProplyeneGlycol50 (a mixture with 50 % glycol).

The TIL library contains components which use the fluid data from TILMedia to model flow in them. The components include for example pipes, heat exchangers and compressors, in addition to sensors for measuring pressure, humidity, volume flow, etc. These components are built-in models. It is also possible to build own models of components, and use these models in other models. In this project, a model of a drying tunnel, containing a model of a tunnel section, containing a model of many hams were used. This was developed in [Kvalsvik, 2014], and used in all models in this work, to obtain the moist air from drying. The library also includes boundaries for fluid flow. Two, one or no boundary conditions can be specified, either pressure, mass flow and/or volume flow.

DYMOLA has two interfaces, one is programming code, another is an icon view, where the components can be moved around and connected by clicking on them. The latter is more intuitive, as it gives a better overview of the process. Pictures of the icon view of the models are shown in Appendix B, and one example of what the heat pumps looked like was given for CO2S in Figure B.46. All simulations were run with 500 time intervals and total time of 1.4×10^7 s unless otherwise stated. All files used in simulation are shown in an overview in Appendix E.

6.2 MEAT DRYING

To represent the meat that being dried, a drying model developed by [Strømmen, 1980], used as described in [Kvalsvik, 2014], was utilized. The equation for the derivative of the mass of a ham was

$$\dot{m}_{ham} = \frac{A(p_{w,sat} - p_{w,a})}{R_w T_a \left(\frac{1}{\beta} + \frac{s\mu}{D_{w,a}} \right)}, \tag{6.1}$$

where A is lean surface area of the meat, $\mathrm{p}_{w,sat}$ saturated vapour pressure, $p_{w,a}$ the vapour pressure of the drying air and their difference was the driving force for mass transfer. R_w is the gas constant for water vapour, T_a the air temperature, β the mass transfer coefficient on the surface, s the thickness of the outer, drier layer of the ham, $D_{w,a}$ the diffusivity of water in air, and μ is the reduction of $D_{w,a}$ due to the ham structure.

The model requires some model parameters, and these were found for ham in [Kvalsvik, 2014] based on results from drying cubic ham slices of four to six cm big. In real production plants, the hams are about eight kg, not cubic and much larger. The model in this work should therefore have a larger surface area and ham thickness than the values used in [Kvalsvik, 2014].

The applied surface area for evaporation was based on the average of 46 measurements of 23 hams (surface area and circumference were estimated for each ham). The data were supplied by Michael Bantle and measured by Animalia. The diameters were calculated from the estimated area and the circumference, assuming a circular area. An average of the resulting diameters, 31.53 cm, was used to estimate the surface area in the simulations. These calculations were performed in Excel, see Appendix E for further details. The thickest part of the ham was on average 14.96 cm from the same measurements, and was also used as input to the model.

In addition to physical parameters, a parameter accounting for the reduced transport of water vapour in meat compared to air was necessary. This depends on the salt content of the ham and was taken from the results in [Kvalsvik, 2014]. Normally, hams are sold with high salt contents, but the trend goes towards lower salt contents for health reasons. The applied parameter in this work was therefore the one for the second highest salt content in [Kvalsvik, 2014], 5.0 % salt on wet basis. This might represent a low salted, but still commercial ham.

Dryin was modelled to take place in a drying tunnel, containing several successive sections with hams. The conditions in a section are the same for all hams within it, but different sections can have different conditions. Completely uniform conditions in each section is not completely realistic, but this simplification was assumed to be small. Based on the conditions in a real plant, the modelled drying tunnel contained six sections, with 900 hams in each, giving 5400 hams in total.

Normally, 3-4 % water is lost during salting and pressing before drying [Raiser, 2014, Toldrà, 2002, p. 40-41], and 3.5 % was assumed. Thus the start weight in the simulations was 7.720 kg. Hams lose 33-36 % of the initial weight in production, and a few percent of this might occur after drying, during the ripening stage [Raiser, 2014, Toldrà, 2002, p. 40-41]. A weight loss of 35 % of initial weight, whereof 31.5 % during drying, was used as a stop criteria for the simulations. Final weight after drying then became 5.2 kg.

Drying was modelled to take place at 13 °C and 68 % relative humidity, which are conditions really applied in the industry. Because the hams were placed in different section, only hams in the first section received these conditions. Other hams received moister, colder air from the sections in front of them, and different drying times for the different sections resulted. Simulations were carried out until all the hams had reached the final weight.

6.3 DRYING AIR

The air in a drying process changes its moisture content and temperature during drying. To describe it, it is convenient to study the process in a Mollier diagram, like that in Figure 6.1. It has absolute humidity x in kg of water vapour per kg of dry air as the abscissa, and enthalpy and temperature as the ordinate. All properties are given per kg of dry air. The enthalpy lines are the black, diagonal ones and the temperature the red, nearly horizontal ones. The diagram is only valid at atmospheric pressure.

Air has a maximum water content depending on temperature. The blue lines displays the relative humidity, where the maximum water content when the air is saturated with water, is the line with 100 % relative humidity. Below this line vapour will condense.

A drying process proceeds as follows: The drying air enters the drying chamber at certain temperature and moisture content. In this work this was 2.8 $\frac{\mathrm{m}^3}{\mathrm{s}}$ at 13 °C and 68 % relative humidity, shown as point A in Figure 6.1. Evaporation of water from the product requires energy, which is taken from the air and reduces its temperature. Because the evaporated water then enters the air, this energy is not lost from the air. The process therefore follows the lines of constant enthalpy in the figure, towards point B.

At point B, the air is saturated with water, and no more evaporation can find place. It must be mentioned that the air does not need to reach this point. It could exit the drying

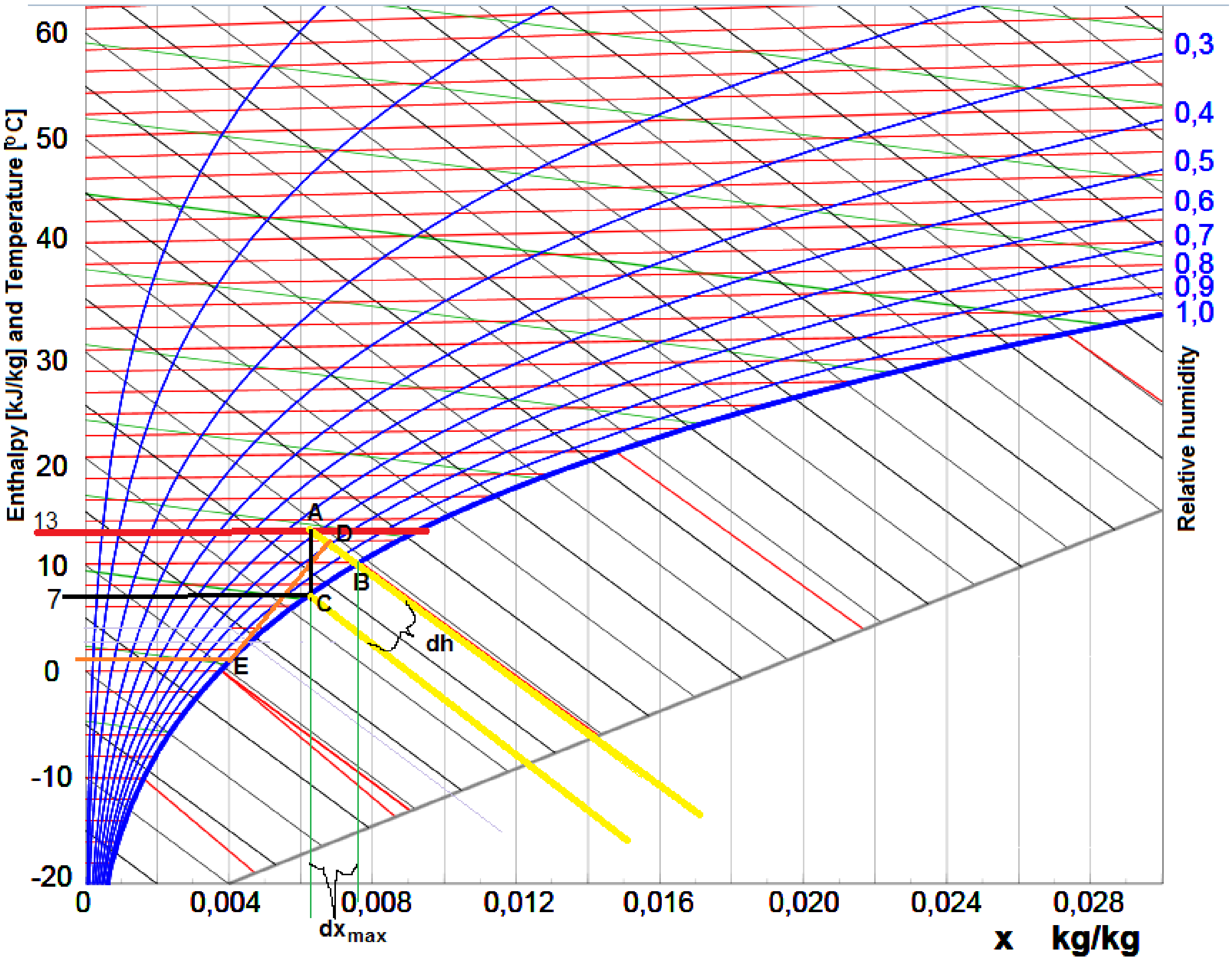

Figure 6.1: The process in a Mollier diagram, showing the start point (A), the wet bulb temperature (B) and the point to which the air must be cooled (C) in order to reach the desired operation point. Required energy per kg air can be read from dh, and change in moisture content is dx.

chamber at point D. The exit state from the drying chamber depends on how much water is removed and the contacting time between the air and the products.

In some existing plants, the drying air is dried and then reused in the drying process, making the air flow a closed loop. This solution was modelled in this work. Reusing the air instead of discharging it to the surroundings prevents energy losses and pollution entrainment from new air, and allows better control of the drying conditions. With the closed loop, one can control both temperature and humidity, not only temperature as with an open process [Jon and Kiang, 2006]. Many studies in [Colak and Hepbasli, 2009b] concluded it is also faster gives better quality.

To bring the used drying air back to its initial state for reuse, one could cool down the air to condense out water. If the air is saturated with water, the cooling will follow the line for saturated air in the diagram (relative humidity $\phi = 100$ %). It should then be cooled to the desired absolute water content. In this case point C in the figure, and then reheated to point A. Thus, if the air is saturated, it must be cooled to about 7 °C , and the process would follow a path described by ABCA.

If the air is not saturated, for example if it exits the drying chamber at D in Figure 6.1, then the required cooling will be less. In the cooling device, a heat exchanger, the surfaces in contact with the air stream must be colder than the desired final temperature for the air. Some of the air will come in contact with the surface and can be cooled to below the desired temperature, and more water (per mass of air) than necessary could condense from it.

Other parts of the air might never come that close to the walls, and thus, the overall state of the air after cooling will be somewhere on a straight line between the inlet state (for example point D) and the saturated state at the wall temperature (point E). This could give an outlet state which is not saturated with water, with a temperature above 7 °C and still the desired water content. The process with drying air exiting the drying chamber in state D would only require cooling to 10 °C if the wall temperature was about 1 °C.

The highest amount of water that it will be necessary to condense from the air, with this method of dehumidification, will be $\dot{m}_a \cdot \mathrm{dx}_{max}$ in Figure 6.1, and the highest amount of power supply can be found from the enthalpy change dh multiplied by mass flow of air, $\dot{m}_a$. Note that the heating and cooling demands are the same.

6.4 SYSTEMS

A basic system, denoted BS, was modelled with the energy system at a real, existing plant. All systems were compared to this to estimate how much the real plant can reduce its energy consumption. This standard process consisted of a closed air-drying system with refrigeration cooling and electric heating. The cooler was a one-step heat pump using ammonia, described in Section 6.7, and a glycol circuit transferring the heat between the heat pump and the process air. The glycol circuit is necessary because ammonia is toxic.

Electrical heating was modelled by a pipe with heat supply controlled to achieve the desired final temperature of 13 °C. The total energy consumption and energy for compression, heating and cooling were all monitored. The electrical heat supply could then easily be converted to that of a boiler or another heater if desired, by introducing its efficiency. No guess on heater efficiency was used. The total power in all systems included power for all fans and pumps in the system in addition to electricity for compression and eventually heating.

It was necessary to run the simulation for 1.43×10^7 seconds. It was ensured that this had no effect on drying, drying time or reported energy needs, as explained in Appendix B and Appendix C.

6.4.1 HPS

A system similar to BS, where the heat from the heat pump heated the air, replacing the electrical heat supply, was called the heat pump system, HPS. It required an extra glycol circuit for heating, in addition to an extra heat exchanger in the heat pump. One heated the process air, the other removed excess heat from the compressor as explained in Section 6.7.

6.4.2 HPSX

Three systems with heating and cooling by an ammonia heat pump and glycol circuits, just like HPS, made use of an extra heat exchanger. This lowered the load on the heat pump and therefore its investment cost and energy consumption. Compressor volume was reduced proportionally with the decrease in ammonia mass flow, which depended on the heat load.

One of these systems was denoted HPSX100, because 100 % of the air was dehumidified. The temperature differences in the process were so small that relatively little heat could be exchanged in the extra heat exchanger. Assuming somewhat reasonable dimensions for the heat exchanger, which can be seen in Table 6.2, the heat load for the heat pump was only reduced by about 15 %.

Heat pump dryers are inefficient for high amounts of drying air [Jon and Kiang, 2006, Colak and Hepbasli, 2009a], because of the great amount of energy it requires. A more efficient cycle could presumably be achieved by condensing water from only a part of the air. This should reduce both the heat load on the heat pump and the dimensions of air heat exchangers. It should also increase the temperature differences in the system. The latter is because when only a part of the air is dehumidified, this part must be even drier than the entire stream if this was dehumidified, and this requires cooling to even lower temperatures.

A first idea was to dehumidify 20 % of the stream. The system would then need to condense $\frac{100\,\%}{20\,\%} = 5$ times more water than for the entire stream. The system must be dimensioned for air at saturated conditions, in other words for a temperature $T \approx 10\,°\mathrm{C}$ and relative humidity $\phi = 100$ %. This is point B in Figure 6.1, and the water content on dry basis is about 7.53 $\frac{\text{g vapour}}{\text{kg air}}$ at this condition. The desired water content, at point A, is about 6.24 $\frac{\text{g vapour}}{\text{kg air}}$. Condensing five times more water than for the entire stream required that

$$5 \cdot (7.53 - 6.24)\,\frac{\text{g vapour}}{\text{kg air}} = 6.45\,\frac{\text{g vapour}}{\text{kg air}}$$

was removed. This meant that after condensation there would remain

$$(7.53 - 6.45)\,\frac{\text{g vapour}}{\text{kg air}} = 1.08\,\frac{\text{g vapour}}{\text{kg air}}.$$

From the Mollier diagram, Figure 6.1, the air should then be cooled to about -16 °C. This is a way too low temperature partly because the pressure ratio in the heat pump would increase and make it ineffective, but mainly because the temperature is below the atmospheric freezing point of water, which will cause trouble with ice formation in the air cooler. Ice must be removed now and then, and in these periods, the cooler will not be available for cooling. Therefore, this should be avoided if possible, and it was concluded that 20 % was a too small part of the air stream.

Starting in the other end of the above calculation, the minimum condensation temperature was set to 1 °C. This gave an absolute humidity of about 4 $\frac{\text{g vapour}}{\text{kg air}}$ after condensation, starting from the saturated state at 10 °C and 100 % relative humidity. Hence

$$\frac{7.53 - 4.00}{7.53 - 6.24} \frac{\text{g vapour}}{\text{kg air}} \approx 2.74$$

times more water could then be condensed than by cooling to 7 °C, and would require that a fraction of $1/2.74 \approx 0.365$ of the air stream was cooled. Rounding up to be safe to avoid too low temperatures, the fraction was set to 37 %, and the system named HPSX37. Reheating to the initial enthalpy then required heating to about 18 °C.

However, the air to be dehumidified became less moist towards the end of the process (see Figure B.2), and then, one could remove sufficient amounts of water by an even smaller stream. Because the large amounts of air seemed to be an important reason for the high energy consumption, a system where the air to be dried was set as low as possible was implemented. The smallest air stream possible was found by controlling it so that it was always cooled to 1 °C. The system denoted HPSX1.

As explained before, the outlet condition for the air after a cooler will be between its inlet state and the saturated state at the cooler surface temperature in the Mollier diagram. Hence, if not saturated air enters a cooler, it can be dried *and* be drier than 100 % humidity at the exit. The required temperature for cooling a constant part of the flow, 37 % would then allow increasing temperatures in the cooler, whereas keeping it low would remove excessive moisture unless the stream was decreased, and this smaller air flow would allow sufficient dehumidification.

To give a fair energy comparison when the extra heat exchange with hot and cold process air were used, the air to air heat exchangers in HPSX100, HPSX37, HPSX1 should be equally effective. This meant that the smallest temperature difference occurring in the exchangers should be equal, and this was achieved in designing calculations. This reduced the load and size of the heat pump by a 25 % for HPSX37 and HPSX1 compared to BS and HPS, the reduction for HPSX100 was 15 %.

6.4.3 CO2S

The best of the systems with an ammonia heat pump was also designed with a CO_2 heat pump, to avoid the glycol circuits and their extra temperature lift. The CO_2 system, CO2S, was designed for cooling the process air to 1 °C and heating it to about 18 °C like explained in Section 6.4.2. The same, quite normal, temperature difference of 7 °C was assumed in all systems, to make energy comparison fair. Thus evaporation temperature was set to -6 °C and condensation at 25 °C.

6.4.4 CS

Compressing used, moist and cold, process air could make it possible to make water condense from it at higher temperatures. This could eliminate completely the need for a heat pump. These are quite expensive, complicated, have working fluids that often are toxic or detrimental for the environment and also contain an energy consuming compressor [Fornasieri et al., 2009]. Hence, one could perhaps leave only a compressor to do the same job.

Compression requires much work, and it was thus desirable to compress only a part of the air stream. The uncompressed stream would then probably need heating because the air temperature sinks during evaporation in the drying tunnel. A good solution would then be to heat it by using a part of the energy added to the other stream from the compressor. The rest of this energy must be removed by other means, for example by heat exchange with ground water.

Water has high heat transfer rates, and ground water has a fairly constant temperature of about 6 °C in Trondheim [TrønderEnergiAS, 2013], making refrigeration superfluous for cooling to temperatures down to $\approx 13\,^{\circ}\mathrm{C}$.

After cooling and condensation of water from the compressed stream, the stream should be throttled to its initial pressure and mixed with the uncompressed stream. The desired moisture content and temperature should then have been achieved. Throttling is normally as good as isenthalpic, and for an air stream, this would also mean it is as good as isothermal. To achieve the final process temperature after mixing the two streams, both streams were cooled or heated to 13 °C before they were mixed.

An alternative solution was of course to allow the streams to have different temperatures, but still ensure that the temperature would become 13 °C after mixing. This would not only complicate the process, but also make it less efficient, because of the following:

Either the uncompressed stream could have a too high temperature, meaning that the compressed stream must be cooled below 13 °C, which was likely to require refrigeration. Groundwater at 6 °C cannot cool down the air too much less than 13 °C in normal heat exchangers. This would especially be a problem if the compressed stream should be smaller than the uncompressed one, which was desirable in this work to minimize the compression work.

Or, the uncompressed stream could be cooled below 13 °C. The compressed stream should then have a higher temperature than 13 °C. This would work, but the entire idea behind this process was to cool down the compressed stream in order to make vapour condense. Less cooling would require a higher pressure to make a sufficient amount of water condense. Higher pressure would increase the energy consumption.

In addition to this, rejecting heat to the uncompressed process stream is a way to recover the heat, simultaneously cooling the compressed one. Therefore, as much heat as possible should be transferred to the uncompressed stream.

From the arguments above, achieving the final temperature for both streams before mixing was a goal in designing. Finding the amount of air that should be compressed, and to which pressure, was the first to be done.

Denoting the part of the *dry* air for compression by $\dot{m}_c$, the rest of the air stream by $\dot{m}_r$, and the absolute humidity before and after any condensation by x_{c1} and x_{c2}, a mass balance for the mixing gives

$$\dot{m}_c(1 + x_{c2}) + \dot{m}_r(1 + x_{c1}) = (\dot{m}_r + \dot{m}_c)(1 + x_{pro}),$$

where x_{pro} is the humidity wanted for the process. In other words, it is the absolute humidity at 13 °C and 68 % relative humidity, which was found to be $\approx 6.24\frac{\text{g vapour}}{\text{kg air}}$ in the Mollier diagram. Rearranging this one gets

$$\frac{\dot{m}_c}{\dot{m}_r} = \frac{x_{pro} - x_{c1}}{x_{c2} - x_{pro}}$$

and so choosing either $\dot{m}_c$ or x_{pro} determines the other one. Choosing $\dot{m}_c$, x_{c2} will given by

$$x_{c2} = \frac{\dot{m}_r(x_{pro} - x_{c1}) + \dot{m}_c x_{pro}}{\dot{m}_c}.$$

From the Mollier diagram, Figure 6.1, one can read $x_{c1,max} \approx 7.53\frac{\text{g vapour}}{\text{kg air}}$ at point B. The total air flow was about

$$\dot{m}_{tot} = \frac{p_{tot,1}\dot{V}\dfrac{M_a + M_w x_{c1}}{1 + x_{c1}}}{RT} = \frac{101250\frac{\text{J}}{\text{m}^3} \cdot 2.8\frac{\text{m}^3}{\text{s}} \cdot \dfrac{28.97 + 18.015 \cdot 0.00753}{1 + 0.00753}\dfrac{\text{kg}}{\text{kmol}}}{8314\,\frac{\text{J}}{\text{kmol K}} \cdot 283.15\text{K}} = 3.44\,\frac{\text{kg}}{\text{s}}$$

whereof

$$\frac{3.44\,\frac{\text{kg}}{\text{s}}}{1 + 0.00753} \approx 3.41\,\frac{\text{kg}}{\text{s}}$$

is air and $(3.44 - 3.41)\,\frac{\text{kg}}{\text{s}} = 0.03\,\frac{\text{kg}}{\text{s}}$ is water. The minimum mass flow to be compressed is one being dried to zero water content, thus

$$\left(\frac{\dot{m}_c}{\dot{m}_r}\right)_{min} \approx \frac{6.24 - 7.53}{0 - 6.24} \approx 0.21.$$

Drying the air to zero water content is ambiguous, but 50 % is realistic, thus setting $\dot{m}_c = 2 \cdot 0.21 \cdot \dot{m}_r = 2 \cdot 0.21 \cdot (3.41 - \dot{m}_c) \leftrightarrow \dot{m}_c = 1.01\,\frac{\text{kg}}{\text{s}}$ seemed appropriate. Making

$$x_{c2} = \frac{(3.41 - 1.01)\frac{\text{kg}}{\text{s}} \cdot (0.00624 - 0.00753)\frac{\text{g vapour}}{\text{kg air}}}{1.01\frac{\text{kg}}{\text{s}}} + 0.00624\frac{\text{g vapour}}{\text{kg air}} \approx 0.00317\frac{\text{g vapour}}{\text{kg air}}.$$

It should be $0.00624/2 = 0.00312$, but the error is due to round off. DYMOLA was allowed to adjust the flow so that the desired final conditions were achieved, and calculated this more accurately. The values calculated here were used for dimensioning, finding good and/or possible operational conditions and as appropriate start values.

Cooling the compressed stream to 13 °C, the condensation that occurred was likely to make the air close to saturated with water. Therefore the saturation pressure of water at 13 °C, divided the high total pressure, should correspond to the desired vapour fraction in the air.

Denoting molar fraction of water vapour by y_w, molar mass of water and air by M_w and M_a and using indices 1 and 2 about before and after condensation,

$$x_{c2} = \frac{M_w y_{w2}}{M_a y_{a2}} = \frac{M_w y_{w2}}{M_a(1 - y_{w2})}.$$

Hence, if $\dot{m}_c$ is chosen, x_{c2} is determined and y_{w2} is known.

The saturated vapour pressure at 13 °C is 1497 Pa, and as explained, the high pressure was set to satisfy $p_{w,sat@13} = p_{tot,2} y_{w2}$. The high pressure was considered constant. If not, backflow would occur. Hence, the cooling was assumed isobaric.

Therefore, choosing $\dot{m}_c$ also gives the high pressure. Eventually one could start in the other end, and choose the high pressure first. With the chosen value for $\dot{m}_c$ the following values were obtained:

$$x_{c2} = \frac{M_w y_{w2}}{M_a(1 - y_{w2})} \quad \Leftrightarrow$$

$$y_{w2} = \frac{x_{c,2} M_a}{M_w + x_{c,2} M_a} \approx \frac{0.00316 \, \frac{\text{kg vapour}}{\text{kg air}} \cdot 28.97 \, \frac{\text{kg air}}{\text{kmol}}}{18.015 \, \frac{\text{kg vapour}}{\text{kmol}} + 0.00316 \, \frac{\text{kg vapour}}{\text{kg air}} \cdot 28.97 \, \frac{\text{kg air}}{\text{kmol}}} \approx 5.056 \times 10^{-3}$$

and the high pressure was then found from

$$p_{w,sat@13} = p_{tot,2} y_{w2} \quad \Leftrightarrow \quad p_{tot,2} = \frac{p_{w,sat@13}}{y_{w2}} \approx \frac{1497 \, \text{Pa}}{5.056 \times 10^{-3}} \approx 3.0 \text{ bars.}$$

This value is a very appropriate pressure. It is not very high, neither is the mass flow very high. If it had been too high, another mass flow for compression should be chosen. It must be large enough to condense out sufficient amounts of water at a not too high pressure.

How the performance of this system varies with pressure was therefore of interest, and three different processes were considered. One was the described process with $\dot{m}_c = 1.01 \, \frac{\text{kg}}{\text{s}}$ and a pressure of ≈ 3.0 bars, one with a 15 % increase in mass flow, 1.16 $\frac{\text{kg}}{\text{s}}$, lowering the pressure to 2.5 bars and one with a 10 % smaller mass flow, 0.91 $\frac{\text{kg}}{\text{s}}$ making the highest pressure 3.5 bars.

6.4.5 ADS

Adsorbers attract some solute or component of a fluid mixture to its surface, thereby removing it from the stream. The component is then the adsorbate, removed from the adsorber material, the adsorbent. In this work the adsorbate was water vapour. The adsorbent must be removed from the stream now and then to remove the amount of adsorbed component. For water adsorption, this is done by a hot, drier air stream. The hotter, the faster desorption [Atuonwu et al., 2012b]. The adsorbent is then regenerated. See also Chapter 2 and Chapter 5.

In the adsorber system, ADS, the adsorber material was assumed to form a rotating disc, the most common arrangement [Atuonwu et al., 2013], contacting the process air on one side and a regeneration stream on the other, allowing continuous operation of the adsorber. Alternatively one could assume that the adsorber material was used for a while, then moved to another regeneration section, and then brought back again.

The drawback of an adsorber system is the regeneration stream. This is normally ambient air, heated and discharged after regenerating the adsorber, and this demands heat and rejects heated air to the atmosphere [Atuonwu et al., 2011b]. Because of this, [Atuonwu et al., 2011b] found it essential for high thermal efficiency to use a heat exchanger between the in- and outgoing regeneration streams, preheating the incoming and cooling the outgoing air, to recover some of the heat. This doubled the thermal efficiency and was done in this work.

Unlike heat pump systems, the drying efficiency for adsorption systems cannot exceed 100 % (see also Section 6.13, but an adsorber called Econosorb, produced by [AG,], combines the two, using a heat pump to heat the regeneration stream, taking heat from moist process air to heat the regeneration air. [AG,] claims that this system is more effective than both normal adsorbers and heat pump systems. This type was considered in this work.

There was one other important reason for considering Econosorb rather than another adsorber. AG reports that most of their adsorbers use regeneration air at 140 °C. This heats the adsorber wheel and thereby the process air to an unacceptably high temperature. This requires cooling in addition to the adsorber, which would require even more energy. Econosorb on the other hand, heats the process air (in °C) to

$$T_{out} = T_{in} + K \cdot 4 + 6.$$

This and other data were taken from a datasheet from [AG,] with specifications for Econosorb, which are given in Table 6.1. K is a correction factor, which was 0.8 for this process, obtained from the same sheet.

Econosorb uses a regeneration temperature of about 55 °C, but this lowers the regeneration potential of the regeneration air. To obtain a sufficiently high level of desorption at a lower temperature than other adsorbers, the amount of regeneration air must be larger. Higher air flow increases the fan power needed, but it was necessary, and also, a heat pump cannot deliver heat to temperatures as high as 140 °C.

Different adsorbers have different maximum water removal capacity, which were given

Name of unit	EF-102E
Process air $[\frac{m^3}{h}]$	4000
Regeneration air $[\frac{m^3}{h}]$	2000-8000*
Correction factor	0.8
Capacity after correction $[\frac{kg}{h}]$	24
Compression power [kW]	7.8
Total power [kW]	10.3

Table 6.1: Data for the chosen Econosorb unit are listed here, as reported by the producer [AG,] in their data sheet. This can be found at `http://docsio.net/doc/69821/econosorb---frigosorb`. *According to the specifications for this type, amount of regeneration air is controlled to keep the desired high pressure in the heat pump, and varies between 50 and 200 % of the process air depending on outdoor temperature.

for drying at 20 °C and 60 % humidity in the datasheet with specifications. Correction factors, K, were given to adjust for other conditions. The capacity was then the product of the given capacity and the correction factor. Assuming that the highest possible inlet moisture content of the process air is 7.53 $\frac{\text{g vapour}}{\text{kg air}}$, the final desired content 6.24 $\frac{\text{g vapour}}{\text{kg air}}$ and that the total amount of air is about 3.41 $\frac{\text{kg air}}{\text{s}}$, the maximum capacity need was found to be

$$(7.53 - 6.24) \times 10^{-3} \frac{\text{kg vapour}}{\text{kg air}} \cdot 3.41 \frac{\text{kg air}}{\text{s}} \cdot 3600 \frac{\text{s}}{\text{h}} \approx 15.8 \frac{\text{kg}}{\text{h}}$$

With a correction factor of about 0.8, the model one must chosen to have a sufficiently large capacity was EF-102E, with $0.8 \cdot 30 \frac{\text{kg}}{\text{h}} = 24 \frac{\text{kg}}{\text{h}}$ capacity. Data for this adsorber were used in this work, and its specifications are shown in Table 6.1.

As seen from Table 6.1, Econosorb withdraws and dries 4000 $\frac{\text{m}^3}{\text{h}}$ of the process air, which is about

$$\frac{4000 \frac{\text{m}^3}{\text{h}}}{2.8 \frac{\text{m}^3}{\text{s}} \cdot 3600 \frac{\text{s}}{\text{h}}} \approx 40\,\%$$

of the air stream in the drying process. Denoting the state of the wet process air by 1, the state after cooling by 2 and air after adsorption, before remixing by 3, the desired water content after desorption of 40 % of the process air must satisfy

$$0.6 x_1 + 0.4 x_3 = x_{pro} \tag{6.2}$$

or

$$x_3 = \frac{0.00624 \frac{\text{kg water}}{\text{kg air}} - 0.6 \cdot 0.00753 \frac{\text{kg water}}{\text{kg air}}}{0.4} \approx 0.00431 \frac{\text{kg water}}{\text{kg air}}.$$

The enthalpy of the dried air should be the same in as out, hence, looking in the Mollier diagram, Figure 6.1, it was desirable to reach an outlet temperature from the absorber of about 18 °C. From Section 6.4.5, Econosorb gives an outlet temperature of about 19.2 °C for the process air, which is close to the desired value.

When the process air has higher temperatures, is less moist, the adsorption load should be lower, yet the outlet temperature should increase according to Section 6.4.5. The producer reported that for this reason, the regeneration temperature is decreased for lower loads. The air streams are kept constant. It is uncertain how the regeneration temperature and mass flow affects Section 6.4.5, but it is likely that a lower regeneration temperature gives a process outlet temperature.

Relations between regeneration air mass flow, temperature and desorption potential and heating was unknown, but the given data show that its operation should be close to the desired one. Due to this lack in knowledge, the small difference between the calculated and desired values, and because the system was modelled close to the deadline, the following simplifying assumption was made: The adsorber wheel delivers the desired conditions for the outgoing stream, and the regeneration stream balances the need for energy. This assumption is somewhat rough, but the theoretical and desired conditions were quite similar, so it was assumed that with small adjustments, the real system can be operate as desired.

To ensure that this assumption did not make the regeneration temperature *too* low, the heat pump was controlled to keep the regeneration temperature *after* the adsorber wheel constant, thereby allowing the regeneration temperature to decrease with higher air flows and lower sorption loads, yet keeping it high. The regeneration stream always had to supply the energy required by the process air, thus at the lowest regeneration air flow, and highest process load, it had to reach 55.0 °C in order to deliver sufficient amounts of energy.

To find operational points for the heat pump and the degree of cooling for the process air, some calculations considering operation, performance, outdoor temperature (which varied from -17 to +30 °C, see Section 6.6), heat exchange and heat pump was necessary. This was an iterative process, and the reader might want to read Section 6.7 and Section 6.8 before reading the rest of this section.

The heat pump must heat up ambient air and the system must handle the worst case, which would be the lowest outdoor temperature, -17 °C. At this temperature, the flow of regeneration air should be about half of the dehumidified process air (see Table 6.1) or

$$\dot{m}_{H,a} = 0.5 \cdot 0.4 \cdot \dot{m}_{pro,a} = 0.5 \cdot 0.4 \cdot 3.41\,\frac{\text{kg air}}{\text{s}} \approx 0.682\,\frac{\text{kg air}}{\text{s}}.$$

The subscript H is used about the hot regeneration air. Denoting ambient and regeneration temperature by 1 and 4, the total heating demand to reach 55.0 °C would be

$$\dot{Q}_{H,a} = (T_4 - T_1)\dot{m}_{H,a}c_{p,a} \approx (55 - 17)\,°\text{C} \cdot 0.682\frac{\text{kg}}{\text{s}} \cdot 1.007\frac{\text{kJ}}{\text{kg K}} \approx 49.45\ \text{kW}.$$

The maximum amount of heat taken from the process without reaching the freezing point is about

$$\dot{Q}_{max} = \dot{m}_{a,pro}(h_{T=10,\phi=100\%} - h_{T=1,\phi=100\%}) \approx 0.4 \cdot 3.41\,\frac{\text{kg air}}{\text{s}} \cdot (29.0 - 11.0)\frac{\text{kJ}}{\text{kg}} = 24.55\ \text{kW}.$$

A heat pump supplies more heat than it rejects, but the heat from the process is far from sufficient, and would give a very low COP if it could be realized at all. In addition, the process air should not be cooled as much as this maximum, because this was found in Section 6.4.2 to be more than sufficient to dehumidify the entire stream without the adsorber. However, if the hot regeneration air exiting the adsorber wheel is still warmer than -17 °C, a realization of the system would not let this air out without heat exchange with the incoming air, reducing the heating need.

To find the temperature of the regeneration air after the wheel, one should consider how much heat must be transfered in it. The adsorber must transfer heat from the hot air stream to the process air. The net heat supplied to the process stream must equal the latent heat for water removed in the wheel. The maximum amount of water to be removed was

$$\Delta x_{pro}\dot{m}_{a,pro,tot} \approx 0.00129\frac{\text{kg vapour}}{\text{kg air}} \cdot 3.41\frac{\text{kg air}}{\text{s}} \approx 0.0044\frac{\text{kg water}}{\text{s}}.$$

Accordingly, the highest net heat supply needed would be

$$\dot{Q}_w = \Delta x_{pro}\dot{m}_{a,pro,tot}h_{fg} \approx 0.00129\frac{\text{kg water}}{\text{kg air}} \cdot 3.41\frac{\text{kg air}}{\text{s}} \cdot 2447\frac{\text{kJ}}{\text{kg}} = 10.76 \text{ kW}.$$

Some of the heat would be recovered by condensation in the heat pump however, so the net supply should always be lower than this.

Because Econosorb cools the process air before adsorption, this energy must also be supplied back by heat exchange with the wheel. Hence, all heat for evaporation *in the adsorber* must be supplied by compressor, because all the «free heat» in the heat pump is taken from the process air and must be given back. This is why the adsorber cannot achieve efficiencies above 100 % without utilizing extra heat recovery by heat pump condensation is used. The heat pump recovers the latent heat and lowers the amount of water that must be removed in the adsorber, and thereby the net heat supply.

An assumption regarding how much the process air should be cooled was necessary to continue. Assuming cooling to 5 °C gives a final air enthalpy of 18.0 $\frac{\text{kJ}}{\text{kg air}}$, starting from 29.0 $\frac{\text{kJ}}{\text{kg air}}$ before cooling. This rejects about

$$0.4 \cdot 3.41\frac{\text{kg air}}{s}(29.0 - 18.0)\frac{\text{kJ}}{\text{kg air}} = 15.00 \text{ kW}.$$

After cooling to 5 °C, the water content is 0.0053, and removed water is

$$0.00753\frac{\text{kg water}}{\text{kg air}} - 0.0053\frac{\text{kg water}}{\text{kg air}} \approx 0.0030\frac{\text{kg water}}{\text{s}},$$

which lowers the net heat supply, or compression power, to about $\frac{4.4-3.0}{4.4} \cdot 10.76 \text{ kW} = 3.42 \text{ kW}$. The outlet temperature for the regeneration air is then

$$T_5 = T_4 - \frac{\dot{Q}_{tot}}{\dot{m}_{H,a}c_{p,a}} = 55.0°\mathrm{C} - \frac{(3.42+15.00)\ \mathrm{kW}}{0.682\frac{\mathrm{kg}}{\mathrm{s}} \cdot 1.007\frac{\mathrm{kJ}}{\mathrm{kg\ K}}} \approx 28.2\,°\mathrm{C}$$

This is more than sufficient to be used in a heat exchanger with the other stream at -17 °C. Assuming heat recovery and the a temperature difference of $\Delta T = 7\,°\mathrm{C}$ as in the other systems, the outgoing stream must be cooled to -10 °C or the cold heated to 21.2 °C. Due to possible condensation, the first might not be possible with $\Delta T_{min} = 7\,°\mathrm{C}$, so the heat load was found from

$$\dot{Q} = \Delta T \dot{m}_{H,a}c_{p,a,in} = (21.2-(-17))°\mathrm{C}\, 0.682\frac{\mathrm{kg}}{\mathrm{s}} \cdot 1.007\frac{\mathrm{kJ}}{\mathrm{kg\ K}} = 26.23\ \mathrm{kW}.$$

The temperature for the stream being cooled depends on its water content. In this work, a constant relative humidity was used, which gives a realistic increase in moisture content wiyth outdoor temperature. At -17 °C there would then be about 1 $\frac{\mathrm{g\ vapour}}{\mathrm{kg\ air}}$ in the incoming regeneration air. The moisture content for the regeneration air after adsorption is then

$$x_1 + \frac{\Delta m_{w,ads}}{\dot{m}_{H,a}} = 0.001\frac{\mathrm{kg\ water}}{\mathrm{kg\ air}} + \frac{0.4(0.00753-0.00531)\frac{\mathrm{kg\ water}}{\mathrm{kg\ air}} \cdot 3.41\frac{\mathrm{kg}}{\mathrm{s}}}{0.682\frac{\mathrm{kg}}{\mathrm{s}}} = 0.00303\frac{\mathrm{kg\ water}}{\mathrm{kg\ air}}$$

which at 28.2 °C, gives an enthalpy of about 36 $\frac{\mathrm{kJ}}{\mathrm{kg\ air}}$. If cooled by $\frac{26.23\ \mathrm{kW}}{0.682\frac{\mathrm{kg}}{\mathrm{s}}} = 38.46\frac{\mathrm{kJ}}{\mathrm{kg}}$ the air gets an outlet enthalpy and temperature from the heat exchanger of $-2.46\frac{\mathrm{kJ}}{\mathrm{kg}}$ and about -7 °C. These values can all be found in Figure 6.1.

Eventually, to avoid ice in the heat exchanger, one should design for outlet air at 1 °C, thus

$$\dot{Q} = \dot{m}_{H,a}(h_{T=28.2,x=3.03} - h_{T=1,\phi=100\%}) \approx 0.682\frac{\mathrm{kg}}{\mathrm{s}}(36-11)\frac{\mathrm{kJ}}{\mathrm{kg\ air}} = 17.05\ \mathrm{kW},$$

and the incoming stream is then heated from $-17\,°\mathrm{C}$ to

$$-17\,°\mathrm{C} + \frac{17.05\,kW}{0.682\frac{\mathrm{kg}}{\mathrm{s}}1.007\frac{\mathrm{kJ}}{\mathrm{kg\ K}}} = 7.8\,°\mathrm{C}.$$

The heat exchanger would then have

$$\Delta T_{lm} = \frac{(28.2-7.8)\,°\mathrm{C} - (1-(-17))\,°\mathrm{C}}{\ln(28.2-7.8) - \ln(1-(-17))} = 19.2\,\mathrm{K}$$

and UA $= \frac{17.05\ \mathrm{kW}}{19.2\mathrm{K}} \approx 890\frac{\mathrm{W}}{\mathrm{K}}$. The heat pump must then supply about

$$(55-7.8)\,°\mathrm{C} \cdot 0.682\frac{\mathrm{kg}}{\mathrm{s}} \cdot 1.007\frac{\mathrm{kJ}}{\mathrm{kg\ K}} = 32.42\ \mathrm{kW},$$

which is still more than twice of what was taken from the process air, and this would mean that the rest of the heat must be supplied by the compressor motor, which is not a very energy efficient solution. Hence it seemed this system could not be realized without auxiliary heat, even when the heat exchanger was included. However, the choice to cool to 5 °C determined the power need, so it was investigated if the power need could be reduced by choosing another temperature.

The same calculations assuming the process air was cooled to 7 °C were performed. The water content after cooling was then 6.24 $\frac{\text{g vapour}}{\text{kg air}}$. The amount of water removed in the heat pump was $0.00129\frac{\text{kg vapour}}{\text{kg air}} \cdot 3.41\,\frac{\text{kg}}{\text{s}} \cdot 0.4 = 0.00176\frac{\text{kg vapour}}{\text{s}}$. An adsorber must supply $10.76\text{ kW} \cdot (4.4 - 1.76)/4.4 = 6.46\text{ kW}$ for evaporation, plus the removed heat of about $(29.0 - 22.5)\frac{\text{kJ}}{\text{kg air}} \cdot 0.4 \cdot 3.41\frac{\text{kg air}}{\text{s}} = 8.87\text{ kW}$.

The temperature after desorption must be

$$55.0\,^{\circ}\text{C} - \frac{6.46 + 8.87\text{ kW}}{0.682\frac{\text{kg}}{\text{s}} \cdot 1.007\frac{\text{kJ}}{\text{kg K}}} = 32.7\,^{\circ}\text{C}.$$

The heat load for the heat exchanger can then be

$$\dot{Q} = \dot{m}_{H,a}(h_{T=32.7,x=3.58} - h_{T=1,\phi=100\%}) \approx 0.682\frac{\text{kg}}{\text{s}} \cdot (42 - 11)\frac{\text{kJ}}{\text{kg}} = 21.14\text{ kW},$$

which is better than for cooling to 5 °C. The incoming air is heated to

$$-17\,^{\circ}\text{C} + \frac{21.14\text{ kW}}{0.682\frac{\text{kg}}{\text{s}} \cdot 1.007\frac{\text{kJ}}{\text{kg K}}} = 13.8\,^{\circ}\text{C},$$

and the heat pump must supply 49.46 kW - 21.14 kW = 28.32 kW. Comparing the two cases calculated, one could either:

- reject 15.00 kW from process air and heat by 32.42 kW, plus 17.05 kW in heat exchanger, $\text{COP} = \frac{32.42}{32.42-15.00} = 1.86$, or
- reject 8.87 kW from the process and heat by 28.32 kW, plus 21.14 kW in heat exchanger, $\text{COP} = 1.46$.

It seems from the numbers above, that less cooling is better. Resulting in the lowest heat load and the highest heat exchange recovery. However, the heat pump cannot supply sufficient heat during the coldest days unless its operation is bad enough to obtain a low very COP. The economics related to a heat pump depend on how much of the heat is «free». The real power demand is 32.42 kW - 15.00 kW = 17.42 kW when cooling to 5 °C and 28.32 kW - 8.87 kW = 19.45 kW when cooling to 7 °C.

Concluding that cooling to a lower temperature improves the energy efficiency, as more latent heat is then recovered, it was decided to design for cooling to 5 °C. The peak loads in heating demand had to be handled by auxiliary heating. This is actually usual when heat pumps are used for heating, they are often dimensioned for about 60 % of peak load [Haukås, 2010], and at higher outdoor temperatures, it would no longer be necessary.

A lower temperature than 5 °C was not chosen, even though it probably would decrease energy demands even further. The temperature should be as low as possible, but there was a lower limit. Cooling to 1 °C would make the system similar to HPSX37, HPSX1 and CO2S, and the adsorber superfluous. The entire purpose was to se how the system could manage without the low temperature cooling. Also, to avoid ice in the evaporator, and yet avoid an extremely small temperature difference, evaporation at 0 °C and cooling to 5 °C were chosen.

Using auxiliary heat, the heat pump had to supply as much heat as possible until the outdoor temperature became high enough for the electric heater to be turned off. An expression for this should be developed. Therefore, the maximum heat supply from the heat pump had to be estimated.

One could obtain a COP around 3.76 with the heat pump chosen and described in Section 6.7. A heat pump could then supply up to $\dot{Q}_{heat}$ given by ($Q_{cool} = 15.00$ kW)

$$\mathrm{COP} = \frac{\dot{Q}_{heat}}{\dot{Q}_{heat} - \dot{Q}_{cool}} \approx 3.76 \qquad \Leftrightarrow \qquad \dot{Q}_{heat} = \frac{\dot{Q}_{cool}\mathrm{COP}}{\mathrm{COP}-1} = 20.43\ \mathrm{kW}$$

as long as the outdoor temperature is low. Denote the states for the regeneration air by 1 at ambient, 2 after heating in exchanger, 3 after heat pump heating, 4 after electrical heating and 5 after the adsorber wheel. The electrical heating was no longer necessary when the temperature after the heat exchanger, T_2, reached

$$T_2 = T_4 - \frac{\dot{Q}_{heat}}{\dot{m}_{H,a}c_{p,a}} = 55.0\,^\circ\mathrm{C} - \frac{20.43\ \mathrm{kW}}{0.682\frac{\mathrm{kg}}{\mathrm{s}} \cdot 1.007\frac{\mathrm{kJ}}{\mathrm{kg\ K}}} = 25.2\,^\circ\mathrm{C}$$

The outdoor temperature when this occured was found using the above calculated UA value. The temperature after wheel was controlled to be constantly 28.2 °C. Assuming similar heat capacities in and out (not far from the truth) gives:

$$T_1 = T_2 - \frac{UA(T_5 - T_2)}{\dot{m}_{H,a}c_{p,a}} \approx 25.2\,^\circ\mathrm{C} - \frac{890\frac{\mathrm{W}}{\mathrm{K}} \cdot (28.2 - 25.2)\ \mathrm{K}}{0.682\frac{\mathrm{kg}}{\mathrm{s}} \cdot 1007\frac{\mathrm{J}}{\mathrm{kg\ K}}} = 21.3\,^\circ\mathrm{C}$$

This was a very high value, meaning that auxiliary heat was necessary nearly all the time. It is therefore uncertain how well this model described reality. This high need for electrical heat made the power need in this system high. It could also be even worse than calculated here, because no increase in mass flow was assumed in calculating it. Theoretically, the electrical heat supply should be $\dot{Q}_{heat}$ satisfying

$$T_2 + \frac{\dot{Q}_{HP} + \dot{Q}_{heat}}{\dot{m}_{H,a}c_{p,a}} = T_4$$

$$T_5 + \frac{\dot{Q}_{cool} + \Delta m_w h_{fg}}{\dot{m}_{H,a}c_{p,a}} = T_4$$

$$\Rightarrow \dot{Q}_{heat} = \dot{m}_{H,a}c_{p,a}(T_5 - T_2) + \dot{Q}_{cool} + \Delta m_w h_{fg} - \dot{Q}_{HP} \tag{6.3}$$

where $\dot{Q}_{cool} = 15.00$ kW, $\dot{Q}_{heat} = 20.43$ kW, $T_5 = 28.2$ °C and the other were measurable variables in the model. The heat from heat leakage explained in Section 6.11 was also added, as this also introduced a heating need. Unfortunately, using Equation 6.3 resulted in excessive cooling of the air when it became drier, making the outlet air too dry and the expression was adjusted to include $1.6 \cdot (3000\text{ W} - \dot{Q}_w)$. This is further discussed in Appendix B and Appendix D

6.5 PRESSURE DROP

In a system with fluid flow in pipes, there will be pressure drop, and the power consumption of the fans was presumably of significance for the overall energy consumption. In addition, flow through components like heat exchangers makes the pressure fall. How large pressure drop there would be in the system depends on the size and length of the pipes, the number of 90 ° bends and U-bends, whether the flow regime is turbulent or laminar and how smooth the walls are [Çengel and Cimbala, 2010]. Due to lack of data on pipes and air distribution system, a theoretical pressure drop for the air flow was made from some, hopefully, reasonable assumptions.

According to Professor Trygve M. Eikevik, a reasonable air velocity in the distribution system would be 3-4 $\frac{\text{m}}{\text{s}}$. This corresponds to an inner pipe diameter between 0.945 and 1.090 m in circular pipes, and 1 m was chosen, giving a velocity of 3.57 $\frac{\text{m}}{\text{s}}$. Furthermore, after having visited a real plant and seen what a large area it covered, it was assumed that the length the air had to be transported was around 100 m both to and from the drying chamber, 200 m in total.

The air flow in such a system is likely to be turbulent, because of fans, bends, heat exchangers and the long flow path. However, to know this for sure, a brief calculation finding the Reynolds number was performed. All information in this analysis was found in [Çengel and Cimbala, 2010]. A Reynolds number below 2300 indicates laminar flow (inserting disturbances in the flow can still create turbulence), and above 4000 the flow is turbulent. Between, the flow is in a transient state between the two.

The Reynolds number, defined in Equation 6.4, varies with pipe diameter and air properties, and thus with temperature and pressure. The two latter changed in the modelled process, and so the Reynolds number also changed. Therefore, it was decided to find a range that will always contain the Reynolds number, by finding the highest and lowest possible values for the properties. Data is taken from [Çengel and Cimbala, 2010, p. 930].

The temperature in the air distribution system should be between 7 and 13 °C as seen in the Mollier diagram, Figure 6.1, but to be sure, and allow a slight variance, 5 and 15 °C was used. At 5 °C, the dynamic viscosity is $1.754 \times 10^{-5} \frac{\text{kg}}{\text{m} \cdot \text{s}}$ and at 15 °C it is $1.802 \times 10^{-5} \frac{\text{kg}}{\text{m} \cdot \text{s}}$. The pressure might vary with a few percent, say $p = 101{,}250\,\text{Pa} \ \pm 1{,}250$ Pa. From this, the density ρ would be between

$$\rho_{min} = \frac{p_{min} M_a}{RT_{max}} = \frac{100,000 \frac{\mathrm{N}}{\mathrm{m}^2} \cdot 28.97 \frac{\mathrm{kg}}{\mathrm{m}^3}}{8314 \frac{\mathrm{Nm}}{\mathrm{kg\ K}} \cdot 288\mathrm{K}} = 1.210\ \frac{\mathrm{kg}}{\mathrm{m}^3}$$

and

$$\rho_{max} = \frac{p_{max} M_a}{RT_{min}} = \frac{102,500 \frac{\mathrm{N}}{\mathrm{m}^2} \cdot 28.97 \frac{\mathrm{kg}}{\mathrm{m}^3}}{8314 \frac{\mathrm{Nm}}{\mathrm{kg\ K}} \cdot 278\mathrm{K}} = 1.285\ \frac{\mathrm{kg}}{\mathrm{m}^3}$$

The Reynolds number is

$$\mathrm{Re} = \frac{\rho v d}{\mu} = \frac{4\rho \dot{V}}{\pi d \mu}, \tag{6.4}$$

where d is diameter, v velocity, μ dynamic viscosity and $\dot{m}$ and $\dot{V}$ the mass and volume flows. This gave a range of Reynolds numbers from

$$\mathrm{Re}_{min} = \frac{4 \cdot 1.210 \frac{\mathrm{kg}}{\mathrm{m}^3} \cdot 2.8 \frac{\mathrm{m}^3}{s}}{\pi \cdot 1\ m \cdot 1.802 \times 10^{-5} \frac{\mathrm{kg}}{\mathrm{m\ s}}} = 239,386$$

to

$$\mathrm{Re}_{max} = \frac{4 \cdot 1.285 \frac{\mathrm{kg}}{\mathrm{m}^3} \cdot 2.8 \frac{\mathrm{m}^3}{\mathrm{s}}}{\pi \cdot 1\ \mathrm{m} \cdot 1.754 \times 10^{-5} \frac{\mathrm{kg}}{\mathrm{m\ s}}} = 261,181$$

The possible range of numbers is seen to be well above both 2300 and 4000, the values for transition to turbulence and fully turbulent conditions. Because of the turbulent regime, pressure drop was calculated from the combination of equations 8.21 and 8.59 for turbulent flow in [Çengel and Cimbala, 2010, p. and 366]. This gave the pressure drop

$$\Delta p = \left(\sum_i K_i + f \frac{L}{d} \right) \frac{\rho v^2}{2} = \left(\sum_i K_i + f \frac{L}{d} \right) \frac{8 \dot{m} \dot{V}}{\pi^2 d^4} \tag{6.5}$$

where K_i gives the pressure drop for different bends, with values found in table 8.4 in [Çengel and Cimbala, 2010, p. 368]. L is the pipe length and f the Darcy-Weisbach friction factor, which is given for turbulent flow in [Çengel and Cimbala, 2010, Eq. 8.50, p.357] as

$$\frac{1}{\sqrt{f}} = -2.0 \lg \left(\frac{\epsilon/d}{3.7} + \frac{2.51}{\mathrm{Re}\sqrt{f}} \right).$$

Here ϵ is here the height of the roughness on the pipe wall and lg is the Brigg's logarithm (with ten as the base number). Unfortunately, DYMOLA would not use this implicit expression and ϵ/d was unknown. The Petukhov equation for smooth pipes, where $\epsilon/d = 0$ and given by [Çengel and Cimbala, 2010, eq. 8.21, p.522] is valid for turbulent flows where $\mathrm{Re} < 5 \times 10^6$, but this expression did not work either. An approximate, explicit expression for f, valid in the relevant range of Reynolds numbers was therefore developed. This was

$$f = 0.011 + \frac{1400}{1.3\mathrm{Re} + 20000}. \tag{6.6}$$

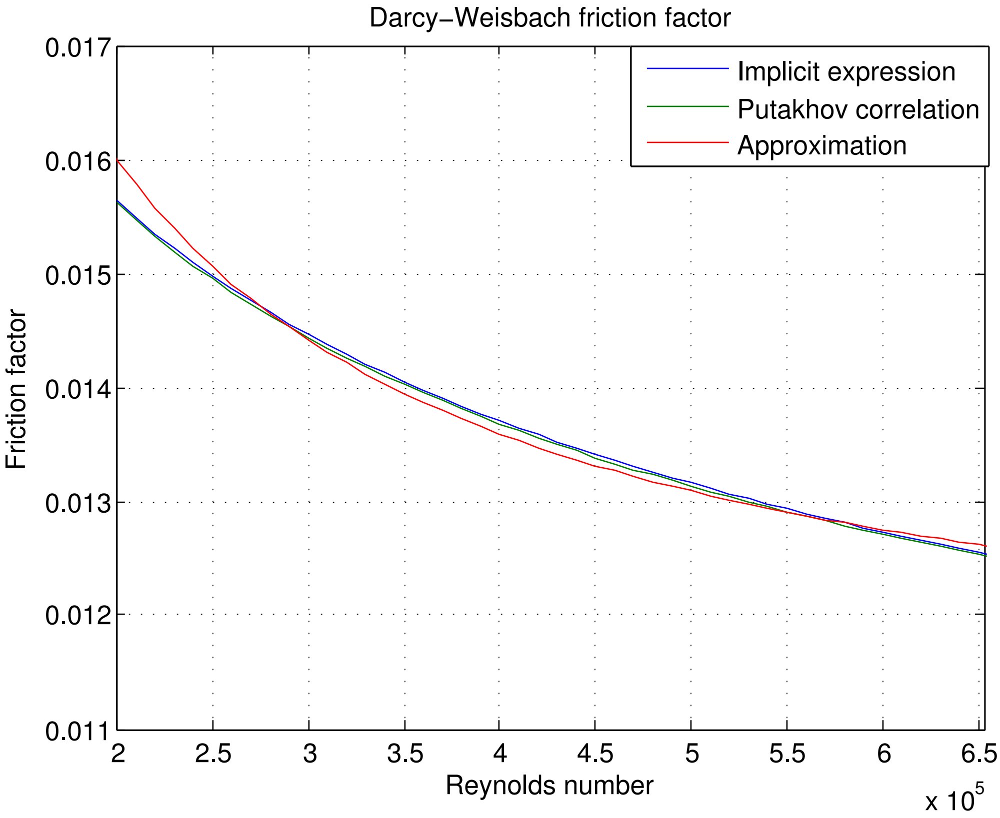

Figure 6.2: Friction Factor as a function of Reynolds number, by two correlations given by Darcy-Weisbach and Petukhov in [Çengel and Cimbala, 2010], and one self-made approximation

It was based on the assumption that the term $\epsilon/d = 0$. This term does not enhance f significantly, especially when the diameter is large. Yet, ignoring it completely is probably an error, hence f was increased with 5 % to account for this. From Example 8-3 in [Çengel and Cimbala, 2010, p. 360-361], the different values obtained by setting ϵ/d to a realistic value or setting it to zero were 0.0169 and 0.0172. The enhancement of f due to rough walls for this case was then 1.6 %, so 5 % seemed to be a safe margin.

Equation 6.6 is plotted together with the correlations from textbooks in Figure 6.2. They are shown for a much larger range of Reynolds numbers than necessary. This is because Equation 6.6 was developed at a point in the work when the pipe diameter was still uncertain. It was assumed to be between 0.4 and 1.2 m, which gave the range $199,488 \leq \text{Re} \leq 652,953$ to which Equation 6.6 was fitted. Because the curve was quite good, it was kept also after the adjustment of the range. Equation 6.6 is 0.17 % too high at Re = 240,000, which is its highest deviation in the final, relevant range of Reynolds numbers. The highest deviation in the figure is 2.3 % at Re = 199,488.

Bends are likely to cause extra pressure drops, and therefore, pipes should be made with as few of them as possible. Six 90 ° flanged bends were assumed in the base and heat pump system. The K-value for such a bend is 0.3 [Çengel and Cimbala, 2010, table 8.4, p. 368]. For other systems, additional bends were assumed, depending on the system sketch compared to that of the basic system. The compression system had two extra bends and two U-bends and the heat pump with heat exchanger had two extra plus a U-bend, each with a K-value of 0.2. Total pressure drop in pipes and bends was then calculated from Equation 6.5.

Pressure drops across heat exchangers in DYMOLA could be modelled as zero, constant or by a built-in relation in DYMOLA. The options differed for liquids and gases. For air, the Haaf model in DYMOLA was normally used, but in air-to-air heat exchangers, this was not an available option. The pressure drop was then calculated from the correlations above, using the hydraulic diameter for the heat exchangers, and the resulting pressure drop was used as a constant value.

The pressure drops for glycol and water were assumed to be quadratic in mass flow, in accordance with theory, as seen in Equation 6.5, and nominal values were taken from [Car, 2013]. From this, three values were read and used, these were among others 8 kPa pressure drop for a flow of 1.2 $\frac{\text{kg}}{\text{s}}$ and 50 kPa for 3.0 $\frac{\text{kg}}{\text{s}}$.They all followed the equation

$$\Delta p = 5.556\dot{m}^2 \text{ [kPa]}$$

This was applied to both water and glycol streams. The data was really for flows in l/s, but for both water and glycol $1\,\text{l} \approx 1\,\text{kg}$, with an error of less than 5 %.

Pressure drops in heat pumps were neglected because these are likely to be very small compared to other pressure drops and because of the small mass flow compared to other flows (see Section 6.7). In addition, the efficiency of the compressor was uncertain, and this error probably had a much larger impact on the system, making the pressure changes in the heat pump insignificant in comparison.

Files with calculation and plotting of the friction factor and the file to create pressure drop in DYMOLA are listed in an overview in Appendix E, where more information on this can be found.

6.6 OUTDOOR TEMPERATURE

The outdoor temperature will affect the energy consumption of the plant. Excess heat from heat pumps is for example normally dumped to the surroundings, and so the temperature in the heat pumps must be high enough to manage this. To model the outdoor temperature, and get results that could represent average values for energy use throughout a whole production year, measured temperature data for a whole year were used.

The values were found at `yr.no`, and were measured at Voll, Trondheim, Norway, from fourth of February 2014 to third of February 2015. Measurements included both minimum and maximum temperatures for each date. These 730 data were then sorted from the lowest to the highest value in Excel to obtain a smooth temperature profile, as in reality.

A MATLAB script was used to find a mathematical expression for the curve. The data could not, as far as the author knows, be imported to DYMOLA. An approximation was therefore made by a combination of assessing the curve shape and trying and failing. MATLAB has own tools to approximate curves by polynomials. These fitted the middle of the curve quite well when polynomials of third to tenth degree were used, but had high deviation at the lowest and highest temperatures.

It was noticed that the measured profile was similar to the tangent function, but an equation based on this became too flat. To improve this, the equation was multiplied first by a linear expression and then by a part of a cosine curve. The latter result was promising, and adjusting parameters gave the curve shown in Figure 6.3. The mathematical expression was

$$T = 7 + \left[18\cos\left(\frac{t}{120} + 4.2\right) + 19\right] \cdot \left[0.2\tan(0.0077t + 300.10)\right]\ [^o\mathrm{C}] \tag{6.7}$$

when the time t is given in days starting at day one and ending at 365.5 (because there were two measurements for each day). This expression was used in DYMOLA. Because DYMOLA counts time in seconds, the t in Equation 6.7 was replaced by $364.5\frac{t}{t_{tot}} + 1$, where t_{tot} is total

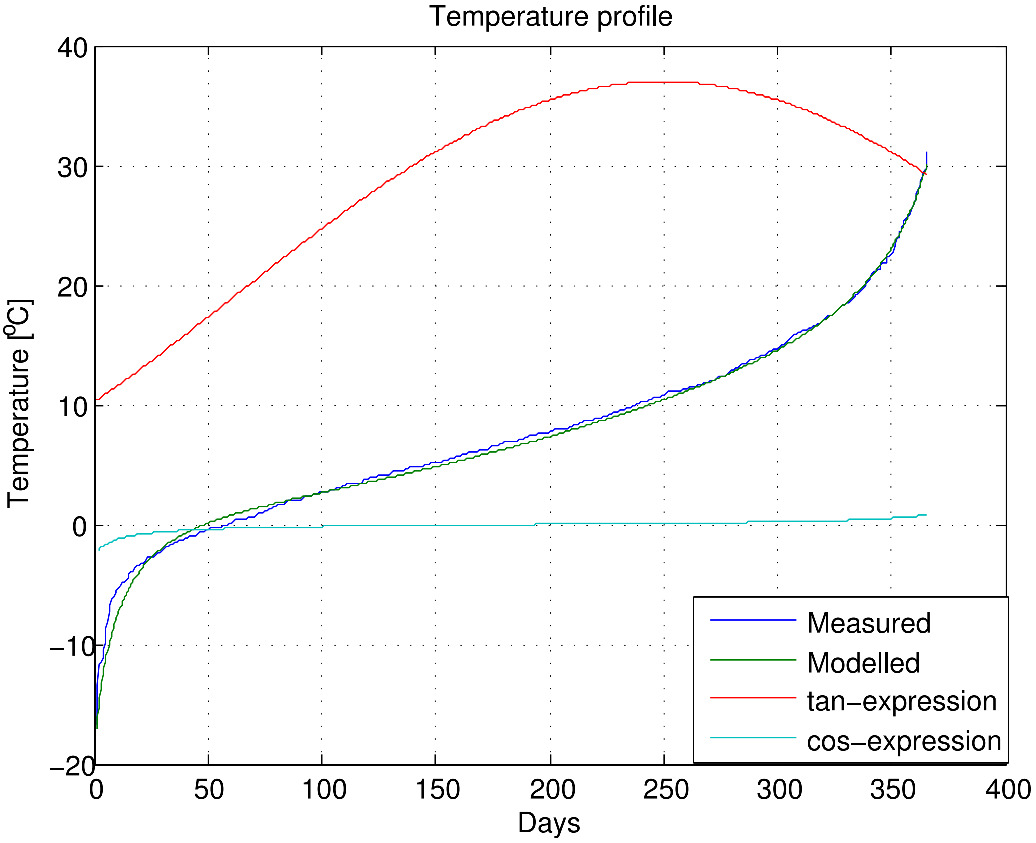

Figure 6.3: Measured and modelled temperature profile, the modelled expression is the product of the tangent and cosine expressions. Measured data was taken from yr.no from fourth of February 2014 to third of February 2015 in Trondheim.

time for the simulation, in seconds. DYMOLA starts time from zero, so one was added to the seconds to be consistent.

The error of this approximation, measured as

$$\sqrt{\frac{(T_{measured} - T_{modelled})^2}{730 - 8}},$$

was only 0.5566. The denominator was $730 - 8 = 722$ because eight parameters were adjusted to fit the expression based on 730 data.

6.7 HEAT PUMP

Heat pumps remove heat from one low temperature reservoir, and deliver heat to another reservoir with higher temperature. This is done by circulating a working fluid between the hot and cold sides. Compressing the fluid increases its temperature, allowing it to deliver heat to a high temperature, whereas expanding it after this heat rejection at high temperature decreases the temperature.

Because of the heat delivery at the high temperature, the fluid contains less thermal energy after expansion than before compression. It can then receive heat at a low temperature, cooling down its environment, before it is compressed again. Compression adds extra energy to the cycle, and therefore, a heat pump always delivers more heat than it rejects.

To make the heat transfer effective, the working fluid is chosen to be one that goes through a phase change at the relevant temperatures. Heat is then transferred at a fairly constant temperature, maintaining a high temperature difference during heat transfer, and the latent heat makes the energy transfer large. The heat exchanger to remove heat by evaporation is called an evaporator, and the heat exchanger to deliver heat by condensation a condenser.

Some of the heat added by compressor often makes the fluid superheated, and thus, a part of the heat rejection from the heat pump is actually gas cooling. If an own heat exchanger is used for this purpose, it is called a desuperheater. This was relevant in HPS, CO2S and all HPSX systems, and as mentioned, an example of what the heat pumps looked like in DYMOLA can be seen in Figure B.46.

Performance of heat pumps is often measured in terms of the amount of useful heat delivered, divided by the power input, called COP or coefficient of performance. If the heat is transferred to a hot reservoir at temperature T_H and the evaporation takes place at the cold reservoir temperature T_C, an ideal cycle that only delivers useful heat transfer as cooling would have

$$\text{COP}_{ideal} = \frac{T_C}{T_H - T_C} > 1$$

and for a pump that only delivers useful heat transfer as heating it would be

$$\text{COP}_{ideal} = \frac{T_H}{T_H - T_C} > 1 \tag{6.8}$$

If both heat rejection at low temperature *and* heat supply at a higher temperature are utilized, the COP_{ideal} would be the sum of these.

Losses in compressor and expander, losses due to the required temperature difference between the working fluid and its surroundings, in addition to pressure drop, superheating and other losses lower the COP to about half of the ideal. Yet, the real COP follows the ideal expression almost linearly. Hence, the temperature lift $(T_H - T_C)$ is of major importance for the performance. A smaller temperature difference gives higher COP. This related to that the pressure difference the compressor must create increases with the temperature difference.

In the considered drying process, the temperature differences are not too big, and a simple, one-stage compression heat pump with an internal heat exchanger was used (more stages of compression lowers energy use at high pressure ratios). In all but two systems, the working fluid was ammonia because this is a usual, highly efficient working fluid, and one of the few which are not forbidden because of environmental concerns.

The major drawback with ammonia is that it is toxic, and an extra medium to transfer heat between the heat pump and food processes was necessary. This secondary fluid was glycol. An extra temperature difference and some temperature glide for the glycol was then necessary. This enhanced the temperature difference for the ammonia cycle and thereby the overall energy consumption.

Another working fluid which has shown good performance, is natural, non-toxic, non-flammable, with no ozone depleting potential and, relative to many other refrigerants, hardly any global warming potential is CO_2 [Fornasieri et al., 2009]. This working fluid becomes increasingly popular [Fornasieri et al., 2009] and does not need an extra glycol system and extra temperature differences. Therefore, it was decided to model the best performing of the ammonia systems with CO_2 as well, to see if and which improvement this could give.

In BS, HPS and HPSX100, the process air required cooling to 7 °C and heating to 13 °C. Assuming a minimum temperature difference of ≈ 7 °C and a temperature glide of ≈ 3 for the glycol, the ammonia heat pump was designed for about -10 °C on the low pressure side and +30 on the high pressure side. This corresponded to pressures of 2.9 bar and 11.67 bars.

In HPSX37, HPSX1 and CO2S the lowest air temperature was 1 °C. Cooling the air to 1 °C instead is 6 °C cooler than in the systems where the entire stream was cooled. Assuming the same temperature differences in all systems to give a fair energy comparison, the new evaporation temperature should be $(-10 - 6)\,°\text{C} = -16\,°\text{C}$, corresponding to 2.26 bars for ammonia.

The highest air temperature increased to 18.1 °C for the systems dehumidifying only a part of the stream, as the dried air was to be remixed with cold, saturated air at 10 °C. In

Figure 6.1, it is clear that they both should lay on the same enthalpy line, as both point A and B are on the same line, and at a water content of about 4 $\frac{\text{g vapour}}{\text{kg dry air}}$, the temperature on this enthalpy line is about 18 °C. The highest pressure of ammonia then became 12.38 bars, corresponding to 32.1 °C.

In the same way, the CO_2 system was designed for cooling and heating the air to 1 and 18.1 °C, with the same temperature difference as the ammonia systems, 7 °C. Resulting operation pressures became 29.63 and 64.34 bars, or 80.07 bars when the outdoor air reached its peak temperature.

With -6 °C on the cold side in the air cooler, there is a concern if there will be ice formation in the glycol cooler or CO_2 evaporator. In this study, the focus was on the energy consumption, and this feature ignored, but if one of the systems in this work this work should be realized, then this must be considered. Energy consumption would then be a part of a larger picture.

A condition that *could* be a problem with CO_2 was that its critical point lies at $\approx 31\,°\mathrm{C}$. The cycle normally cannot operate well close to this point, because the latent heat decreases to zero at this point, thus the heat rejection diminishes. However, if sufficient subcooling below the saturated temperature is available, the sensible heat would increase the possible heat rejection. As the process air was found to have an inlet temperature around 6 °C, such subcooling was possible.

Above the critical point, the fluid is in a transcritical state, not really a gas, neither a liquid, and no phase change occurs. This might always be relevant at the highest outdoor temperatures. Heat must then be rejected at gliding temperature and with lower heat transfer coefficients. Designing *one* heat exchanger for heat rejection both by condensation and gliding temperature might be optimistic. However, the fluid will be superheated after compression, which means that its temperature will be higher than the saturated one. Some of the heat rejection therefore finds place at higher temperature, and if this is sufficient to reject enough heat to outdoor air at 30 °C , the cycle can operate subcritical throughout the year.

A transcritical cycle could be very profitable all year if there is a need for hot water production, as it reaches very high temperatures. However, including hot water production required extra assumptions on the need for hot water and then one should consider the possibility and profitability to rebuild the water supplying system at a plant.

Rather than assuming that such a convenient heat sink existed, allowing to subtract all compressor power from the result (and perhaps obtain an unfair comparison with other systems), all models were made without this possibility, but compression power and energy were both reported and discussed.

The operation of heat pumps will be less good when the surroundings are warm, but this was only relevant for a small part of the time, and the system should be designed for optimal operation at a more typical condition. Thus, somewhat worse performance at this point should be a part of the design. All models were allowed to vary both pressures and mass flow to adapt the operational conditions to the changing cooling load and the outdoor temperature.

The adsorption system included a heat pump as shown in Figure 5.6. This heat pump delivered all excess heat to the regeneration stream, and was made with a CO_2 heat pump at 0 °C, or 34.85 bars to avoid ice in the evaporator and 95 bars. Hence, its operation was always transcritical.

CO_2 was chosen because the air would have a gliding temperature and a quite big temperature change during heating. It is then better to heat up by heat exchange with a fluid at a gliding than a constant temperature. Otherwise, there would be large temperature differences in the coldest end. When there are such large differences, high temperature heat, and therefore high quality heat, is used to heat up a fluid that did not need this high quality. A fluid at a lower temperature would suffice. If one should apply heating at constant temperature, then the entire refrigerant flow must be compressed to a high pressure, but this is only necessary for a small part of the heating. Thus, it is not energy effective.

All models and their components were designed with the above described temperatures and pressures, unless something else was more congruous. This would include that the heat pumps should handle the worst operational conditions, for example very high outdoor temperatures, requiring higher temperature in the heat pump than 30 °C. The heat exchangers with outdoor air were therefore modelled with saturation at 35 °C, or 80.87 bars for CO_2, giving 35 °C above the critical point. The process air handled the remaining heat rejection.

Calculations were performed for each system with their respective temperatures, heat loads and pressures, and one example calculation for the systems BS and HPS, which had the same dimensions in the heat pump as they had the same cooling demand, is shown in the sections to follow.

6.7.1 COMPRESSOR

Much of the losses in a heat pump are due to the compressor, and these are minimized by maximizing its isentropic efficiency. For compressors, isentropic efficiency is defined as the ratio between required power for isentropic operation, to real shaft power consumption. This is generally a function of the pressure ratio Π. Including losses in driving mechanism and other components, the overall efficiency might be lower. The isentropic efficiency for the compressor was calculated from the formula

$$\eta_{is} = 0.3862 + 0.0016\Pi^3 - 0.0333\Pi^2 + 0.1892\Pi \tag{6.9}$$

given in the subject TEP4255 at NTNU the spring 2014. For ammonia one finds $\Pi_{NH_3} = \frac{11.67}{2.9} = 4.0$ when cooling and heating the entire air stream to respectively 7 and 13 °C like in

BS and HPS.This gave $\eta_{is} = 0.71$. A heat loss from the compressor of 4 % was included in the modelling as this normally will occur.

To calculate the size of the compressor, one must consider how much energy it shall deliver and find the necessary mass flow. For a closed loop air system, the cooling load will be determining for the dimensioning of the heat pump, because it delivers more heat than it removes from the cold side. (Closed loop was assumed because this is used in an actual plant to avoid pollution of or impurities in the incoming air.)

The change in enthalpy between point A, B and point C in Figure 6.1 is approximately

$$h_{(T=10,\phi=100\%)} - h_{(T=7,\phi=100\%)} \approx (29.0 - 22.5)\,\frac{\text{kJ}}{\text{kg}} = 6.5\,\frac{\text{kJ}}{\text{kg}}$$

The amount of air was 2.8 $\frac{\text{m}^3}{\text{s}}$ at the inlet to the drying chamber, with 13 °C and from Figure 6.1, an absolute humidity of about 6.24 $\frac{\text{g vapour}}{\text{kg dry air}}$. Thus the mass flow of air and vapour must be

$$\dot{V}_a \rho_a = \dot{V}_a \frac{p(M_a + M_w x)}{RT(1+x)} = \frac{2.8\,\frac{\text{m}^3}{\text{kg}} \cdot 101250\,\text{Pa} \cdot (28.97 + 18.015 \cdot 0.00624)\,\frac{\text{kg}}{\text{kmol}}}{8314\,\frac{\text{J}}{\text{kmol K}}\,286.15\,\text{K} \cdot 1.00624} = 3.44\,\frac{\text{kg}}{\text{s}}$$

The mass flow of dry air is then

$$\dot{m}_{dry,a} = \frac{\dot{m}_a}{1+x} = \frac{3.44\,\frac{\text{kg}}{\text{s}}}{1.00624} = 3.42\,\frac{\text{kg}}{\text{s}}$$

Thus the cooling load on the heat pump was $\Delta h \dot{m}_{dry,a} \approx 6.5\,\frac{\text{kJ}}{\text{kg}} \cdot 3.42\,\frac{\text{kg}}{\text{s}} \approx 22.23$ kW.

Assuming purely saturated ammonia gas at the compressor inlet (enthalpy of 1448.53 $\frac{\text{kJ}}{\text{kg}}$), and saturated liquid before isenthalpic throttling at 30 °C (enthalpy of 339.71 $\frac{\text{kJ}}{\text{kg}}$), the mass of ammonia flow must be $22.23\,\text{kW}/(1448.53 - 339.71)\,\frac{\text{kJ}}{\text{kg}} = 0.020\,\frac{\text{kg}}{\text{s}}$. Enthalpies can be read in saturation tables or on pressure-enthalpy charts for ammonia.

The heat load will vary depending on the amount of water to be evaporated, thus, the mass flow of ammonia was allowed to vary. 0.020 $\frac{\text{kg}}{\text{s}}$ was used as the design mass flow in calculations.

To find the heat load on the desuperheaters, or the excess heat that had to be removed, the energy added by the compressor was found. Isentropic compression to 11.67 bars gives a final enthalpy of $\approx 1644.12\,\frac{\text{kJ}}{\text{kg}}$. With an isentropic efficiency of 0.71 and 4 % heat loss, the power added to the cycle in the compressor is

$$\dot{W} = \frac{\dot{W}}{\eta_{is}} \cdot (1 - 0.04) = \frac{(1644.12 - 1448.53)\,\frac{\text{kJ}}{\text{kg}}}{0.71} \cdot 0.96 = 246.46\,\frac{\text{kJ}}{\text{kg}}$$

From an enthalpy-pressure chart for ammonia, this means that the outlet temperature from the compressor will be about 110 °C .

The volume of the compressor and its speed, together with the opening of the throttling valve, determine how much working fluid is circulated and the pressures in the heat pump. The ratio between actual volumetric flow at the compressor inlet and its geometrically swept volume is called the volumetric efficiency λ, and was found from

$$\lambda = 0.002\Pi^2 - 0.0761\Pi + 1.0556 \tag{6.10}$$

taken from TEP4255 at NTNU the spring 2014. The volume of the compressor, V_{compr} was found from

$$\dot{V} = n\lambda V_{compr} = \dot{m}v_1$$

where n is the frequency, set to 50 Hz in designing. v_1 was found to be about 0.42 $\frac{\mathrm{m}^3}{\mathrm{kg}}$ in a pressure-enthalpy diagram for ammonia. From the given correlation for λ, Equation 6.10, assuming that the compressor must handle the highest outdoor temperature, this parameter became 0.745. Using the design mass flow of 0.020 $\frac{\mathrm{kg}}{\mathrm{s}}$, one finds

$$V_{compr} = \frac{0.020\frac{\mathrm{kg}}{\mathrm{s}} \cdot 0.42\frac{m^3}{\mathrm{kg}}}{50\ \mathrm{Hz} \cdot 0.745} = 225.5 \times 10^{-6}\ \mathrm{m}^3$$

At the highest loads, it could be neceassary to enhance the mass flow a bit, so a 5 % increase was used, giving $236.8 \times 10^{-6}\,\mathrm{m}^3$. However, during the work, this turned out to be unnecessary.

The speed of the compressor was controlled in order to control the mass flow rate and appropriate cooling, but compressor volumes were calculated like above and used as they should have more or less appropriate values.

Because the temperatures and pressures varied, the isentropic and volumetric efficiencies should vary too. The existing compressors in DYMOLA did not allow for varying efficiencies. Therefore, the DYMOLA compressor called «effective compressor» was duplicated, and a new compressor made, for which the code was changed to allow changing isentropic and volumetric efficiencies. The models all used Equation 6.10 and Equation 6.9 during simulation. This new compressor was simply named «Compressor» and is in all other aspects a copy of the «effective compressor» in DYMOLA.

6.8 HEAT EXCHANGERS

Heat exchangers are constructions through which two (or more) fluids can flow and exchange heat. There are many configurations of these, shell and tube is a quite normal one, but new plate heat exchangers are often both smaller, more effective, and more expensive [Wadekar, 2000]. One fluid flowing in finned pipes and the other flowing across it is another usual type, which was used in this work for heat exchangers when one of the fluids was a gas. The shell and tube configuration was used for glycol-ammonia heat exchangers, and plate heat exchangers were used for air-air heat exchangers. This is discussed in Section 6.8.2.

Generally, smaller flow channels enhances both heat transfer and pressure drop for the fluids and heat exchangers are characterized by the amount of surface area for heat transfer per volume. A high value gives high heat transfer and small flow channels [Wadekar, 2000]. The thermal efficiency of a heat exchanger is defined as

$$\eta_{th} = \frac{\dot{Q}}{\dot{Q}_{max}} = \frac{\dot{Q}}{C_{min}(T_{H,in} - T_{C,in})} \tag{6.11}$$

where $\dot{Q}$ is heat transfer, C_{min} the smallest product of a stream's mass flow and specific heat, and subscripts C and H refer to the cold and the hot stream. All presented theory and relations for heat exchangers were found from [Bergman et al., 2011].

The flow pattern can be counterflow, crossflow or a combination. Parallel flow is of course also possible, but gives poorer heat transfer and is therefore not commonly used. Counterflow gives higher heat transfer, which can be further enhanced by turbulence and larger areas (this is seen in Equation 6.13). Making the heat transfer area large in a small exchanger calls for small channels and twisting and bending the them. This makes the flow deviate from pure counterflow.

Smaller channels tend to create more laminar flows, and herringbone patterns and obstacles are used to prevent this. Other measures to enhance heat transfer is by adding fins to flow pipes. These are metal plates extending the surface of a pipe, giving larger surface area for the fluid outside [Bergman et al., 2011, p. 155]. All heat exchangers used in DYMOLA were arranged to let the inlets for each fluid on each their side, to achieve countercurrent, or close to countercurrent flow. The air-air heat exchangers were designed for crossflow, which will be discussed in Section 6.8.2.

Transferring heat, $\dot{Q}$, in a heat exchanger involves transfer from fluid 1 to the heat exchanger wall, through the wall, from the wall to fluid 2. The heat transfer from fluid 1 to the wall is described by $\dot{Q} = A_1\alpha_1(T_1 - T_{wall})$. For stream 2 it is of course opposite. Transfer through the wall depends on its thermal conductivity k_{wall} and thickness s. This means both fluids have their own heat transfer coefficient with the wall, and the overall heat transfer coefficient is then

$$U = \left(\frac{A_i}{\frac{1}{A_1\alpha_1} + \frac{s}{k_{wall}} + \frac{1}{A_2\alpha_2}} \right)^{-1} \tag{6.12}$$

The subscript i should be either 1 or 2, and U is then referred to that area of the heat exchanger. From Equation 6.12, U will always be different depending on which area it is referred to, and lower than both α_i.

The heat transfer in a parallel or counterflow heat exchanger is given by

$$\dot{Q} = UA\Delta T_{lm} \tag{6.13}$$

where U is the overall heat transfer coefficient, referred to the area A, and ΔT_{lm} is the logarithmic mean temperature difference between the fluids. Final values and which formulas from [Bergman et al., 2011] that were applied are given in Table 6.2.

The logarithmic mean temperature difference is derived for counterflow with the c_p of both flows constant in [Bergman et al., 2011, p. 712-714], and is

$$\Delta T_{lm} = \frac{(T_{H,in} - T_{C,out}) - (T_{H,out} - T_{C,in})}{\ln\left(\dfrac{T_{H,in} - T_{C,out}}{T_{H,out} - T_{C,in}}\right)} = \frac{\Delta T_1 - \Delta T_2}{\ln\left(\dfrac{\Delta T_1}{\Delta T_2}\right)} \tag{6.14}$$

The same, smallest temperature difference, $\Delta T_{min} = 7\,°\mathrm{C}$ was used in the design of the heat exchangers, to make the energy comparisons fair. There were, however, a few exceptions from this: In HPSX100, the largest possible temperature difference was about 3 °C. Hence, a heat exchanger of reasonable size was designed, the possible heat load and smallest temperature difference found to be 1.7 °C. The comparison with other HPSX systems would only be fair if they had the same smallest ΔT, so this value was used in all HPSX systems.

The other exception was that, at the worst conditions for the systems, desuperheaters were designed for 5 °C, as they would rarely operate at this point, and somewhat worse conditions could result. Similarly, in the worst case for the adsorption system, it was also allowed this smaller temperature difference of 5 °C, to be consistent with the other systems.

6.8.1 NTU METHOD

Heat exchangers for which the assumptions for Equation 6.13 and Equation 6.14 were not satisfied (not constant c_p or not pure parallel flow for example) should be designed by the NTU method. It applies to both crossflow, parallel and counterflow, handles that the outlet temperatures are unknown and can be used for constant temperature cases. It involves the equations

$$C_{min} = \min(\dot{m}_H\, c_{H,p}, \dot{m}_C\, c_{C,p}), \qquad NTU = \frac{UA}{C_{min}} = F\left(\eta_{th}, \frac{C_{min}}{C_{max}}\right)$$

and Equation 6.11. NTU is the number of transfer units. The function F varies with flow configuration, and all formulas for this one are found in [Bergman et al., 2011, p. 724-724]. The NTU method applied to some of the evaporators and condensers gave the exact same UA-value as the first method described, but because the first method was not always valid, the NTU method was applied in these cases, if differences between them should occur, especially related to cross flow.

6.8.2 CHOICE OF CONFIGURATIONS

For most heat exchangers in this work, one fluid had was the determining for the heat transfer, as its heat transfer coefficient was significantly lower than for the other fluid, and therefore, this fluid was combined with the largest area.

Gases have poor heat transfer due to their low density, and was therefore placed on the outside of the tubes in the heat exchangers, and these tubes were modelled as finned tubes, because this enhances the area and heat transfer [Bergman et al., 2011, p. 155]. Therefore, refrigerants and liquids exchanging heat with air, which CO_2 always did, were always modelled inside finned tubes.

It was assumed that the fins, surfaces and flow pattern induced turbulence in the air flow, in addition to that the analysis in Section 6.5 showed that the air is turbulent even before entering the exchangers. Thus, turbulent heat transfer correlations were used in these cases.

In the plate heat exchangers, the small channels, without any pipes and fins, could result in laminar flow, even at high Reynolds numbers [Bergman et al., 2011, p. 558-559], and laminar correlations were used.

Evaporation or condensation has very high heat transfer due to the latent heat. Shell and tube heat exchangers were chosen for ammonia-glycol exchangers, because these are normally applied, and not too expensive [Wadekar, 2000].

Tube and tube exchangers consist of an outer tube for one fluid, with several smaller tubes inside for the other. Many of them have baffles that force the flow in the shell move across these pipes several times. It was assumed that the baffles had a surface area corresponding to 85 % of the tube diameter, to allow the flow to pass by them.

Condensing ammonia was assumed to flow in the shell, since dripping from one pipe with glycol to another can enhance heat transfer [Bergman et al., 2011, p. 686]. In addition, it allows liquid ammonia in the shell to bah the lowest pipes in ammonia, giving more efficient heat transfer than gaseous ammonia and allowing subcooling of it. Subcooling enhances the performance of a heat pump. It lowers the enthalpy of the working fluid before throttling, and thereby the enthalpy after throttling, which means that heat rejection at the low temperature can be larger for the same mass flow of working fluid.

Evaporating fluids wet the walls around them, which gives good heat transfer. The gas is normally in the middle, and the fluid expands upon the phase change. This accelerates the fluid, and can drive it through the channel without extra pumping power, thus, evaporation was assumed to find place inside the pipes, and the hotter glycol surrounded them [Bergman et al., 2011, p. 670-672].

In DYMOLA, there is no air-air heat exchanger, but there are tubes for gas flow, and these can exchange heat. These were used in the simulations. Heat exchangers were designed for the relevant cases, but could not be used in simulations. Data for the designed ones are shown in Table 6.2.

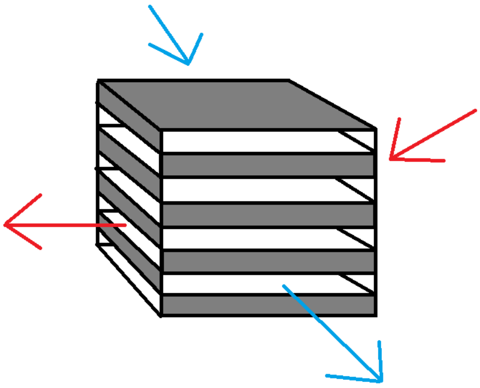

Figure 6.4: Chosen type of air-air heat exchanger, where the red arrows represent the hot fluid flow being cooled and the blue ones the colder fluid. The figure is strongly inspired by a picture from `http://www.uk-exchangers.com/air-to-air-heat-exchangers.htm`.

Designing air-air heat exchangers involved considering three normal types, choosing the, hopefully, most suitable. A quite simple configuration were several plates form air channels like in Figure 6.4 was chosen. Each air stream flows in every other channel, and the streams cross each other.

A considered but rejected option involved an exchanger with glycol in between, giving good heat transfer to and from the liquid, but also requiring extra pumps and equipment for the glycol circuit, and an extra temperature difference. Because of this, and because the temperature differences in most of the air-air heat exchangers in this work were not big to begin with, this solution was rejected.

Another option considered was a rotating air-air heat exchanger. This is a wheel where the air streams flow through each their half of a desk and the material absorbs and delivers heat. Rotating heat exchangers can both transfer heat and adsorb moisture, not unlike adsorption systems. (The difference is that adsorption systems do not transfer moisture between two streams of drying air.) The moisture transfer was the reason this solution was discarded, as it could transfer moisture *from the wet* process air *to the dried* process air, counteracting the entire purpose of this work.

6.8.3 DIMENSIONING

Materials in the heat exchangers are normally metals that have high thermal conductivity, like copper, and the fins are often made from aluminium due to low cost and weight. For air-to-air heat exchangers, aluminium is the usual material according to Professor Hans Martin Mathisen at NTNU. These materials were therefore chosen in the models except for in one special case: For some fluids, the metal must be non-corrosive or withstand high pressures. One such fluid is ammonia, for which heat exchangers were modelled with stainless steel, AISI 302, with a thermal conductivity of $15.1\ \frac{\mathrm{W}}{\mathrm{m\ K}}$. Conductivities used for copper and aluminium, in that order, were 401 and 237 $\frac{\mathrm{W}}{\mathrm{m\ K}}$, all taken from [Bergman et al., 2011, Table A.1].

Table 6.2: Sizes and operational conditions for heat exchangers applied: Heat, $\dot{Q}$, is always transferred from fluid 1 (with mass flow rate, velocity and inlet temperature denoted $\dot{m}_1$, v_1, and $T_{i,1}$) to fluid 2 (with properties denoted in the same way); the dimensions of the heat exchangers are given as LxDxW, length times depth times width or in terms of length and diameter (Lxd) for tube and tube exchangers. The reported area is always the largest area, and U is referred to this side. Formulas for calculations were all found in [Bergman et al., 2011]. «Air» is always process air, unlike the «o. air» and «r. air», being short for «outdoor air» and «regeneration air», respectively.

System	Fluid 1	Fluid 2	$\dot{Q}$ [kW]	WxDxH or LxD [m]	A [m^2]	U [$\frac{\text{W}}{\text{m}^2\text{K}}$]	Formulas	$T_{i,1}$ [°C]	$T_{i,2}$ [^{o}C]	$\dot{m}_1$ [$\frac{\text{kg}}{\text{s}}$]	$\dot{m}_2$ [$\frac{\text{kg}}{\text{s}}$]	v_1 [$\frac{\text{m}}{\text{s}}$]	v_2 [$\frac{\text{m}}{\text{s}}$]
BS	ammonia	o. air	28.34	2x1x1.1	176.37	16.85	10.43, 8.60	42.6	30	0.020	5.0	-	2.0
BS, HPS	air	glycol	22.23	1x1.1x1.4	150.11	10.62	8.60, 8.58	10	−5.2	3.4	1.2	2.0	0.79
BS, HPS	glycol	ammonia	22.23	1.86x0.26	9.51	330.13	8.58, 10.51a	0	−10	1.2	0.020	3.7	-
HPS	ammonia	glycol	22.23	6.3x0.6	190.79	19.76	10.46, 8.58	27	20	0.020	3.0	-	0.29
HPS	ammonia	o. air	6.08	0.4x1x1.4	47.42	16.82	10.43, 8.60	41.0	30	0.020	1.0	-	2.0
HPS	glycol	air	22.23	1x1.5x1.4	173.33	12.18	8.58, 8.60	22.1	7	3.0	3.4	1.9	2.0
HPSX100	air	glycol	19.13	1x0.85x1.4	111.44	10.27	8.60, 8.58	3.1	−5.2	3.4	1.2	2.0	0.59
	glycol	air	19.13	1x1.2x1.4	158.20	12.03	8.58, 8.60	21.8	7.9	3.0	3.4	2.4	2.0
	glycol	ammonia	19.13	1.716x0.26	6.75	376.06	8.58, 10.51a	0	−10	1.2	0.017	3.7	-
	ammonia	glycol	19.13	4.9x0.6	148.33	21.28	10.46, 8.58	27	20	0.017	3.0	-	0.29
	ammonia	o. air	5.17	0.4x0.5x1	13.23	16.83	10.43, 8.60	110	30	0.017	1.0	-	2.0
	air (at 10)	air (at 7)	3.10	1.61x1.61x1.5	383.63	3.48	8.57, 8.57	10	7	3.4	3.4	2.5	2.5
HPSX37, HPSX1 + CO2S	air	glycol	16.35	1x2.15x0.55	111.61	9.81	8.60, 8.58	7.7	−9.8	1.3	1.2	2.0	0.41
	glycol	air	16.35	1x2.5x0.5	117.52	11.27	8.58, 8.60	26.6	6.0	3.0	1.3	1.2	2
	glycol	ammonia	16.35	0.94x0.35	6.52	428.38	8.58, 10.51a	−6	−16	1.2	0.015	3.7	-
	ammonia	glycol	16.35	3.8x0.6	114.63	23.00	10.46, 8.58	32.1	25.1	0.015	3.0	-	0.29
	ammonia	o. air	5.04	0.4x0.5x1	16.20	16.82	10.43, 8.60	125	30	0.015	1.0	-	2.0
	air (at 7.7)	air (at 1)	6.42	1.57x1.57x1.57	384.52	3.47	8.57, 8.57	10	1	1.3	1.3	0.94	0.91
CO2S	CO_2	air	16.35	0.51x0.9x1	38.60	16.58	8.60, 8.60	36	6.0	0.092	1.3	-	2.0
	CO_2	o. air	4.58	0.4x2.1x2.05	143.32	2.07	8.58, 8.60	65	30	0.092	1.0	-	2.0
	air	CO_2	16.35	1x0.7x0.55	36.42	16.70	8.60, 10.51a	7.7	−6	1.3	0.092	2	-
CS	air	air	7.35	0.21x0.93x1.3	0.78	72.62	8.60, 8.60	144.3	10	1.0	2.4	2.6	2.8
	air	water	137.80	0.6x2.85x0.35	106.77	28.73	8.60, 8.60	137.3	6	1.0	7.0	2	2.2
ADS	CO_2	r. air	20.43	0.55x1.85x0.5	4.81	15.89	8.60, 8.60	87	7.8	0.095	0.68	0.70	2.0
	air	CO_2	15.00	1x0.7x0.55	36.55	16.59	8.60, 10.51a	10	0	1.3	0.095	2.0	-
	r. air (at 28.2)	r. air (at -17)	17.05	1.5x1.5x1.38	306	3.47	8.57, 8.57	28.2	−17	0.69	0.68	0.54	0.54

Other assumptions in the heat exchangers, which were used consistently, were the following:

- fin and wall thickness = 1 mm
- distance between pipes = 50 mm
- distance between fins/extended surfaces = 12 mm
- outer pipe diameter = 10 mm
- air inlet velocity = 2.0 $\frac{\text{m}}{\text{s}}$ in finned tube exchangers

Distance between plates in air to air exchangers were normally assumed 9 mm, but in the compression system, this gave a high heat transfer in a very small volume, making the air velocity in the exchanger unacceptably high (far above 10 $\frac{\text{m}}{\text{s}}$). For this case therefore, the distance was adjusted to as much as 249 mm, making heat transfer and velocities acceptable.

Heat transfer for all fluids and sizes of heat exchangers were calculated in Excel from relevant formulas in [Bergman et al., 2011], see Appendix E for further details. Results are shown in Table 6.2 along with characteristics for designed conditions. Both Equation 6.13 and Equation 6.12 must be modified slightly if a heat exchanger has different conditions than they were derived for. This could for example involve accounting for fouling of the surfaces. In order not to make this work to complex and extensive, this was ignored in this work, and the equations were used as they are shown here.

All heat exchangers were designed at most difficult conditions, since they had to be large enough to provide sufficient cooling and heating also in the worst cases. This meant that for example air-ammonia condensers and desuperheaters were designed for the highest outdoor temperature, 30 °C. Exchangers were all tested separately in own DYMOLA files before they were used in a model, to ensure their operation was satisfactory. Length or depth was adjusted to achieve this. The dimensions after testing are the ones reported here.

The shape of the temperature profile in a desuperheater and/or condenser can in many cases be neither smoothly decreasing nor constant becauseboth sensible and latent heat is transferred. This created problems in designing the condenser of BS and desuperheater in HPS, because the appropriate value for ΔT_{lm} was unknown. The problem was simply solved by assuming a slightly higher and constant condensing temperature. This gave a logarithmic mean temperature difference closer to the real one. New calculations gave slight changes in design and proper exit conditions for both flows in DYMOLA, which were then used.

A more correct and cumbersome method would be to divide this calculation in two, and use one heat exchanger for desuperheating (changing temperature) and one for the constant temperature condenser, using the NTU method. However, because the modelled exchangers had performed as desired in DYMOLA, they were kept as they were, and this new, more correct method were used in the remaining models. As exchangers were all tested to perform as desired, no model had any unfair advantage of this in the energy comparison.

6.9 Fans and Pumps

All fans and pumps have losses, and were modelled with the default efficiencies in DYMOLA, 0.6 for fans and for 0.4 for pumps. These values are quite realistic and were the same for all systems to give a fair comparison. The energy losses were added to the fluids.

6.10 Placement

The systems using a heat pump for heating had two heat exchangers on the high pressure side. The process needed the same amount of cooling and heating, but extra energy was added in the heat pumps by the compressor, so that the heat pump always has surplus heat. One heat exchanger rejected excess heat to the surroundings, and one exchanged heat with the drying process.

The two heat exchangers were placed in series. A desuperheater was placed directly after the compressor, and cooled the superheated vapours to saturation. This was done to avoid extra high pressures and temperatures in the heat pump when it was 30 °C outside, as the outdoor air could then utilize the highest temperatures of the superheated gas from compression. After the desuperheater came a condenser with heat supply to the process. This allowed subcooling of the refrigerant also during summer, and a lower condensation pressure.

Fans and pumps were always placed after heaters in the system. They add heat, and should therefore not be placed in front of cooling or heating devices. Adding heat before a heating device decreases the temperature difference in the heater, and thus makes it less efficient. Instead, they were placed directly after. All flows in the heating devices were controlled to achieve the desired temperature after the pumps or fans, and the heat transfer *to* the process air was therefore slightly less than the heat removed from it. The heat load from fans and pumps were not included in the dimensioning of heat exchangers because their effects were unknown and likely to be negligible.

The electrical heater in the adsorption system, ADS, was placed after the heat pump for similar reasons as just explained.

6.11 Heat leakage

It is likely that the process will have heat leakages through the walls. This could be either to or from the surroundings, depending on the season. No data was available to find the heat load this imposed on the system, but it was assumed that at up to 10 % of the cooling and heating load for the air in BS was exchanged with the surroundings. Therefore, a pipe for airflow with heat exchange was inserted in the model. It was placed after the drying tunnel, before the dewatering system, so that the coolers and heaters could deliver the necessary heat or cooling this imposed on the system.

The modelled outdoor air was set as the thermal outside boundary for the pipe, to make the heat exchange somewhat realistic. The highest temperature difference between the process air and the outdoor air was about that between the wet bulb temperature for the drying process, $\approx 10\,^{\circ}\mathrm{C}$, and the lowest outdoor temperature, $\approx -17\,^{\circ}\mathrm{C}$. Both these occurred at the start of simulation and gave $\Delta T_{max} \approx 27\,^{\circ}\mathrm{C}$.

The process heat load for BS was 22.23 kW. The outdoor air temperature would not be notably affected by this exchange and the change in temperature for the process air was also likely to be small. Due to this, the inserted pipe was given a constant UA-value equal to $22230\,\mathrm{W} \cdot 0.10/27\,\mathrm{K}$.

6.12 Regulation

To control the temperatures and conditions in the dynamic systems, several parameters were adjusted as the process developed. These were for example compressor speed, valve areas, supply of electrical heat or fan power and amount cooling air or water. Both DYMOLA and the TIL library contain controllers that take in one measurement signal and one desired value for this signal, and then adjust output signals of their own to minimize the difference between them.

One such controller type is the P-controller. This gives an output signal proportional to the difference between measurement and its desired value. Hence, with these controllers, there will always be a deviation, but this can be negligibly small.

PI-controllers are more accurate, as they can achieve the exact output to diminish any deviation. However, PI-controllers need long time to reach the appropriate output unless their parameter Ti is small. A very small Ti tends to make the systems unstable, resulting in oscillations or simply a stop in simulation. Some simulations kept running for a whole day without ever moving on due to a decrease in some Ti.

A PID-controller can decrease instabilities resulting in oscillations, but this type is rarely necessary to use, and was not needed in this work. All controllers used were from the TIL library with lower and upper limits for output signals. Normally they were of PI-type, but a few were P-controllers.

6.12.1 CHOOSING PARAMETERS

The parameters in the controllers could be proportionality constants, initial output, which turned out to be extremely important to make the models start, and time constants, Ti, that determined the speed of regulation.

Parameters were obtained by starting with a P-regulator and find a suitable proportionality constant. First, the order of magnitude in difference between deviation and output signal was found. For example, if the input should be a pressure, measured in pascals, and the output a valve area, measured in square metres, the proportionality constant would be given a value somewhat smaller than the ratio between a normal valve area and a normal pressure. This could be around $1\ \mathrm{cm}^2/800,000\ \mathrm{Pa} = 10^{-4}/(8 \times 10^5) \approx 10^{-10}$.

The next step was then to apply this value and run the simulation (or the first part of it as it often did not run to completion during the first tries) and investigate which values the controllers ended up with, and when and how the conditions deviated from the desired values. Then, the parameters were adjusted, larger if the controller was too bad or slow, lower if the simulation stopped or values oscillated. The model was then tested again.

If the controller responded to changes in a correct manner, but yet a constant deviation resulted, the controller was changed into a PI-controller. Normally, the time constants were set big at first, giving stable, but somewhat slow regulation. If they were set too small at first the regulation did not run. From the slowly regulated, but possible simulation, suitable operation points were found, giving good values for initial output, which were then applied, and Ti was then decreased to increase accuracy from this better start point. Sometimes the proportionality constant was also decreased when Ti decreased, as this also stabilized the regulation and allowed a smaller Ti. During regulation of one parameter, one or more other parameters were sometimes set constant to avoid them to interfere too much with the process.

6.12.2 CONTROL STRATEGIES

To control sufficient cooling of the process, without an excessively low temperature and pressure in the heat pump, the mass flow in heat pump compressors were controlled to achieve desired absolute humidity in the process air. Humidity also determined the mass flow of compressed air in CS. The absolute humidity was generally used, because it presumably was easier for DYMOLA to calculate this than the relative humidity, as the latter depends on temperature. Its exact value was found by measuring the absolute humidity of the air before the drying tunnel.

One exception from the strategy above was the heat pump in the adsorber system, which primarily delivered heat, not cooling. Here, the temperature of regeneration air after adsorption was controlled to be 28.2 °C. Compressor mass flow was controlled by changing the compressor speed, which is usual.

Valve areas in heat pumps were controlled to feed sufficient, but not too much, working fluid to the cold side of the heat pump. This is normal and done by ensuring a slight superheating of the evaporated gas after the evaporator, which is easily measured as the temperature then rises above the saturated one.

Similarly, air flow of outdoor air to condensers and desuperheaters could be regulated to obtain a small subcooling of the condensed liquid in BS, whereas in the systems that used the heat of condensation, the flow was controlled to ensure 13 °C in the process air at the end of the process/before re-entering the drying tunnel. Electrical heat supply and mass flows of cooling water were adjusted to give the desired air temperatures. The mass flow of air to be dehumidified in HPSX1 and CO2S was controlled to keep the lowest air temperature at 1 °C.

6.13 PERFORMANCE MEASURES

The results were reported in terms of energy consumption, SMER and drying efficiency. These were defined in Chapter 2 but are briefly repeated here. SMER, specific moisture extraction rate, is defined as amount of energy used divided by evaporated water, or

$$\mathrm{SMER} = \frac{\Delta m_w}{E_{tot}}$$

and the drying efficiency for the process is the ratio between energy actually used for evaporation and energy consumed by the process,

$$\eta_{dry} = \frac{\Delta m_w h_{fg}}{E_{tot}}.$$

For a dryer without a heat pump for heating, the highest possible efficiency is 100 %, as no more energy can be supplied for evaporation than that delivered to the process. Systems using a heat pump on the other hand, recover latent heat when the water is condensed in the evaporator, and deliver the heat back. Their efficiencies can therefore exceed 100 %. Typical values given in [Jon and Kiang, 2006] showed $\eta_{dry} \in \{0.35, 0.40\}$ and SMER $\in \{0.12, 1.28\}$ for conventional hot air dryers and $\eta_{dry} \approx 95$ % and SMER$\in \{1.0, 4.0\}$ for heat pump dryers.

6.14 COST ANALYSIS

Any energy system requires an investment, and the most effective system might also be the most expensive, and could therefore not be of interest for the industry despite its better operation. To find out whether or not the investment will be profitable, a simple cost analysis was performed. By assuming an energy price of 0.65 $\frac{\text{NOK}}{\text{kWh}}$ the investments that could be justified by the energy savings were found. The value of future savings were corrected to their net present value (NPV) by the formula

$$NPV = \frac{S}{(1+r)^t} \tag{6.15}$$

where S is the amount of saved money each year, r the discount rent and t is time in years. The discount rent was assumed to be 7 %. Energy savings per year was calculated as simulated energy saving for system j relative to BS, multiplied by one year divided by simulated drying time for the hams in the first section, t_{pro}. This was multiplied by the cost of energy, c, to obtain the economical savings S, as follows:

$$S = (E_{tot,BS} - E_{tot,j})\frac{1 \text{ year}}{t_{pro}} \cdot c \tag{6.16}$$

From these relations, an estimation for possible investments for a payback time of one, two or three years was found.

Chapter 7

RESULTS

The total amount of required energy in each system is shown in Table 7.1. The total energy included energy to compressors, pumps and fans and electrically supplied heat, in other words, the total amount of energy one must pay for. The energy for compression is shown separately, to give an idea of how much of the total it comprised and to calculate available excess heat in Chapter 8. The energy for heating and cooling are the amounts of heat received by or rejected from the process air, excluding exchange with itself. They are generally larger than the total energy, due to the use of heat pumps. An assessment of how the systems performed is given in Appendix B.

Not reported in Table 7.1 are the used amounts of cooling water in the compression system CS. They were 3.01, 2.83 and 2.16 tonnes of water, the first value for the lowest and the last value for the highest pressure applied. It should also be mentioned that the required energy per kg produced ham in the basic system, BS, was 2.58 $\frac{\text{kWh}}{\text{kg}}$.

Table 7.1: Resulting energy flows and improvements compared to the basic system BS: The total energy was E_{tot}, energy for compression E_{compr}, and energy for heating and cooling the air, E_{heat} and E_{cool}. SMER is the specific moisture extraction ratio, giving amount of evaporated water per kWh used, and η_{dry} is drying efficiency, defined in Section 6.13. Three results are given for the compression system; CS2.5 compressed the drying air to 2.5 bars; CS3.0 compressed the air to 3.0 bars and CS3.5 to 3.5 bars. Energy for heating in the adsorption system was 18.67 MWh from electrical heating and 33.45 MWh from the heat pump. ***Preliminary result, model not entirely completed.

System	E_{tot} [MWh]	E_{cool} [MWh]	E_{heat} [MWh]	E_{compr} [MWh]	SMER $\left[\frac{\text{kg water}}{\text{kWh}}\right]$	Improvement [%]	η_{dry} [%]
BS	69.64	60.60	58.13	6.54	0.21	0	15
HPS	21.05	60.55	54.63	10.23	0.70	70	48
HPSX100	17.25	48.51	43.68	7.87	0.85	75	59
HPSX37	14.88	29.98	24.50	4.68	0.99	79	68
HPSX1	8.93	22.66	22.01	4.39	1.65	87	113
CO2S	5.32	25.13	23.88	3.81	2.76	92	190
CS2.5	196.19	194.71	0.00	194.92	0.07	−182	5.2
CS3.0	192.27	190.76	0.00	191.00	0.08	−176	5.3
CS3.5	192.69	191.15	0.00	191.42	0.08	−177	5.3
ADS***	27.60	26.54	52.12	6.63	0.53	60	37

Chapter 8

DISCUSSION

From the energy results, the CO_2 system had the lowest energy demand, 40 % better than the second best, HPSX1. A disadvantage with running simulations was that no measure of uncertainty for the results was found, but this difference in energy needs was so large it seems to be significant. The only difference between the two best systems was the use of CO_2 rather than ammonia and glycol, with extra temperature differences for the latter. Hence, based on results in this work, using CO_2 is a good solution, in accordance with findings in [Fornasieri et al., 2009]. It is unclear whether this was solely caused by the lower temperature lift or if CO_2 is also a better refrigerant in this temperature range.

A presentation and discussion of how the systems operated is given in Appendix B. From the results shown, the choice to model the closed air process as an open one can be defended, as all systems achieved final conditions very close to the initial ones.

Specific energy for a real plant is about $3.79 \pm 0.22 \, \frac{\text{kWh}}{\text{kg ham produced}}$. For the basic system it was somewhat lower, $2.58 \, \frac{\text{kWh}}{\text{kg ham produced}}$. The simulation involved a quite long time with low drying load, seen in Figure B.2 in Appendix B, which could partially explain the difference. In addition, operation in the simulation was close to ideal, lowering the power consumption.

Other reasons are that the real plant sometimes faces challenges to maintain the drying conditions, which could result in both excessive heating and cooling. There are extra heat loads from opening and closing doors and from people working in the rooms. In addition, there might be errors in assumptions on efficiencies for fans and pumps or in assumptions for the air distribution system. Pressure drop for refrigerants were neglected, and the applied temperature differences in the industry might be higher, increasing energy needs but allowing smaller heat exchangers.

The obtained SMER values were in the lower range of what one should expect from the values given by [Jon and Kiang, 2006], which will be repeated here. The normal values for heat pump drying were reported to be SMER $\in \{1.0, 4.0\}$, whereas in Table 7.1, none of the systems which cooled the entire air stream reached these values. HPSX100 had the highest value, 0.85, HPS only 0.70. BS had a value of 0.21, which is even among the worse results for conventional hot air drying for which SMER$\in \{0.12, 1.28\}$. This might be because hot air dryers heat the air just like BS, but they do not apply cooling, thus saving this energy.

SMER values for the systems where only a fraction of air was dewatered were within the reported range, 0.99 - 2.76, but this is still not close to the reported value of four. However, other drying processes apply higher temperatures, which is far more efficient in terms of removing water, but detrimental for meat quality [Strømmen, 1980], which explains much of the difference. High water removal is what SMER really measures. The reported total energy included energy needs caused by pressure drops in the air distribution system, which lowered the SMER values compared to other studies where this was not included. In addition, the process is low temperature drying for a long time, with low humidity and large amounts of air. This is also likely to make its performance lower than quick, high temperature drying.

Drying efficiencies were also lower than reported values. BS performed worse than the hot air dryers, with 15 % against $\eta_{dry} \in \{35, 40\}$ % for hot air drying. Only the systems with smaller mass flows of air managed to reach higher values. $\eta_{dry} \approx 95$ % was reported by [Jon and Kiang, 2006]. Both HPSX1 and CO2S achieved $\eta_{dry} > 100$ %, CO2S as high as 190 %, more than twice of HPSX37 and 68 % higher than for HPSX1.

All compression systems showed an increase in energy compared to BS, and a substantially increase too. Their SMER and efficiencies were much worse than those of all other types of dryers considered, but no other study of air compression to compare the result with was found. The adsorption system achieved results similar to those of HPS, but was not finished, and only a preliminary result is shown. Therefore, one should not trust these results completely, see also Appendix B and Appendix D, presenting the challenges related to the adsorption system. Key findings in Appendix B will be discussed in this section.

The energy reductions in Table 7.1 obtained for other systems were similar to other findings. The heat pump system reduced the needs by 70 %. In the review articles [Colak and Hepbasli, 2009b, Colak and Hepbasli, 2009a], the highest improvements were 60-80 %, found by [Strømmen et al., 2002], but most reductions reported were 30-50 %. Most of these studies compared heat pump drying to hot air drying, which does not involve refrigeration, so it is reasonable that the value in this work was relatively high.

A key factor to achieve low power consumption seemed to be to dehumidify as little air as possible, not only using the extra heat exchanger. This results from comparing HPSX37 and HPSX1, which were identical in equipment and only differed in mass flow of air. This is in accordance with several findings reviewed in [Colak and Hepbasli, 2009a], concluding that dryers with high airflows are not suited for heat pump drying. No matter how well a system performed, one must ask how much it would cost to buy the system, and whether it would be profitable in a sufficiently short time to be relevant for the industry. Some plants have already invested in adsorbers and heat pumps, but there were extra heat exchangers in the best systems, not only the heat pump. Equipment for monitoring and controlling the process adequately was also of major importance for the lower energy use in both this work and many existing firms [Strumillo et al., 2006].

Assuming a discount rent of 7 %, and an energy cost of 0.65 $\frac{\text{NOK}}{\text{kWh}}$, the possible investments for payback times of one to three years were calculated from Equation 6.16 and Equation 6.15. This was done for systems with lower energy consumption than BS, and savings were

Table 8.1: Calculated savings or investments that can be repaid in payback times of one to three years, compared to BS assuming the discount rent is 7 %, and the price of energy 0.65 $\frac{\text{NOK}}{\text{kWh}}$

System	Energy		Saved money	Investment that can be repaid in:		
	Required [MWh]	Saved [MWh/year]	[NOK/year]	1 year [NOK]	2 years [NOK]	3 years [NOK]
HPS	21.0	145.8	94 753	88 555	171 316	248 663
HPSX100	17.2	157.2	102 164	95 481	184 715	268 111
HPSX37	14.9	164.3	106 777	99 792	193 055	280 217
HPSX1	8.9	182.1	118 369	110 626	214 014	310 639
CO2S	5.3	193.0	125 418	117 213	226 758	329 137
ADS	27.6	126.1	81 971	76 608	148 205	215 117

calculated relative to this system. The results are shown in Table 8.1. Values for CS are not shown, as these numbers would be negative, and therefore not of interest.

Note that the numbers are based on drying 5400 hams of initially 8 kg, ending up with a total of 26 987 kg after drying. For larger production plants, the savings must be scaled up accordingly. Payback times beyond three years are normally not of interest to the industry and therefore not calculated.

Due to the lower energy demand in the basic system compared to the existing plant, the numbers in Table 8.1 might be too low. If the savings had instead been calculated from the energy required at the existing plant, either as differences in energy use or as the same percentage of saving as relative to BS, the savings would have been larger.

Subtracting the modelled energy needs in the different systems from the energy needed in the existing plant probably gives too optimistic estimates. Whatever made the energy demand of BS lower, the same assumptions and simplifications were used in all other systems. Their results are therefore also likely to be a bit lower than they would have been in reality.

Using the same relative savings as those compared to BS might be more correct, as BS should have had the same result as the real plant. One should then scale up all the results and savings by the ratio between real and modelled energy demand at the plant. This would make all the numbers in Table 8.1 about $\frac{3.79}{2.58} \approx 1.47$ times larger.

The fine thing about this uncertainty is that these three different ways of finding the savings could give a quite certain range for the true values, hence, it says something about the variance of the results, which is otherwise very difficult to obtain when using simulations.

From Table 8.1, the difference in profitable investments are not so different for the three first systems, the jump between each system is small, only that between HPSX37 and HPSX1 is somewhat larger. This shows that the benefit in decreasing the airflow was significant and lowered the energy consumption more than many other changes. The mass flow of air was the *only* difference between HPSX37 and HPSX1. The improvement might be somewhat optimistic though. All heat exchange was based on constant heat transfer coefficients.

Table 8.2: Savings if excess heat can be used elsewhere in the plant, equivalent with profitable investments, shown for payback times of one to three years, assuming a discount rent of 7 % and an energy price of 0.65 $\frac{\text{NOK}}{\text{kWh}}$.

System	Energy		Saved money	Investment that can be repaid in:		
	Required [MWh]	Saved [MWh/year]	[NOK/year]	1 year [NOK]	2 years [NOK]	3 years [NOK]
HPS	4.9	194.2	126 238	117 980	228 241	331 290
HPSX100	4.6	195.3	126 916	118 613	229 467	333 068
HPSX37	4.7	194.8	126 593	118 311	228 882	332 219
HPSX1	3.9	197.2	128 195	119 808	231 779	336 424
CO2S	0.3	208.1	135 281	126 431	244 591	355 021
CS	1.5	204.4	132 855	124 163	240 203	348 652

In reality, these will decrease with decreasing flows, thus, the actual amount of energy required for HPSX1 and CO2S might be somewhat higher than found here.

The small benefit of the extra heat exchanger in HPSX100 is not likely to pay off, as the heat transfer was small, and the reported saving was only about 20 000 NOK after three years. If an extra heat exchanger should be installed, it should be one for dehumidifying only a fraction of the air. An advantage with the systems using extra heat exchangers is that they use smaller heat pumps, 15 % smaller in HPSX100 and 25 % smaller in the other two, which could make the overall investment lower. Using CO_2 would also allow to buy much smaller compressors and other heat pump equipment, due to its high density. The calculated compressor volume was $28.5 \times 10^{-6}\,\text{m}^3$ compared to $201.3 \times 10^{-6}\,\text{m}^3$ for HPSX1, which was an identical system except for the use of ammonia and glycol. The high pressures are a challenge for the equipment, but it is commercially available [Fornasieri et al., 2009].

Calculations resulting in Table 8.1 were only conducted for systems that actually caused a reduction in energy demand. The compression system did not cause any such reduction, rather opposite. However, if the heated cooling water could reduce the energy demand somewhere else in a plant, for example to heat tap water, then all the energy for cooling in this system could be subtracted. Most food producers would need hot water for cleaning and other purposes. All the heat pump systems also rejected heat to the surroundings. This energy waste is equal to $E_{cool} + E_{compr} - E_{heat}$, and could be treated in a similar fashion. Table 8.2 shows the savings and possible investments if excess heat can be utilized.

For CS, only the results for compression to 3.0 bars is shown, because the differences in used energy for the other cases were very small, perhaps insignificant, and this was the lowest of the results. The adsorption system could not reject any excess heat, and is not included in Table 8.2. What is clear from Table 8.1 and Table 8.2 is that if there is a use for excess heat, then the adsorption system modelled here almost certainly would be worse than the other systems, as the true energy need for the system must be $\frac{(27.6-0.3)\text{ MWh}}{27.6\text{ MWh}} = 99\ \%$

lower. As it was not well modelled, nothing can be absolutely concluded, but it is highly unlikely that it could be improved this much.

Comparing Table 8.2 with Table 8.1 one must conclude that excess heat should not be dumped if there are heating demands somewhere else in the plant. Utilizing this heat increased the possible investments much more than any of the system changes did. It is then important to also consider the quality of the heat, though, not only the amount of it. The compression systems generally reached higher temperatures than the other systems, and these were constantly high, see also Appendix B. The temperatures in ammonia systems, despite that they are often high, can perhaps not be fully utilized, because the fluid is toxic and could require an extra glycol circuit and temperature difference for this purpose too.

Subtracting the excess heat, the compression system was actually one of the definite best systems, even better than HPSX1. The difference in profitable investments for these two was not big, but CS would remove entirely the need for a heat pump, which is not cheap, and avoid usage of a refrigerant with leakage and environmental concerns, and pressures that could cause explosion dangers at break downs [Fornasieri et al., 2009]. The required investment might be lower, and give fewer concerns. It reached temperatures well above 100 °C, making hot water production more than possible, and followed a very simple principle. Hence, if the heat sink is there, this appears to be a very good choice.

Implementation of CS would require that sufficient amounts of sufficiently cold groundwater is available. The latter could be a problem in countries with warmer climates than the temperate climate in Norway. Groundwater with a temperature of about 6 °C plus a reasonable temperature difference cannot cool further down than to about 13 °C. Hence, it cannot be applied for drying temperatures much lower than 13 °C unless: highly efficient heat exchangers are installed [Wadekar, 2000], more air than in this work is compressed to the same high pressure, or the same amount of air was compressed to a higher pressure. The first would simply allow a smaller temperature difference. The two latter would allow condensation of vapour at even higher temperatures than 13 °C, but also be less energy efficient. Other issues are whether necessary equipment is available and how well the process could be controlled, but the drying process is so slow that regulating it should be possible.

However, tap water could be heated by a heat pump rather than by excess heat from CS, which stemmed from the electrical power supply to the compressor. A heat pump would require a much smaller fraction of electric power, about one fourth of the total heating demand, and thus, the figures in Table 8.2 could be misleading. If the surplus heat should replace heat from a heat pump with an average COP of four, the energy requirements in Table 8.2 would be, in MWh:

- HPS: 17.0
- HPSX100: 14.1
- HPSX37: 12.3
- HPSX1: 7.7
- CO2S: 4.1
- CS: 144.6

CS would then again use more power than BS, and in this calculation, utilization of surplus heat had a similar effect as other system changes. Thus, what type of heat the surplus heat replaces is of great importance. Using these numbers to again find the necessary improvement of ADS to be equally good as CO2S, it must be $\frac{(27.6-4.1)\ \mathrm{MWh}}{27.6\ \mathrm{MWh}} = 85\ \%$ lower, which is still a major improvement.

Only if a heat pump cannot be used due to its cost, complexity or environmental problems related to the refrigerant, would CS truly be a good choice. In fact, if heat pumps should not be used, there are only two options left in Table 7.1.

CO2S was still the superior system. The difference between this and HPSX1 was regarded significant, and the two only possible explanations are that the temperature differences with glycol were not present in CO2S, and that a different working fluid was used.

Interestingly, HPSX37 and HPSX100 are about equally good in Table 8.2, actually HPSX100 is a bit better. The differences between them and HPS are also very small, so small they are probably insignificant. This indicates that if one can utilize the excess heat, then it does not matter which of these systems is used; they all recovered all latent heat from the same amount of vapour. The rejected and supplied heat within each system was more or less the same, so when all excess heat was useful, it did not matter much how large the air stream was and how much heat was transferred back and forth.

The reason HPSX1 was a bit better than the recently mentioned systems might be that its significantly smaller air flow (see Appendix B) reduced the pressure drop, thereby the fan power and heat from fans, and allowed the system to deliver more excess heat to the process air and less to outdoor air. Thus, fanning power for outdoor air was smaller. Overall, this reduced the energy demand a bit.

Section B.5.3 discusses whether the two parts of the airflow in HPSX37 and HPSX1 should be mixed before or after heating the air. The result was that the differences in pressure drop made it more efficient to mix after heating when the dehumidified air fraction was $\lessapprox 28\ \%$. This would presumably also be true for CO2S. How large the air fraction had to be depended on how moist the air was, so one should consider how moist the drying air normally is before choosing solution. The modelled batch process had a high drying rate initially and a low drying rate towards the end. However, in a drying tunnel one can put in new meat in one end and remove that which have been dried for a while from the other, achieving semi-continuous operation. All systems performed differently at different dehumidification loads. Which drying loads that normally occur should therefore be investigated. Simulating the systems at, or close to, full moisture load all the time could be equally relevant as the solution used here, and this could alter the results.

Some further questions that must be asked. One is whether it would be possible to realize CO2S in reality, especially with regards to subcritical and transcritical operation. In this work, Figure B.52 shows that the system managed to stay at subcritical operation throughout, but this should be discussed with a vendor.

Another question is the issue of frost formation in the air coolers of CO2S, HPSX1 and HPSX37, and in the air-air heat exchanger of ADS. This was ignored in this study where the focus was on energy, provided the air temperature did not reach the freezing point. Some defrosting technique could solve this, but also increase the energy demand a bit, or a very efficient heat exchanger with temperature difference of 1 °C could be bought to avoid it [Wadekar, 2000]. This would increase the pressure drop, and make a smaller airflow even more important. Eventually, one could conclude that the low temperature cooling in HPSX1 and HPSX37 was not a good solution, especially because the extra economical savings compared to HPS and HPSX100 were not *very* large.

The heat pump systems had the advantage of having their easiest outdoor conditions at the highest drying load. This might have made the comparison to the adsorption system a bit unfair. If the temperature profile had started at the highest value instead, there would have been full load and 30 °C outside at the same time. A real plant must handle this, and if this had occurred in the models, this could have made the energy results somewhat higher. This could be another explaination to why the power consumption of BS was lower than that of the existing plant. It would be interesting to run the temperature profile from the highest to the lowest temperature and see how this changed the results. This would for example remove the free cooling from ambient at the beginning, when highest need for cooling occurred. Perhaps it should be run in the opposite way for the adsorption and heat pump systems, to make the comparison more reasonable.

More research on the adsorption system is required to give a fair and valid comparison. The adsorption system was based on some assumptions that might be incorrect, further outlined in Section B.8, and unlike the other systems, it experienced the highest load from the process at the same time as the most difficult outdoor conditions for this system.

The system was not properly operated. It was designed to supply some electrical heat, but a heat pump should deliver most of the energy required. Doing so, in Appendix D, the heat pump simultaneously cooled the process air. When the air from the drying tunnel became drier (Figure B.2), if sufficient heat was supplied by the heat pump, then the air was cooled so much that excessive amounts of water were condensed. The air became too dry unless the heat pump supplied less, but then, the electrical heating had to increase, and likewise the total power. This resulted in the reported version of ADS, using 27.6 MWh.

If the system was run as planned, and dewatered the air more than it should, the energy need was 23.9 MWh. The rated power in the specifications for the adsorber was 10.3 kW. Assuming on-off operation as the producer, [AG,], informed was normal, and that the adsorber was on 60 % of the time, this would give a total energy demand of ≈ 24 MWh, calculated in Section B.8. The preliminary results therefore seem to be in the right range.

Most of the unfinished issues in this system would not affect the power consumption much. One main deviation from the real adsorbers was that the highest pressure in the heat pump decreased, though it should be kept constant by changing the amount of air for cooling.

The smallest reported airflow was used all the time, as it was considered unrealistic to use a lower value than the lowest applied in reality, and a too low airflow would not regenerate the adsorber sufficiently. However, increasing the amount of air, but reaching the same regeneration temperature would enhance power consumption even more. Recovering heat from the outgoing regeneration air was found to be of major importance in Section B.8. This amount could be increased if an additional evaporator replaced the air-air heat exchanger.

Nothing decisive can be said, but it does seem peculiar that the adsorber system should be better than the best heat pump systems when its energy demand was nearly 5.2 times higher than for the CO_2 system. On the other side, the system did remove *too much* vapour from the air. Perhaps would it be better at higher moisture loads, so one should really find out whether there are some more typical dehumidification loads, and what these are. Eventually, if the drying temperature had been higher, then the heat pump systems would have had lower performance, and an adsorber could perhaps be better. However, at the applied conditions, this much was clear: The adsorption system required less energy the more heat its heat pump supplied (see Section 6.4.5 or Section B.8 and Appendix D), because less electrical heating was then required. Thus, the closer the system operated to pure heat pump drying, the better it performed.

An important question for choice of energy system is whether a new plant shall be built or an existing one upgraded. If a plant were already built, then the investments would be smaller if only a part of the system should be implemented.

If one should upgrade BS to HPS, then one would only need to install an extra glycol circuit with two extra heat exchangers. If there is a use for the excess heat, this should be utilized, and a new heat exchanger could heat or preheat tap water. Because ammonia is toxic, it could be necessary with a third glycol circuit between the water and ammonia.

If no heat sink is available, the existing condenser could still be used, and because this one would be large, capable of rejecting all heat to outdoor air, this largest heat exchanger should be used for heating the process air if possible. This would allow smaller temperature differences in the system because the heat transfer area would be large. A small, new heat exchanger would then remove excess heat.

Changing BS to HPS would not be too big a change. Utilization of excess heat also requires investments, and changing the water supply system could be a larger change. Yet, comparing Table 8.1 and Table 8.2, this is likely to pay off.

An extra heat exchanger in addition could be uneconomical, as the differences in profitable investments were not too big. One should keep in mind though, that a larger production than assumed here would make all the numbers in Table 8.1 and Table 8.2 larger. In other words, the production should be of some size for the investments to pay off.

Some of the ideas in the best systems could be implemented inexpensively, though. If the amount of air for dehumidification is lowered when it is drier than saturated, then the power consumption would decrease without buying any new exchangers at all. Only monitoring and controlling equipment would be needed. This has been important for energy saving in several plants [Strumillo et al., 2006].

This simple, energy saving change could be implemented in either HPS and BS, and would not be costly. The results indicate that this would significantly lower the energy consumption, HPSX1 was about 40 % better than HPSX37, but again, it is an important question how moist the air normally is, as the difference between the mentioned systems depended on that.

Another, cheap change that could be made to any of the heat pump systems, either if it was a new plant or an upgrade of BS, is to vary which heat exchanger the ammonia enters directly after compression. In the heat pump systems, the heat exchanger with outdoor air was placed first and the glycol circuit after it. During the winter, however, this would be a disadvantage. If the exchangers were placed in the opposite order, the outdoor air could have subcooled the vapours significantly, and reduced overall power consumption much. Therefore it would have been even better to use a valve that allowed both options, depending on the present conditions.

A good strategy for an existing plant using ammonia and glycol could perhaps be to upgrade stepwise, first from BS to HPS, eventually also with decreasing flowrate of air for dehumidification and tap water heating, then to HPSX1. One could also keep BS, but utilize surplus heat and reduced airflow for a period, and then invest in HPS and finally HPSX1.

For the strategies above, one thing is highly important to notice. If heating of water was originally done by electricity, then the change from that the heat pump in BS heats the water and electricity heats the drying air, to that electricity heats water and the heat pump heats the air and partially the water, would not pay off at all. Then it would be better to keep the original strategy, or upgrade to HPSX1, but with electric heating of the air and heat pump heating of tap water.

Rebuilding a plant from using an ammonia heat pump to using a CO_2 heat pump could be a large investment. Equipment for CO_2 heat pumps is available and in use [Fornasieri et al., 2009], but due to the high pressures in a CO_2 heat pump, no, or at least very few, parts of the existing system could be used in the new installation. Hence, this is mainly an option if a new plant should be built.

The results of this work have some limitations. Simulations are not reality, and simplifications were used. No pipes between the components were assumed. There were thus no temperature or pressure changes between components. All fluid changes found place in heat exchangers, pipes and a pressure drop model. In addition, efficiencies in this study might deviate from the real ones.

Heat exchangers and compressors were, like in reality, modelled especially for each case and tested, but the author is unexperienced with this and a real producer must be consulted. The heat load in the calculations did not include any heat leakage because the idea of including it was introduced after all heat exchangers in several systems were designed. This was therefore done consistently in later heat exchanger designs too. In reality, several other heat loads should be estimated before dimensioning both exchangers and heat pumps. These would stem from opening and closing of doors, workers and equipment.

Many of the extra heat loads would be difficult to implement in DYMOLA, and require a large amount of guesses, as no data on this was available. They were therefore neglected, giving a lower energy demand than at the real plant. Heat from fans and pumps were included though. Their heat loads were unknown in size, but likely to be small, and the heaters and coolers were allowed to increase their supply if necessary. The assumed heat leakage with the surroundings was a rough guess, again because no data was available.

A more energy efficient process and smaller heat exchangers could have been achieved by newer types of exchangers [Wadekar, 2000]. For this work to be of interest to the industry, it was decided that the simulations should not use equipment so expensive that the industry will not buy it. Better heat exchangers also give higher pressure drops [Wadekar, 2000]. It was discovered in Section B.5.3 that higher pressure drops alone could increase power consumption to a high extent. In HPSX1, lower flow and pressure drops in the heat exchangers were determining for the final energy result.

Really, drying of cured meat is a very slow, quasi-steady process, and running a dynamic simulation of it could be questioned. An alternative would of course be to assume constant conditions in the drying air after the tunnel, especially if semi-continuous operation is used. The same would be the case for a plant with many drying chambers using the same air supply system, filling and emptying the chambers at different times. Doing so, one must find out whether the constant conditions should be saturated air or another condition, and in the latter case which one.

Studying Figure B.2, it is seen that the dynamics of the process diminished with time. Only at the very start, when the drying tunnel contained only undried hams, was the air moist with steep changes in conditions. 80 % of the time or so, the temperature and humidity profiles from drying were relatively flat. Hence, the drying was quasi-steady most of the time, and the simulations were, if not entirely realistic, not far from it either. Most of the dynamics stemmed from the dynamic outdoor temperature.

Finally, it must be emphasized that this work only is a part of a larger picture. Only energy was considered. No discussion on fouling and maintenance was included. The quality of surplus heat was only briefly mentioned; perhaps an exergy study of the process would have been better. Important issues like flavour and texture development during ripening, avoiding mites and ensuring meat quality were only included through the decision to model the drying conditions applied in reality, hoping this would ensure satisfactory meat quality. From this, many other aspects than energy must be considered in the choice of drying system.

Chapter 9

CONCLUSIONS

The CO_2 system was the most energy efficient system, 92 % better than the basic system, BS, followed by the same system using ammonia, HPSX1. Changing from ammonia to CO_2 reduced the required energy by 40 %, mainly due to the avoided temperature differences with glycol.

The energy used in the basic system was lower than in reality, but it was in the right range. The deviation was due to, among other factors, the near-ideal operation in the simulation and neglection of heat loads from equipment, workers and opening of doors. Changing BS to the heat pump system HPS, decreased the energy needs by 70 %.

All systems showed satisfactory operational conditions. Some instabilities occurred, though, making simulation of a closed air system apparently impossible, but the final air conditions were so close to the initial ones that modelling the closed process as an open one was justified.

Most of the obtained SMER values and drying efficiencies were in the lower range for heat pump drying, probably because of the inclusion of pressure drops and the long time, low temperature drying with low moisture content and large airflow. Dehumidifying less of the air increased these numbers to more typical values. Because of the use of simulations, it was difficult to say anything about the variance of the results.

Utilization of excess heat lowered energy requirements substantially, potentially more than any other system change, but this strongly depended on which energy supply it should replace, and its quality. Another highly important factor for high efficiency was the recovery of latent heat from the water vapour in a heat pump, as no system can achieve efficiencies above 100 % without it. A third was to dehumidify an as small part of the air as possible.

The last of the three was possible because the amount of moisture in the air decreased with time. How moist the air would typically be is important for choice of energy system. All systems should be dimensioned for maximal load, but optimized for a typical condition.

Investments that could be paid back in one, two or three years were found, and realization of the systems was discussed. Decreasing the airflow being dehumidified, was a simple change that could easily and inexpensively be implemented in an existing plant. Rebuilding the supply system for tap water could be a larger change, but large savings could also be achieved.

Existing plants using ammonia systems could upgrade stepwise to ammonia systems with better performance. For new plants, a system similar to CO2S should be chosen. Suggestions for further improvements were found, and are repeated in Chapter 10.

Frost formation could be a problem in CO2S, HPSX1, HPSX37 and the adsorption system ADS. Suggestions to face this challenge were defrosting and highly efficient heat exchangers, but further investigation is needed before these systems can be implemented.

The compression system, CS, had the advantages of simplicity and a probably low investment cost, but the running cost would be so high it would only be beneficial if surplus heat could be utilized and heat pumps for some reason should be avoided.

The adsorber system was not completed. A preliminary result presented seemed to be in the right range, and indicated that its performance was similar to that of HPS. If surplus heat could be used, the adsorber was much worse than the heat pump systems. Its true result must be 85 % lower if it should be equally good, and the closer to heat pump drying it operated, the less energy it used. Some obtained drying efficiencies exceeded 100 %. Hence, adsorbers *must* use a heat pump to outperform good heat pump dryers. It could perhaps perform better at higher drying temperatures or for higher moisture loads.

Comparing energy needs is just one of many aspects that should be considered in choosing system solution. Quality, fouling, maintenance and many other issues were not covered in this study, but real drying conditions were modelled to ensure meat quality. Hence, this work is a small part of a larger picture, but an important one, as potential energy savings up to 92 % were found. This is of both economical and environmental importance, as use of most energy resources pollute and the prices increase. Efficient energy systems is therefore becoming even more important for producers to retain liquidity and stay competitive.

A proposal for further work is given in Chapter 10, and an article about the work is found in Appendix A. All tasks in the project description, on the first page in this work, were thus completed.

Chapter 10

PROPOSAL FOR FURTHER WORK

Further work should look into adding missing data, improving systems further and evaluate their realization. One should investigate typical air conditions and the quality aspects of meat during drying, to find optimal drying conditions and methods, like in [Stollewerk et al., 2012]. A detailed list of suggestions is presented here.

- It should be measured which conditions of the drying air, if any, are typical when it exits the drying tunnel. If they exist, one should optimize dehumidification for these.
- How to implement and realize the systems must be considered in greater detail. Possible challenges with ice formation, and trans- or subcritical operation for CO_2 should be investigated, to find out whether or not this could be successfully realized.
- The adsorption system should be properly modelled, preferably in contact with the producer [AG,], and data on adsorbers in use should be found.
- [AG,] informed that the air streams in their adsorbers are kept constant, but decreasing them could probably lower energy needs much, similar to for heat pump systems, and this should be considered.
- Other ways of heat recovery and other sources of free heat to the adsorption system could lower its energy requirements substantially. One promising suggestion to look into is the use of an additional evaporator in the exiting regeneration air.
- All systems should be run with the temperature profile staring both at high and low temperatures, to obtain fairer comparisons.
- An exergy analysis of the systems should be performed.
- Possible improvements by utilization of better heat exchangers as reported by [Wadekar, 2000] should be quantified, including the drawback of higher pressure drops.
- One should investigate the possibility of allowing refrigerants to alternate between the heat exchangers cooling it, depending on which option gives more subcooling.
- Optimal drying and ripening conditions for meat quality is of great importance, and should be optimized, applying experiments.

- A promising method for faster drying and ripening is reported to lower power consumption substantially [Stollewerk et al., 2012]. Faster production could also be achieved by boning and skinning before drying according to [Montgomery et al., 1976]. This should be looked closer into.

Appendix A

ARTICLE SUMMARIZING THE WORK

Efficient energy systems for the dry-cured meat industry

Karoline Husevåg Kvalsvik
Norwegian University of Science and Technology, Trondheim, 7491, Norway
karolinehk@broadpark.no

ABSTRACT

Eight energy systems for dry-cured meat drying were modelled and simulated in DYMOLA and their energy consumptions compared. The systems included heat pumps, electrical heat, air compression and adsorption. All but an adsorption system were satisfactorily modelled, and a system using CO_2, with an additional heat exchanger and controlled to dehumidify as little of the air as possible, showed the best performance. A similar ammonia system was the second best if excess heat could be utilized, using 8.9 MWh against 5.3 MWh in the simulation. Drying efficiencies up to 190 % were found. Utilization of excess heat and minimizing the fraction of air for dehumidification had large impacts.

1. INTRODUCTION

To minimize production costs in the energy intensive industry of dry-cured meat, an energy effective drying process is necessary (Bantle et al., 2014, Colak and Hepbasli, 2009b). Dry-cured meat is meat that is salted and dried, often for very long times, to achieve desired aromas and preservation (Toldrá, 2002). Many techniques to lower drying time have been performed, but frequently, these either harm the product, drying the meat too hard or increase energy consumption or both (Toldrá, 2002, Bantle et al., 2014). For high quality products, faster drying must be accompanied by faster ripening processes in the meat, which determines the flavour, but this is difficult to achieve (Toldrà, 2002). Alternatively, the required drying conditions and time can be kept, but the system supplying them be made as efficiently as possible. Higher efficiency could be achieved by using heat pumps (Colak and Hepbasli, 2009a and b), using adsorbers (AG), reducing fanning power (Alcazár-Ortega et al., 2011) or including extra heat exchangers (Haukås, 2010). This work considered all these methods and a system compressing air for high-temperature condensation. As ammonia is a usual medium in heat pumps and CO_2 a promising one (Fornasieri et al., 2009), both were included.

2. METHOD

Modelling and simulation of 5400 hams in a drying tunnel with six successive sections, each with uniform conditions, were performed in DYMOLA. To ensure satisfactory quality, real drying

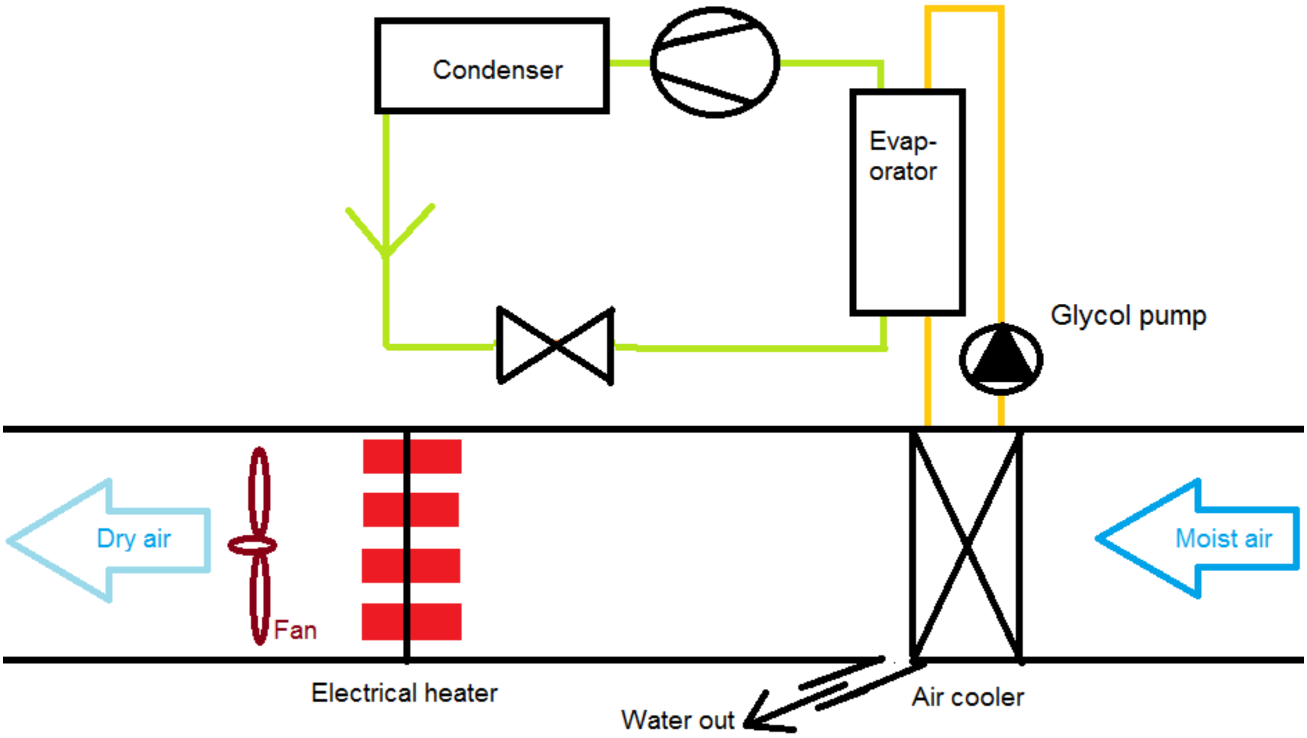

Figure 1: The basic system involved cooling by an ammonia and glycol system for condensing water, rejecting surplus heat to ambient and electrical heating.

conditions were used. Simulation lasted until all hams had lost 35 % of their original weight of eight kg assuming a loss of 3.5 % before drying (Toldrà, 2002). To model the meat being dried a model developed by Strømmen (1980) was used. Its parameters were based on experiments by Inna Petrova and Michael Bantle, described by Kvalsvik (2014). Medium salted ham was assumed, and the drying conditions were 13 ^{0}C and 68 % relative humidity.

An energy system similar to a system at an existing plant was modelled. All results were compared to this basic system, denoted BS. It used refrigeration with ammonia to condense vapour from moist drying air, and electrical heating, as seen in figure 1.

Table 1: Overview over the energy systems considered, where the adsorber system used a CO_2 heat pump and all heat pump systems except CO2S used an ammonia heat pump and glycol circuits for heat transfer

System name	Description
BS	Basic system with refrigeration for cooling and electrical heating
HPS	Heat pump system with a heat pump for both cooling and heating
HPSX100	Heat pump system with extra heat exchanger, dehumidifying 100 % of the air
HPSX37	Heat pump system with extra heat exchanger, dehumidifying 37 % of the air
HPSX1	Heat pump system with extra heat exchanger, always cooling to 1 ^{0}C
CO2S	Best performing ammonia system made with CO_2 heat pump, without glycol
CS	Compression system where air is compressed to condense water
ADS	Adsorption system using Econosorb and recovering heat in a heat exchanger

The drying involved a closed air system, because otherwise, energy is rejected to ambient, and closed systems gives higher quality (Colak and Hepbasli, 2009b) A glycol circuit exchanged heat between the ammonia evaporator and the air, as ammonia is toxic. Excess heat was rejected to ambient.

Heat pump systems use some of this excess heat for reheating the air. These systems were abbreviated HPS (which was otherwise equal to BS) or HPSX followed by a number. All these used ammonia and required an additional glycol circuit for heating the air. See also figure 2.

Using an extra heat exchanger between cooled, dehumidified air and the uncooled, wet air, some free cooling and heating is obtainable (Haukås, 2010). Systems denoted HPSX plus a number, which are further explained in table 1, used such an extra exchanger. Some of them dewatered only a part of the drying air to save energy, but this also requires condensation at a lower temperature to remove sufficient amounts of water from this smaller stream.

Studying a Mollier diagram, required cooling and heating was found for all systems. Cooling all the air, it should be cooled to 7 ^{0}C if it was saturated before cooling. Systems cooling a fraction of the air, cooled it to 1 ^{0}C if it was saturated, and heated it to about 18 ^{0}C. 1 ^{0}C was chosen to stay above the freezing point of water. The smallest fraction of saturated air one could dewater by cooling to 1 ^{0}C is ≈37 %, and was done in HPSX37.

Less cooling is required for unsaturated air, and so the temperature for condensation rises for drier air. Eventually the same temperatures can be kept if an even lower air fraction is dried. The last principle was applied in HPSX1 and a system denoted CO2S, keeping the lowest air temperature constant by decreasing the airflow for dehumidification for drier air.

CO2S was equal to HPSX1 except that it used CO_2 as refrigerant, and avoided the glycol circuits and extra temperature differences. This should lower its power consumption.

Another possible technique for dehumidification was to compress the air, increasing the dew point and allowing condensation at a higher temperature. Cooling could then be achieved by heat exchange with ground water at 6 ^{0}C (TrønderEnergi AS, 2013), avoiding a heat pump. Only a fraction of the air was compressed, and this fraction decreased with drier air, to avoid excessive drying while maintaining the same high pressure. Calculations showed that an appropriate operation point would be compressing 1.01 kg air/s to 3.0 bars at saturated inlet conditions. Pressures of 2.5 and 3.5 bars were also investigated for comparison.

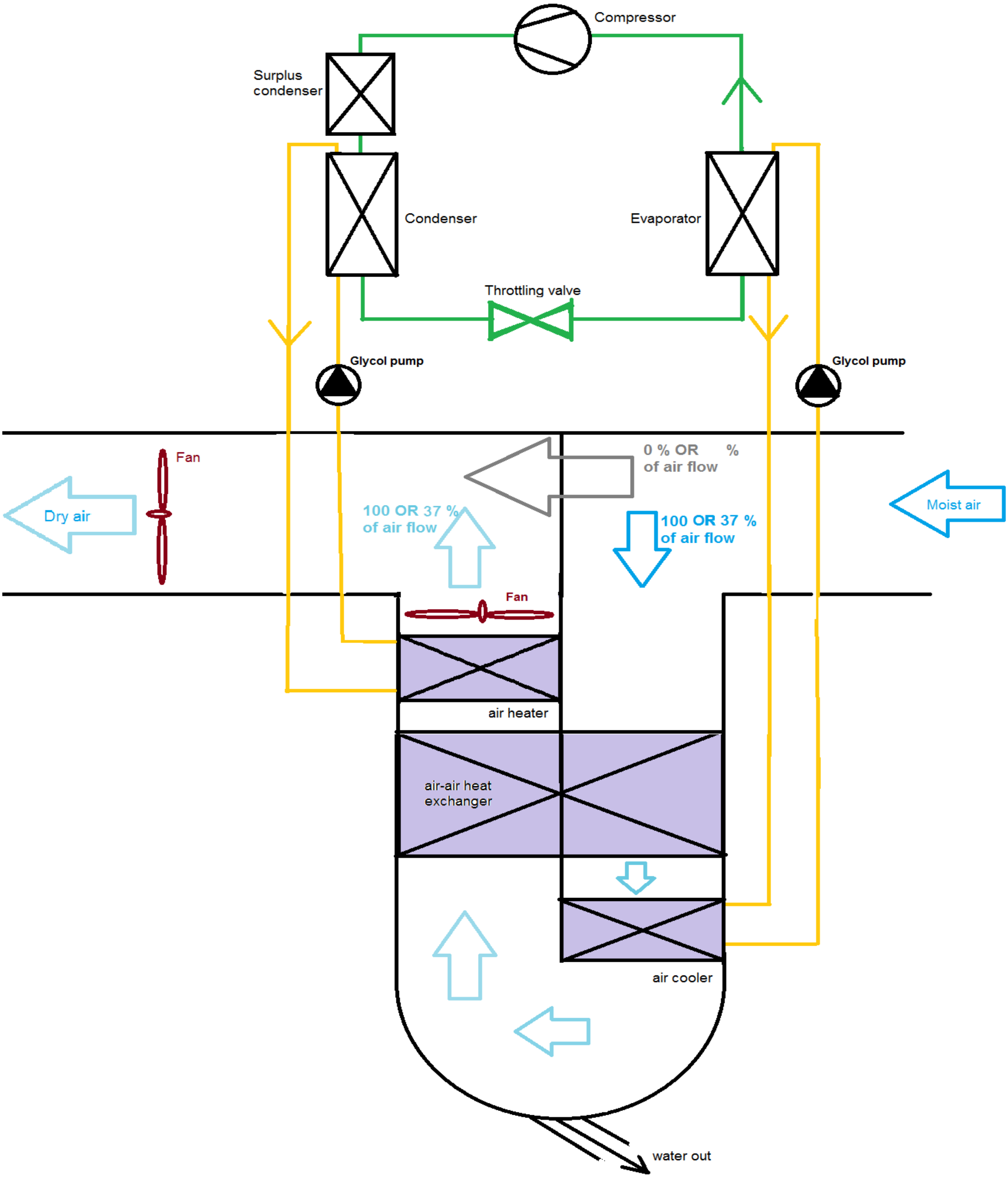

Figure 2: The HPSX systems involved cooling and heating one part of the air (blue arrows), and bypassing some of it (grey arrow). In HPSX100, The grey arrow would have zero flow; all air entered the air-air-heat exchanger, the cooler, air-air exchanger and air heater. In HPSX37, the grey arrow had a value of 63 % and the blue ones 37 %, in HPSX1 and CO2S the fraction for cooling decreased. In CO2S, the heater and cooler would be condenser and evaporator in a CO_2 heat pump, unlike the ammonia and glycol circuits shown. In HPS, the grey arrow would have a flow of zero, and the air-air heat exchanger would not be present.

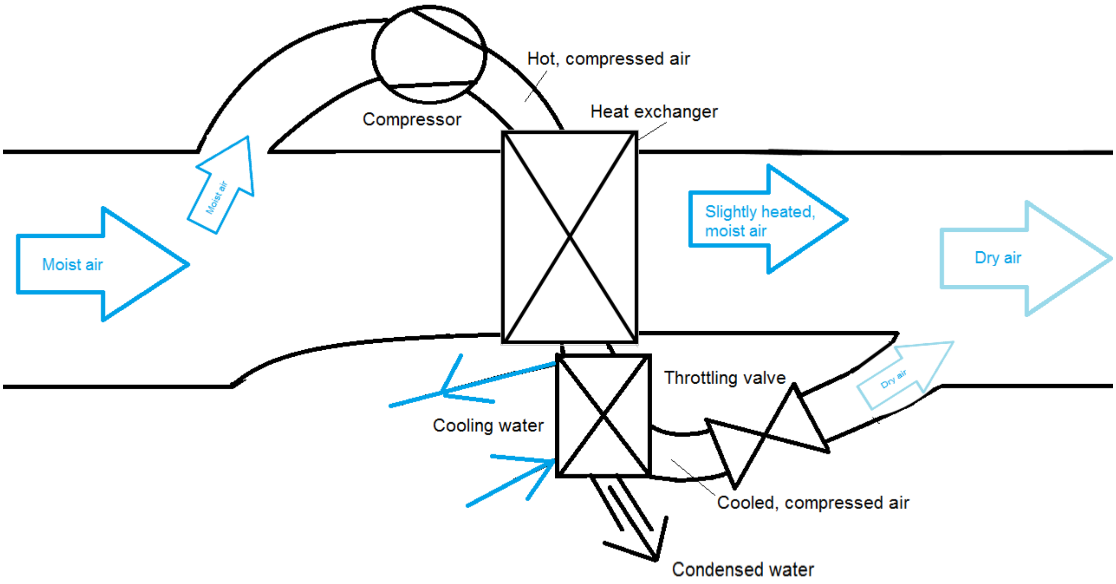

Figure 3: The principle of the air compression system, CS, where a part of the moist air is compressed, heats the uncompressed air and is cooled in an air-water heat exchanger before throttling and remixing of air

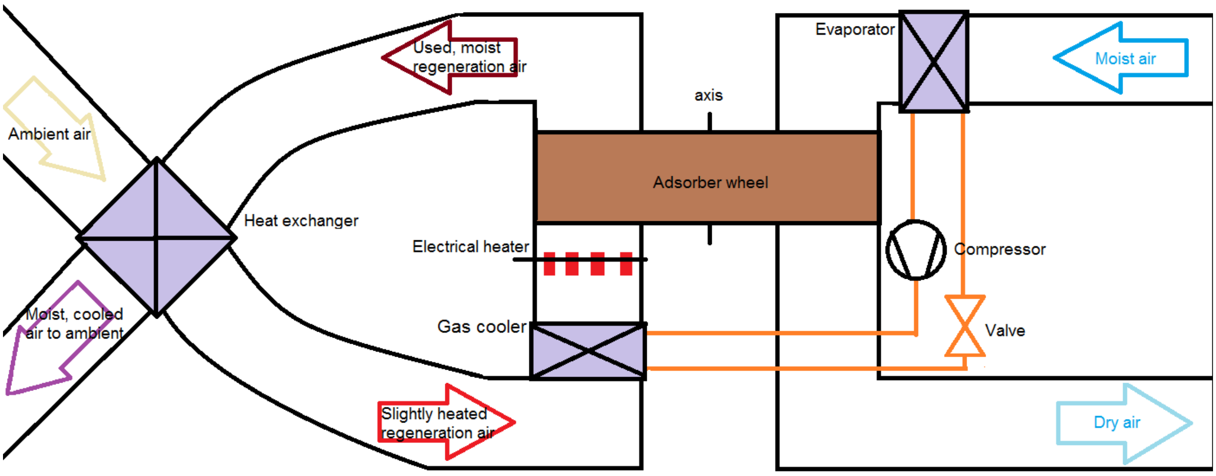

Figure 4: The modelled adsorber system, ADS, based on Econosorb from AG, except that an additional air-air heat exchanger was added to recover heat: From the upper left corner, ambient air enters the exchanger, is partially heated to regenerate the adsorber wheel. It is further heated by a heat pump and eventually an electrical heater, it desorbs moisture in the right part of the wheel, which rotates about the drawn axis. It preheats incoming air before it exits. The moist drying air, in the upper right corner, is cooled by the heat pump, some moisture condenses, remaining moisture is adsorbed in the wheel.

A final system used an adsorber from AG, and the modelled unit was Econosorb, EF-102E, using data from its specifications, available at http://docsio.net/doc/69821/econosorb---frigosorb, and assuming the correction factor given in a diagram here was 0.8. It involved adsorbing the air moisture to one part of a rotating disc, comprised by an adsorbing material. The other part of this wheel was dried by an air stream at 55 ^{0}C, regenerating the material for reuse upon next rotation. This regeneration air was taken from ambient. It was heated by a transcritical CO_2 heat pump, which also cooled the drying air before adsorption. The principle is shown in figure 4. At low outdoor temperatures, the lowest -17 ^{0}C, the heat pump could not manage the heating alone, and electrical heat was needed in addition.

This adsorber system, ADS, was modelled with the simplification that the adsorber worked as desired, provided the regeneration air was hot enough to have the same high temperature after regeneration as initially, 28.2 ^{0}C. Real adsorbers do operate well, but the relations between regeneration temperature and operation were unknown, making this simplification necessary.

Ambient temperature was modelled from climate data at www.yr.no from Voll, Trondheim, Norway, by fitting a curve to the data, as seen in figure 5.

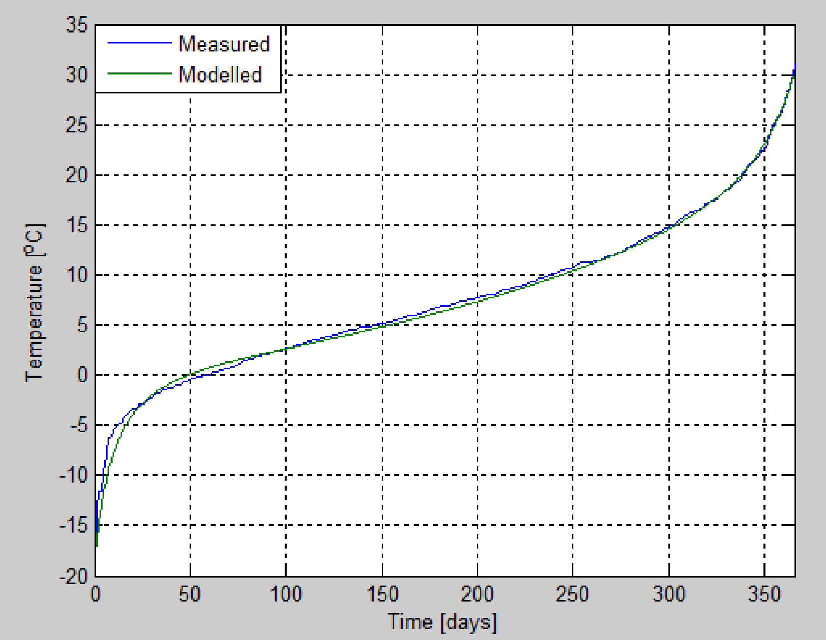

Figure 5: Measured and modelled outdoor temperature, based on data from www.yr.no, from Voll, Trondheim, Norway from fourth of February 2014 to third of Feruary 2015: Minimum and maximum temperatures for each day were used.

Heat pumps were designed with one stage compression, internal heat exchange after condensation and before compression and varying isentropic and volumetric efficiencies, given in the subject TEP4255 at NTNU the spring 2014. Pressure drops for refrigerants were neglected.

Pressure drops for air were modelled by the Haaf model in DYMOLA. For glycol and water, a quadratic expression, $dp=0.556\dot{m}^2$, fitted to values from Carrier (2013) was used. Pressure drops occurred in heat exchangers and in an assumed air distribution system, 2x100 m long (to and from) and circular pipes 1 m in diameter. Fans and pumps had efficiencies of 0.6 and 0.4, in that order, and losses were added to the fluids' energy balance.

All heat exchangers were specially designed for each case, using the method $Q\Delta = \Delta T_{lm}$ UA when possible, and the NTU method otherwise, both described in (Bergman et al., 2011). The methods give the same answers, so no inconsistency resulted. The first one is simpler, but not always applicable. A temperature difference of 7 ^{0}C was used except for at the worst operational conditions, were 5 ^{0}C was allowed, mainly to avoid too high pressures, and in the air-air heat exchangers in heat pump systems.

In the latter ones, a difference of 7 ^{0}C was not always obtainable due to the inlet temperatures, and 1.7 ^{0}C was used consistently instead. More details on this work can be found in (Kvalsvik, 2015).

Performance was reported as required energy, drying efficiency, and SMER. Efficiency is the ratio of energy to evaporate the water from the product to the total amount of energy used. SMER is specific moisture extraction ratio, kg of water evaporated divided by energy needed. Typical values are given in table 1.

Table 2: Typical values for drying efficiency and SMER, taken from Jon and Kiang (2006)

	Hot air drying	Heat pump drying
SMER	0.12-1.28	1.0-4.0
Efficiency	0.35-0.40	0.95

A cost analysis for how large investments would be profitable was also performed, assuming a discount rent of 7 % and an energy price of 0.65 NOK/kWh. Savings in terms of energy and money per year were calculated relative to BS, and investments with payback times of one to three years found.

3. RESULTS

Required energy per kg of produced ham in BS was 2.58 kWh, or ≈68 % of the average value for a real plant, 3.79 kWh/kg. The used amounts of groundwater in the compression system, listing values corresponding to from the lowest to the highest pressure were 3.01, 2.83 and 2.16 tonnes.

*Table 3: Resulting energy flows and improvements compared to the basic system BS: The total energy was E_{tot}, energy for compression E_{compr}, and energy for heating and cooling the air, E_q and E_{cool}. SMER is the specific moisture extraction ratio, or kg evaporated water per kWh used. Three results are given for the compression system; CS2.5 compressed the drying air to 2.5 bars; CS3.0 compressed the air to 3.0 bars and CS3.5 to 3.5 bars. Energy for heating in the adsorption system was 18.67 MWh from electrical heating and 33.45 MWh from the heat pump. ***Preliminary result, model not entirely completed*

System:	E_{tot} [MWh]	E_{compr} [MWh]	E_{cool} [MWh]	E_q [MWh]	SMER [kg water/kWh]	Efficiency	Improvement
BS	69.64	6.54	60.60	58.13	0.21	15 %	0 %
HPS	21.05	10.23	60.55	54.63	0.70	48 %	70 %
HPSX100	17.25	7.87	48.51	43.68	0.85	59 %	75 %
HPSX37	14.88	4.68	29.98	24.50	0.99	68 %	79 %
HPSX1	8.93	4.39	22.66	22.01	1.65	113 %	87 %
CO2S	5.32	3.81	25.13	23.88	2.76	190 %	92 %
CS2.5	196.19	194.92	194.71	0.00	0.07	5 %	-182 %
CS3.0	192.27	191.00	190.76	0.00	0.08	5 %	-176 %
CS3.5	192.69	191.42	191.15	0.00	0.08	5 %	-177 %
ADS***	27.60	6.63	26.54	52.12	0.53	37 %	60 %

4. DISCUSSION

Best results were obtained for CO2S, which performed 40 % better than the second best, HPSX1. Avoidance of extra temperature differences with glycol was probable the main reason for the large difference. Both these dehumidified an as small part of the airflow as possible, and HPSX37 performed better than HPSX100, thus this seemed to be important for high efficiency. The effect of changing refrigerant in itself cannot be seen from the results.

The result for BS was lower than for a real plant, probably because of the near ideal operation in simulation, and possibly wrong assumptions on efficiencies, air distribution systems and temperature differences.

Upgrading from BS to HPS, required energy was reduced by 70 %, similar to a result reported by Strømmen et al. (2002) in a review by Colak and Hepbasli (2009a). Most energy savings reported in this review were lower, normally 30-50 %, but they also compared heat pump drying to hot air drying, not to BS, which involves cooling as well as heating, and so a higher improvement should be expected here.

SMER and efficiency for BS was also lower than typical values for hot air drying, shown in table 1. Inclusion of pressure drops, the low temperature, long drying time and large airflow could also be reasons for this, as most of the heat pump systems also had lower SMER and efficiency than the typical values. CO2S and HPSX1 on the other side, had high efficiencies and typical SMER values, but not as high as the highest reported by Jon and Kiang (2006).

Table 4: Calculated savings or investments that can be repaid in payback times of one to three years, compared to BS, assuming the discount rent is 7 %, and the price of energy 0.65 NOK/kWh.

System	Required energy [MWh]	Saved energy [MWh/year]	Saved money [NOK/year]	Investment [NOK] that can be repaid in:		
				1 year	2 years	3 years
HPS	21.05	145.8	94 753	88 555	171 316	248 663
HPSX100	17.25	157.2	102 164	95 481	184 715	268 111
HPSX37	14.88	164.3	106 777	99 792	193 055	280 217
HPSX1	8.93	182.1	118 369	110 626	214 014	310 639
CO2S	5.32	193.0	125 418	117 213	226 758	329 137
ADS	27.60	126.1	81 971	76 608	148 205	215 117

A cost analysis resulted in table 4, and showed that the differences in possible investments between the heat pump systems using ammonia were relatively small, but the simulation results were valid for 5400 hams of initially eight kg each. After drying the total weight of all hams were 26 987 kg. For larger production, one must scale up these numbers accordingly. Because BS used less energy than the real plant, the values shown are probably a bit low. One should perhaps multiply by a factor 3.79/2.58≈1.47. This says something about uncertainty for the results. Only results for systems requiring less energy than BS were included.

Most systems had surplus heat, which was dumped to the surroundings. An energy efficient plant would rather use it for heat demands, like heating tap water, if possible. In this case, subtracting the excess heat, all systems but ADS would have other results, shown in table 5.

Table 5: Savings if excess heat can be utilized, equivalent with profitable investments, shown for payback times of one to three years, assuming a discount rent of 7 % and an energy price of 0.65 NOK/kWh.

System	Required energy [MWh]	Saved energy [MWh/year]	Saved money [NOK/year]	Investment [NOK] that can be repaid in:		
				1 year	2 years	3 years
HPS	4.90	194.2	126238	117980	228241	331290
HPSX100	4.55	195.3	126916	118613	229467	333068
HPSX37	4.72	194.8	126593	118311	228882	332219
HPSX1	3.90	197.2	128195	119808	231779	336424
CO2S	0.26	208.1	135281	126431	244591	355021
CS3.0	1.51	204.4	132855	124163	240203	348652

In this case, CS was actually the second best system. Only the best result is shown as the results were nearly identical. This system would also be fair simpler, probably cheaper than the others, and avoid refrigerants and their environmental concerns (Fornasieri et al., 2009). It also reached higher temperatures than the other systems, ≈145 ^{0}C against about 80-120 ^{0}C in other systems. The quality of the surplus heat is not shown in any of these calculations, and perhaps an exergy analysis would be more appropriate. It did however, require a low groundwater temperature, and might only be applicable in temperate or colder climates.

An efficient plant would heat tap water by a heat pump, though, not electricity, thus, only a fraction of the heat should be subtracted. Assuming heating with COP=4, then only ¼ of the energy should be subtracted, giving values for E_{tot} [MWh] of HPS: 17.0, HPSX100: 14.1, HPSX37: 12.3, HPSX1: 7.7, CO2S: 4.1 and CS: 144.6. Thus, the value for CS is again higher than that of BS, and this system is only economical if heat pumps should be avoided. However, one should utilize surplus heat, as it resulted in savings of significant sizes.

The adsorption system was not entirely completed, but a preliminary result is shown. The heat demand for the regeneration air was high, and designing the system, it was assumed that much of this heat

could be taken form the drying air. However, as the drying air became less moist as the process proceeded, the same amount of cooling resulted in excessive condensation of vapour before the adsorber. Too dry final conditions, and total energy needs of ≈23.9 MWh, were achieved unless more heat was supplied electrically, which increased the energy demand to 27.60 MWh.
Unsolved challenges then were that the heat pump pressure, which should be kept constant by higher airflows at higher outdoor temperatures, fell despite that the minimum airflow of regeneration air was used. It would be unrealistic to use less than the reported minimum, but then the high pressure was not constant, as it should. Therefore, the obtained results probably differ somewhat from the true value, but using the rated total power, 10.3 kW, and assuming that it was run 60 \% of the time due to the normally applied on-off operation, total energy should be 10.3 kW · 0.6 · 1.4e7 s ≈24 MWh. Hence, the obtained results seemed to be in the right range. If excess heat could be utilized, the energy required should be 85-99 % lower to be equally good as CO2S, depending on whether one fourth or all of the heat was subtracted.

Whether a new plant should be built or an existing upgraded determines which investments would be good. Plants using ammonia cannot use the same equipment with CO_2 in it instead, due to its much higher pressure. The higher density of CO_2 means that its equipment would be smaller, and avoiding the glycol, new plants should be built with CO_2, as this would be more efficient and perhaps cheaper to buy. Existing plants using ammonia should rather upgrade stepwise to better ammonia systems. Both solutions should utilize surplus heat if possible. One efficient but simple and inexpensive change that any system could implement is to dehumidify as little of the air as possible. However, one should also evaluate the adsorber more properly than managed here before making any decision.

Ice formation could be a problem in systems were air is cooled to 1 ^{0}C (CO2S, HPSX37, HPSX1 and ADS), because the surfaces might be colder than this. Defrosting or highly efficient heat exchangers, allowing 0 ^{0}C in the other fluid could solve this (Wadekar, 2000), but both would increase energy needs somewhat. However, this increase is likely to be quite small.

A concern related to the use of CO_2 in a heat pump is that the process might operate very close to the critical point, which could make the compression cycle perform very poorly. In this simulation, the allowance to heat up the process air, which was cold throughout the year, was highly determining for good operation. Placing the heat exchanger with outdoor air before the heat exchanger with process air, like in figure 2, was also important for this, and it should be especially considered upon realization of such a system.

5. CONCLUSIONS

The highest efficiency was obtained for CO2S. Avoiding extra temperature differences, decreased energy needs by 40 %. Utilization of excess heat and dewatering as little air as possible were also important ways to decrease energy needs. Heat pump drying is efficient, as latent heat can be recovered, and efficiencies up to 190 % were achieved. To compete with this, an adsorber must also use a heat pump. A preliminary result indicated it was no better than heat pump systems at the applied conditions, but this system was not completed. The advantages of heat pump drying would increase even more if surplus heat could be used. Compressing the air showed poor results unless surplus heat could replace electrical heating, which would rarely be relevant.

6. FURTHER WORK

Realization of the systems must be further investigated. Especially ice formation and use of CO_2 close its critical point could bid on challenges. Because utilization of excess heat had a great impact, an exergy analysis should be carried out. Modelling of the adsorption system should be completed, and data on real adsorbers collected.

7. ACKNOWLEDGEMENTS

Professor Trygve M. Eikevik, NTNU shall have thanks for supervising this work. It was supported by the Research Council of Norway, Nortura AS, BWL Maskin and Alfsen & Gunderson through the project DryMeat (grant 225262/E40). Many thanks to the Food Technology Group of NTNU and the Sintef Energy Research for their support. Especially PhD. Michael Bantle, Civil engineer Erlend Indergård and PhD. Cand. Nicolas Fidorra at Sintef Energy Research and Sales engineer Willy Bruràs at BWL Maskin and Alfsen \& Gunderson have all been very helpful, supplied both data, information and other help, for which the author is very grateful.

8. REFERENCES

AG. Alfsen og Gunderson: Luftavfuktning - avfuktere. http://ag.no/produkter-og-tjenester/luftavfuktning-avfuktere-1.aspx. Accessed: 15.12.2014.

Carrier (2013). 30rb/rq modular. http://www.carrier.co.th/pdcarrier/catalogue/Chiller_Catalog/air_cooled/30RBRQ_Modular.pdf. Accessed: 30.01.2015.

Alcazár-Ortega, M., Erscrivá-Escrivá, G., Álvarez Bel, C., and Domijan, A. (2011). Active demand response strategies to improve energy efficiency in the meat industry. In *World renewable Energy Congress 2011 - Sweden*.

Bantle, M. and Eikevik, T. M. (2014). A study of the energy efficiency of convective drying systems assisted by ultrasound in the production of clipfish. *Journal of Cleaner Production*, 65(0):217 – 223.

Bantle, M., Petrova, I., Raiser, J., and Eikevik, T. M. (2014). Dynamic model and kinetics for convective drying of ham with different salt contents. In *19th International drying Symposium (IDS).*

Bergman, T. L., DeWitt, D. P., Incropera, F. P., and Lavine, A. S. (2011). *Heat and mass transfer in capillary porous bodies*. Wiley, New York, 7th edition.

Colak, N. and Hepbasli, A. (2009a). A review of heat-pump drying (hpd): Part 2–applications and performance assessments. *Energy Conversion and Management*, 50(9):2187 – 2199.

Colak, N. and Hepbasli, A. (2009b). A review of heat pump drying: Part 1 – systems, models and studies. *Energy Conversion and Management,* 50(9):2180 –2186.

Fornasieri, E., Zilio, C., Cecchinato, L., Corradi, M., and Minetto, S. (2009). Natural refrigerant CO_2. Technical report, University of Padova. Part of Leonard project ”NARECO2”, edited by Walter Reulens.

Haukås, H. T. (2010). Heat pumps for various applications.

Jon, C. K. and Kiang, C. S. (2006). Heat pump drying systems. In Mujumdar, A. S., editor, *Handbook of Industrial Drying*. CRC Press.

Kvalsvik, K. H. (2014). Evaluation of three drying models for dry-cured ham. Project work, NTNU. Available from the Department of Energy and Process Engineering at NTNU.

Kvalsvik, K. H. (2015). Energy efficient drying systems for the dried cured meat industry. Master thesis, NTNU.

Strømmen, I. (1980). *Tørking av klippfisk*. PhD thesis, Norges tekniske høgskole.

Strømmen, I., Eikevik, T. M., Alves-Filho, O., Syverud, K., and Jonassen, O. (2002). Low temperature drying with heat pumps new generations of high quality dried products. In *13th International drying symposium*. In (Colak and Hepbasli, 2009b).

Toldrà, F. (2002). *Dry-Cured Meat Products*. Food & Nutrition press, Trumbull, Connecticut 06611, USA, 1 edition.

TrønderEnergi AS (2013). Lokal energiutredning i Trondheim kommune. Technical report, TrønderEnergi AS.

Wadekar, V. V. (2000). A che’s guide to ches. *Chemical Engineering Progress*.

Appendix B

EVALUATION OF THE SIMULATIONS

To ensure that the results could be considered as realistic, an evaluation of the operational conditions in the systems is given here. First, there will be an assessment of the meat model and some general considerations about the energy systems, then follows a brief section about each system.

B.1 ASSESSING THE MEAT MODEL

Using the measured dimensions for hams and a typical weight of eight kilogram (as described in Section 6.2), the assumed total weight loss of 35 % gave a drying time for the hams in the first tunnel section of four months. In an actual plant where the modelled drying conditions are applied, the time is three months. The prediction was hence neither exact, nor far off. The drying time for the last section was of course longer, and lasted for nearly six months. The drying curves are shown in Figure B.1 and look physiologically reasonable.

The model was fitted to data for small, cubic samples; hence, a shape factor could explain some of the difference in drying time. It could also be due to that the real plant alternates the airflow and creates air swirls among the hams, which can enhance drying [Jon and Kiang, 2006]. This was not possible to incorporate in the meat model at hand.

An important factor for drying time is the assumed surface area in the model. It was found that if the diameter was increased from 31.53 cm to 33.85 cm, the model predicted a drying time of three months or 92 days. This is quite a big change in diameter as it was calculated that a 95 % confidence interval was $\{30.59, 32.48\}$. Therefore, the surface area was unlikely to be the explanation for the difference, at least not entirely.

One could point out that the model was developed for lean meat, not including the fat, whereas the used weight of eight kg included both bone and fat. However, this did not affect the derivative of the mass, which is governed by the lean surface area (which had a realistic value) and its relation to the amount of *removed* water, humidity and temperature. Thus, this had no influence on the result.

Despite the deviation, four months is a realistic value for ham drying; [Hui, 2012, p. 683] reported that Parma and Iberian hams, dried at 60-80 % relative humidity and 15 to 30 °C,

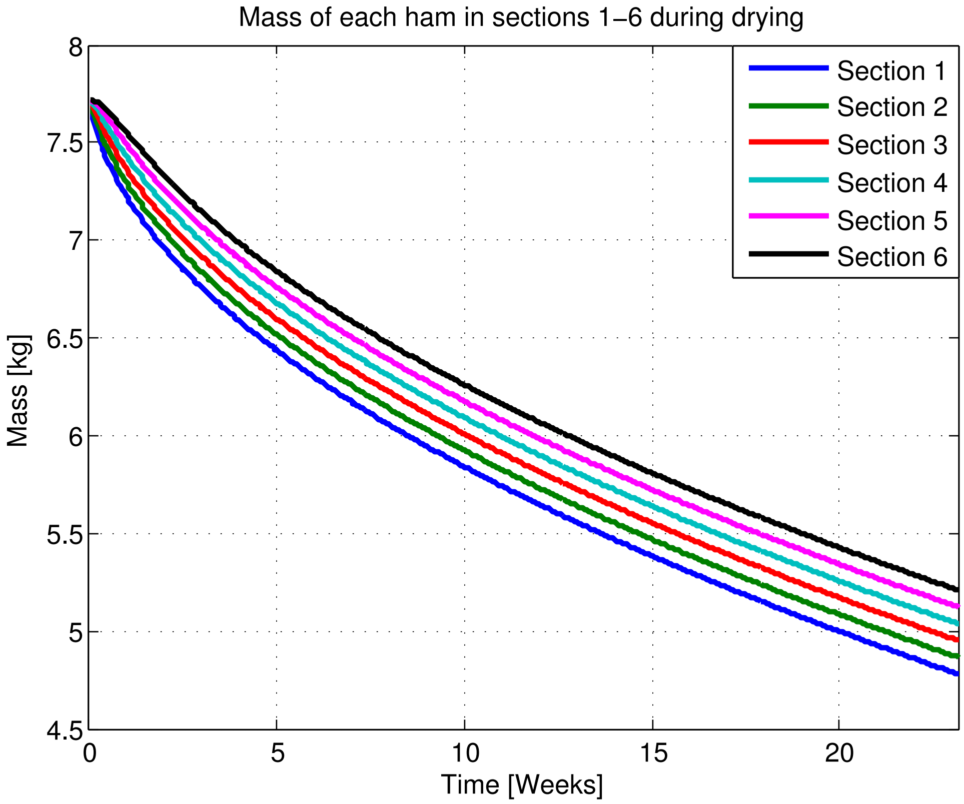

Figure B.1: The mass of one ham in each tunnel section versus drying time, drying until all hams had reached the final value of 5.2 kg

Tunnel	Mass [kg]		
section	Initial	Final	Removed
1	7.72	4.78	2.94
2	7.72	4.87	2.85
3	7.72	4.95	2.77
4	7.72	5.04	2.68
5	7.72	5.13	2.59
6	7.72	5.22	2.50
All	41688	26987	14701

Table B.1: Mass of one ham in each section (rows two through seven) and the total mass of all hams in all sections, 900 in each, before and after simulation (row eight)

are dried for respectively six to eight and four to four and a half months. Drying-ripening times for six ham types presented by [Toldrà, 2002, p. 36] vary from one to twelve months for the different hams. The conditions for these hams vary though, so these are not fully comparable to the result here.

It was concluded that the model behaved satisfactory if not optimally. Realistic drying curves and quite realistic drying times from realistic input were obtained. Because of this, the model was used as it was.

B.2 GENERAL

All the simulations had a short initial period with very high and/or low values for nearly every variable, which changed much and rapidly, before they reached a proper operation point. This was probably because the initial values were not exactly those that developed during the simulation, and the initial process conditions changed very fast initially. Examples of this are the outdoor temperature and moisture and temperature from the drying tunnel, see Figure 6.3 and Figure B.2.

After initialization, conditions developed reasonably for the rest of the simulation time. The initialization period was too short to have any significant influence on the results, and since all processes had similar start periods, the resulting error was also similar for all the systems. Therefore, this was accepted.

The only consequence of the initialization was that it made it apparently impossible to let the drying airflow in a closed loop like in reality. Instead, an open process with two boundaries for the air was used. The desired inlet conditions for drying were specified on the inlet boundary. This is seen in Figure B.4, where the airflow, the yellow or orange line, has two ends instead of forming a complete square.

Using an open process, controlling the final variables at the outlet boundary became especially important to defend this choice. If they were close enough to the inlet values, the open loop could be said to represent a closed one. An example of outlet conditions is shown in Figure B.11. All other systems reported showed similar behaviour, with large initial changes and then fairly constant outlet conditions at the desired 13 °C and 68 % humidity (and 1.0125 bars).

Attempts to use a closed loop were performed. Allowing the air to move in a closed loop, removing the boundaries and the stable inlet conditions in the simulation, resulted in extreme temperatures, pressures, drying, moisture content and heating. The variables became unreasonably high or low and simulation stopped.

A reason for the problem, and generally a big challenge, was that the process conditions changed very fast at the start of the simulation. Both the outdoor temperature in Figure 6.3 and the temperature and humidity of the process air, seen in Figure B.2, changed rapidly in the first part of the simulation. This made the initial stabilization highly difficult.

Another reason for the large initial changes in all systems was that the humidity in pipes could not be specified. It always started at zero. Heat leakage was modelled in a pipe directly after the drying tunnel, which can also be seen in Figure B.4. Thus the first air arriving at the air cooler had zero humidity. Controllers were made too increase cooling when humidity was too high and opposite, hence, all regulators tried to stop the heat pump when the dry air arrived.

When the moist air suddenly arrived, all regulators would suddenly change their outputs, simultaneously, and regulate strongly in the opposite direction. This caused simulation stop.

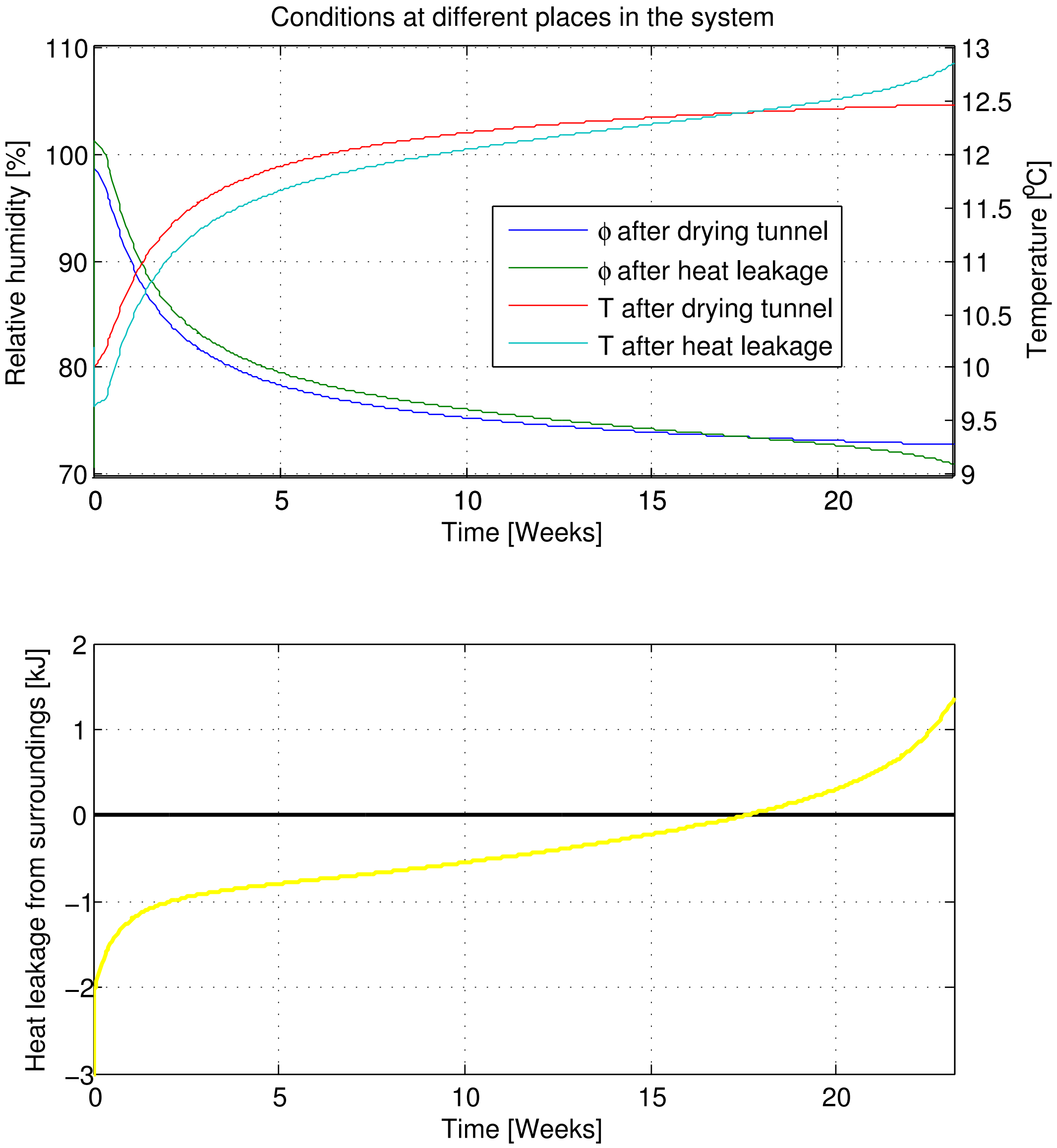

Figure B.2: Temperature T and relative humidity ϕ of the drying air after the drying tunnel and after heat exchange with the surroundings

From Figure B.2 it is seen that the drying rate and cooling load both decreased with time. This is reasonable, but also means that the systems, designed to handle saturated air, would not need to work on full load throughout most of the simulations. A real system must be designed to both handle the peak loads, but it should have its optimal operational conditions at a more normal point of operation.

The heat exchange with the surroundings provided some free cooling when the surroundings were cold, decreasing the load for the energy systems applying cooling and condensation. This made the overall energy needs somewhat lower in all but the adsorption system.

Heat leakage increased the cooling load at high outdoor temperatures, which is also clear from Figure B.2. At this point in simulation, the drying air had a quite low moisture content, thus the systems applying condensation never needed to use their full capacity for cooling and heating. Either, free cooling reduced the cooling load, or the drier air caused a low cooling load.

Most systems therefore behaved a bit better than planned, with for example somewhat lower flows of refrigerants. The lower power demand for BS compared to that in reality can also be explained by this. This was somewhat unfair for the adsorption system, which experienced its most difficult process and surrounding conditions at the same time.

Regulation of the processes has been the most challenging in this work. Systems using heat pumps required sufficient streams of outdoor air, which varied with outdoor temperature; sufficient working medium flow, which varied with the cooling load, which varied with the moisture and humidity of the process air; a suitable valve area to obtain desirable pressures, temperatures and mass flow; and appropriate subcooling after the condensers.

Mainly, it was the complexity and quickly changing conditions of the systems that made controlling challenging. There were so many different things that required simultanuous regulation, and all depended on and affected one another. Simulations were extremely sensitive to process changes, deviations, sudden changes and disturbances. Inserting the pipe that allowed heat leakage for example, changed a simulation model from functioning to not functioning. The regulation of the system then had to be performed again.

B.3 BS

Simulations of BS showed good final humidity and temperature, which both were at their proper values at all outdoor temperatures. Thus, its performance in this respect was satisfactory, and the open loop solution could be defended. The system sketch is shown in Figure B.3 and the interface from DYMOLA in Figure B.4.

BS was the most problematic system to start, because not only did the process air temperature and humidity and the outdoor air temperature vary steeply, but also, unlike the other systems, the pressure on the high-pressure side in the heat pump was governed by this varying outdoor temperature. For the other systems, this high pressure at least, was nearly constant as it was governed by heat supply to the process.

Another challenge was that the surroundings were so cold that the high pressure required to reject heat to the ambient was actually lower than the low pressure. Therefore, initial cooling created problems unless only a small airflow was allowed, preventing such a large heat rejection that the high pressure sank below the low pressure. During this work however, excessive cooling occurred several times, and caused simulation errors and stop. Many attempts of making the airflow smaller, resulted in too small heat rejection, and the high

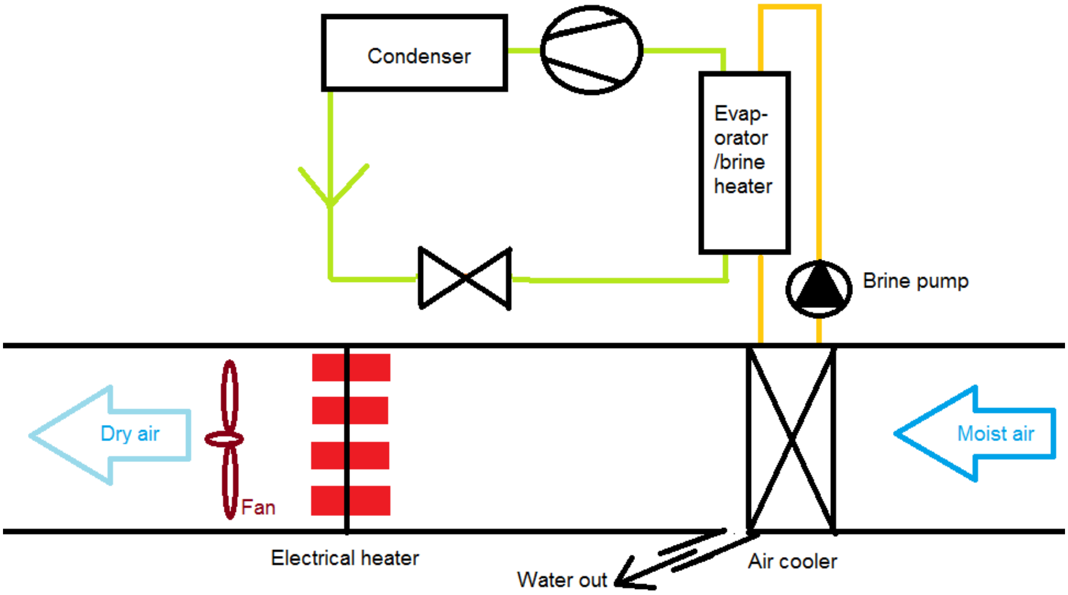

Figure B.3: Basic system

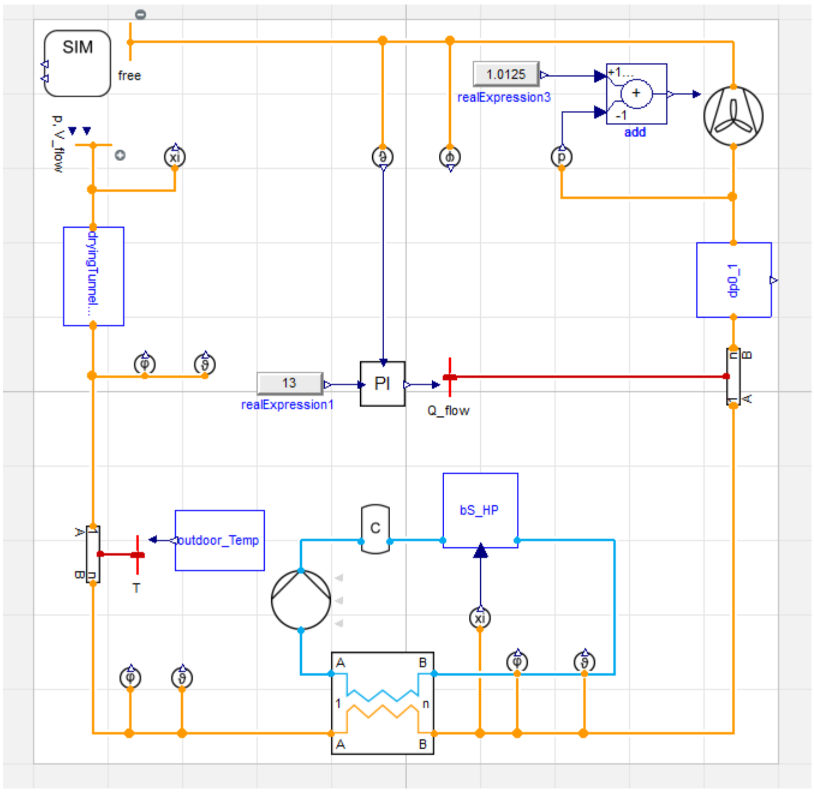

Figure B.4: Basic system as it looks in DYMOLA: An air source with desired temperature and humidity starts the airflow (yellow/orange) to the drying tunnel, followed by a pipe with heat exchange with the surroundings. Then followed a heat exchanger with a glycol circuit (blue) cooled by the heat pump (the white square). After this the air entered a pipe with heat supply (red line), which modelled the electrical heating. A block involving the pressure drop of the system and a fan finished the system before the air sink.

pressure raised to some 100,000 bars.

For this system, the general initial instability, in addition to the steeply varying conditions, made it necessary to use an extra initialization period with constant conditions before changing conditions could start. All the results and graphs have this period subtracted. The initialization period was 3e5 seconds, and total simulation time was therefore correspondingly longer. No contribution from this period was included in the energy calculations. Energy variables were all set to zero initially. Their derivatives were zero during the initialization period and equal to the power consumption after it.

Likewise, no drying was allowed in this period, to give a fair comparison with other systems. Saturated conditions for the air gave exactly no drying in the drying tunnel, and so the inlet conditions to the tunnel were set to 10 °C and ϕ=99 % in the initialization period and 13 °C and ϕ=68 % after.

When the process then started to change, the changes were fast and came abruptly, giving the system a second initialization period, similar to that of other systems. More about why this initialization period was used and why the heat pump was programmed with a divided control strategy for airflow and valve area, is explained in Appendix C.

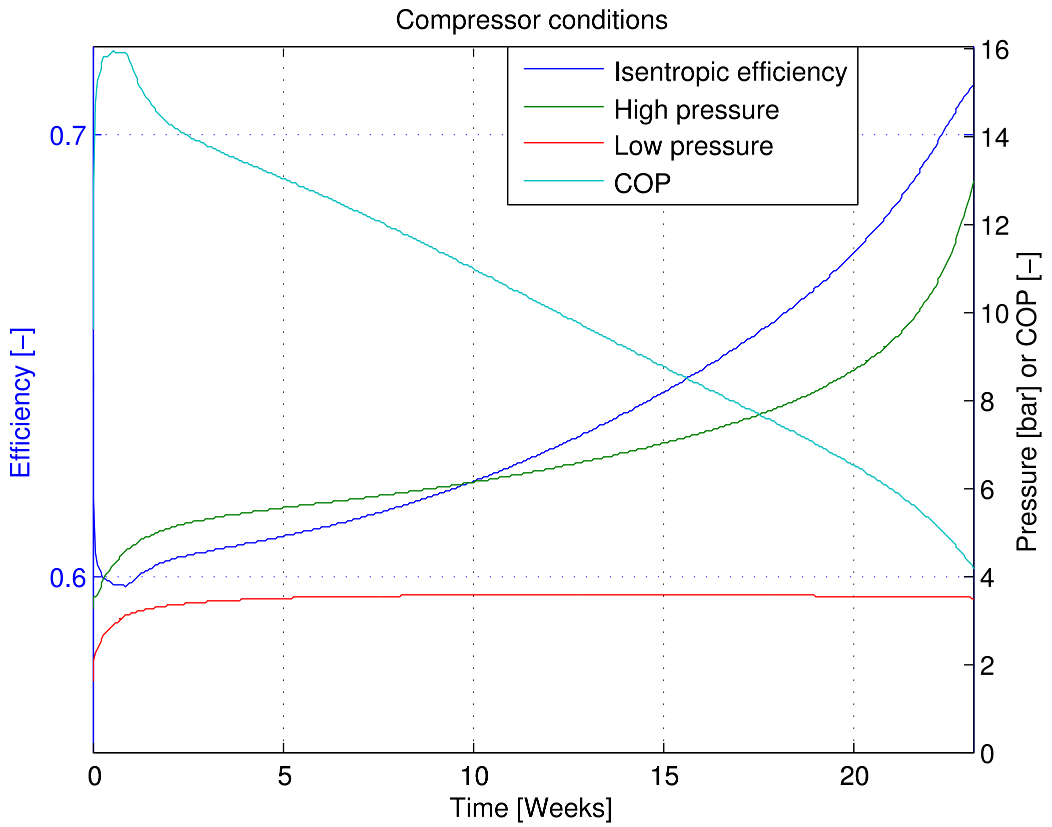

Figure B.5: The isentropic efficiency in BS (left axis) was a function of the pressure ratio. The high pressure and COP (right axis) were mainly functions of the ambient temperature and opposite of one another, because the low pressure was quite stable.

The operational conditions were somewhat off the design point most of the time. This was just as it should, because most of the time, the process air was not saturated as in the design phase either.

The low pressure was in general around 3.5 bars instead of 2.9, as seen in Figure B.5. However, it started at 2.9 bars and increased as the cooling load decreased. The high pressure followed the outdoor temperature, which is reasonable. An exception was at the start, when a very small amount of cooling air kept the highest pressure above the lowest one. The highest pressure was slightly lower than the assumed 13.5 bars, corresponding to 35 °C. The final pressure corresponded to a saturation temperature slightly below 34 °C.

The isentropic efficiency, also shown in Figure B.5, increased with the increasing pressure ratio, and was a bit low during most of the process. Again, it was apparent that one should design the system to have optimal conditions for the most typical operation point, not at the worst conditions.

The small pressure difference resulted in very low necessary compression power at the start, as seen in Figure B.6, but this increased with the outdoor temperature. This was unique for this system. The power for heating and the delivered cooling in Figure B.6, had much larger values, thus the COP was high, starting around 16, but decreasing due to the increasing compression power.

The total power consumption included power for pumps and fans, but was only a tiny bit higher than the sum of heating and compressor power, which made up the most of the power need. The higher energy need due to higher heating and cooling load in the start and higher pressure ratio at the end is reflected in the shapes of the curves in Figure B.6. Initially, the cooling and heating demand were high, at the end, the compressor needed more power.

The energy consumed is shown in Figure B.7. It looks nearly linear with time, but really, the curves bend a bit up and down with the changing power consumption. The heating and cooling supplied were about equal, but heat leakage and heat from fans made them slightly different.

The resulting mass flow in BS was smaller than calculated, generally between 0.016 and 0.012 instead of 0.020 $\frac{\text{kg}}{\text{s}}$, and larger at the start and at the end of the simulation. Calculating the mass flow, it was assumed that the ammonia was saturated before the valve, but it actually it was subcooled after the condenser, and the subcooling was large at the lowest outdoor temperature. This meant that more heat was rejected at the high temperature than in the calculation, giving more cooling potential per mass flow at the low-pressure side, so less ammonia than planned was required to provide sufficient cooling.

The mass flow was higher at the start than later because the heat load decreased with time, as less water was evaporated from the hams, and less water needed to be condensed. In addition, the cooling was partly done by the heat leakage in the model. As the high pressure increased, the subcooling and the latent heat at this pressure became smaller, the first is seen in Figure B.8. Thus, an increase in mass flow was needed.

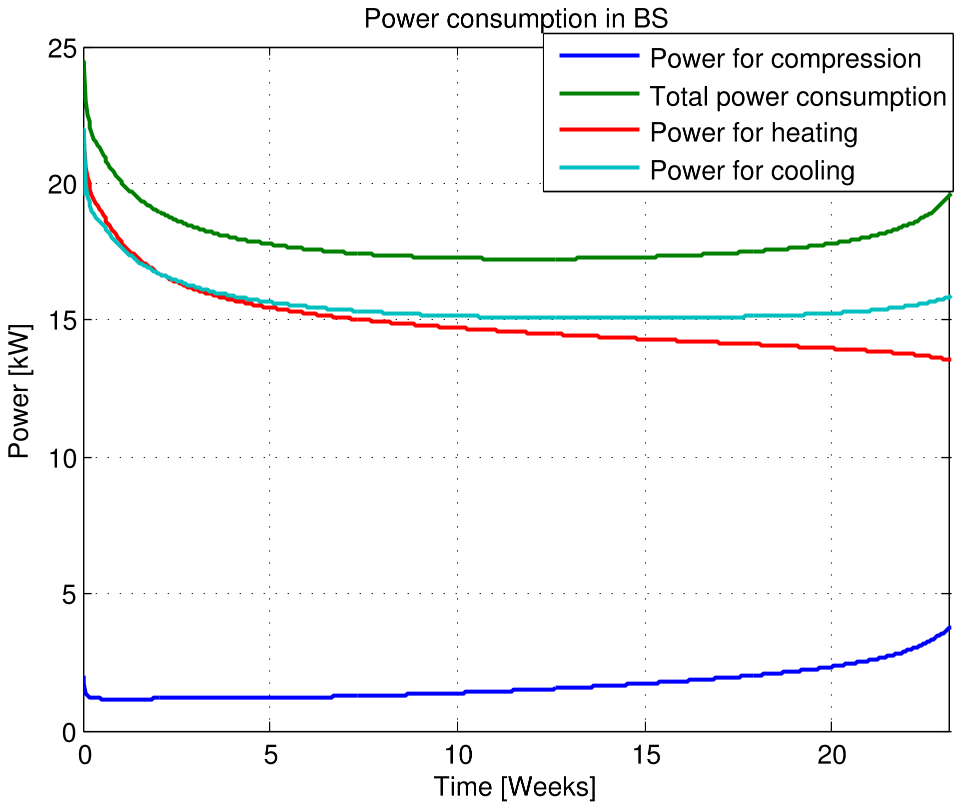

Figure B.6: Power supply to BS

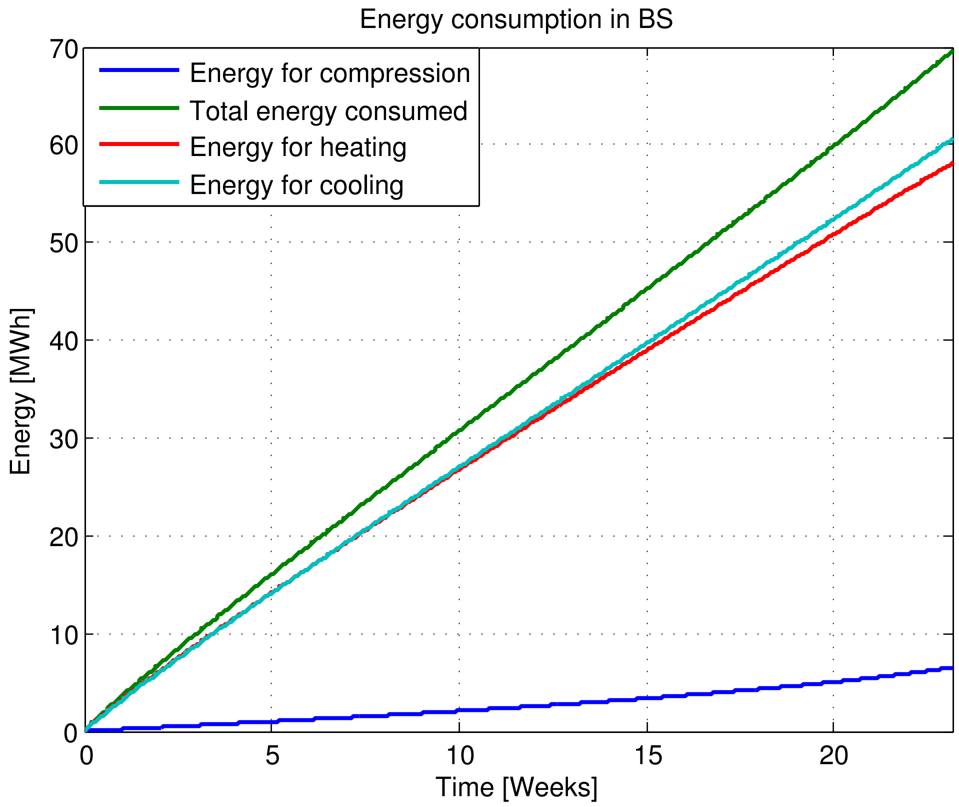

Figure B.7: Energy consumed in the BS as a function of time

The heat exchangers were designed to handle the worst case, which was the highest outdoor temperature or that all the drying air had reached the wet bulb temperature, which it also nearly did at the start of the process. These two conditions never occurred simultaneously, and the exchangers generally performed more than well enough. The decreasing heat loads in the condensers and thereby decreasing flows of ammonia, also contributed to this. The temperature difference between ammonia and air after exchange was therefore very small in the condenser, $T_{NH3,out}$ and $T_{air,in}$ in Figure B.8. The ammonia temperature after compression increased in a similar fashion to the outdoor temperature, following the pressure in Figure B.5. The temperature difference for the air decreased at higher temperatures because more air was supplied to avoid a too high pressure in the condenser. This airflow seems to have been appropriate, as the ammonia was sufficiently subcooled at all outdoor temperatures.

The temperatures in the evaporator again reflect the initial high cooling load, which then decreased. The temperature differences were generally about 5 °C, except for at the very start of the process. This was again because less heat should be transferred when the air became drier.

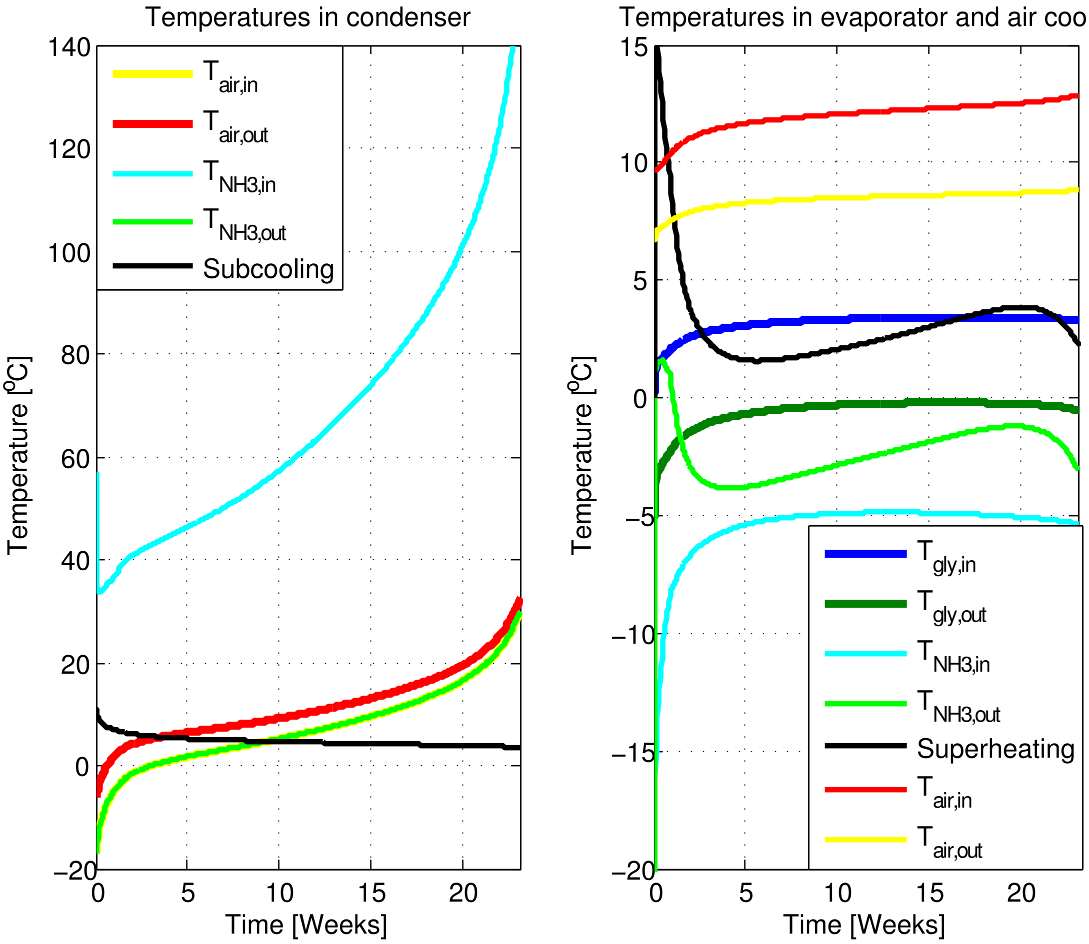

Figure B.8: Heat exchanger temperatures in BS

Despite that the process had its initial evaporation temperature set to start at -10 °C, this dropped during initialization, and increased quickly to more reasonable values afterwards. Regulating this was difficult, as fast regulators made simulation stop. Hence, the start of the process was somewhat peculiar. This was also because the heat pump had to deliver heat to a colder reservoir than the heat was taken from, opposite of its real purpose.

Studying the process in a p-h-diagram in StateViewer, the operation was good and reasonable. The internal heat exchanger became increasingly important at higher temperatures, but was insignificant in the coldest period.

B.4 HPS

How HPS looked in DYMOLA and the system sketch are shown in Figure B.10 and Figure B.9.

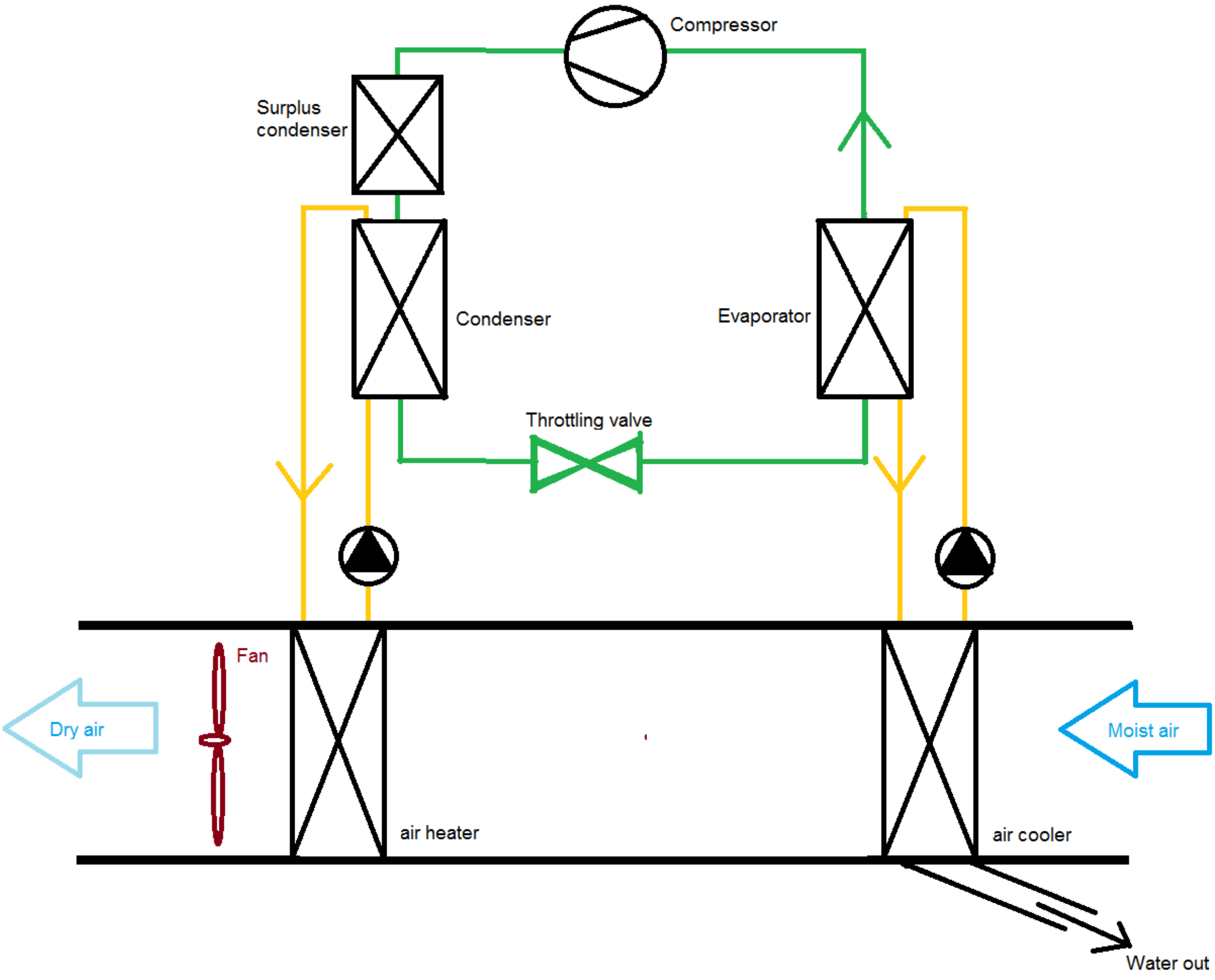

Figure B.9: The system sketch for the heat pump system

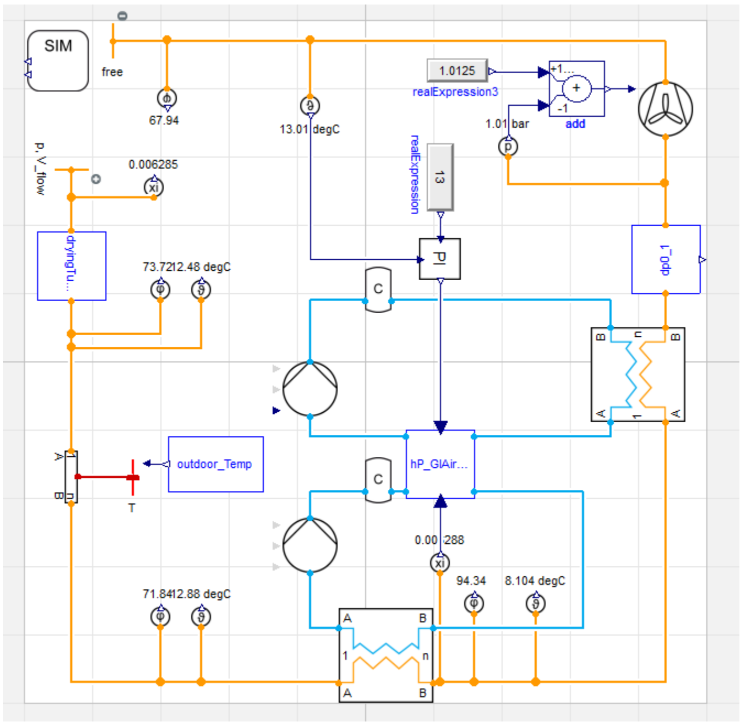

Figure B.10: Heat pump system as it looks in DYMOLA: An air source with desired temperature and humidity starts the airflow (yellow/orange) to the drying tunnel, followed by a pipe with heat exchange with the surroundings. Then a heat exchanger with a glycol circuit (lower blue circuit) cooled by the heat pump (the white square) supplied cooling. Another glycol heat exchanger supplied heat from the heat pump. A block involving the pressure drop of the system and a fan finished the system before the air sink.

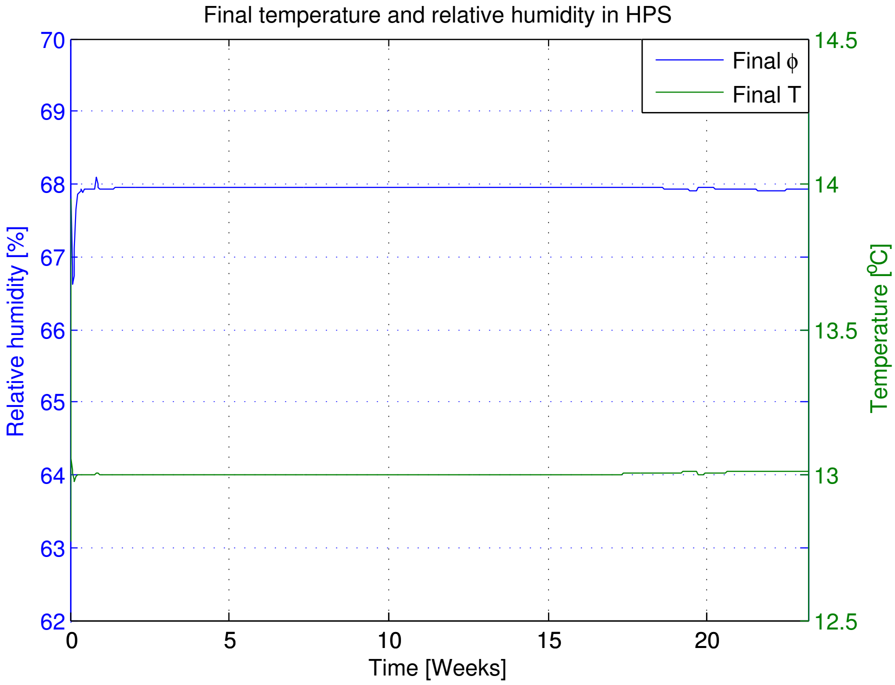

Figure B.11: Final temperature and relative humidty in HPS

The outlet conditions for HPS are shown in Figure B.11, and its performance was considered satisfactory. At an early point in this work, the process temperature raised when the outdoor temperature increased steeply towards the end of the simulation. When the outdoor temperature raised, less cooling to the desuperheater should result in more gas on the high-pressure side, causing the pressure and temperature to rise until sufficient heat could be removed and a new balance be found. In HPS, however, the heat pump did not rise its pressure because it *did* get sufficient cooling by dumping more heat to the process.

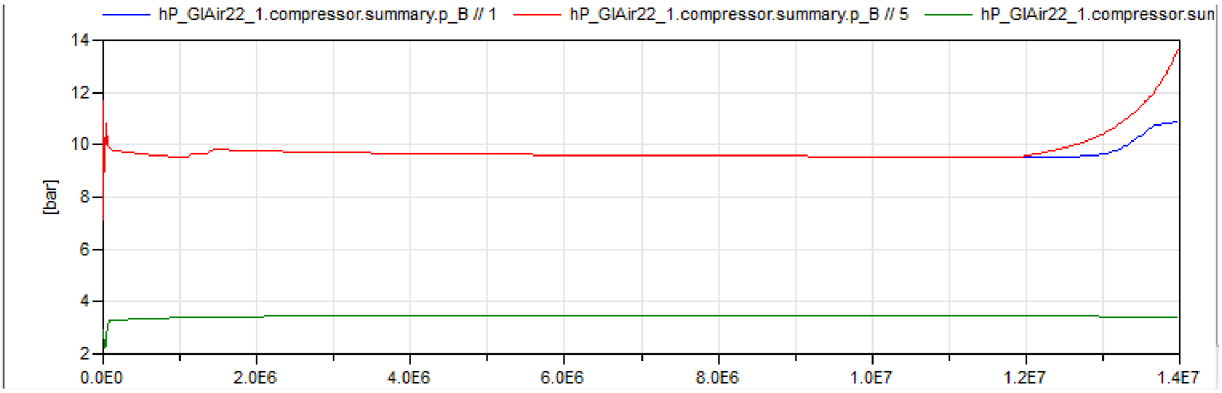

Figure B.12: Pressures in the heat pump in HPS before (blue line) and after (red line) the problem as it looks in a DYMOLA graph, the green line shows the low pressure, which was unchanged.

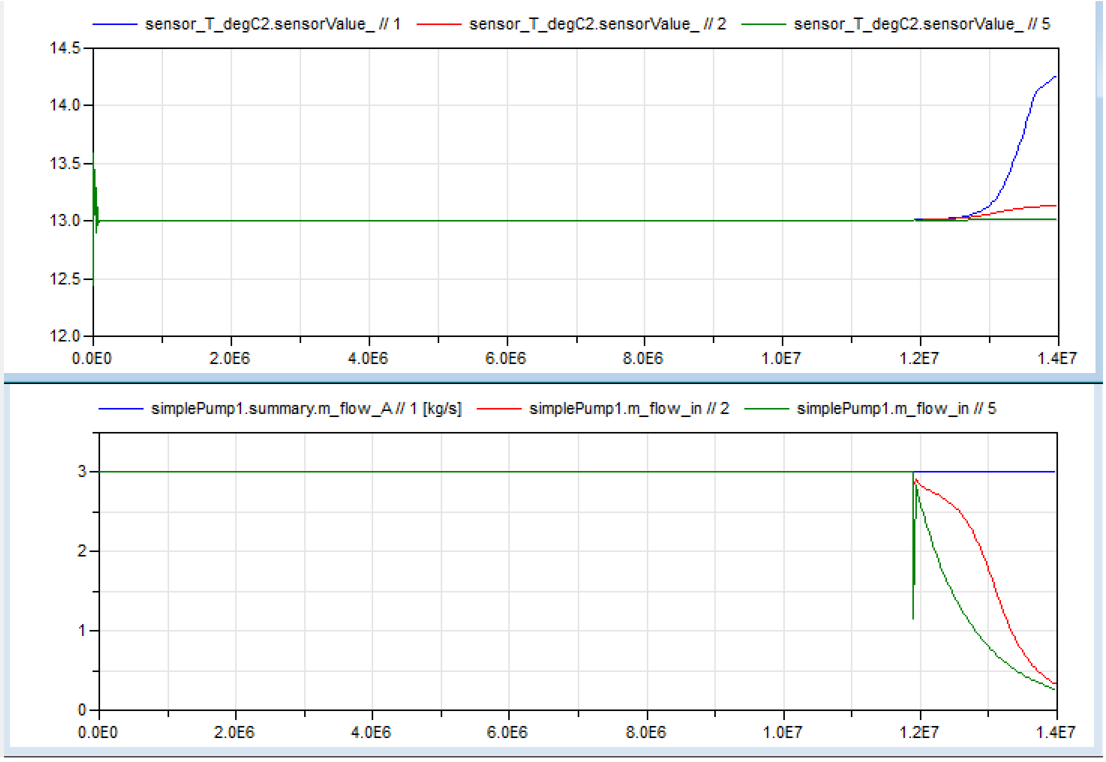

Figure B.13: Final process temperature (upper) and glycol mass flow (lower figure) in HPS before and after the problem as it looks in a DYMOLA graph, shown for three cases: no regulation of the glycol pump (blue), regulation using Equation B.1 and C=20 (red) and C=200 (green)

Many ideas for solving this was considered, but most of them would result in an unsatisfactory condition elsewhere in the process, and just move the problem. A solution without this drawback, was to change the mass flow of glycol, so that less heat could be delivered to it. Then, the desired lower condensing rate would be obtained and the pressure would rise.

When the deviation occurred, after about 1.2×10^7 seconds, the mass flow of glycol was set to 3 $\frac{\text{kg}}{\text{s}}$ minus a constant times the deviation, or

$$\dot{m}_{glycol} = 3 - C \cdot (T_a - 13) \tag{B.1}$$

T_a denotes the air temperature. Setting $C = 20$ gave a deviation of about 0.1 °C, shown by the red line in Figure B.13. A value of 200 reduced the deviation to 0.014 °C, which was an acceptable deviation, no larger than for other systems.

The power consumption for this system and the accumulative energy consumption are shown in Figure B.14 and Figure B.15. The heating and cooling were naturally enough similar to those in the BS, but the total power was much lower as it did not include all the power for heating in BS. The total power has small jump, which resulted from the change in glycol flow and power for the glycol pump.

The compressor power was much higher than in BS during most of the process, because the compressor in HPS delivered heat to a high temperature and did not have the advantage

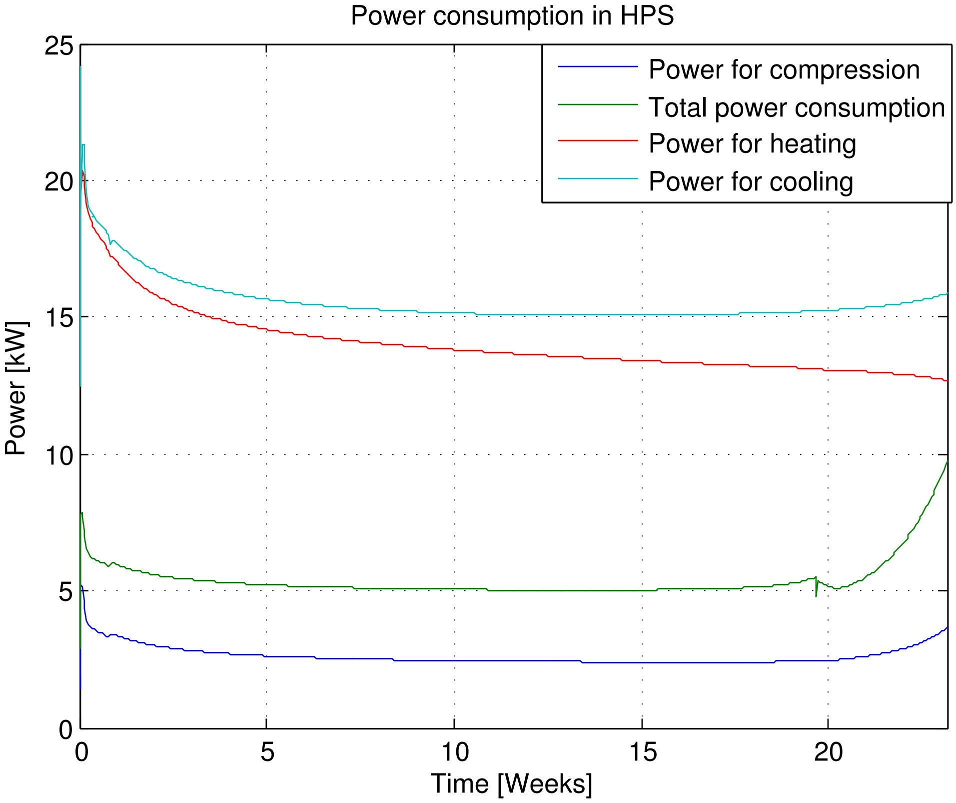

Figure B.14: Power supply to HPS

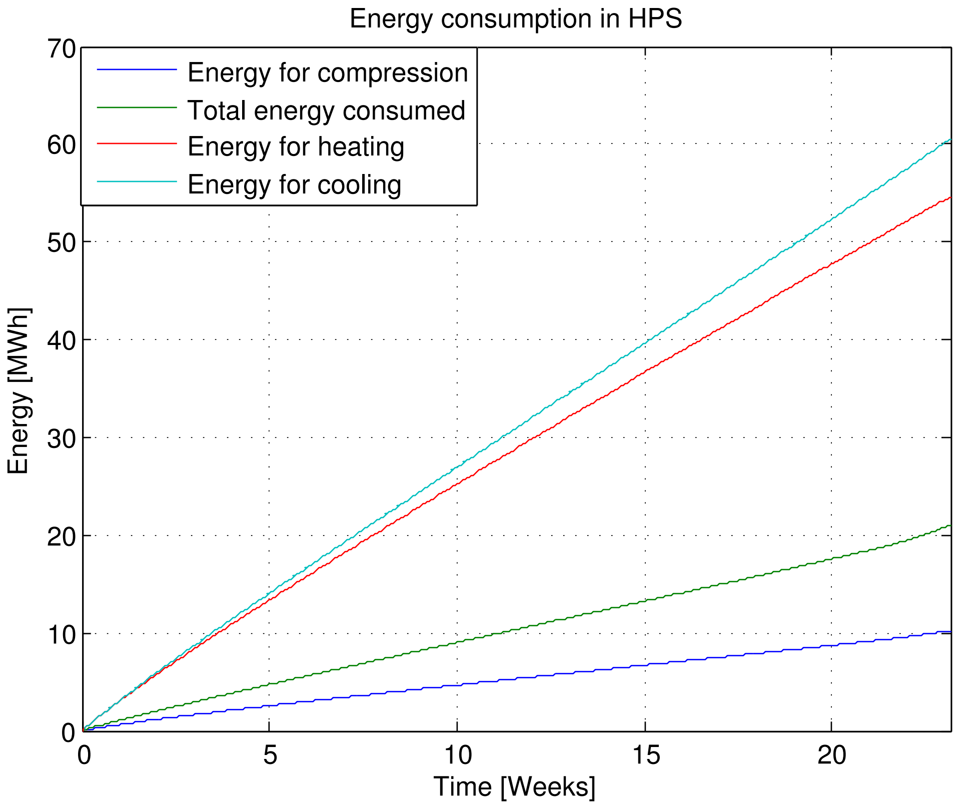

Figure B.15: Energy consumed in HPS as a function of time

of dumping it to the ice cold air outside. This resulted in that the COP was lower in HPS than in BS, despite the lower overall power need.

The total energy was again nearly linear with time, which is natural when the heating and cooling temperatures were about the same most of the time. At the end, when the temperature and pressure in condenser increased, the energy bends up a bit, because more compressor and fan power for cooling air was needed. The compressor power had a smaller increase than the total power (this is seen in Figure B.14) probably because the isentropic efficiency increased as well, shown in Figure B.16.

The isentropic efficiency in Figure B.16 started at the value calculated at design point, because the cooling and heating load were close to the designed values. However, the load decreased fast, the low pressure increased to cool down less, and so the high pressure sank a bit to heat up less than at the start. The pressure ratio Π decreased and so did η_{is}, until the high pressure again had to increase because of the outdoor temperature and both Π and η_{is} increased again.

Towards the end of simulation, the high pressure reached a similar value to that in BS, corresponding to a saturation temperature slightly above 34 °C. The low pressure showed a small drop in Figure B.16, probably caused by the heat leakage from the surroundings. During most of the process, it provided free cooling due to the relatively cold climate, but it started to add heat at the end, thus increasing the cooling load slightly.

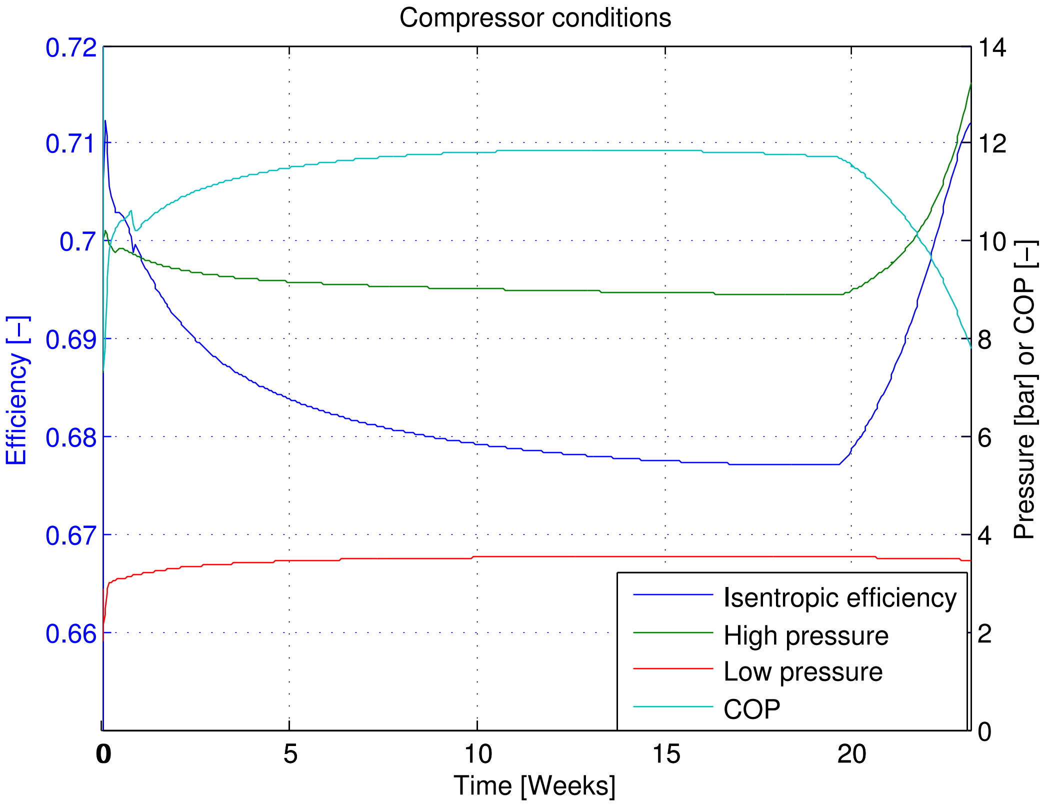

Figure B.16: The pressures, COP and isentropic efficiency for HPS

The temperatures in the heat exchangers developed in a quite reasonable way, though exceptions often occurred during initialization, as seen in Figure B.17 and Figure B.18. The temperatures in the evaporator started at the design point for full cooling load and increased smoothly as the load decreased. The small drop in temperature at the end can be attributed to the heat leakage from ambient air. The temperature difference was reasonable, about 5 °C at the outlet for the glycol, and the ammonia was a few degrees superheated at its outlet at the other side as it should.

In the desuperheater, the airflow was controlled to leave the exact right amount of heat to the condenser, and thus, the airflow was always as small as possible, and it exited at a temperature very close to the ammonia saturation temperature.

There was a peculiar jump in the inlet temperature for the ammonia. It was found that there was no superheat of the ammonia at the compressor inlet, and the jump in temperature after the compressor happened at the same time as the first superheating occurred. There should always be superheat, so the valve controlling the superheat was too slow. Faster valve regulation ensured that the ammonia was always superheated before the compressor, but the jump in temperature in the desuperheater did not disappear. It just moved to the left in Figure B.17, despite that the always present superheating.

Why it was still there is unclear, but the one explanation is that the superheating oscillated and was quite unstable at the beginning, like most other variable in the initialization period.

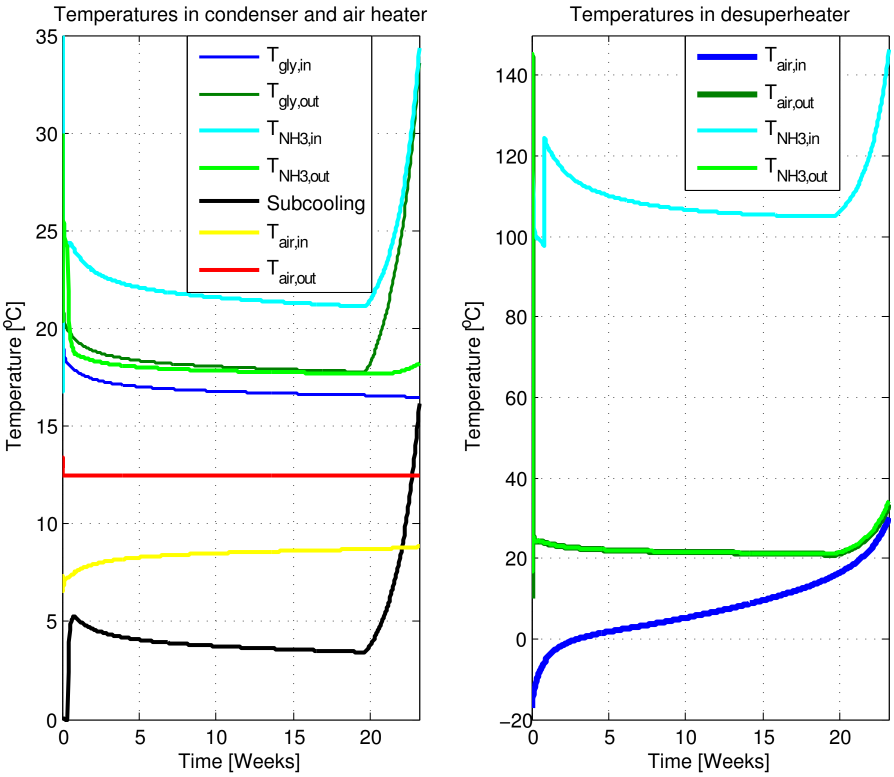

Figure B.17: Heat exchanger temperatures in HPS on the high-pressure side

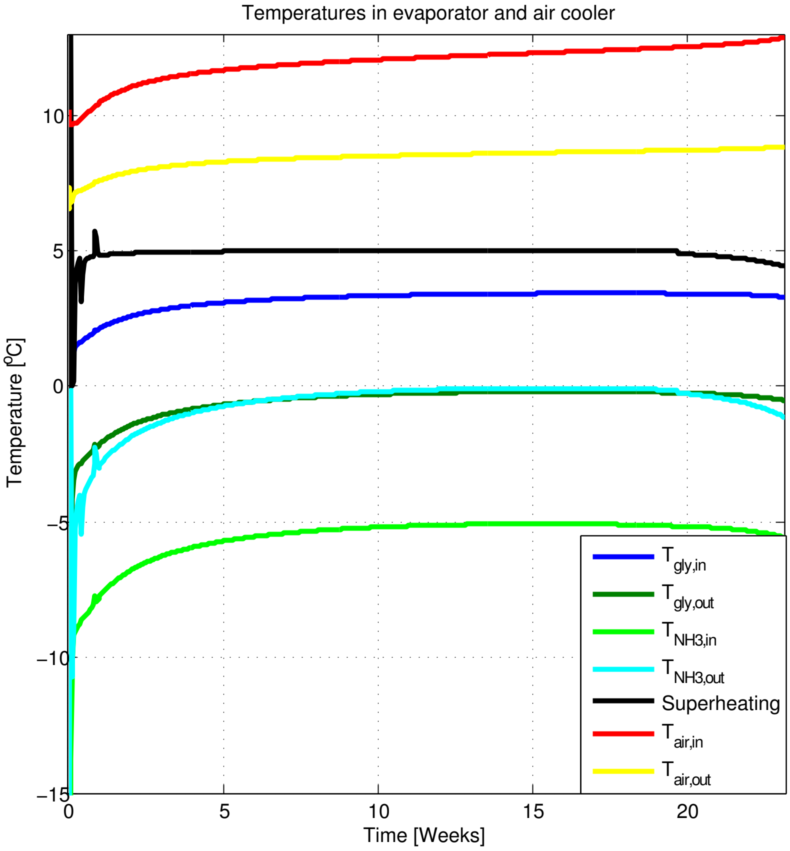

Figure B.18: Heat exchanger temperatures in HPS on the low-pressure side

Subcooling was generally around 4 °C, and increased steeply towards the end of the process. This is related to the pressure increase. At the end of simulation, the outdoor temperature rather than the process governed the high pressure and temperature. The difference in inlet temperatures between ammonia and glycol increased, while the mass flow of glycol decreased. This made the temperature of the glycol rise more quickly, and to a higher level than before, decreasing the driving forces for heat transfer faster and keeping the heat delivery to the process correct. Ammonia left the condenser at about the same temperature as before, because the glycol entered at the same temperature as before. Because the pressure had risen, the degree of subcooling increased much.

The mass flow of ammonia developed in a similar way to that in BS, but was somewhat higher to begin with, around 0.019 $\frac{\text{kg}}{\text{s}}$, before it decreased with the cooling load to around 0.013 $\frac{\text{kg}}{\text{s}}$. As for BS, the degree of subcooling could explain that it initially was a bit lower than calculated, and the reason the mass flow in HPS was higher than in BS was that the degree of subcooling was smaller when heat was rejected to the process temperature rather than ambient. An even better system would perhaps use a valve to allow ammonia to always be desuperheated by the process if the ambient air was colder, and opposite if the process temperatures were colder.

B.5 HPSX

All the heat pump systems with extra heat exchange can be represented by Figure B.19, depending on whether the airflows in the figure are set to 100 %, 37 % or dependent on initial air moisture content. The icon view from DYMOLA looked as in Figure B.20. Really, Figure B.20 shows HPSX1, but the other systems were identical except that HPSX37 did not include the PI-controller connected to the fan, which controlled the airflow for dehumidification, keeping the lowest control at 1 °C. HPSX100 lacked both this controller and the possibility for air to bypass the coolers, which is the yellow line shaped like an L in the middle of Figure B.20.

B.5.1 HPSX100

The HPSX systems behaved in a similar manner to HPS, but with a smaller heat load for the heat pump, and somewhat different temperatures. When only an extra heat exchanger was added to HPS, resulting in HPSX100, the power and energy consumption only became slightly smaller, as seen from Figure B.21 and Figure B.22. This should also be expected, because the system only recovered a small part of the heat.

The inlet temperatures also were only slightly changed, which is seen in Figure B.25 and Figure B.26. The ammonia mass flow decreased with time, so did the high pressure,

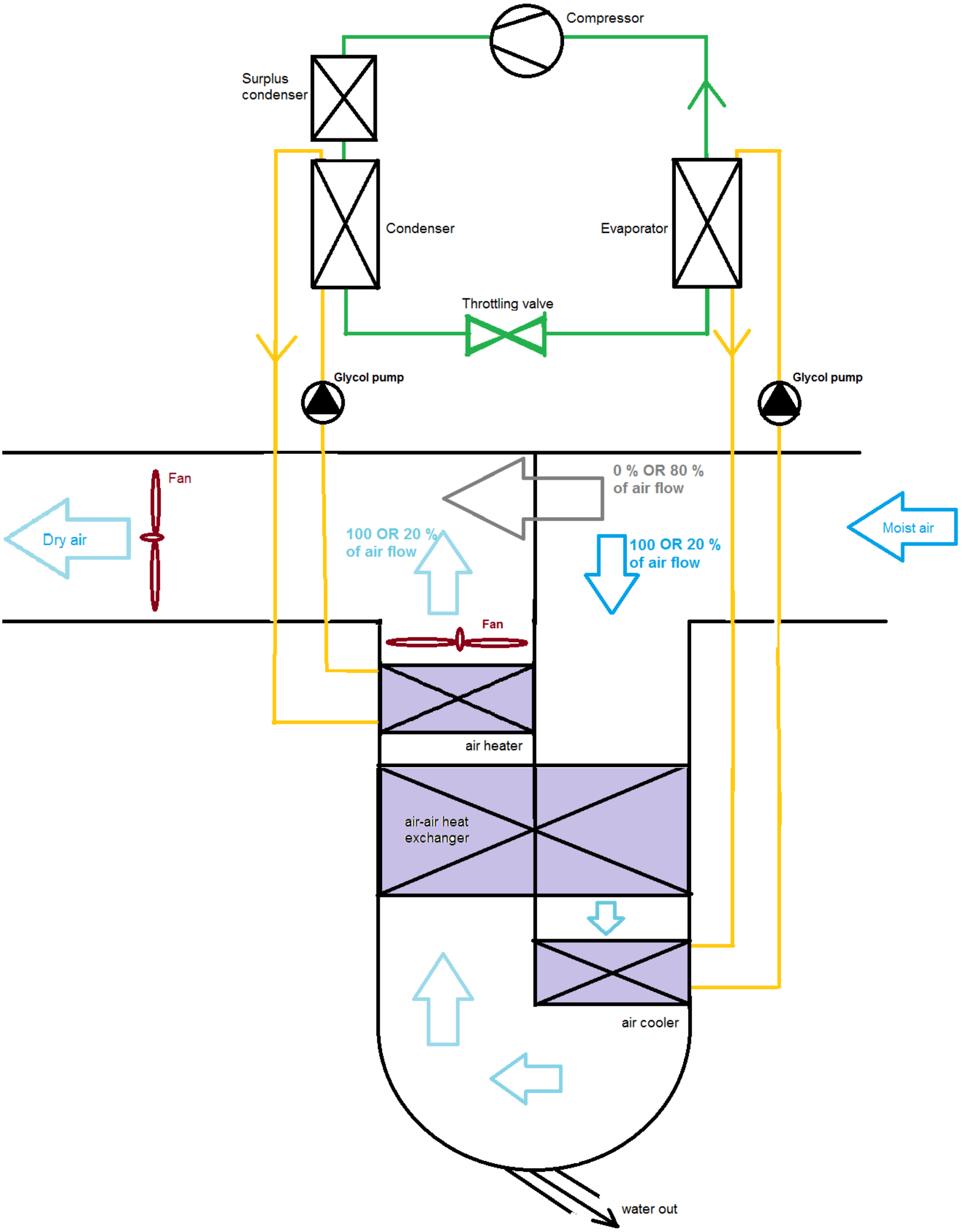

Figure B.19: HPSX, heat pump drying with extra heat exchanger, the entire airflow could be cooled and heated, or only a part of it.

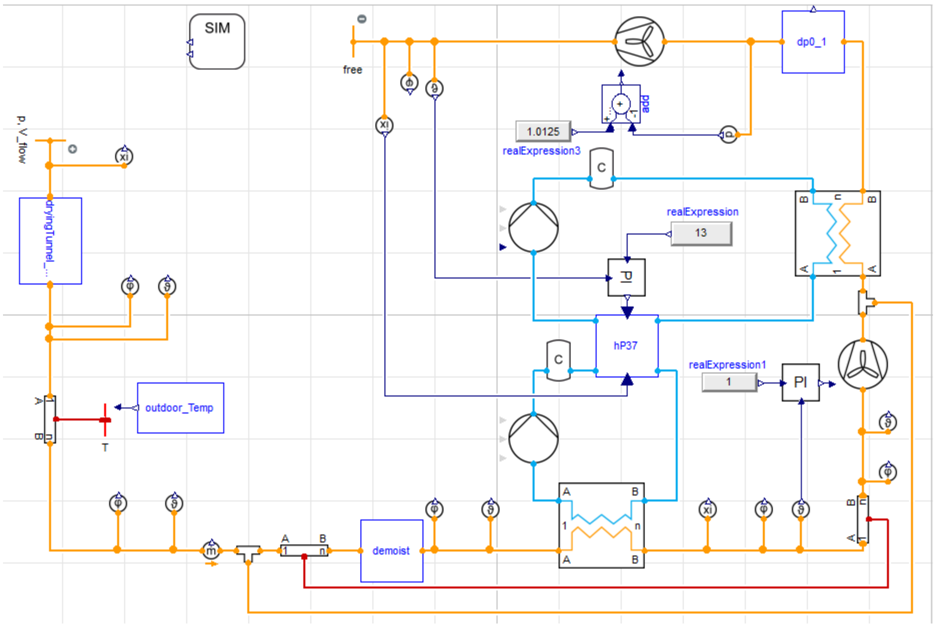

Figure B.20: Icon view of HPSX1 in DYMOLA: Yellow lines are airflows. Starting from the air boundary on the left side, where inlet conditions were determined, the air flew through the drying tunnel before it exchanged heat with surroundings in the pipe. It was then split up into two streams. One stream exchanged heat with already cooled air through the pipes connected by the red line (red lines represent heat transfer). It was then cooled by glycol (blue lines) from the heat pump, entered the air-air heat exchanger again and was heated, before a fan restored its pressure and the air streams were remixed. A final pressure drop in the air distribution system finished the cycle.

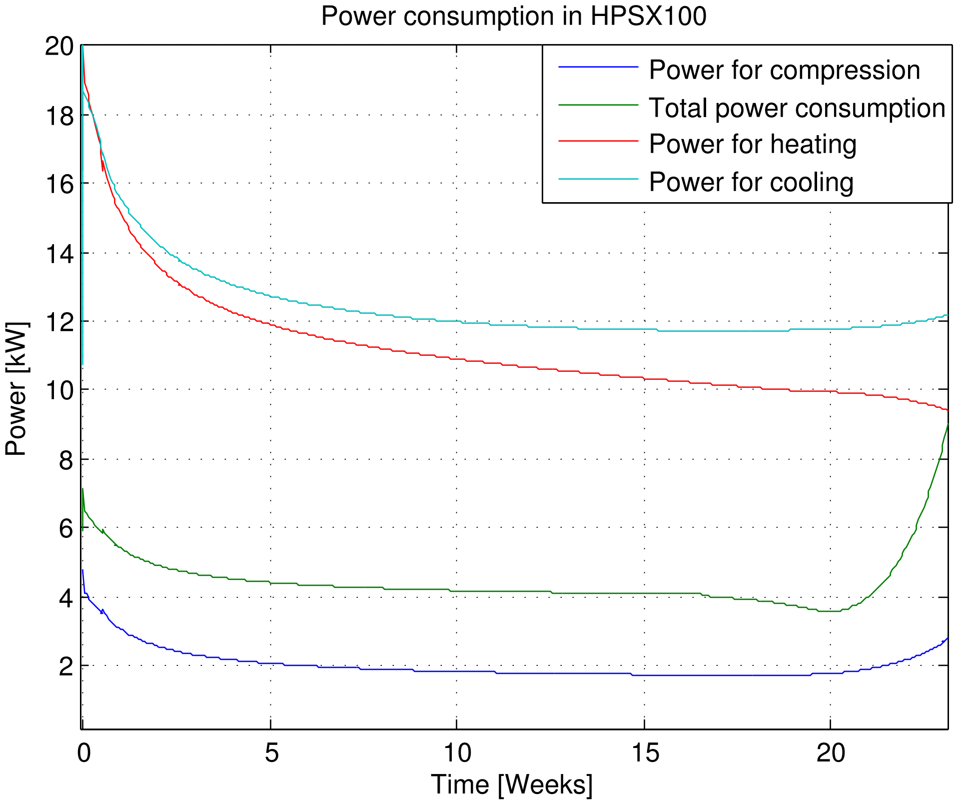

Figure B.21: Power supply to the HPSX100

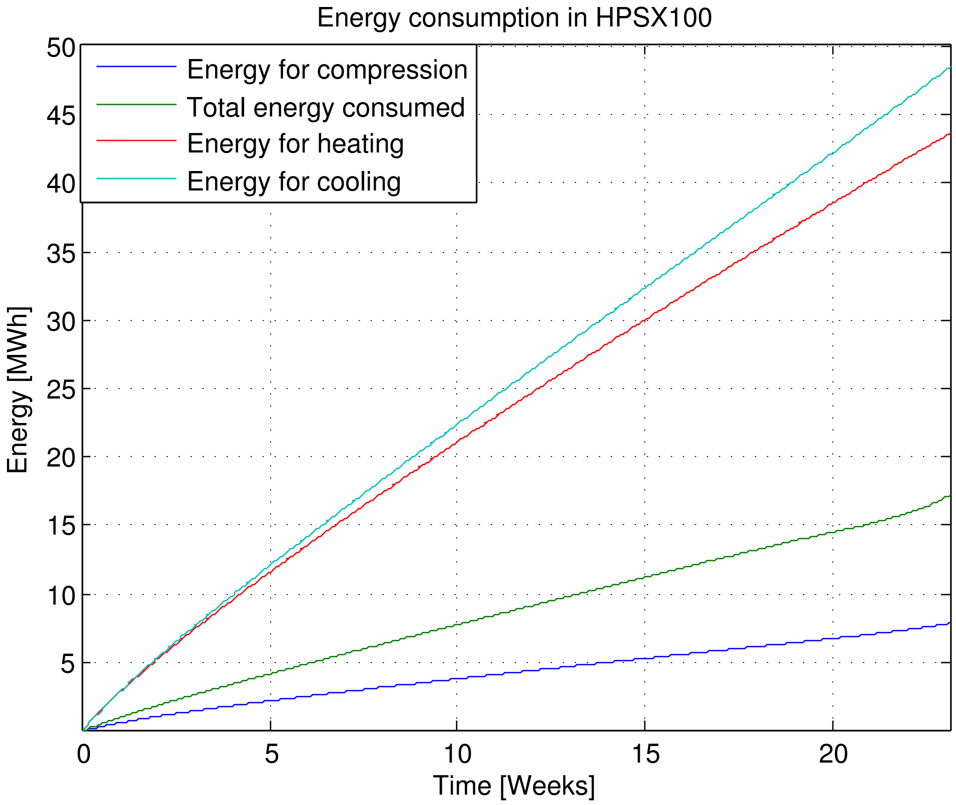

Figure B.22: Energy consumed in the HPSX100 as a function of time

because the smaller amount of cooling needed to condense sufficient water vapour also called for lower heating. This lowered the compression power, and as a result, the COP increased initially, but increased again towards the end, when the highest pressure raised due to the increasing outdoor temperature. The latter is seen in Figure B.24.

Another important reason for the power increase towards the end of the processes was the extra fanning power to remove the heat in the desuperheaters at higher air temperatures. At these conditions, a decreasing mass flow of glycol was necessary to ensure that the process air was not excessively heated, just like in HPS. This was the case in all HPSX systems. The tendency for the power consumption to fall, which can also be seen in Figure B.21, was due to the reduced need for pumping power in the glycol pump.

The final conditions were quite satisfactory, as seen in Figure B.23 and so was the high pressure in the heat pump, seen in Figure B.24, where also the COP is seen. COP was mainly a function of the pressure ratio, because sufficient subcooling and superheating were always obtained, as seen in Figure B.25 and Figure B.26. The pressure ratio strongly affected the compressor work, which was high at the start and at the end. In the beginning, this was due to high cooling and heating loads, at the end it was caused by higher outdoor temperature and thereby higher pressure ratio.

When the heating and cooling demand decreased, as seen in Figure B.21, the temperatures rose on the cold side, Figure B.26, and sank on the high pressure side, Figure B.25. The

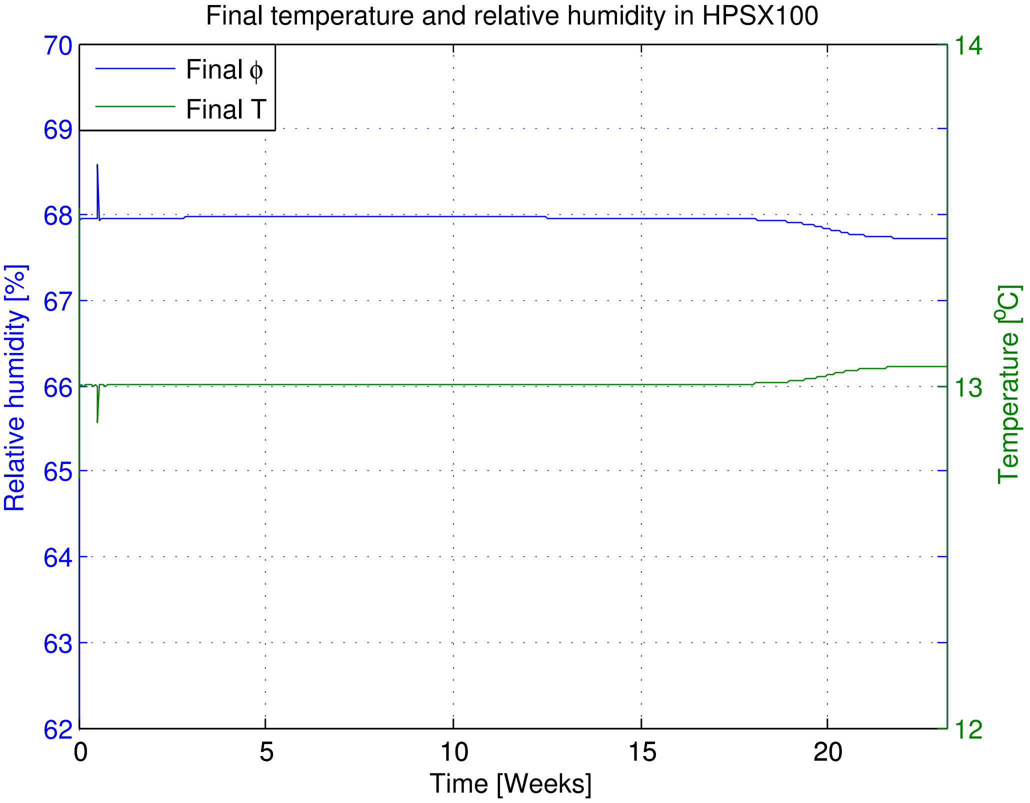

Figure B.23: The resulting temperature and humidity delivered to the drying tunnel

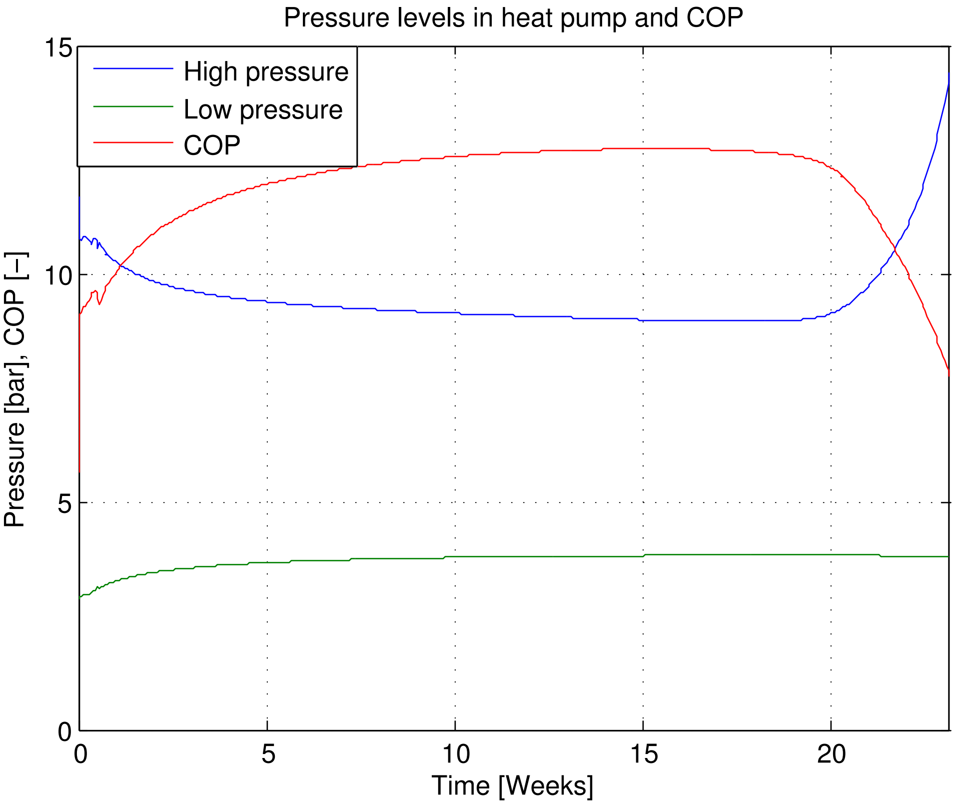

Figure B.24: Pressures and COP for the heat pump in HPSX100

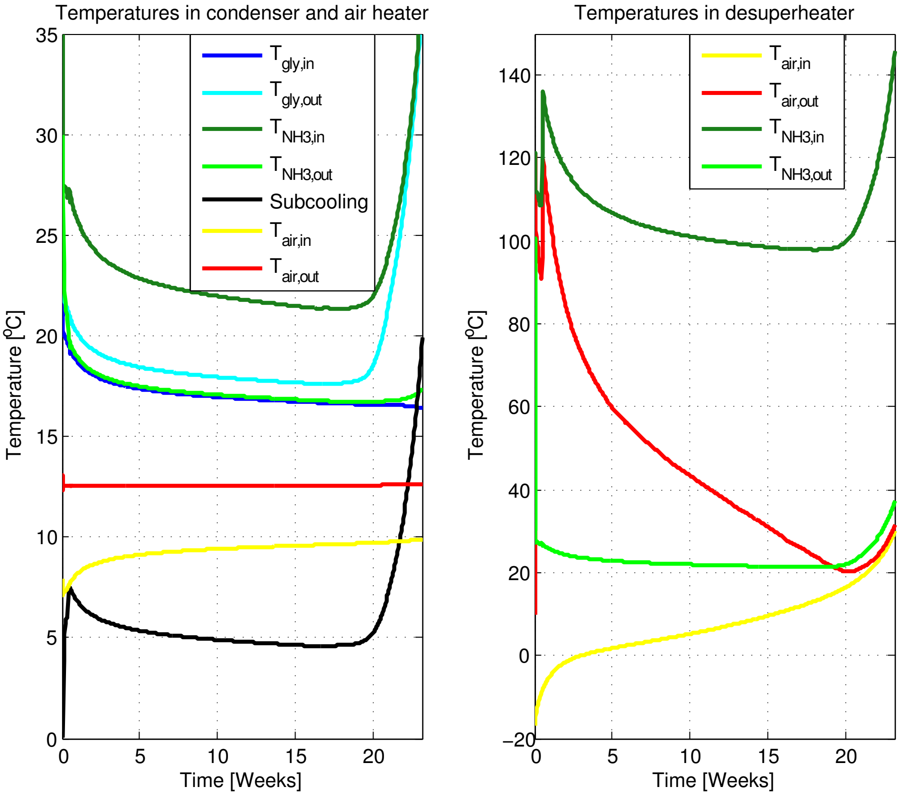

Figure B.25: Heat exchanger temperatures in desuperheater, where ammonia is cooled by ambient air, and temperatures in condenser and air heater in HPSX100: For glycol, the subscripts «in» and «out» refer to in and out of the condenser.

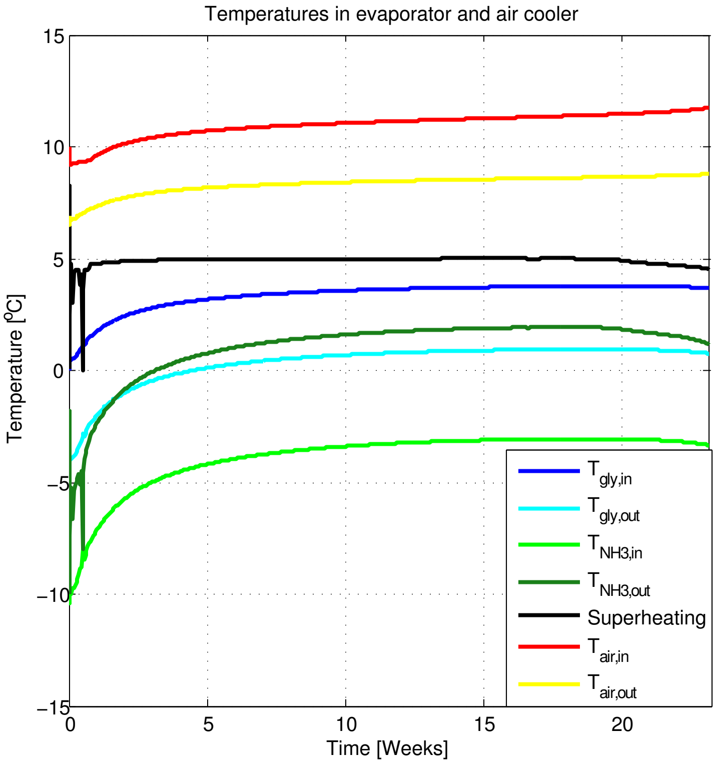

Figure B.26: Temperatures in HPSX100 on the low pressure side

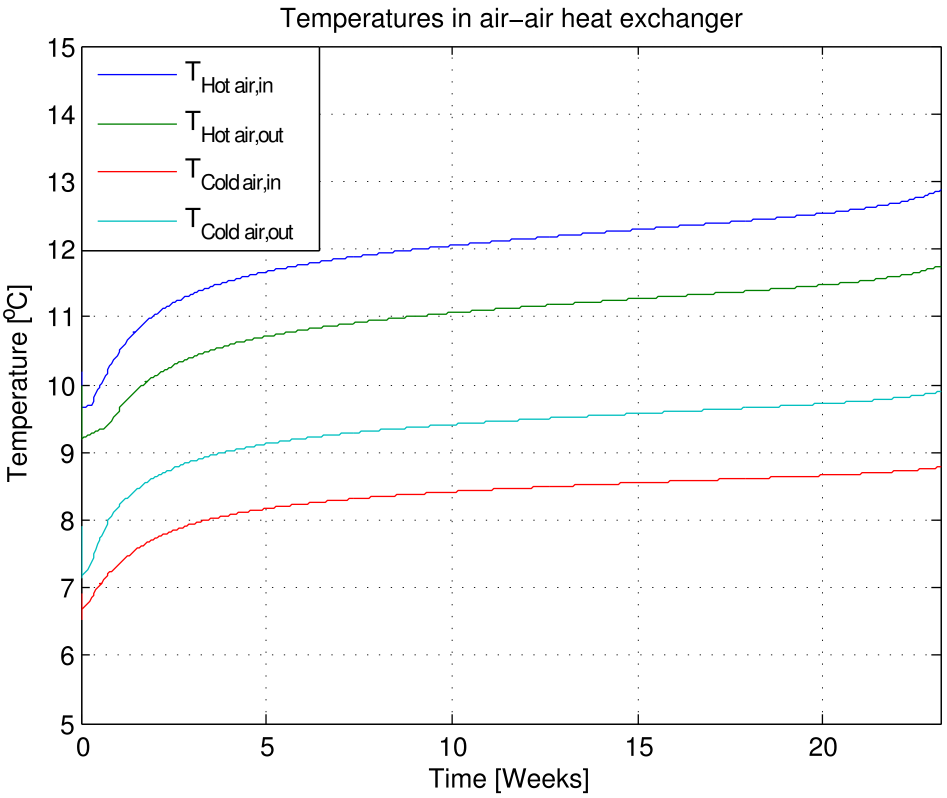

Figure B.27: Air-Air heat exchanger temperatures in HPSX100

subcooling increased much towards the end because the higher pressure, with cooling to about the same temperature, resulted in a similar outlet enthalpy but larger subcooling.

The temperature differences were close to the designed, but some superheat and subcooling made them very small in one end of the exchangers. This change in temperature only occurred towards the end, most of the heat exchange in condenser and evaporator found place at the constant saturation temperatures, so this was regarded as all fine. Some instabilities are seen in all graphs, but nothing unacceptable.

The changes in air temperatures in the air-air heat exchanger are shown in Figure B.27. They followed the rest of the process temperatures, and showed a small effect on the cooling need. However, initially, cooling from about 10 to 7 °C was desired. Achieving a reduction of nearly 1 °C was not bad, especially when considering the small temperature differences in the heat exchanger. The designed outlet temperature difference of 1.7 was obtained.

B.5.2 HPSX37

All systems had satisfactory final conditions, even though several systems heated by heat pumps suffered from some extra heating of the process air at the end, when the surroundings were modelled to have high temperature. This also meant that all systems had a small drop in relative humidity like the one in Figure B.28. Correct absolute humidity was obtained,

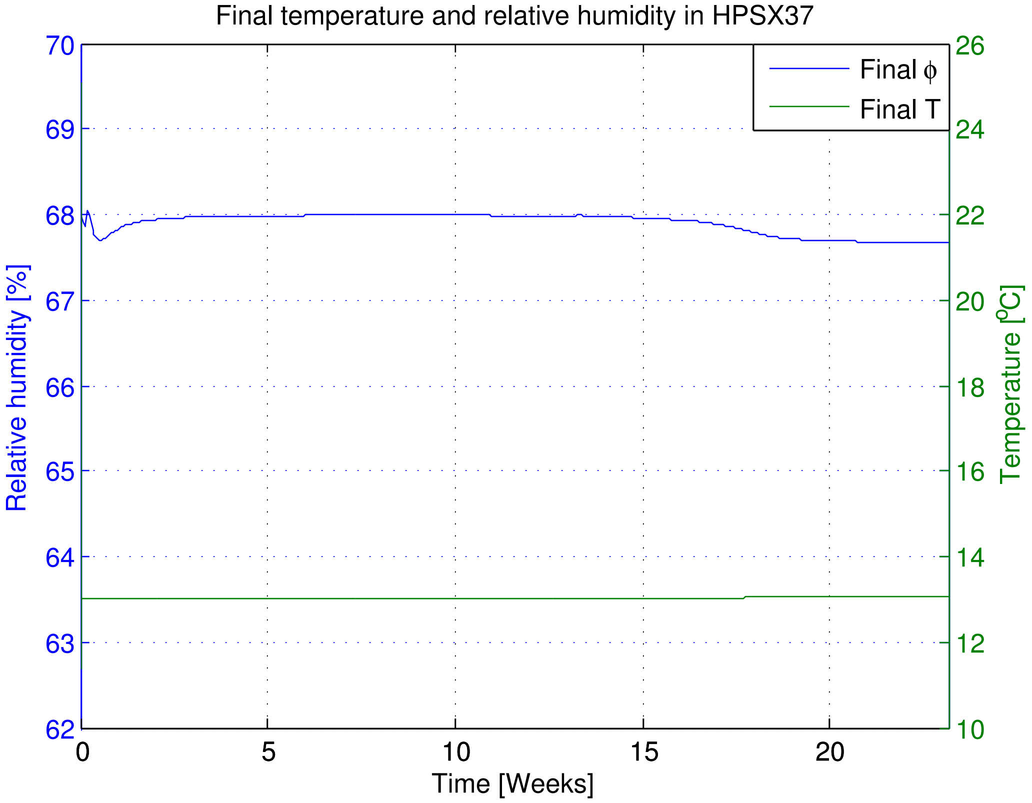

Figure B.28: Resulting temperature and humidity delivered to the drying chamber

the drop in relative humidity was purely due to the higher temperature.

Some noise and initial error before stabilization was also present in this as all other systems. Reasons could be that there were dynamical changes or small disturbances that the controllers needed some time to handle. A deviation from set point must occur before the controllers can calculate how much their output should change, and in which direction. Numerical errors, due to an inappropriate number of time intervals, is another possibility.

The power and energy needs, displayed in Figure B.29 and Figure B.30, were a bit lower in this system than in HPSX100, and markedly better than for HPS. In all other respects, they followed the same trends as the two just mentioned systems.

The COPs for all heat pump systems were high during most of the time, which is reasonable when both heating and cooling are used. The highest possible would vary just like the temperatures and pressures, but a value for heating and cooling to 18 and 1 °C would give $\text{COP}_{max} \approx \frac{273.15+18+273.15+1}{18-1} \approx 33$. Hence, the values obtained were good, but still about half or so of the maximum. The extra temperature differences with glycol is an important reason for this. When the inlet process air became drier, the temperature differences in the heat pump decreased, seen in Figure B.32 and Figure B.33, and the highest possible COP increased.

The temperature differences were in several cases very small, especially in the evaporator and condenser for the incoming glycol in Figure B.32 and Figure B.33. This was due to the

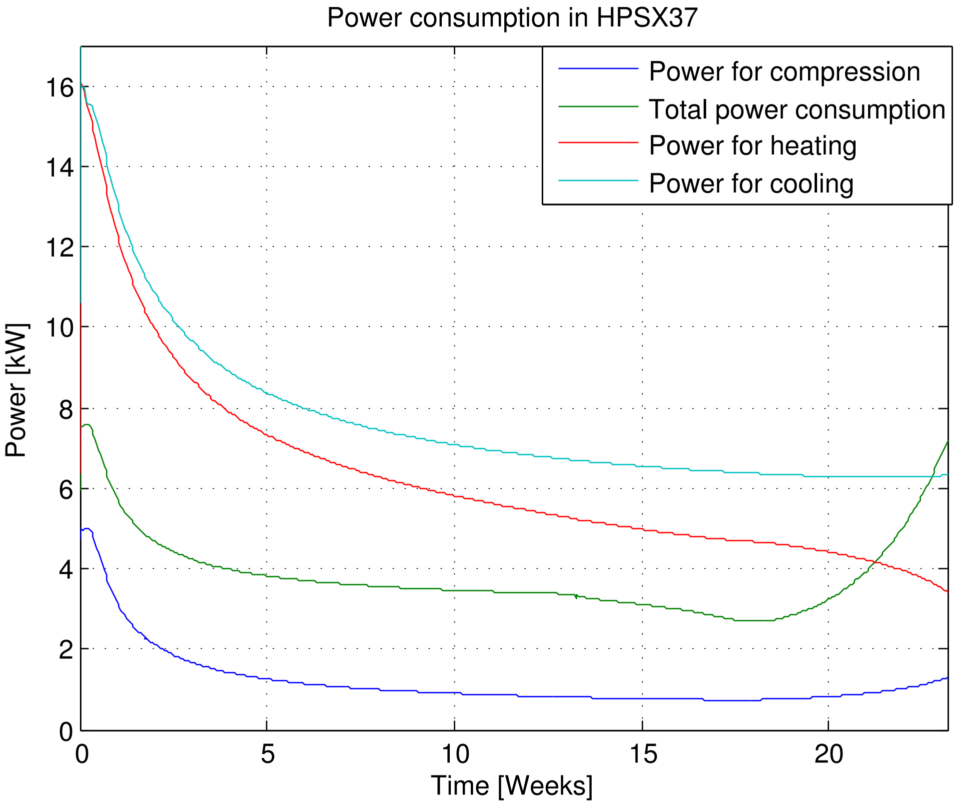

Figure B.29: Power supply to the HPSX37

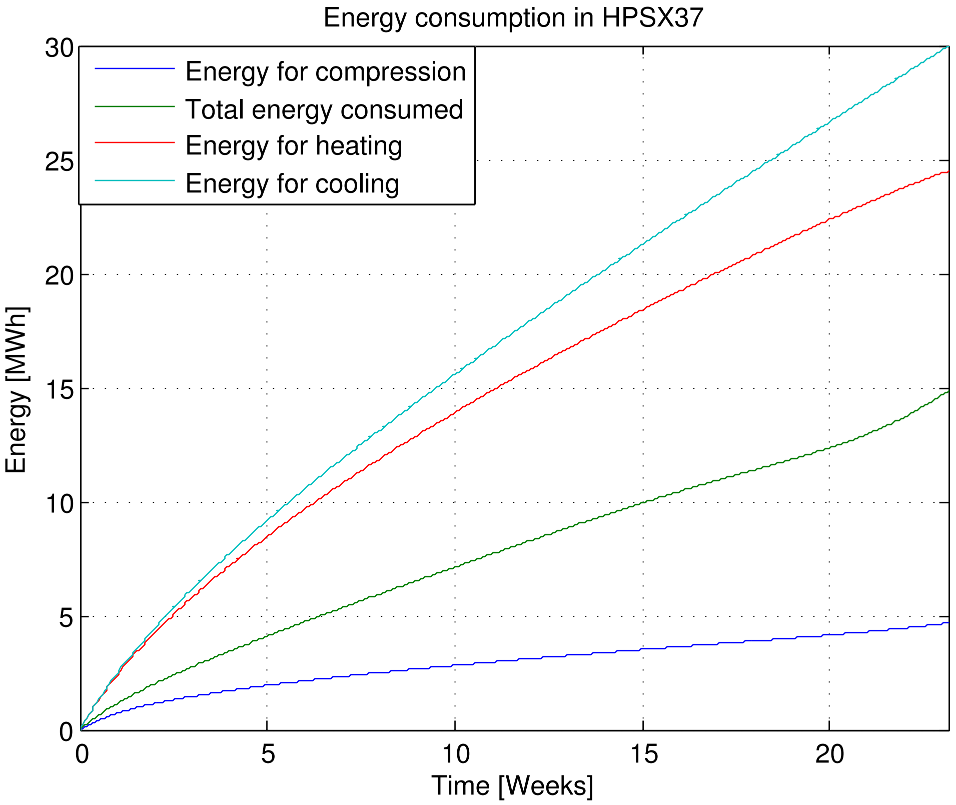

Figure B.30: Energy consumed in the HPSX37 as a function of time

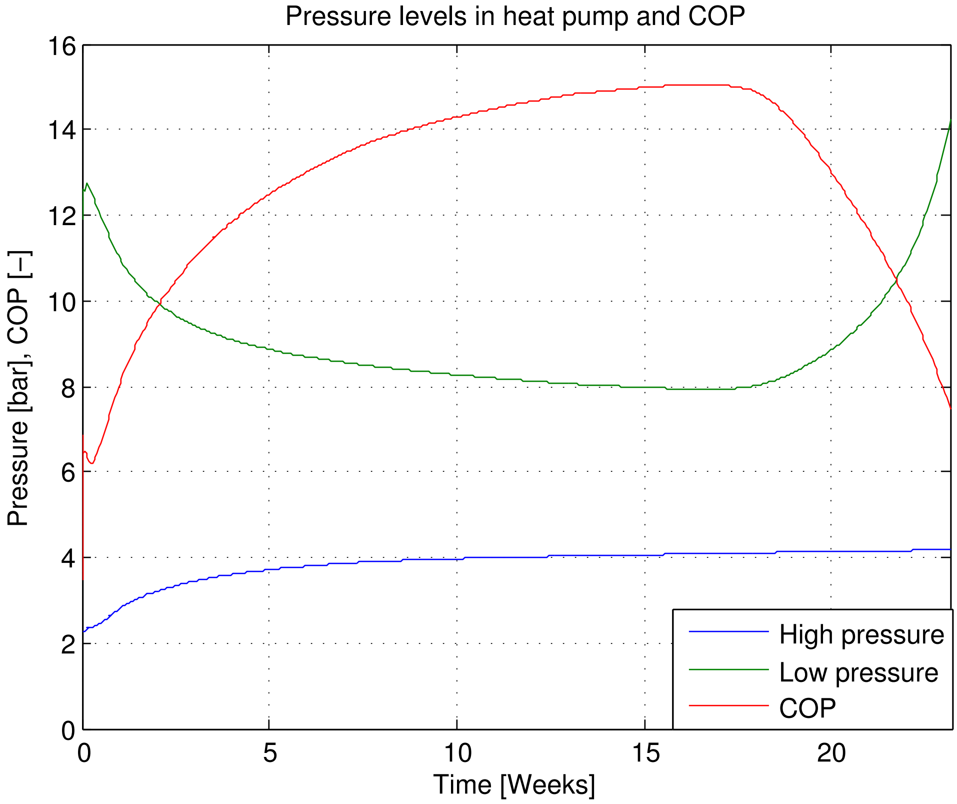

Figure B.31: Development of pressures and COP for the compressor in HPSX37

superheat and subcooling in the process, and occurred only in a small part of the exchangers. Most of the heat exchange took place with the saturated, working fluid, at a much higher temperature difference than what it appears to be.

The decreasing outlet temperature of the ambient air was due to that the incoming temperature increased, and this called for a higher airflow to obtain the same heat rejection. The larger airflow absorbed more heat without increasing much in temperature, and at the highest outdoor temperatures, the systems could not have had a much lower flow of this warm cooling air. As seen in Figure B.31, the highest pressure increased quite a bit when the airflow and outdoor temperature increased. The pressure should not increase to much, as the power consumption to compressor and the COP changed to the worse when this happened, which also clear from Figure B.31. At lower ambient temperatures, this was not a problem, as heat could be rejected to the air at the same pressure as the process required.

Except for this, temperature differences were quite reasonable and did not differ from the other ones presented. The air temperatures on the other side, were lower and higher after cooling and heating than in the first systems. The lowest air temperature was designed to start at 1 °C. However, air could have relative humidity above 100 % after cooling in DYMOLA, and the heat pump cooled the air until the correct absolute humidity was reached. Hence, some excessive cooling resulted, and the initial air temperature was closer to zero.

The effect of the air-air heat exchanger was substantially better than in HPSX100 and is

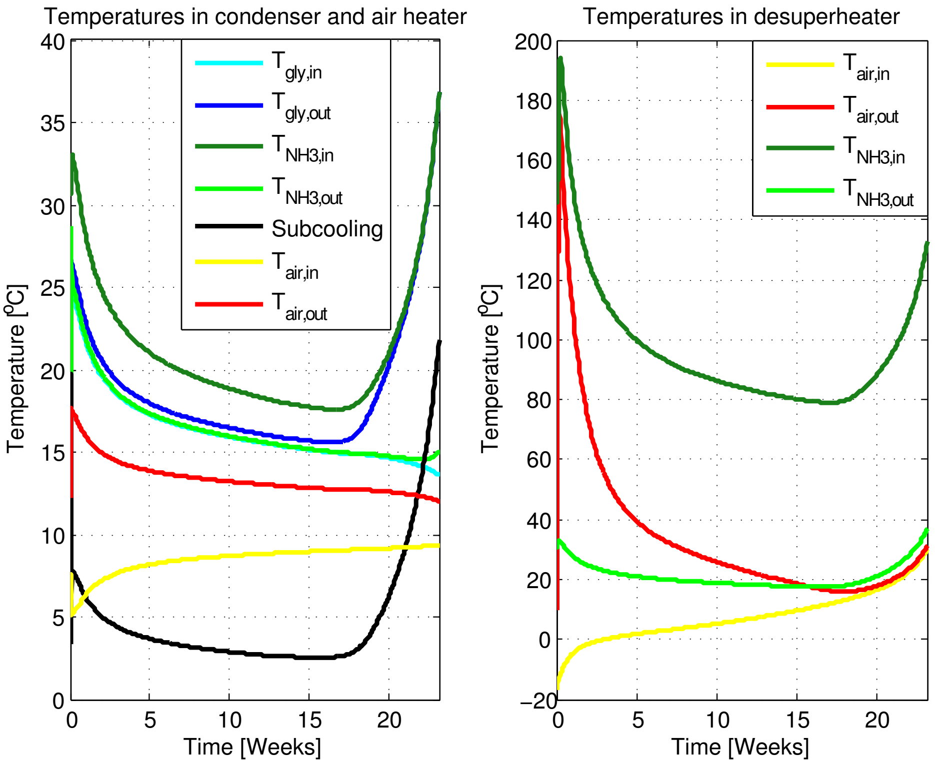

Figure B.32: Heat exchanger temperatures in desuperheater, where ammonia is cooled by ambient air, and temperatures in condenser and air heater in HPSX37: For glycol, the subscripts «in» and «out» refer to in and out of the condenser.

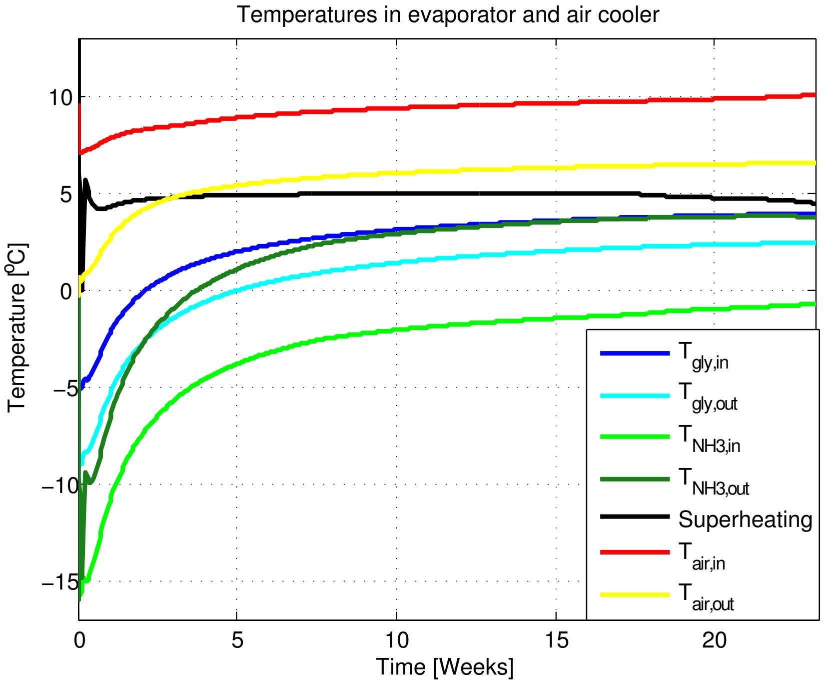

Figure B.33: Temperatures in evaporator and air cooler in HPSX37: For glycol, the subscripts «in» and «out» refer to in and out of the evaporator.

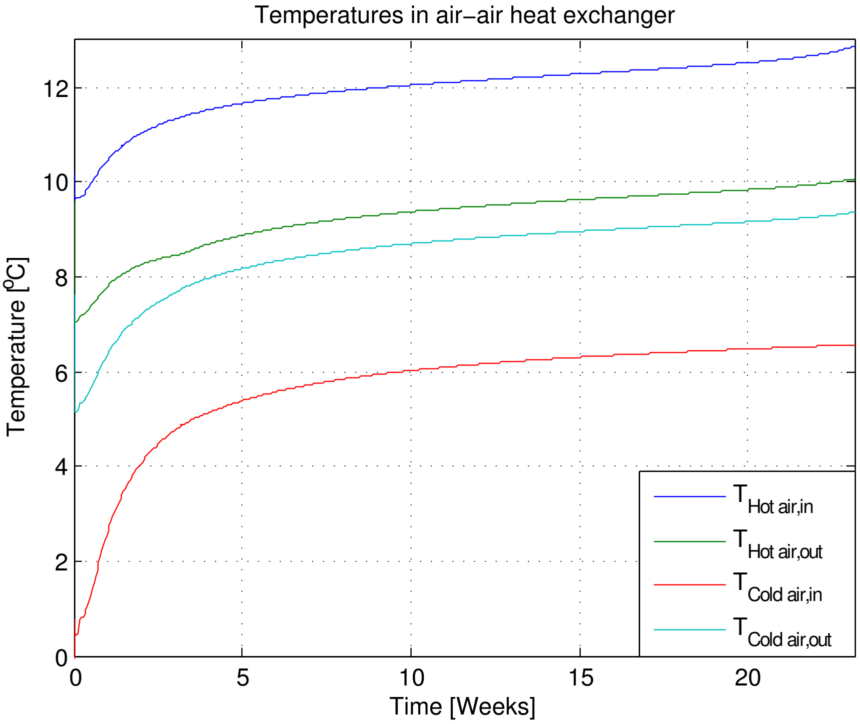

Figure B.34: Air-Air heat exchanger temperatures in HPSX37

shown in Figure B.34. The inlet temperatures differed more, and the exchanger played a more significant role. The smallest temperature difference was designed to be 1.7 °C at the start, and there was a relatively constant difference between in- and outflowing streams.

B.5.3 HPSX1

This system was the best performing of all ammonia systems, and its power and accumulated energy is shown in Figure B.35 and Figure B.36. Power needed was high at first, but decreased steeply when less air was cooled and less water condensed.

The initial values in this system should be similar to those in HPSX37, as the system always cooled the minimum amount of air to achieve satisfactory conditions, which was about 37 % to begin with. Some initial deviations were always present, so in the simulation, initial airflow being dehumidified was a bit higher. The mass flow of air is displayed in Figure B.37.

In all heat pump systems, the energy for compression comprised about half of the total. Fans and pumps were the other power sinks, which is seen in for example Figure B.35. This might be a higher portion than fans normally contribute with, but it also includes fan power to transport the entire air stream through the plant, and there are unusually many heat exchangers in the systems, making the pressure drops significant for overall energy needs.

Despite the low energy consumption, the final conditions shown in Figure B.38 were just as good as for the other systems. It showed the same small temperature increase as the

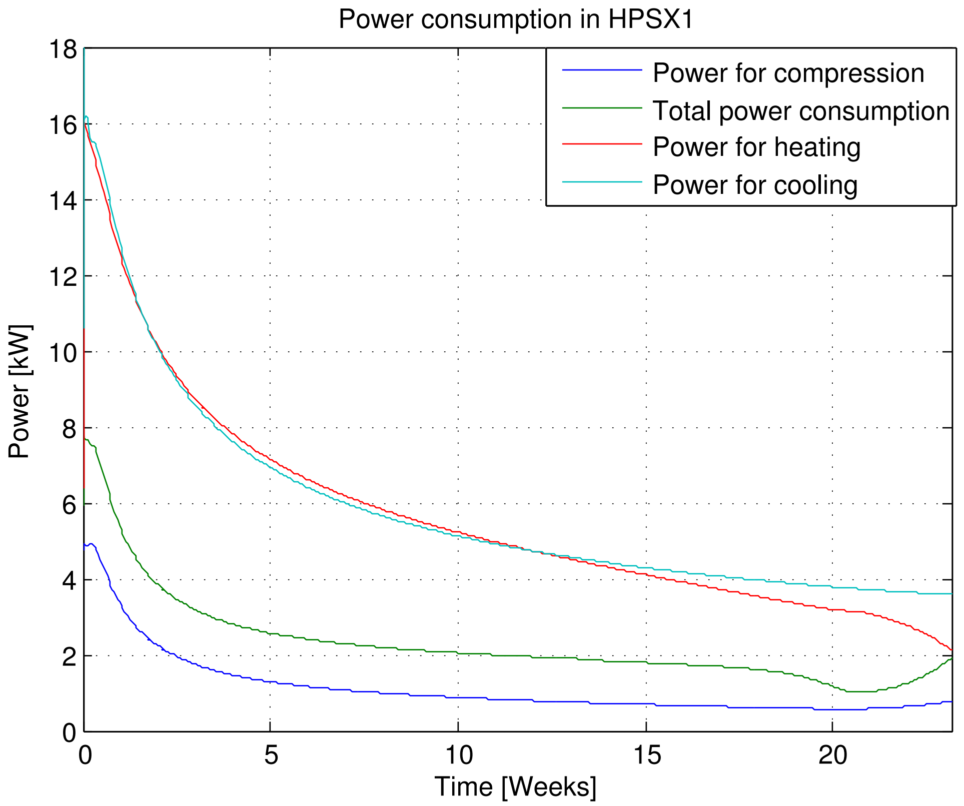

Figure B.35: Power supply to HPSX1 as a function of time

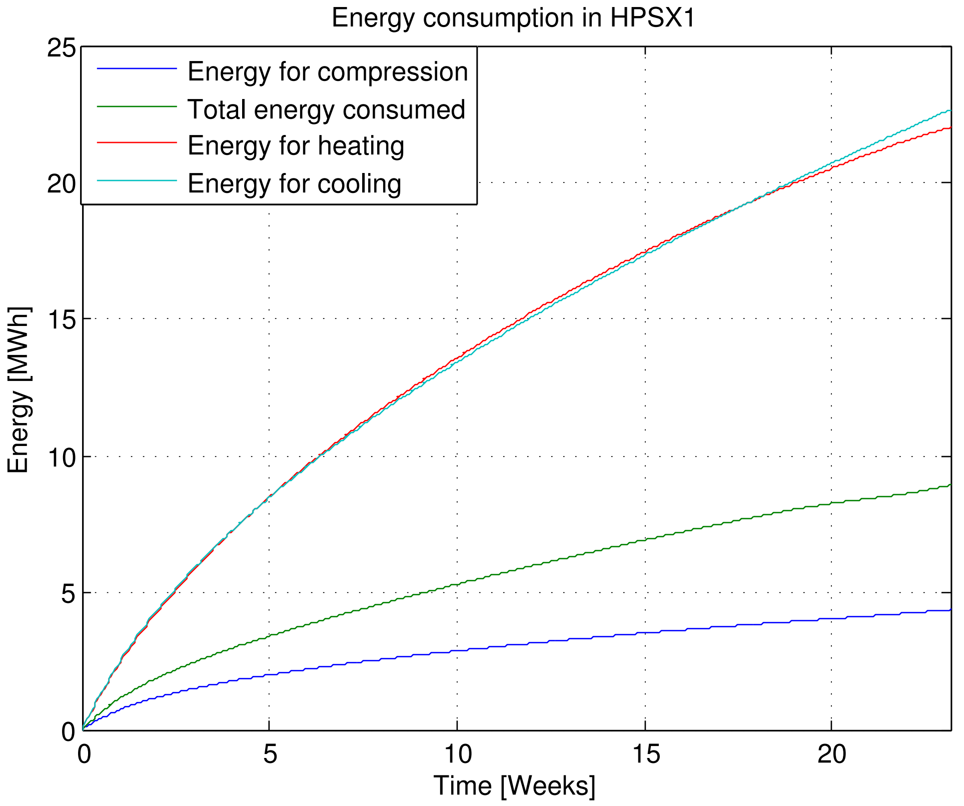

Figure B.36: Energy required in the HPSX1 as a function of time

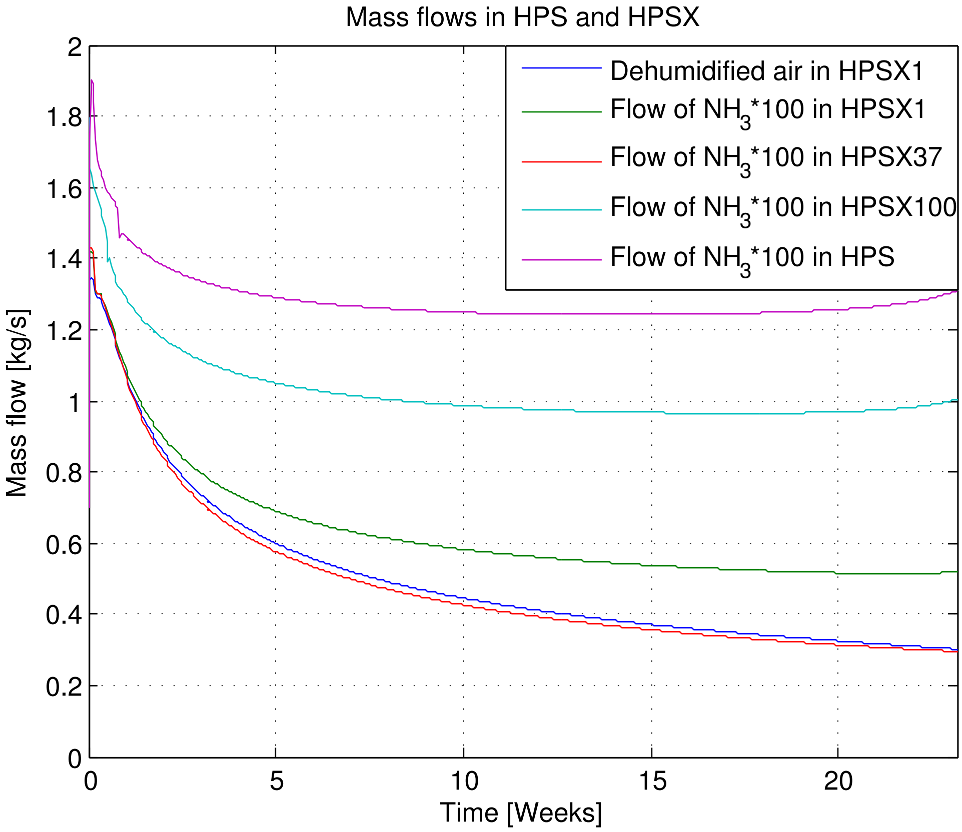

Figure B.37: Mass flow of air being dehumidified in HPSX1, and mass flows of ammonia (NH_3) multiplied by 100 in all HPSX systems and HPS, shown for comparison

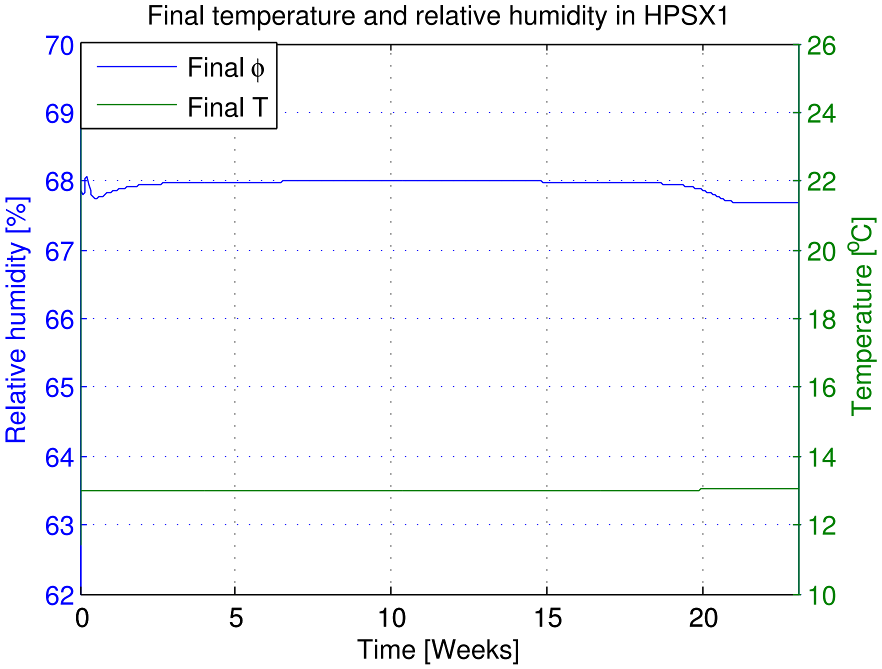

Figure B.38: The resulting temperature and humidity delivered to the drying chamber in HPSX1

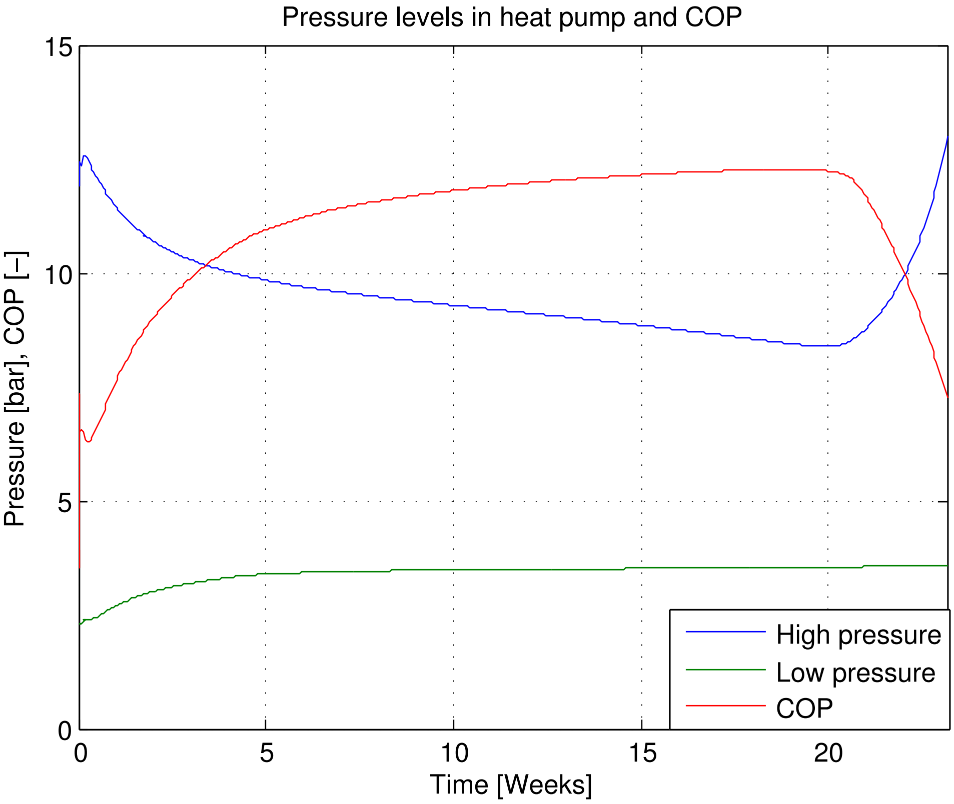

Figure B.39: Development of pressures and COP for the heat pump in HPSX1 as a function of drying time

other heat pump systems at the highest temperature. The amount of cooling air to the heat pump could be set many times higher without decreasing this further, as the temperature lift for ambient air in the desuperheater, Figure B.40, was already minimal.

More cooling air lowered the highest pressure, but there was of course a lower limit, because lower pressure and saturation temperature diminished the temperature differences in the desuperheater, and lowered the heat rejection. In addition, the extra fan power to supply the cooling air increased very much if this was done, so the small temperature increase was accepted.

The pressures and COP all behaved in a similar manner as in the other systems, and are shown in Figure B.39. The COP of this system and that of HPSX37 were actually surprisingly equal.

The interesting and special about this system, is that much of the dynamics disappeared when the lowest temperature for the process air, 1 °C, was set constant, as seen in Figure B.41. This was especially because this had a back coupled effect through the air-air heat exchanger, as seen in Figure B.42. This constantly low temperature made the air temperature into the cooler more stable and similar features were seen around the entire system. An example is the hot outlet temperature from the air-air heat exchanger. The mass flow of process air though, changed, and so did the mass flow of ammonia, and they followed each other

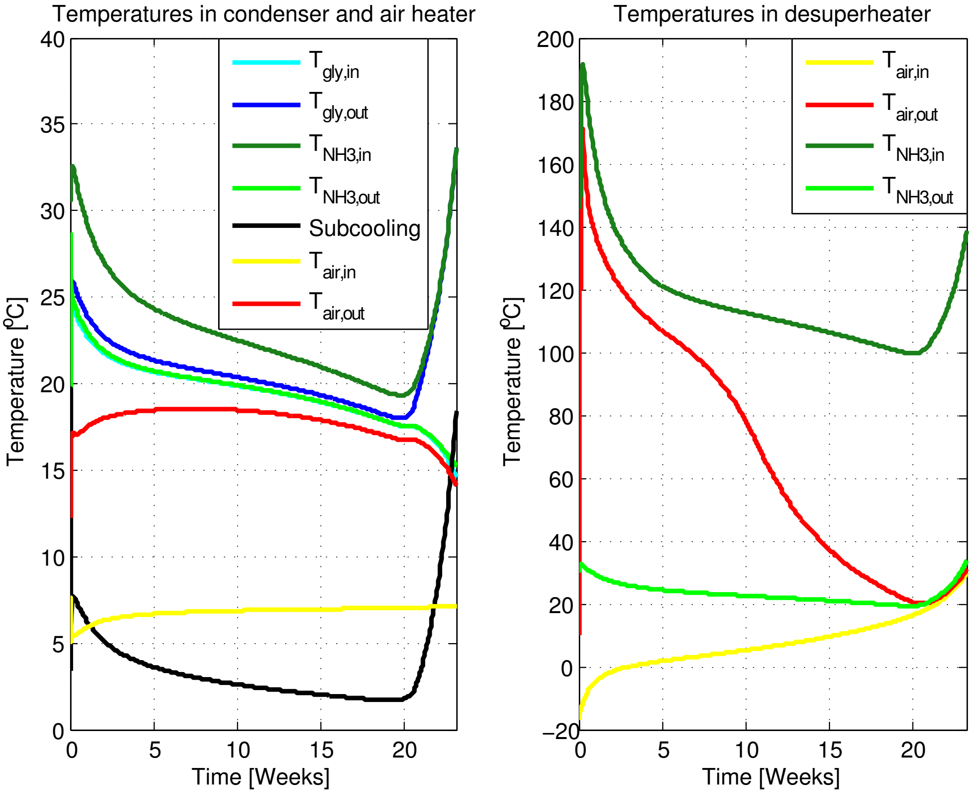

Figure B.40: Heat exchanger temperatures in desuperheater, where ammonia is cooled by ambient air, and temperatures in condenser and air heater in HPSX1: For glycol, the subscripts «in» and «out» refer to in and out of the condenser.

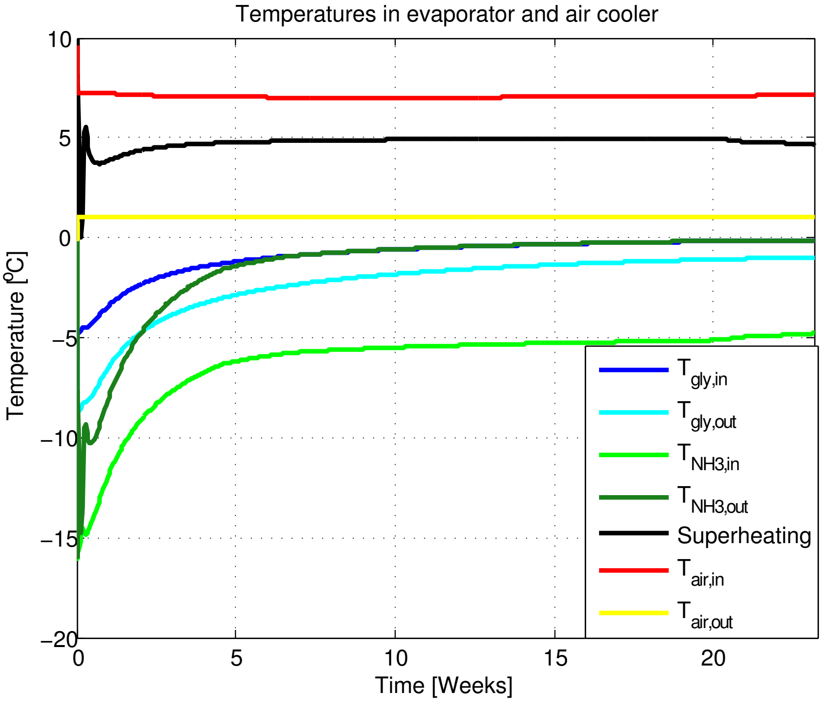

Figure B.41: Heat exchanger temperatures in evaporator and air cooler in HPSX1: For glycol, the subscripts «in» and «out» refer to in and out of the

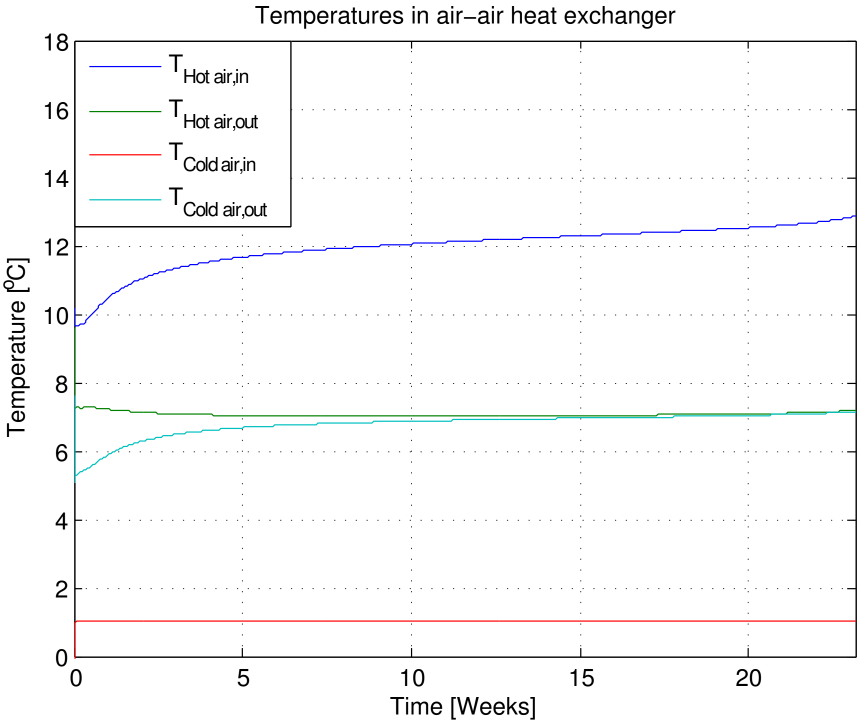

Figure B.42: Air-Air heat exchanger temperatures in HPSX1

almost entirely, which is reasonable as less air required less cooling, but in return, this air should not be cooled less with time like in the other systems. Because the temperature was constant, but less heat was rejected and supplied, the flow of ammonia became much smaller than for other systems. So did the compression power. The mass flows of ammonia in all HPSX and HPS are visualized in Figure B.37 for comparison. Lower flow of ammonia was one of the main reasons for lower energy consumption.

Exchanging heat between the cooled and uncooled air showed good heat transfer with the inlet temperature differences seen in Figure B.42. These actually increased when the inlet air was drier and warmer, and the coldest air always 1 °C. The temperature difference between the outgoing flows decreased as the air mass flows decreased steeply, which is different from all other HPSX. The reason is that the heat exchanger was dimensioned for the initial airflow, 37 % of the total, and for smaller flows one could perhaps say that it became over dimensioned. This reduced the load on the heat pump, causing the energy consumption to be lower than for any other of the ammonia systems.

Like in the other systems, the pressure ratio decreased and so did the temperature differences, seen in Figure B.41 and Figure B.40. This was again because, despite the constantly lower and higher air temperatures after heat exchange, less heat should be transferred, and a lower temperature difference resulted.

DEMOIST

The air-air heat exchangers were modelled as pipes with heat transport between them in DYMOLA, like the two pipes seen in Figure B.20, as no built-in air-air heat exchanger was available. The red line in Figure B.20 represents heat flow. The performance of these exchangers were tested similarly to that of other exchangers before they were used.

A problem was that the pipes lacked the possibility to withdraw condensed water. Hence, the relative humidity after these exchangers could exceed 100 % quite much. For HPSX100, the exchanged heat was so small that this did not have any strong effect. Most other systems also showed a relative humidity slightly above 100 % after condensation in heat exchangers. For HPSX37, HPSX1 and CO2S on the other hand, where much cooling was obtained in the air-air heat exchanger, this caused the humidity to be more than 120 %, and made the evaporator unable to remove the large amount of water. The result was that the heat pump cooled the air several °C too much, in order to condense more water. This affected the energy results, and gave unacceptable conditions in the models.

To solve this, a model block called «Demoist» was made and placed *after* the first pipe. It contains a glycol-air heat exchanger, able to withdraw condensed water, and a pipe for airflow. The glycol had nearly the same temperature as the incoming air, and only changed the air temperature slightly (0.01 °C hotter at all times except at the start when it was nearly 0.25 °C). The pipe was modelled with a heat supply set *equal*, by equation, to the heat flow in the exchanger, but in opposite direction to diminish this difference further. The exit humidity from «Demoist» was still a bit higher than 100 %, but lower than 120 %, and it was similar to that in other systems. This solution was thus kept because this made comparison fairer.

REMARK ON PRESSURE

The pressure drop for the air-air heat exchangers in all HPSX were placed only in the second pipe, with no loss in the first pipe. This should not have any great impact on the results, if any at all. It was done because the simulations would not run if there was a pressure drop in the first tube, perhaps because this created an initially lower pressure in front of the cooling heat exchangers. DYMOLA then calculated that the air should flow backwards, which was not allowed in the model heat exchangers, and caused a system error and stop.

HEATING A FRACTION OR ALL THE AIR

For systems dehumidifying only a fraction of the air, it was a question concerning whether one should let the two air streams be mixed before or after the heater. Mixing them before heating would require heating to a lower temperature (to 13 degreees instead of 18 °C, se Figure 6.1), but also cause more air through the heat exchanger, and thereby a larger

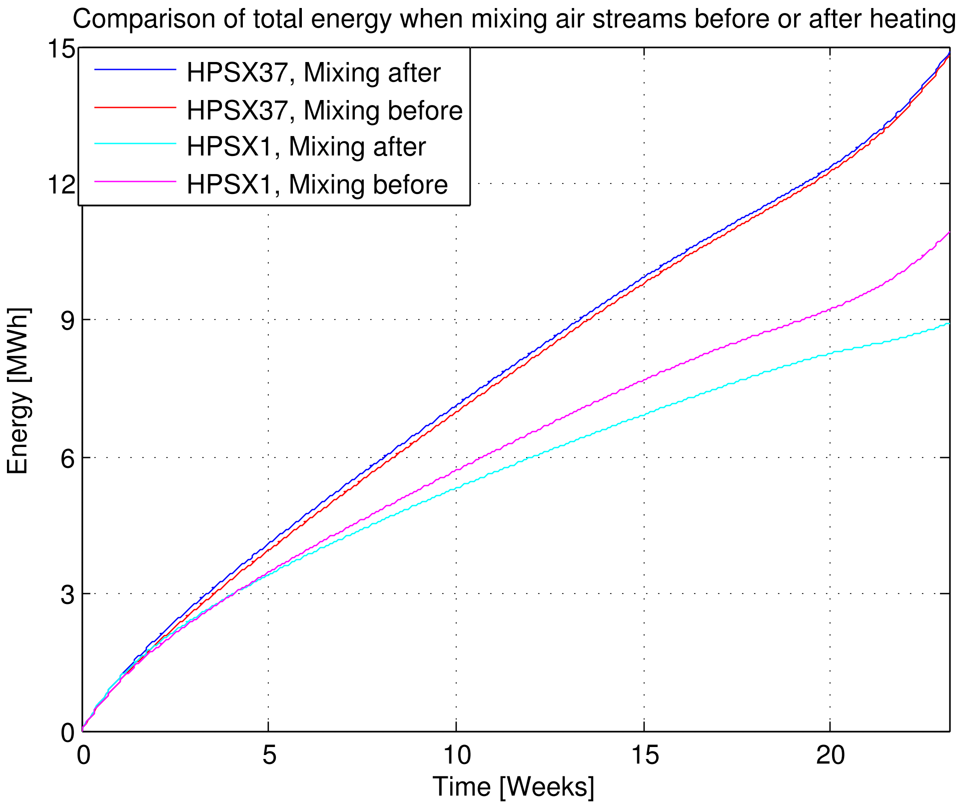

Figure B.43: Comparison of energy when

pressure drop and fanning power. More supplied fan power again meant that less heating was necessary to the process, so more outdoor air for cooling would be required, requiring further more fan power. Mixing the streams after heating is the usual solution. Both solutions have been tried and discussed, but numerous results were only reported for the best case, which was mixing after heating.

The system with a decreasing fraction of air to be dehumidified (HPSX1) was significantly improved by mixing the air streams after heating, visualized in Figure B.43. Reported energy would have been about 22.5 % higher if they were premixed. This was probably because the process air, when unmixed before heating, had a lower temperature and smaller flow rate at the heat exchanger inlet. The low air temperature actually made the high pressure in this process lower than when the air was mixed beforehand, and allowed more subcooling. The lower mass flow in the exchanger decreased the system pressure drop and fan power, thus the air could also be heated more in the heater, seen from the heat supplies in Figure B.44. This in turn made the amount of cooling air to the desuperheater smaller. It obtained the same process conditions by supplying only half as much cooling air, and thus the fan power for outdoor air also decreased.

It must be mentioned, however, that at the start of the process, mixing before heating was a bit better because the airflows to be dried were larger to begin with, which is seen in Figure B.44, and the difference between heating all or only a part of the air was smaller.

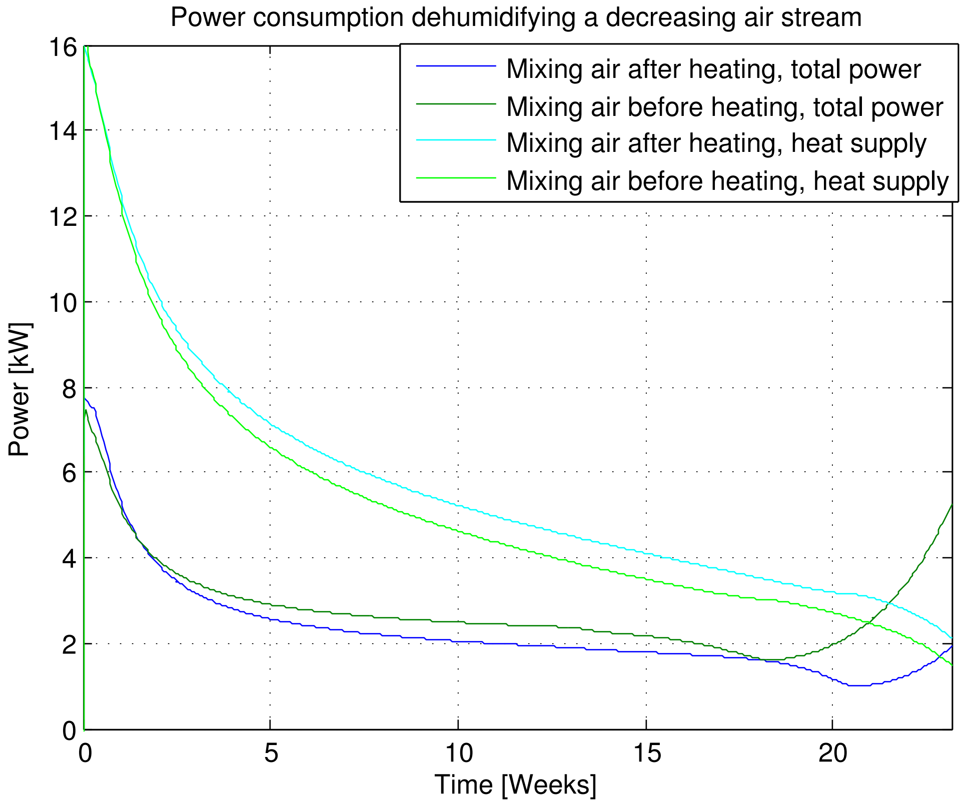

Figure B.44: Total power and power for heating the dried air in HPSX1 for the two cases that heating was conducted before or after that the air streams were remixed

Heating both streams was better as long as the air from the drying tunnel was colder than about 11 °C and had a moisture content above ≈ 90 % and $\approx \frac{0.95\frac{kg}{s}}{3.44\frac{kg}{s}} \approx 28$ % of the air was dried. This means that the extra fan power and compression power were very similar for airflow fractions of ≈ 25 − 40 %, and heating before or after remixing would not matter much. Mixing after heating was better for lower flows than this.

When a constant fraction of the air was dehumidified, in HPSX37, both solutions obtained similar results. Mixing streams after heating was better, but the difference was insignificantly small. The difference also seemed to be constant, 74.5 kWh or 0.5 % of the total, throughout. This is in accordance with the explanation above. Only at the highest heating and cooling loads, for a large enough fraction of air, will mixing before heating be beneficial. This would be important to notice if a plant has a high dehumidification load at all times, for example because there are several drying chambers or the process in the tunnel is operated in a semi-continuous way.

B.6 CO2S

As HPSX1 was the best performing of all the energy systems, this was made with CO_2 to see if any further improvement could be achieved. The model is shown in DYMOLA in Figure B.45, and the heat pump in Figure B.46. Except for the lack of glycol circuits and that the heat pump had another refrigerant with corresponding dimensions, the system was excactly like HPSX1. Its energy and power needs, seen in Figure B.47 and Figure B.48, were the lowest obtained in any system.

Surprisingly, this system, even though being simpler than the other ones, was even harder to control, and several simulations stopped halfway without any apparent reason. Sudden drops in the simulation curves caused large problems unless the regulation was very slow, too slow to reach the desired operational point.

The reason why this occurred is not clear, but one possibility is that the water removal before the heat pump was a bit uneven (the «Demoist» block was used in this model just as in HPSX1), and caused small disturbances. A small drop in moisture content before cooling

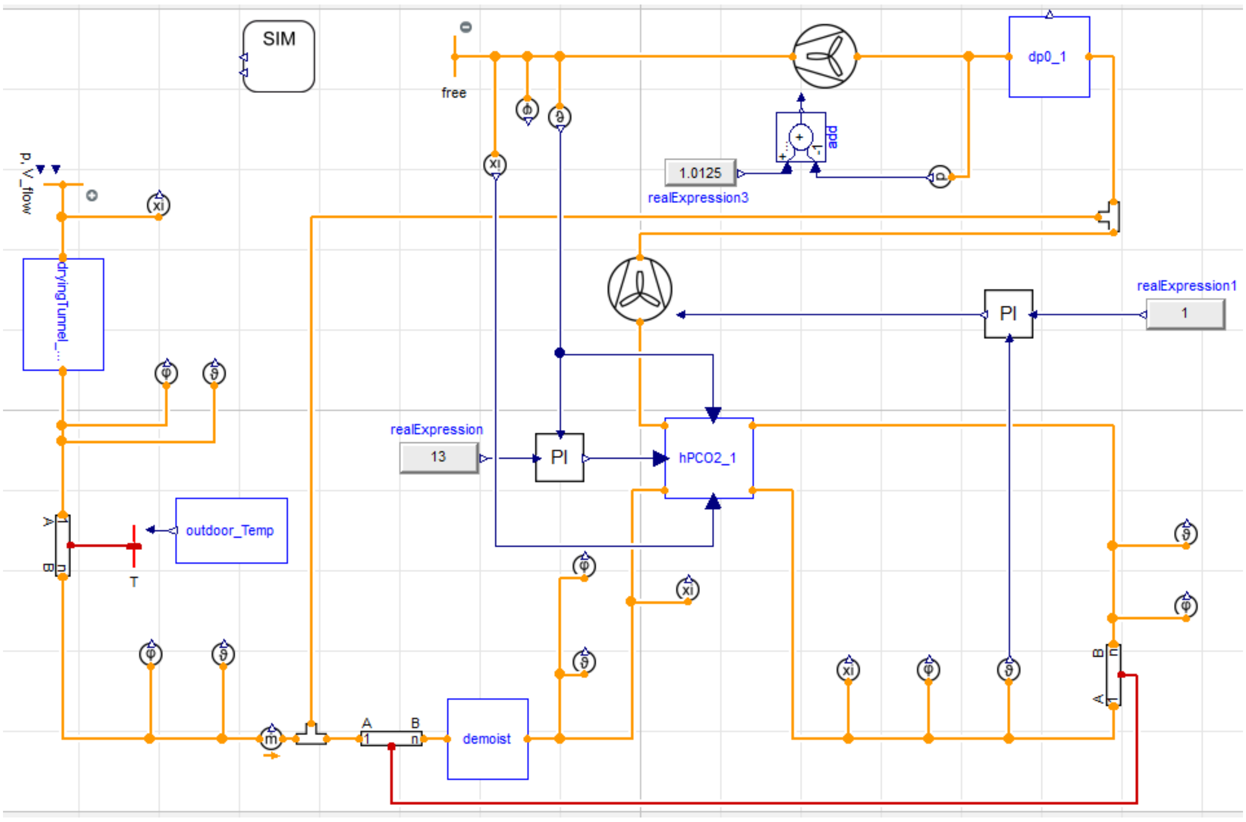

Figure B.45: The icon view of CO2S in DYMOLA: Yellow lines represent airflow, the pipes allow heat exchange through the red lines and the heat pump is the white square close to the centre of the figure: The air enters the heat pump in its lower left corner and exits after cooling from the right lower corner. It is partially heated in the tube to the right before entering the heat pump in the upper right corner, and its condenser, and exits in the upper left corner after heating.

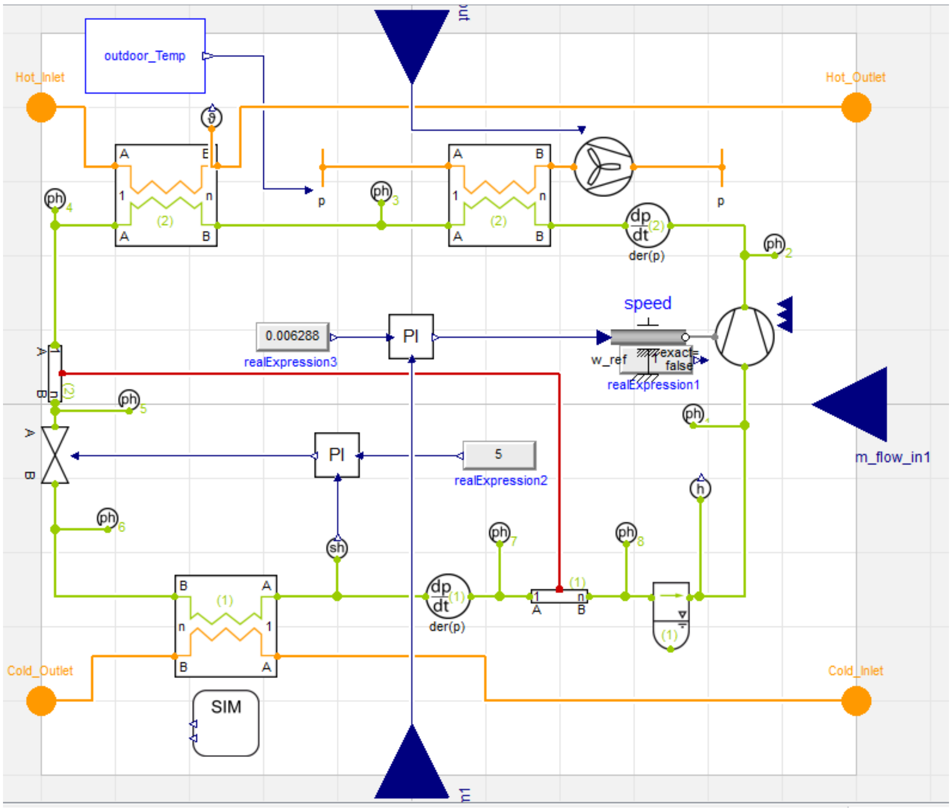

Figure B.46: The icon view of a heat pump using CO_2 in DYMOLA, used in CO2S: the green lines represent flow of CO_2, the yellow airflow, which enters the heat pump in its lower left corner, is cooled in the heat exchanger close to the bottom, and exits in the right lower corner. A sensor for superheating, denoted «sh», controlled the valve to the left. The compressor is seen to the right. The desuperheater and condensers exchanges heat with each their air stream. The process air enters the heat pump a second time in the upper right corner, then the condenser, and exits in the upper left corner after heating. The two tubes connected by a read line is an internal heat exchanger, and the red line represents heat flow. All heat pumps looked like this, except that some exchanged heat with glycol instead of process air, and some only contained one heat exchanger on the high-pressure side (in BS and ADS).

in the heat pump then caused a drop in the compressor speed and flow of refrigerant. This made the low pressure somewhat higher, and made the cooling decrease.

Less cooling increased the lowest temperature unless the mass flow of air also dropped. The system was controlled to constantly achieve 1 °C after cooling, hence the airflow was decreased. Then, the amount of subcooling, cooling by outdoor air and the pressures in the heat pump were affected, and so were all the regulators.

A lower airflow required even less cooling, making the compressor speed fall even further. After the cooling, partial heating by heat exchange with uncooled process air, seen as the red heat flow line in Figure B.45 caused the air to be affected by this even before the heat pump. Several values dropped to about half of their values before the error became large in the other direction. When the final moisture content suddenly became too high, because too little of the air was dried, everything abruptly changed in the opposite direction and the proper operation point was found again.

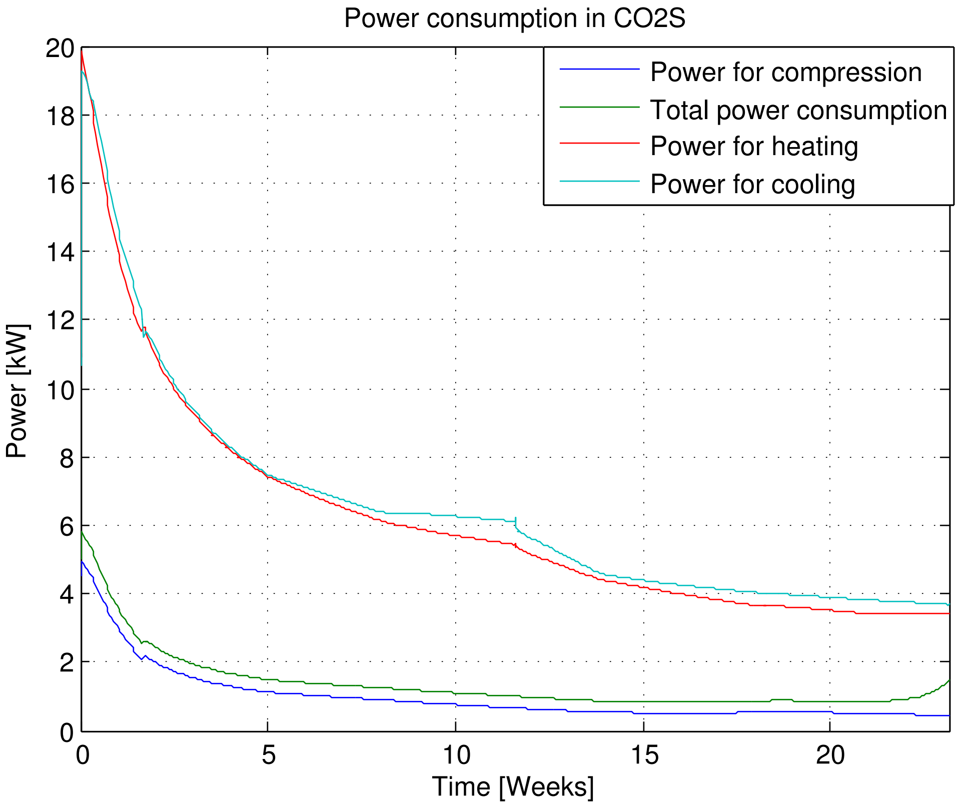

Figure B.47: Power supply to CO2S as a function of time

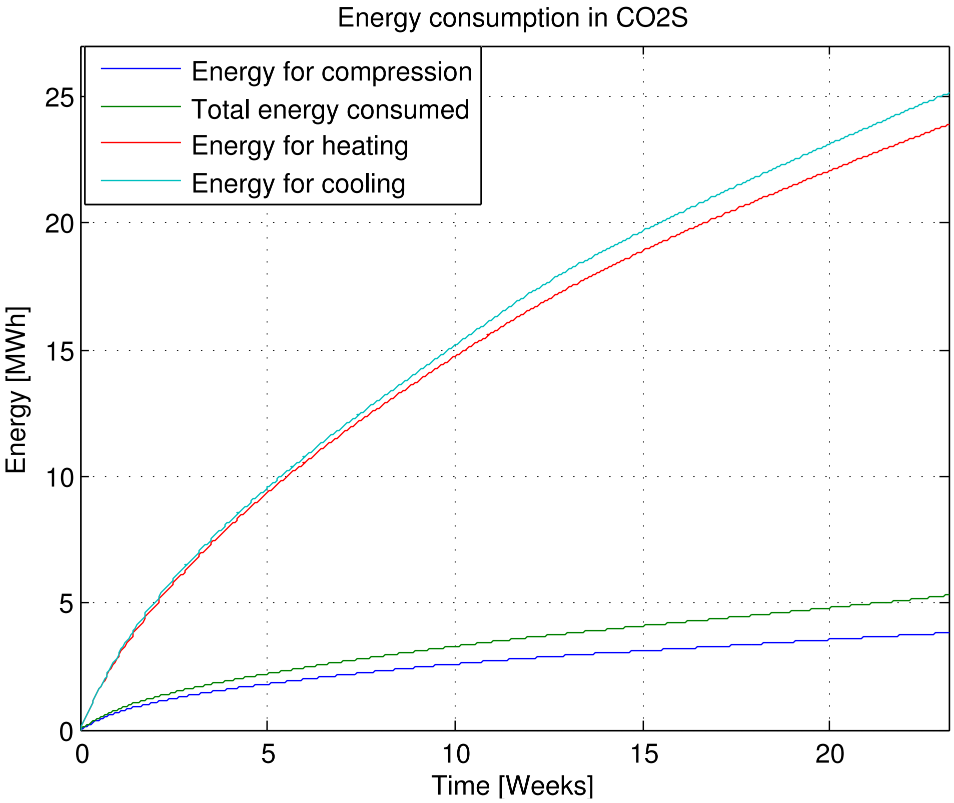

Figure B.48: Energy consumed in the CO2S as a function of time

These disturbances made simulation very hard to accomplish, and impossible to run unless the regulation was too slow to react to such changes. Then the values did not drop so far before the error was corrected, but the controllers were also too slow to maintain the desired final values.

Why this was a particular problem with CO_2, and not with the exact same system using ammonia is uncertain. One possible explanation is the smoothening effect of the glycol circuits. In the ammonia systems, the glycol circuit between the refrigerant and the air smoothened out any sudden temperature change before it arrived on the other heat exchanger in the circuit. A disturbance did not affect superheating and enthalpies in the heat pump as abruptly and strongly as when the refrigerant exchanged heat with the air directly. Thus, a disturbance would affect the compressor speed, but the impact had a smaller, and somewhat delayed effect on other operational conditions. This made the impact far less severe, and the system more stable, so that it could more easily maintain proper operation. The problem was solved by partially using the controllers, and partially equations that were made to follow the smooth lines the regulator ought to follow instead of dropping, avoiding the sudden peaks in the simulation. These desired curves were visible from the simulations where the drop occurred, and they stabilized the system. In a real plant, where the process is slow, sudden peaks and jumps could hopefully be avoided, or at least not be a problem, as the final conditions showed in Figure B.49 were actually achieved despite these instabilities.

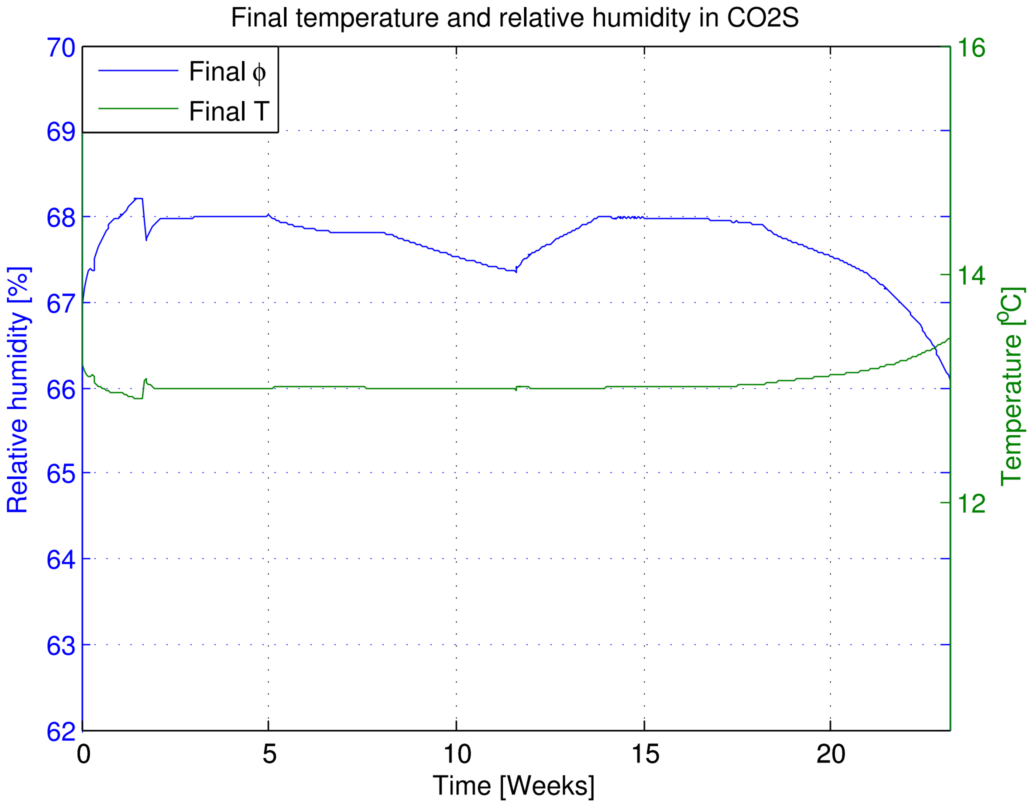

Figure B.49: The resulting temperature and humidity delivered to the drying chamber in CO2S

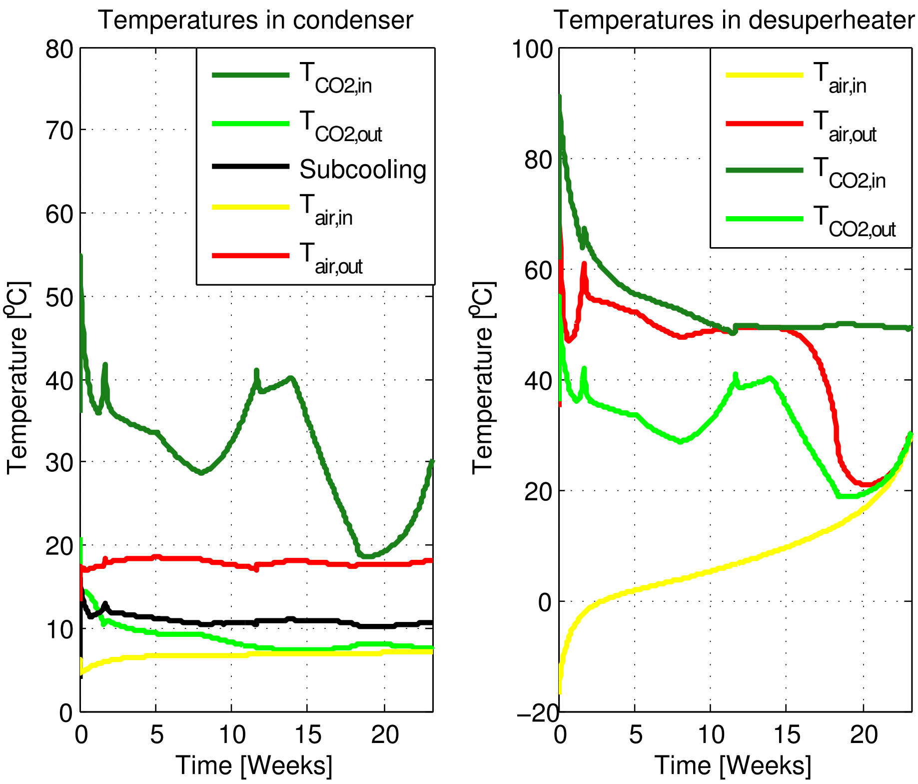

Figure B.50: Heat exchanger temperatures in the desuperheater, where CO_2 was cooled by ambient air, and the condenser in CO2S

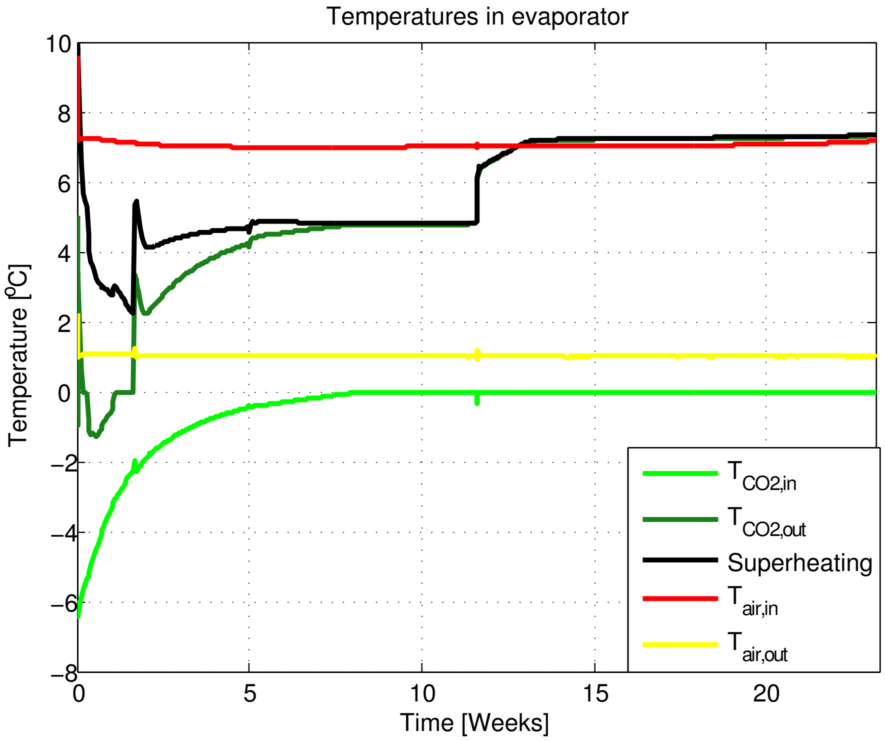

Figure B.51: Temperatures in the evaporator of CO2S

Some jumps in the obtained conditions can still be seen, which the values in Figure B.50 and Figure B.51 are examples of, and the final values were not as good as desired. Figure B.49 show that they are not as smooth as in other systems, but CO2S did remove sufficient amounts of water and the conditions were close enough to the set point for the system to be accepted as the best performing energy system.

The main argument against this acceptance, was that the temperature increase in Figure B.49, at the highest outdoor temperatures, was higher than in any other system. A final process temperature half a degree above set point is not a big error, but it would be better to reduce it. Unlike in other systems using a heat pump, it was not possible to reduce the process temperature by reducing the glycol flow. The only way to reduce the process temperature seemed to be by applying more cooling air, which would increase the overall energy consumption.

However, just like in HPSX1, there was a limit for how much heat ambient air could reject as the higher airflow reduced the CO_2 pressure and temperature, and thereby the temperature difference for heat transfer.

In addition, when much cooling air was supplied, its temperature change was nearly zero, like in Figure B.50 and most other systems. Hence, no improvement from higher airflows was obtained. The CO_2 was practically cooled to the air temperature, but could not be cooled any further. Thus, it would not help to apply more air.

One could wonder if the desuperheater was too small, even though it had been tested for the worst conditions. The explanation was that the cooling, both from the outdoor and from the process air which entered at about 7 °C, prevented the pressure from increasing, so that the designed conditions with CO_2 at 65 °C and transcritical operation at 80.7 bars did not occur. Instead, the CO_2 entered at about 50 °C and 55 bars (see Figure B.50 and Figure B.52). Subcritical operation was obtained throughout, and the temperature difference for the outdoor air was much lower than assumed in the planning phase.

However, this might actually be good, as it was a concern whether it would be possible to cool the CO_2 sufficiently to use it in such a system. Bad performance could easily occur close to the critical point, and it is uncertain how the condenser and desuperheater would perform if they should be designed for both subcritical and transcritical operation.

Achieving only subcritical operation should therefore be seen as a good thing. The low inlet temperature of the process air, giving a high degree of subcooling, Figure B.50, was probably the reason for this. The CO_2 left the condenser below 10 °C most of the time, which is utterly good. Subcritical operation caused a small pressure ratio, making the cycle efficient. The high COP, which Figure B.52 shows, was constantly high, and unlike in the other heat pump systems, it remained high throughout.

A solution to avoid the final temperature increase could be to allow CO_2 to bypass the heater. Unfortunately, this idea was thought of after all simulations were completed, and therefore not tried. Nevertheless, this would increase the high pressure and lower the

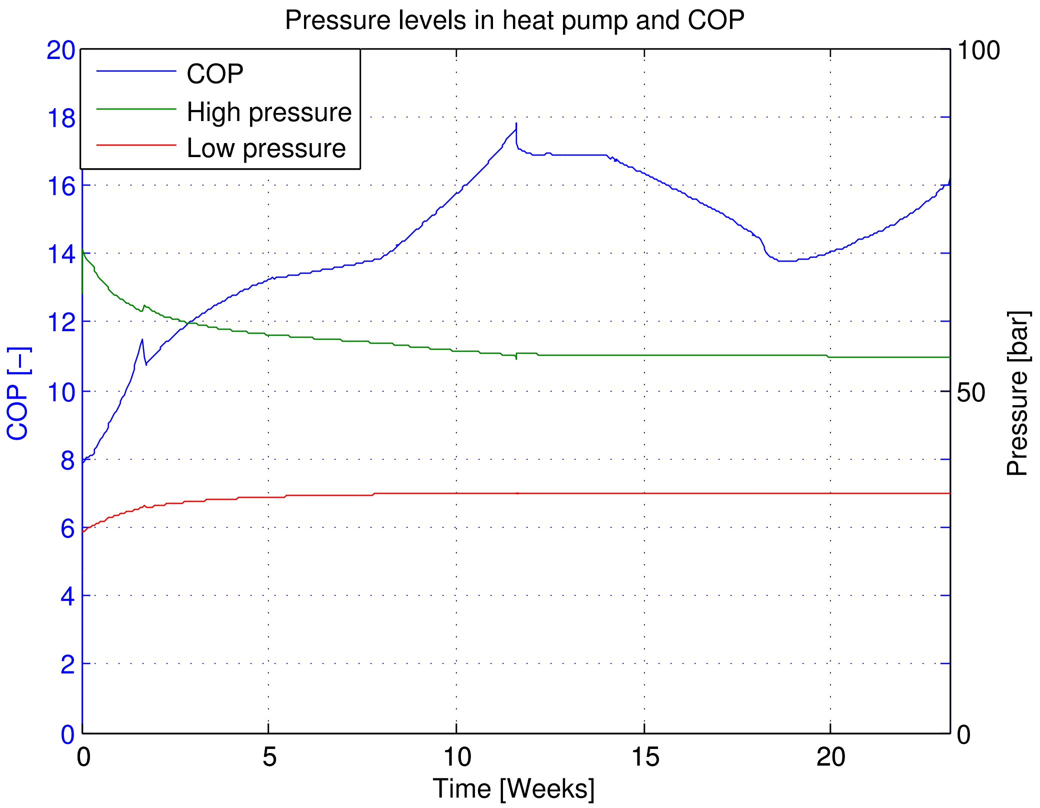

Figure B.52: Development of pressures (right axis) and COP (left axis) for the heat pump in CO2S as a function of drying time

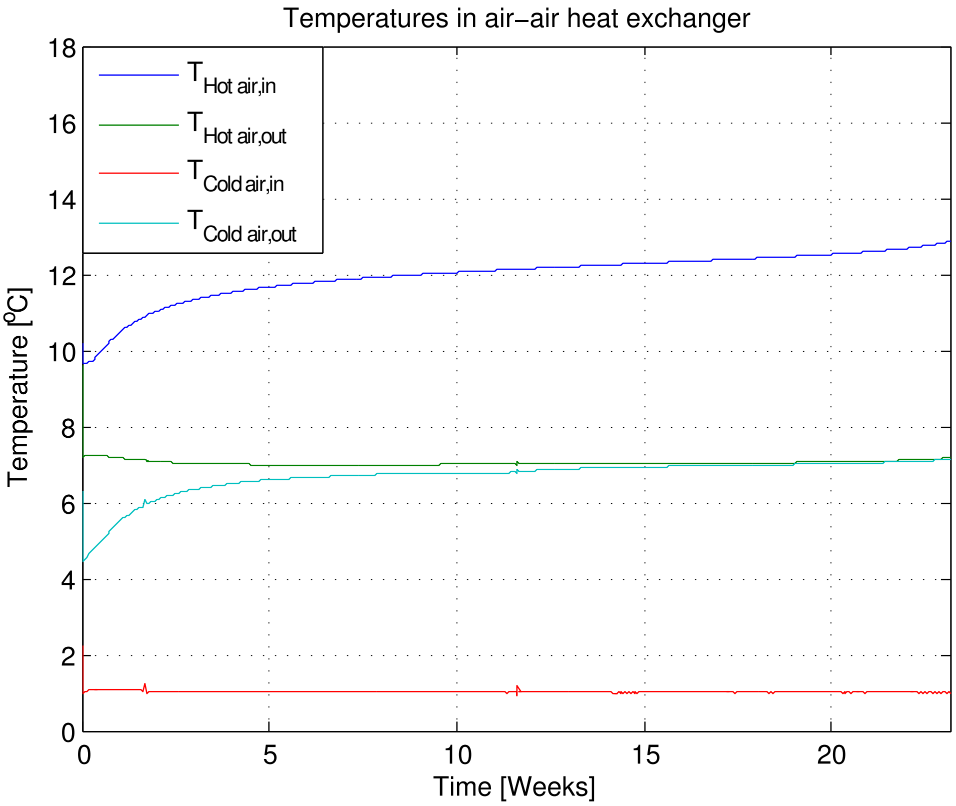

Figure B.53: Air-Air heat exchanger temperatures in CO2S system pressure drop. From the discussion in Section B.5.3, it would not increase the energy consumption much, if it would cause any change at all. Even if it did, CO2S would probably still be the best performing system. The amount of heat that should be avoided in the process was very small, but the difference in energy needed for HPSX1 and CO2S was large.

The temperatures in the air-air heat exchanger behaved just like in HPSX1, which is just as it should be.

B.7 CS

Energy and water required for CS at the three different pressures chosen are presented here, to see how the energy needs varied with pressure. Operational conditions are only shown for the case of a high pressure of 3.0 bars, because these were similar for all the compression systems. The system and its icon view from DYMOLA are given in Figure B.54 and Figure B.55.

All three systems managed to obtain satisfactory humidity and temperature, like those in Figure B.56. The energy consumption for all systems, displayed in Figure B.57, were also very similar, and about equal to that for compression, which should be expected as no other

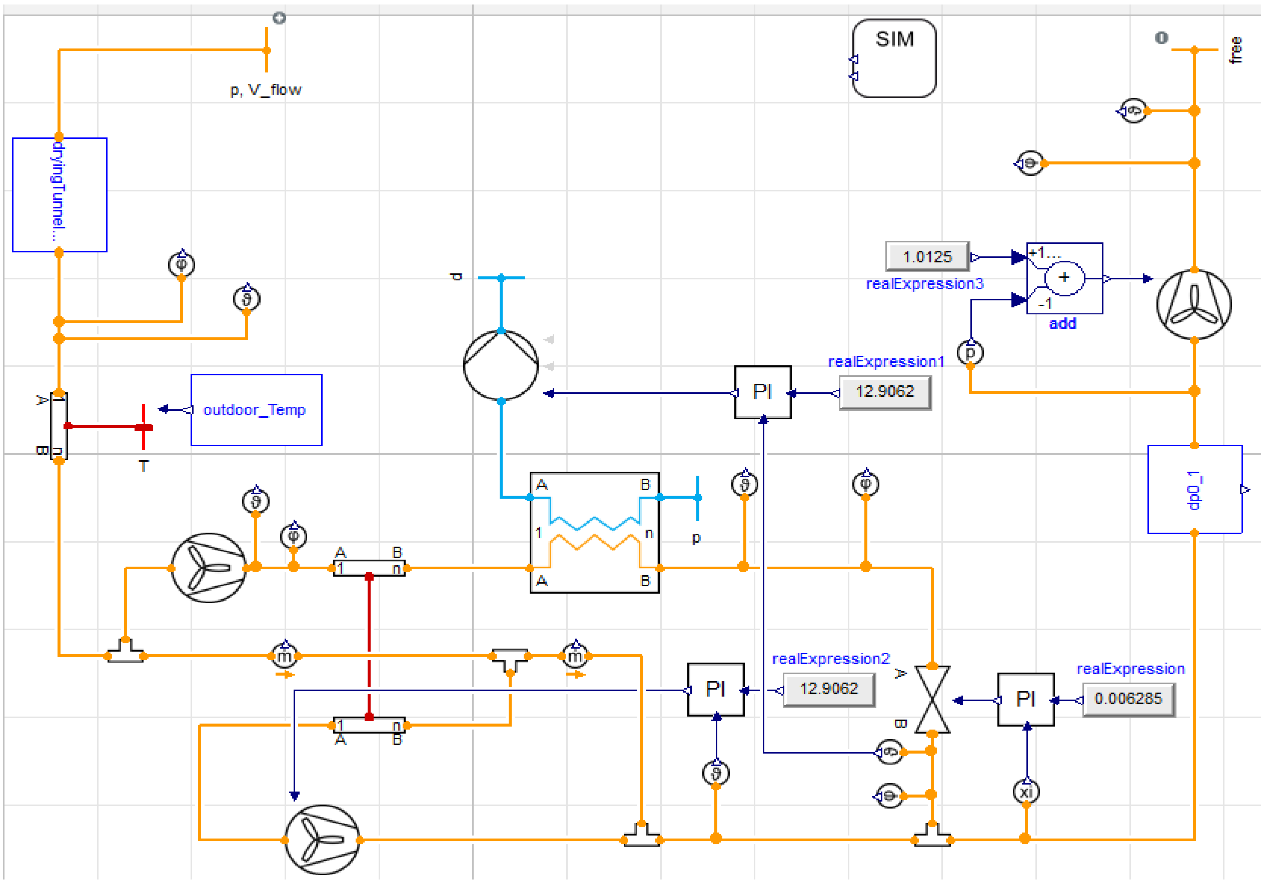

Figure B.54: Compression system as it looks in DYMOLA

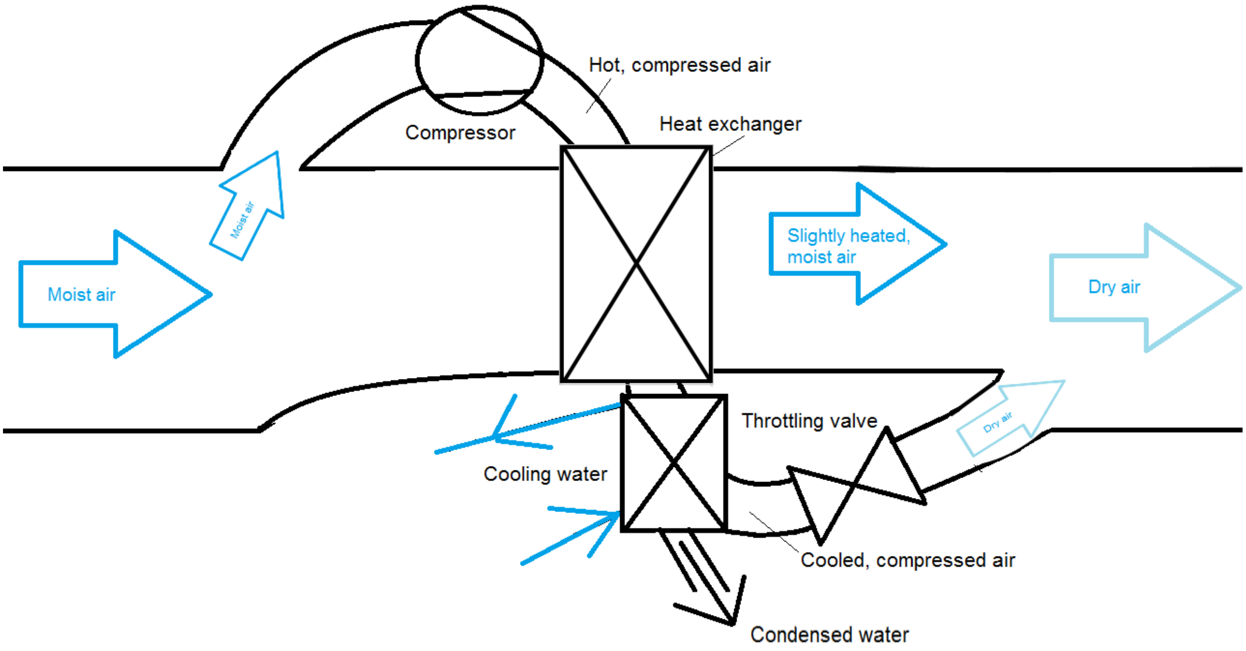

Figure B.55: CS compressing the air to condense water and deliver heat, excess heat was removed by heat exchange with water

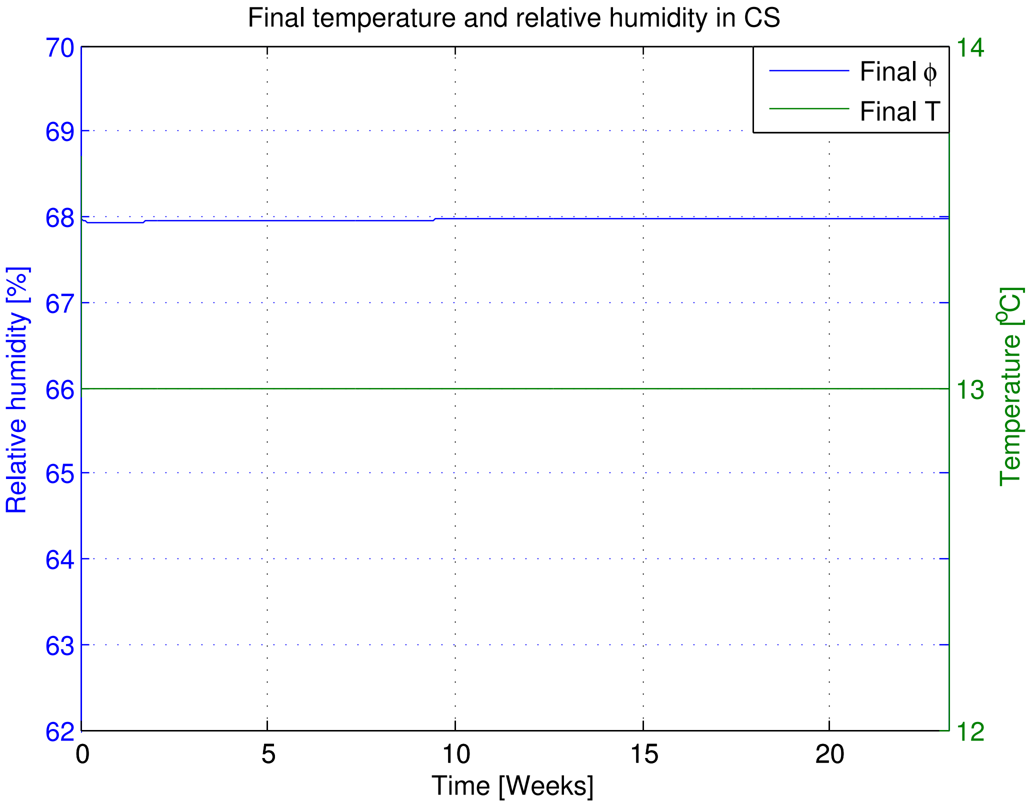

Figure B.56: Final temperature and relative humidity obtained when the air was compressed to 3.0 bars

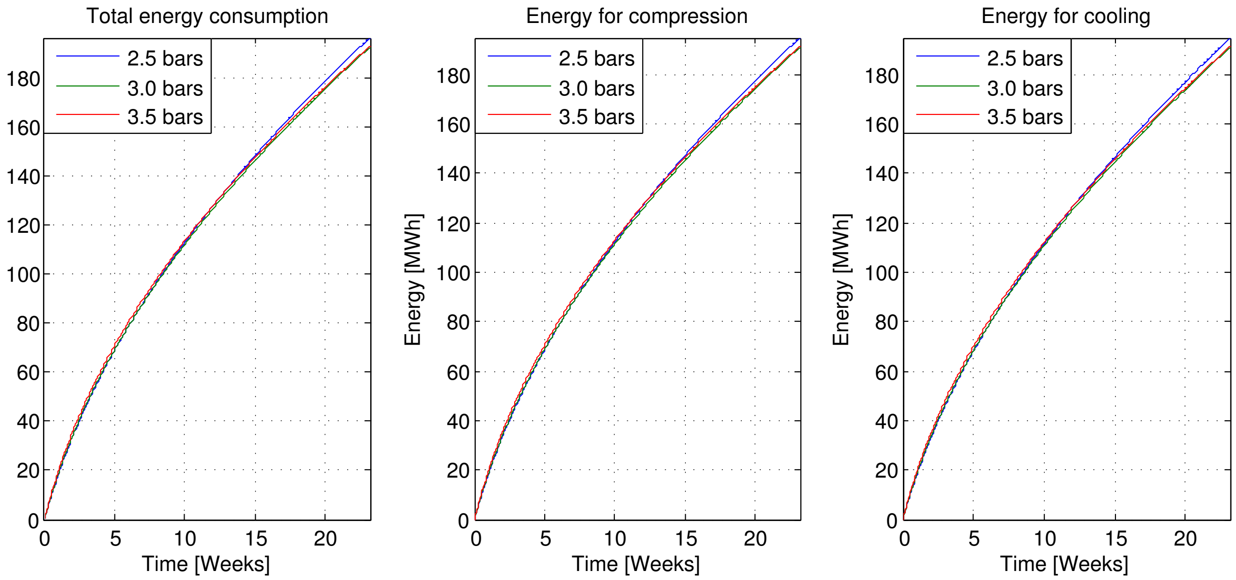

Figure B.57: Accumulated energy consumption for CS at three different high pressure levels

energy consuming equipment was present. Energy to the water pump and air fan are the only differences in total energy and energy for compression.

The cooling need was the same as the heat supplied and therefore also similar. The system at 3.0 bars had a slightly lower energy consumption than both the other two. This could indicate that the optimum energy consumption is found near this operation point, because it is close to the optimum trade-off between amount of air to be compressed and the corresponding high pressure required. Still, this was more probably a coincidence, because the differences in energy were very small.

The amount of cooling water needed on the other hand, clearly decreased with pressure as seen from Figure B.58. The explanations are that the higher air temperature after compression at higher pressures allowed less water to remove the same amount of heat. The compressed air stream was also smaller at higher pressure.

The temperature levels in the heat exchanger were quite reasonable, as seen in Figure B.59. One could heat up the water to a higher temperature and use it as a way to deliver hot water to the plant, but one would then need a much larger heat exchanger and have a need for this water. Such a solution would lower the amount of water used and the energy consumption at some other point in the plant.

The proper amount of air to be compressed varied with time and load. A part of the uncompressed air had to bypass the air-air heat exchanger in order to obtain acceptable heating, which otherwise became too high. The temperature levels and mass flows of air in the heat exchanger are shown in Figure B.59 and Figure B.60. Towards the end of the process, the uncompressed air hardly needed heating at all, and hardly any of it entered the heat exchanger, causing the temperature difference in the exchanger to become very small.

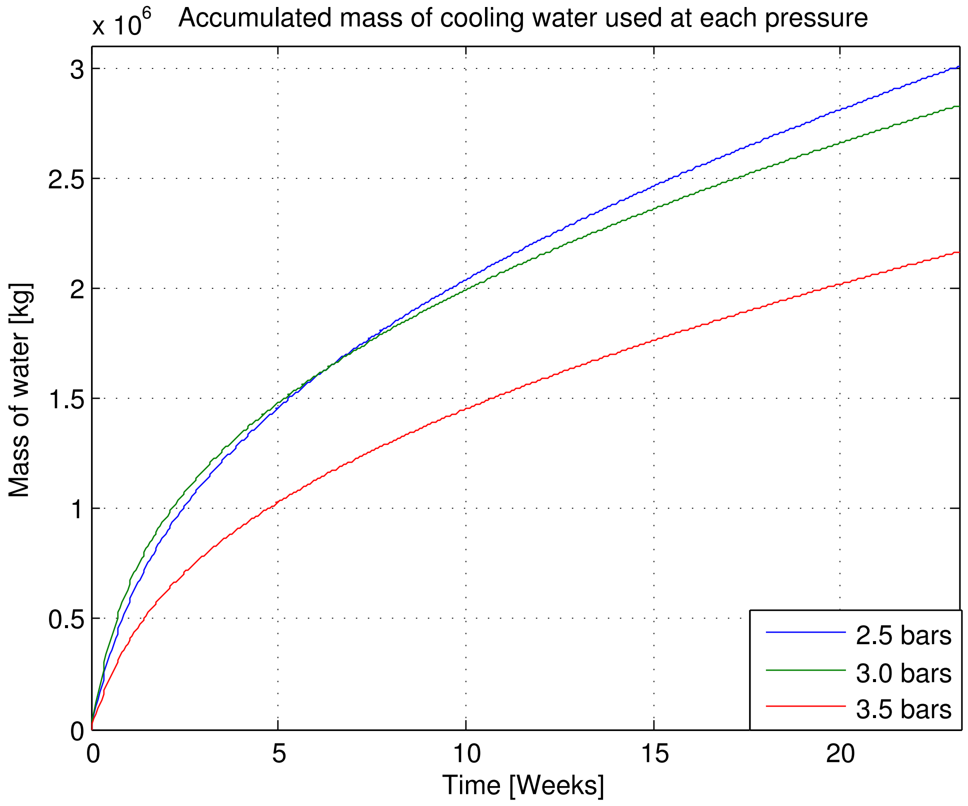

Figure B.58: Accumulated use of cooling water for three different high pressure levels in CS

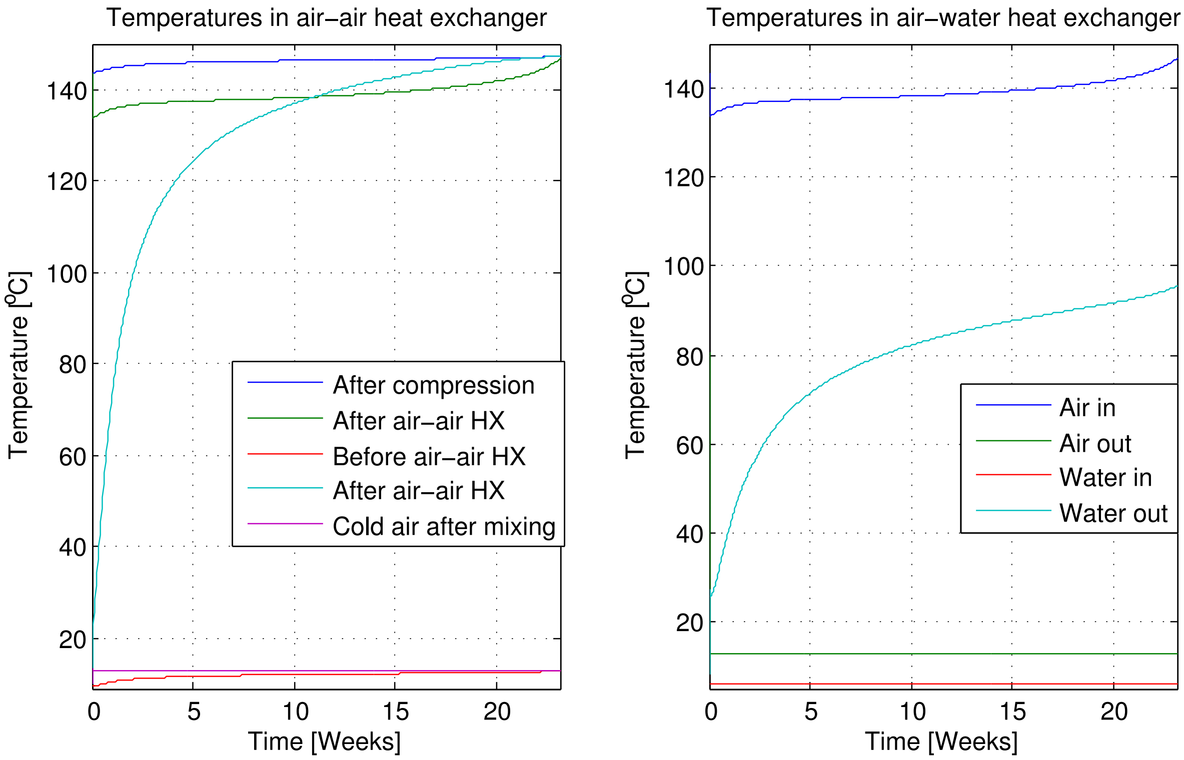

Figure B.59: Temperature levels in the water cooler (left) and air-air heat exchanger (right)

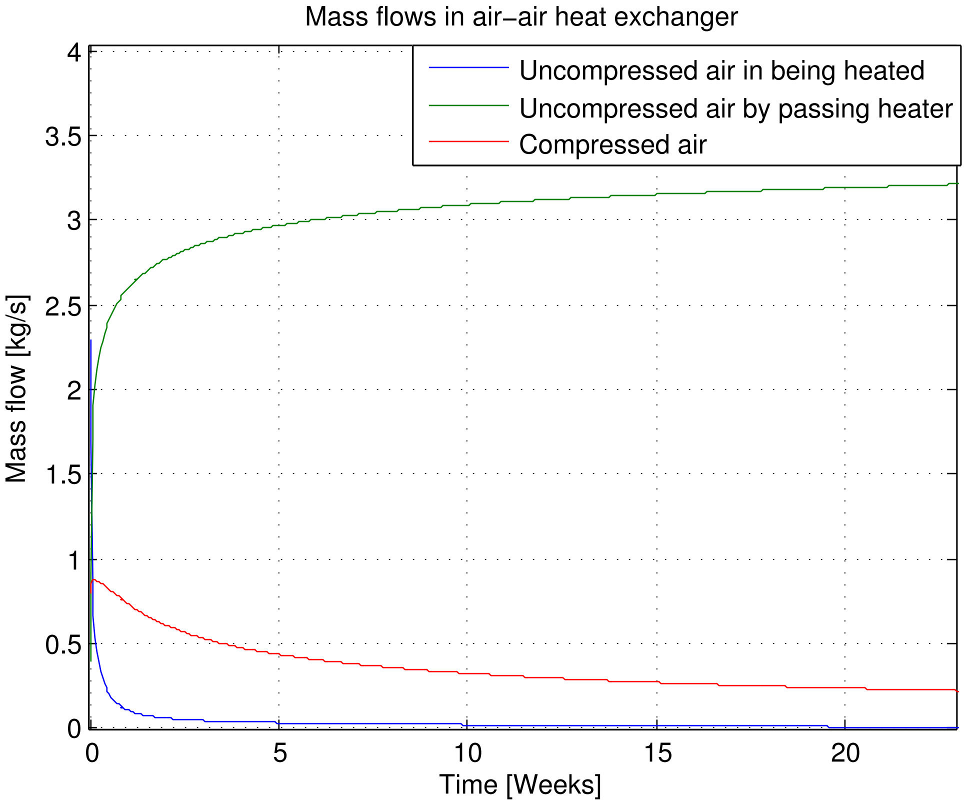

Figure B.60: Mass flows of air passing by or through the air-air heat exchanger

The valve for throttling the compressed air after cooling was not entirely isothermal, thus the temperature after the valve was controlled instead of the temperature directly after the heat exchanger (before the valve). It was quite difficult to control the air temperature in this system, and this might be even more difficult in reality, because the exact right amount of air must be withdrawn and compressed and cooled to the exact right points.

The mass flows and thereby pressure drops for the cooling water varied when the mass flow of cooling air varied. It was controlled that the pressure drops for the liquid, at other mass flows than the nominal values corresponded to assumed pressure drops and nominal values in other systems. For example, the mass flow of 1.2 in CS gave a pressure drop of 0.080 bars, which was also exactly the value for BS were nominal flow was 1.2 $\frac{\mathrm{kg}}{\mathrm{s}}$, even though nominal flow in CS was set to 4 $\frac{\mathrm{kg}}{\mathrm{s}}$ with a nominal drop of 0.89 bars.

The calculated pressure drop in the air-air heat exchanger was negligible (less than 1 Pa), probably due to the very small size of the heat exchanger and that its channels had to be quite wide in order to allow reasonable air velocities despite the small size and heat load.

B.8 ADS

This system was not completed, which will be further discussed, but a preliminary result could still be presented. The system as it looks in DYMOLA and the system sketch are shown in Figure B.61 and Figure B.62.

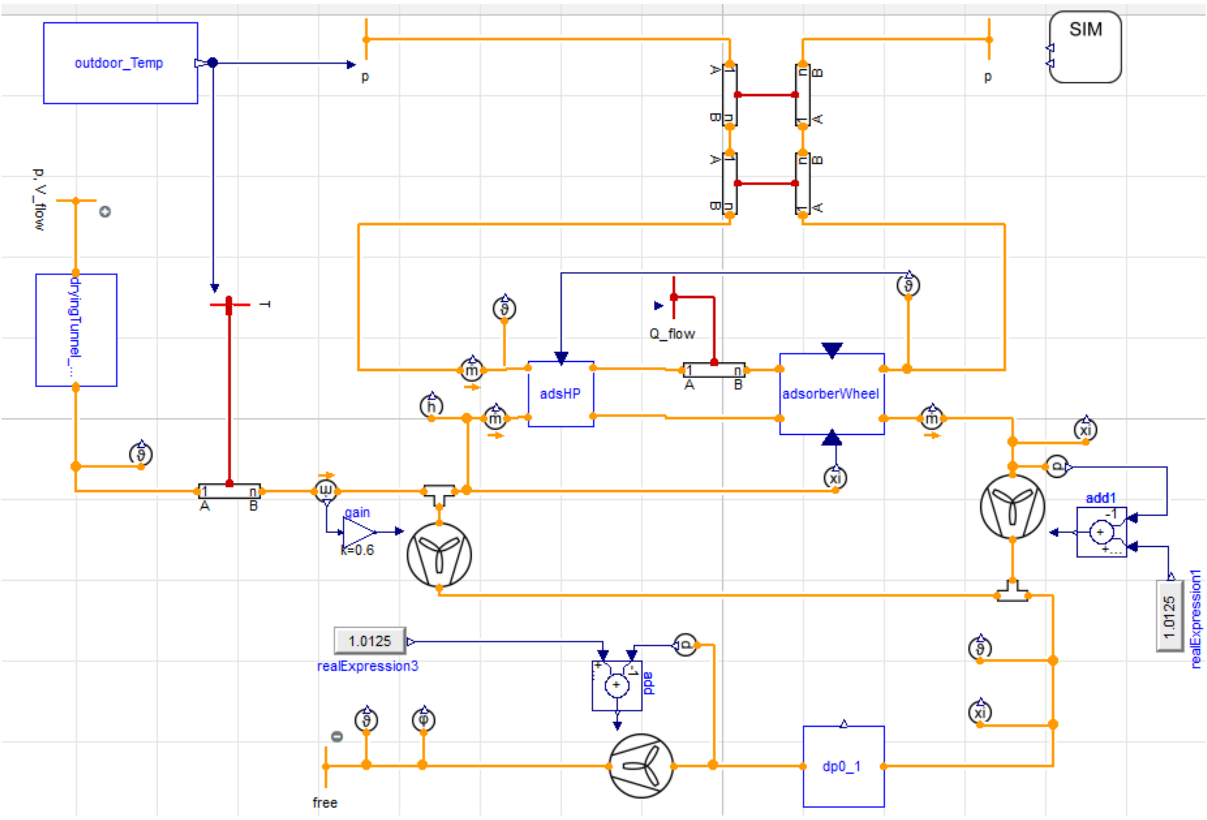

Figure B.61: In DYMOLA, the adsorption system had four air boundaries. Two were for the process air, the other two, the ones entering and exiting the pipes in on the top, for outdoor air. These exchanged heat, marked by the red lines. The process air entered the drying tunnel to the left, and exchanged heat with the surroundings in the following tube. The airflow was split in two. The upper branch was cooled in the heat pump evaporator, entered the adsorber, represented by a white square, and after a fan, the two streams were mixed. The outdoor air entered the heat exchanger from the left boundary, was heated in the heat pump and eventually in the following pipe, it then removed moisture in the adsorber and exited through the air-air heat exchanger.

Resulting power and energy needs are displayed in Figure B.64 and Figure B.63. The energy consumption mainly consisted of energy for compression and electrical heat supply. They comprised about 25 and 75 % of the total, and the system would indeed perform much better if the electrical heater was unnecessary. As in the heat pump systems, the heating and cooling from the heat pump were larger than total energy usage.

As the process proceeded however, the heat pump delivered much less power than necessary, and the electrical heating was thus higher than planned. This was because it was discovered that the system could not operate as planned. If the heat pump should deliver

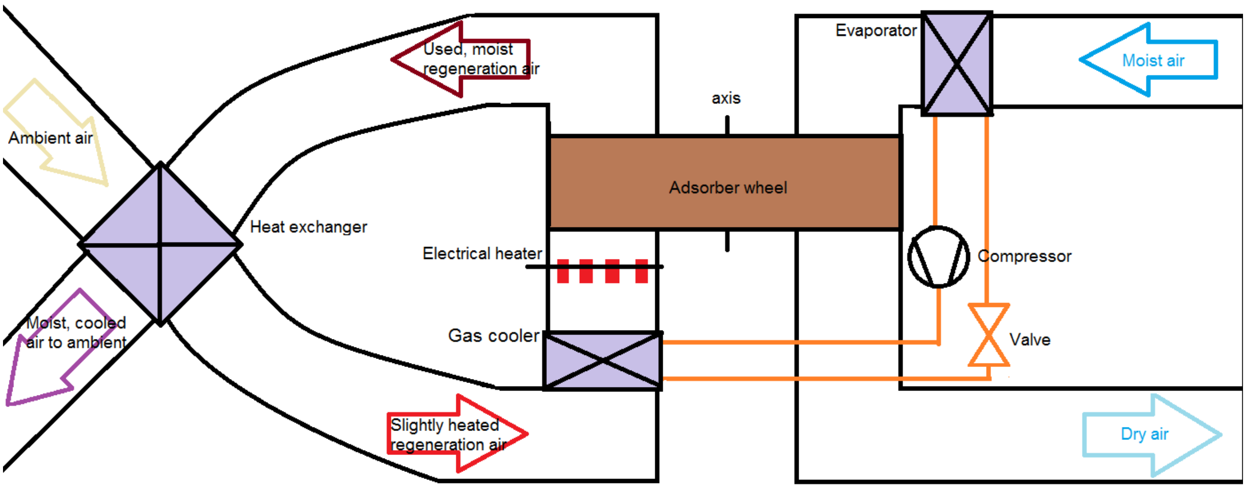

Figure B.62: Adsorption systems with heat pump, most of the principle shown is taken from [AG,], only the heat exchanger to the left is added

more heat, excessive cooling and condensation resulted, removing excessively much moisture, see also Appendix D.

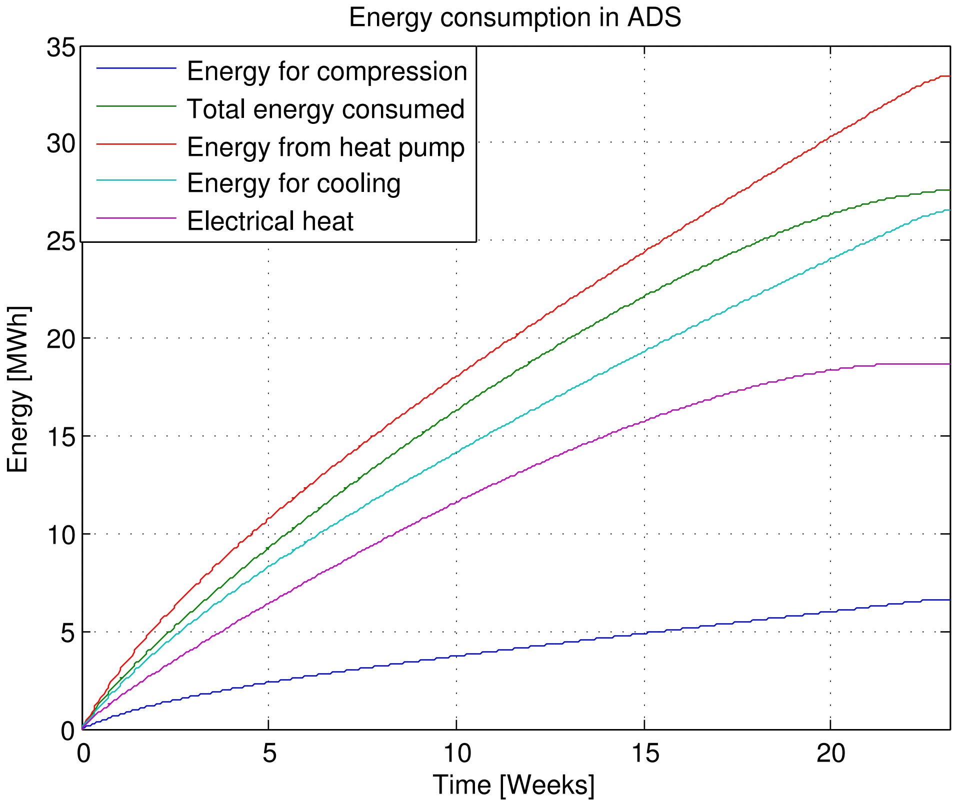

Figure B.63: Amounts of energy for heating, both by electricity and heat pump, for cooling and total energy consumed in ADS are shown. The electrical heat was not necessary towards the end, thus its derivative was then flat.

The reasons the system cannot be said to be completed have several reasons. One is the

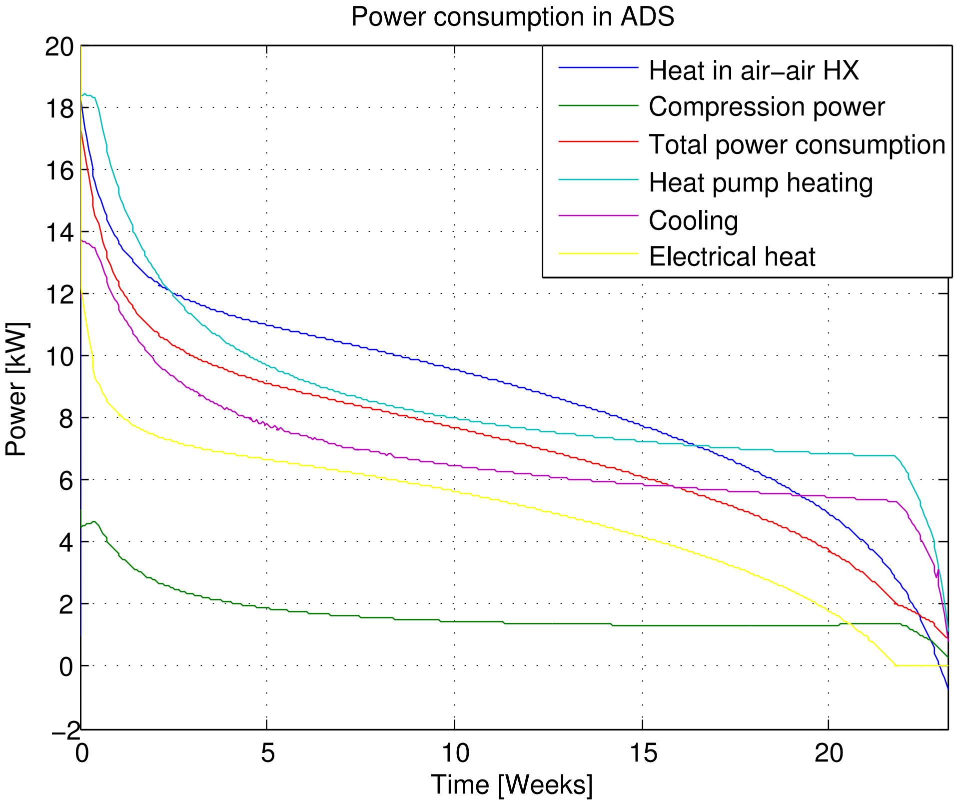

[t!]

Figure B.64: Power for heating, both by electricity and heat pump, cooling, evaporation in adsorber and heat recovered in the air-air heat exchanger are shown, together with the total power consumption. «Energy from heat pump» includes heat delivered by the heat pump alone; the electrical heat was not a part of it.

rough assumption made in Section 6.4, that the adsorber wheel always managed to achieve the desired conditions. The final conditions achieved were good, mainly due this rough simplification. However, real plants using adsorbers do achieve the desired conditions, so this in itself is not the problem with this model, but rather how the dryer manages this.

A second reason is that the high pressure in the heat pump should have been controlled to be constant by changing the mass flow of air. More air would decrease the pressure, and as seen in Figure B.65, the pressure was not constant, but rather too low during most of the time. The minimum amount of air reported was therefore constantly used. A lower value was not applied, as it was a concern whether the regeneration could actually be realized with an airstream lower than any value reported, also at lower regeneration temperatures. Another problem was that the heat pump supply was controlled to achieve 28.2 °C in regeneration air after regeneration. Attempts with higher mass flows in Appendix D required more heat to achieve this, and the pressure rose. Another control strategy should have been used.

A third problem that should be mentioned was the heat supply. The electrical heat supply was set equal to the heating need, including heat for evaporation and due to heat leakage, minus the 20.43 kW which the heat pump was designed to deliver. However, 15.00 kW

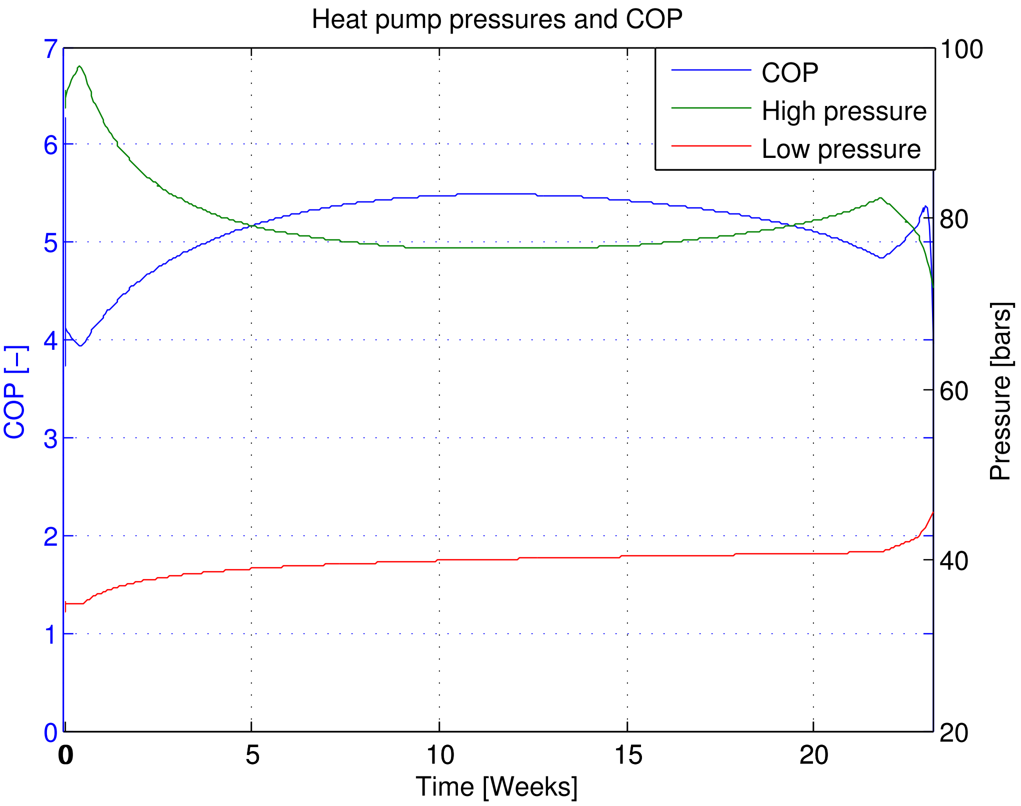

Figure B.65: The pressures (right axis) and COP (left axis) in the adsorption system are shown. The planned transcritical operation was achieved. The high pressure should have been controlled to be constant, but this task was not completed. The COP was calculated as heat supplied divided by compression power, this and the high pressure ratio made it lower than in other systems.

of the latter were taken from the process air. As the dynamic process proceeded, the air became drier, and if the same cooling was allowed, this condensed too much water. This is clearly seen in Appendix D, where the system operated very close to designed, and too dry air resulted. A higher electrical heat supply was necessary, forcing the heat pump to contribute with some heat, but without condensing excessive amounts of water. An additional term of $1.6 \cdot (3000\ \mathrm{W} - \dot{Q}_w)$ where $\dot{Q}_w$ is heat for evaporation in the adsorber, was introduced into Equation 6.3. Because less heat could be taken from the drier process air, the electrical heat supply was large most of the time, and the power flows in the heat pump, in Figure B.64, dropped instead of remaining high as long as the electric heat was supplied, as they otherwise should have. The heat recovery in the air-air heat exchanger was therefore of major importance.

Figure B.64 shows that despite the falling contributions from the heat pump, the initial conditions were closed to the designed ones. Power for compression was close to its targeted value of 5.43 kW, and so were the cooling and the heat from the heat pump, though they were all a bit lower than planned. One reason was that initially, 17.05 kW should have been recovered in the heat exchanger. It delivered about 18 kW instead, as the enthalpies read

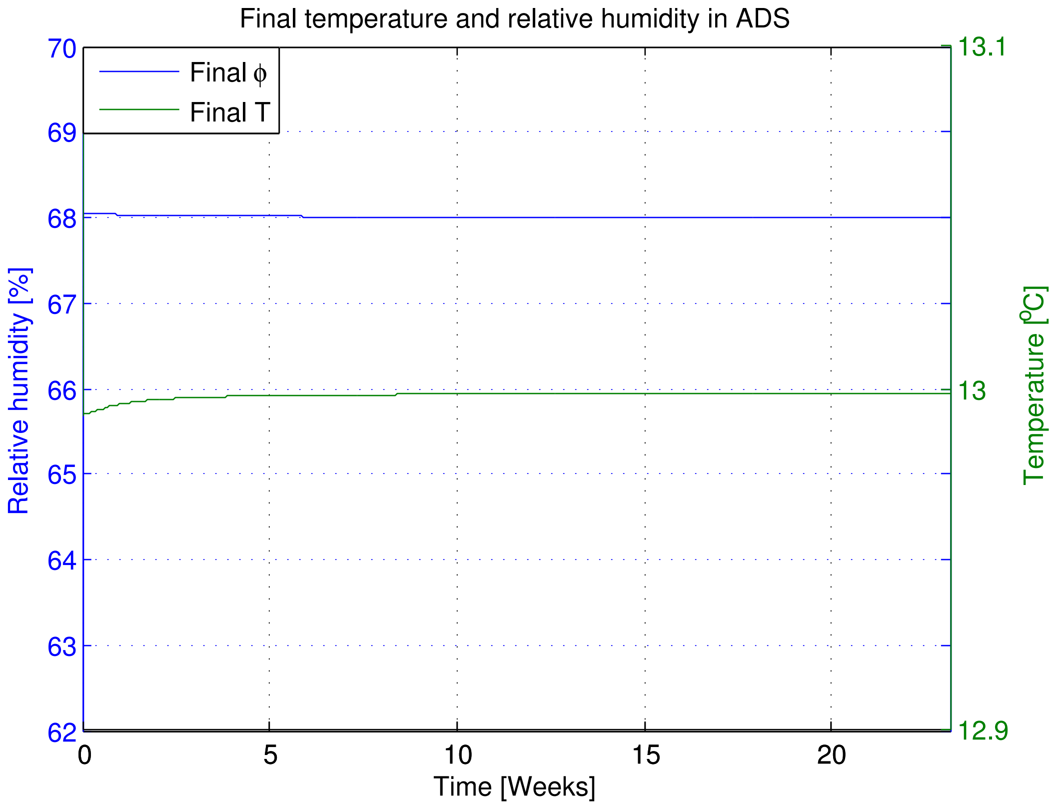

Figure B.66: The final temperature and relative humidity in ADS were very close to the desired values. The deviation was due to the heat leakage, and even though this effect was minimized by extra heat supply in the wheel, the effect was not entirely diminished.

from Figure 6.1 in the planning phase were not accurate. Because the electrical heat followed Equation 6.3, which was made so that it delivered sufficient heat if the heat pump contributed with a net value of 5.43 kW, and the exchanger recovered more heat than planned, the heat pump delivered somewhat less. (All heat rejected from the process air was delivered back, so the heating and cooling in the heat pump were not really controlled, but their difference should be 5.43 kW.)

Econosorb EF-102E has a rated total power of 10.3 kW. Initial total power, with or without excessive cooling, was about 17.5 kW, which is quite reasonable, because the simulation added fan power for the distribution system and the low outdoor temperature naturally made initial needs somewhat higher. It soon decreased below 10 kW, and followed the outdoor temperature to a high extent. Towards the end, all power needs drop, because the incoming air for regeneration was close to or even above the necessary value after heating, seen in Figure B.67. The heat pump then tried to deliver as heat little as possible.

Other unfinished aspects in the system were that not all pressure drops could be implemented, as the simulation then did not start, but this was of minor importance. In the summer, the air-air heat exchanger was actually cooling the incoming air a bit. This is neither of great importance, but makes the system performance somewhat worse. Attempts

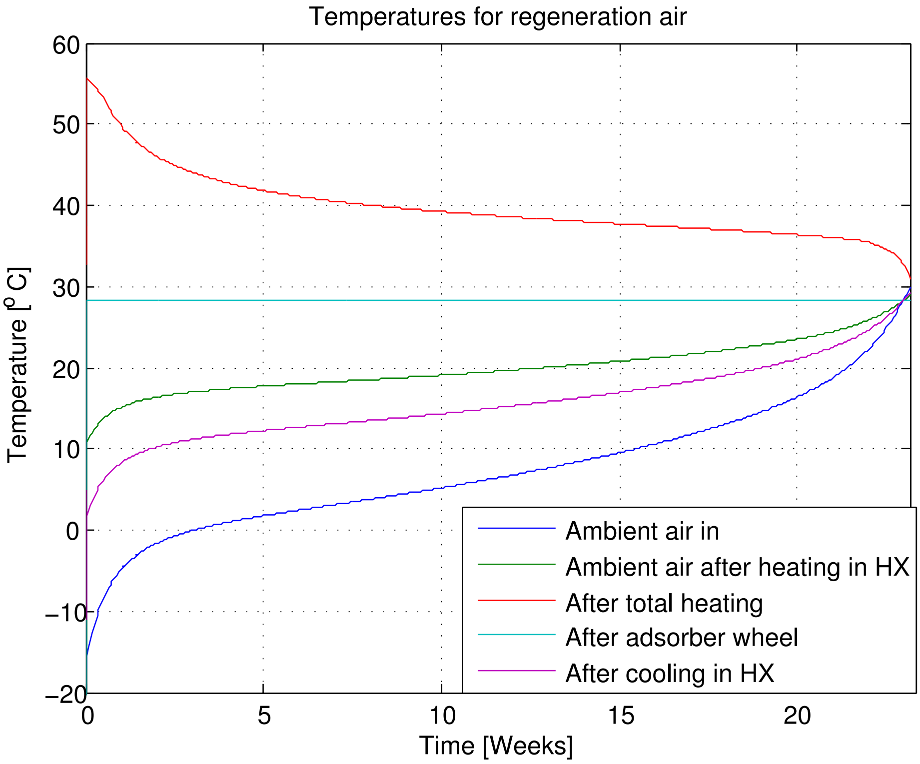

Figure B.67: The temperatures of the regeneration air at different positions in the system. The temperature after the adsorber wheel was controlled to reach 28.2 °C, and this was also achieved. The outdoor temperature increased to 30 and the energy supply to the process was nearly zero at the end, hence all temperatures met at the end of simulation.

to bypass the heat exchanger or supply back the same amount of heat both failed, as the simulation then refused to run more than about 1.5 seconds.

One interesting notion was that, even though too much cooling made the adsorber superfluous, the power consumption also went down when this happened, like it was also found in Section 6.4.5. The final total energy consumption was 27.60 MWh in the system reported here, giving desired final humidity, against 23.86 MWh for the planned system in Appendix D, drying excessively. Thus, this system might be better when it comes to drying quite moist air quite much, so that much cooling is good for the process, and much free heat can be supplied to the regeneration air. In addition, the adsorbers from [AG,] operate in on off mode, unlike here, where the system was run the entire time. This could significantly lower the energy consumption.

Assuming that the system is operating 60 % of the time, and that the rated power of 10.3 kW is a representative value over the whole year, this simulation of 1.4×10^7 seconds should give $10.3\ \text{kW} \cdot 1.4 \times 10^7\ \text{s} \cdot \frac{1\ \text{h}}{3600\ \text{s}} \cdot 0.6 = 24\ \text{MWh}$, which is very close to the results obtained here. Thus, it seems that the results are, if not correct, so in the right range.

After regeneration and heat recovery, the outlet temperature in Figure B.67 was at first the targeted value, 1 °C, but then rose above this value. This increased the load on the heat

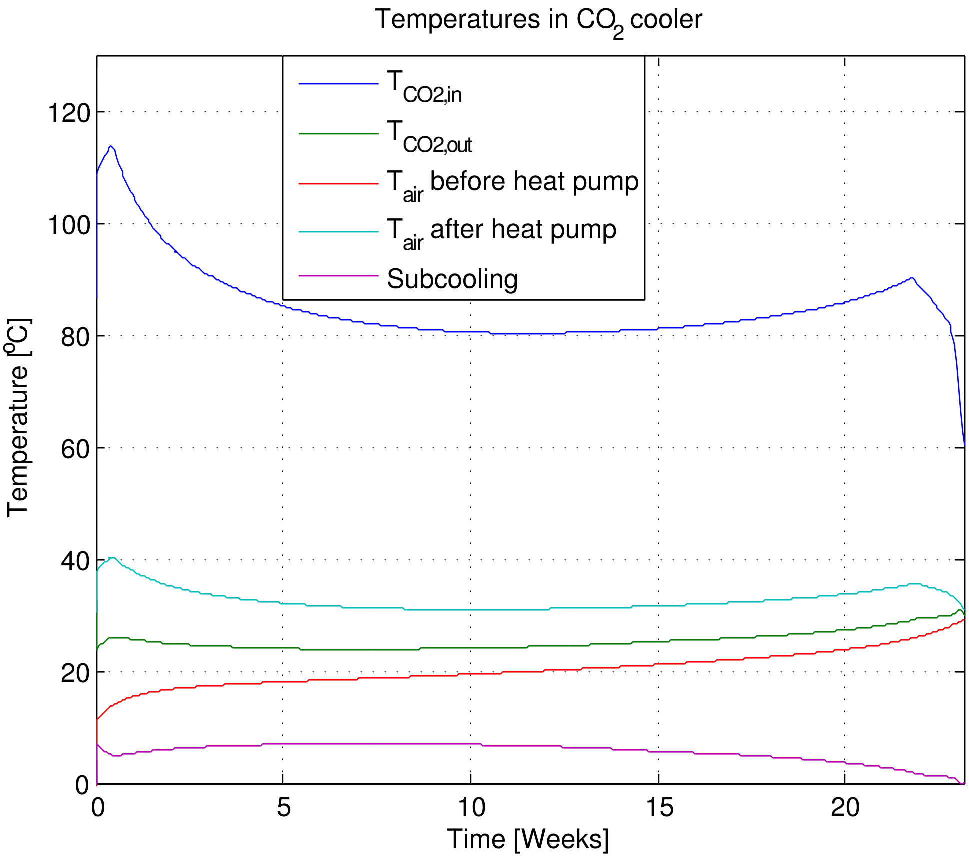

Figure B.68: The temperatures of the CO_2 and regeneration air varied with outdoor temperature and the pressure in the gas cooler. DYMOLA reported subcooling, also shown, but in transcritical mode, its meaning is unclear. The exit temperature for CO_2 was satisfactory, normally about 20-25 °C, up to 30 °C in the worst case.

pump and electrical heater, and meant that more heat could have been recovered. Perhaps it would be an idea to place an additional evaporator in this stream instead of using the heat exchanger.

Figure B.69 shows how the lowest temperature for the process air had to increase when it became drier. Precooling the process air before adsorber is probably an important reason to ensure lower outlet temperature than in other adsorbers. Otherwise, extra cooling after adsorption would be necessary. The precooling also removes some water initially, recovering its heat on the heat pump evaporator, thereby reducing the power the wheel must supply for evaporation. Hence, cooling as much as possible seems desirable, but cooling too much would make the process similar to HPS, or HPSX and the adsorber would be superfluous. Its advantage must lie in that less cooling than otherwise is necessary.

Perhaps one could conclude that the system seems to work well when the air from drying is relatively moist, but bad when it is relatively dry, and that this unfortunately was the case during most of this simulation. Finding the most typical state(s) of drying air after the process would be important to consider the systems more properly. The adsorption

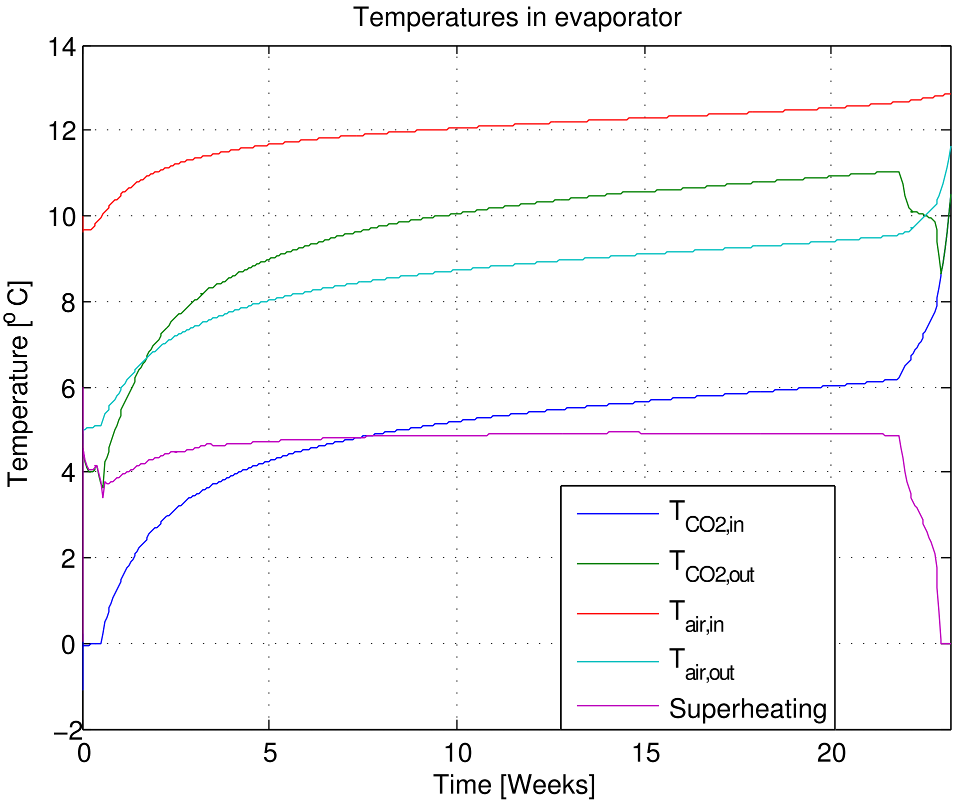

Figure B.69: In the evaporator, the temperatures increased like in many of the heat pump systems, due to the lower moisture content of the air and thereby lower cooling demands for sufficient condensation

calculations were an iterative process, subject to further optimization.

Yet, it seemed clear that the closer to heat pump operation the system came, the better it performed, and the total power consumption of the best heat pump systems were several times lower than that of ADS. This was also true at high ambient temperatures, which should be the better condition for ADS and the worst for HPS, but because ADS never had a condition with quite moist air and relatively normal outdoor temperature, it is difficult to say for sure. Many small changes should be made to make this model operate realistically, but most of them would affect the energy consumption little. Control of the highest pressure by more air, yet achieving the same regeneration temperature, should mean higher energy needs. The high pressure was also lower than planned, and if it had been kept high, the power need would have increased. An extra evaporator in the used regeneration stream would reduce power needs.

Appendix C

REGULATION PROBLEMS IN BS

The flow of outdoor air in BS to the condenser in the heat pump was extremely difficult to control. It should ensure that excess heat was removed. Normally, one would increase the airflow so that the working fluid would become subcooled, which is easy to measure. However, this value of subcooling was so unstable at the start of simulation that it made the entire model too unstable to run. Eventually, it started, but stopped and never finished.

Other strategies were then investigated: Setting the value of airflow constant was only possible for a very low, very narrow range of mass flows. This gave insufficient cooling as the temperature increased. The value should then be higher, but the model did not start with this high value from the beginning. Controlling the supply of ambient air to provide the correct, low temperature in the process air was difficult, as this temperature varied with amount of evaporated water (se Figure B.2). The same applied when it was attempted to control any of the pressures in the heat pump.

Controlling the enthalpy after condenser worked quite well, but was very sensitive to changes, and did not manage to make the working fluid saturated, as it should be. A small change gave either a too high mass flow of working fluid, several times too high or a too high pressure (some 1000 bars) depending on valve area. The cooling of the condenser affected the pressure on the high-pressure side, and a too low or a too high value could make the pressure infinitely large and stop the simulation.

It might seem weird that both high and low values of airflow could give the same value, but the explanation might be that a too low airflow did not cool the working fluid sufficiently, leaving too much gas in the condenser, which then accumulated and increased the pressure. The high pressure forces more mass through the valve, also gas, with high enthalpy and low potential for cooling. This required more working fluid to provide sufficient cooling, and made the compressor push more mass to the high-pressure side and so on.

Too high cooling on the other hand, sometimes seemed to be treated as a heating demand in DYMOLA, and the compressor/system tried to deliver sufficient heating to the outdoor air and raised the mass flow and pressure to the high-pressure side. Too high flow of cooling air could also make the rate of condensation so high that the pressure in the condenser sank below that in the evaporator, stopping the simulation. The compressor could not handle this unrealistic situation. It became clear that constant outdoor airflow did not work at all.

The heat pump was also tested alone, outside the system. Without changing process conditions, it worked fine after some regulation, but as soon as this heat pump was given a non-constant cooling load, which required fast regulation, the entire system stopped. Conversely, a dynamic process with a constant outdoor temperature was applied (-17.0 °C, which is the start temperature for the varying outdoor temperature). A well performing controller was developed, but the system failed when the temperature increased.

It appeared that the initialization of the process was highly unstable and required much time and a big variation in air mass flow. This is why models with constant airflow rates did not start and others obtained infinite pressures: Different flows were required before and after initialization. When the outdoor temperature varied in addition, this initialization was even more difficult. Values that work in the start do not work at the end and opposite, and the process changes were faster than the controllers managed to follow. The input to the controllers were also unstable, making the output unstable and so on. Quickly changing conditions require fast regulation, but this always made the process unstable.

The solution was therefore to regulate the airflow as proportional to temperature, as more cooling air was needed for higher outdoor temperature. This made the flow stable, undisturbed by all the initial instabilities. To start the process was still difficult, because not all variables had reached proper operational points, so an initialization period with constant conditions were added to the process. The airflow was controlled by the regulator in an initialization period, with all values constant and then be proportional to temperature.

The chosen curve for air supply to condenser started at the value after the initialization period and ended at 8 $\frac{\text{kg}}{\text{s}}$. This value was tested to work well at the highest outdoor air temperature in the testing of the condenser alone. The strategy gave very reasonable results and conditions, and was thus kept. The increase had to be very slow to begin with, but could then be increased much.

In addition, it was a problem was to provide superheating of the ammonia on the low-pressure side. This did not work, because the valve that should adjust it, did not manage to keep up with the process changes, and the value remained zero. It was discovered that a faster controller stopped simulation, but stronger regulation was required at the end of the process than in the start.

To avoid initial instability and process stop and still obtain fast enough regulation towards the end, an expression dependent on both time and deviation was applied. This then corresponds to a time dependent P-controller. The gain was proportional to the process deviation, but also, the output changed with time. Regulation of the deviation alone was too weak and slow when the process conditions varied so fast. This was not the case for the heat pumps that also delivered heat to the process, as the high pressure side only changed a little bit at the end, when the outdoor air became very hot.

To avoid influences on the results from that the drying started before the energy was counted and before outdoor temperature varied, more options were tried. One included using a pipe with flow area sufficiently large to make the flow speed 1 $\frac{\text{m}}{\text{s}}$ and of length 3×10^5 m, with no pressure drop or heat conductance, before the cooler. The air from the drying tunnel would then be delayed by 3×10^5 s before it arrived the remaining part of the process. The initial temperature and relative humidity in the pipe were set equal to the initial output values from the drying tunnel. However, the initial humidity could not be specified and the outlet conditions from the pipe were far from constant.

Instead, evaporation in the initialization period was prevented by letting the inlet conditions to the drying tunnel be $T = 10\,°\mathrm{C}$ and $\phi_a = 99$, to cause a drying potential of exactly zero. When the initialization period was over, this gave a small jump in the relative humidity and temperature after the tunnel. Choosing the initial output from the drying tunnel created a drying potential in the drying tunnel, because section one then got the same conditions as a seventh section would have had, and the air was not saturated with water. 10 °C and $\phi = 99$ was thus kept.

The condensers and desuperheaters in the systems that delivered heat had relatively constant conditions for the high pressure and cooling nee, thus, these did not show this problem.

Appendix D

THE PLANNED VERSION OF ADS

The planned but not used version of ADS performed as desired in nearly all ways, except that it removed an excessive amount of vapour from the air, which is seen in Figure D.1. The outlet enthalpy from the adsorber wheel was set to the correct value, and the exiting regeneration air always left the wheel at 28.2 °C as designed in Section 6.4.5. Due to that the process air was too dry at the inlet of the adsorber, so was the exiting air, and hence, it became too hot.

In Figure D.2, both the water content in the process air at different places and the amount of removed water are shown. At the point where the amount of removed water reaches zero, the inlet moisture content to the adsorber falls below the required outlet water content. The latter was calculated from Equation 6.2 to obtain the desired final moisture

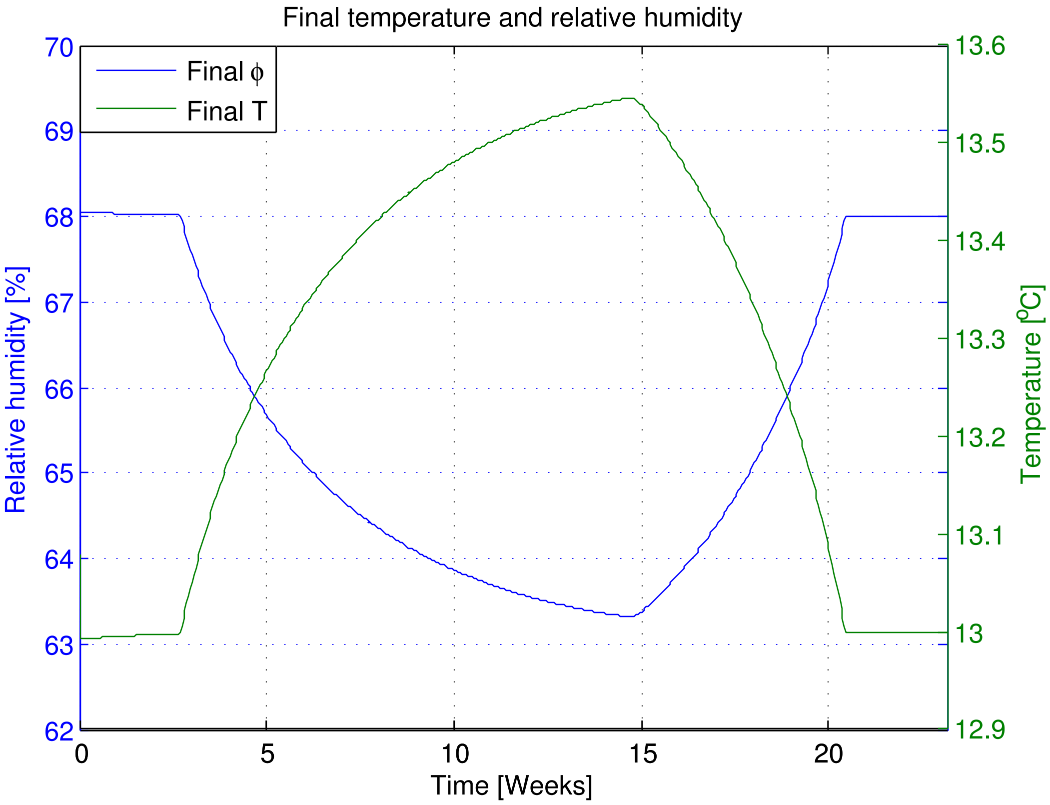

Figure D.1: The resulting temperature and humidity delivered to the drying chamber in ADS when excessive drying resulted

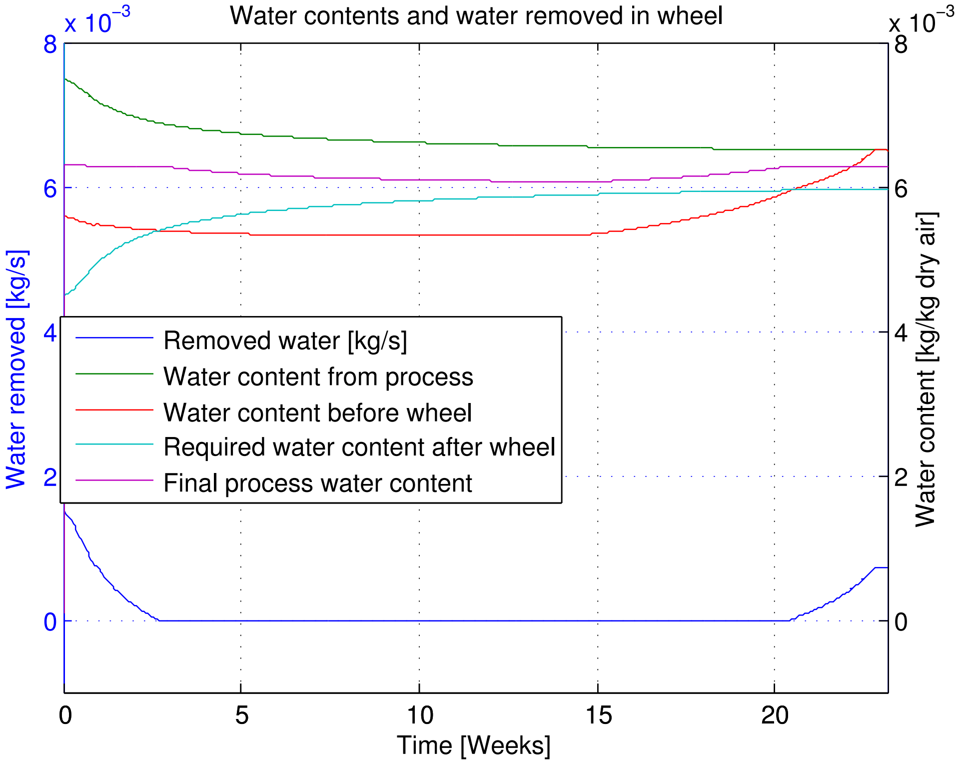

Figure D.2: Amount of water adsorbed in adsorber wheel (left axis) and moisture content in the process air at different places, in addition to the desired water content after adsorption, found from Equation 6.2

content. The model was made so that no water was adsorbed if the inlet air was too dry, but this is probably not realistic, hence in reality, the result would have been worse. Results after adjusting the heat supply, discussed in Appendix B, can be seen in Figure D.3, for comparison.

Why the air became too dry occurred is seen in Figure D.5. Here, the power for compression, cooling and heating are shown. As planned in Section 6.4.5, a fairly constant fraction of heat, close to the targeted value of 15.00 kW, was taken from the process air, thereby cooling it and condensing vapour. At the start of the process, with conditions for which the system was designed, this worked fine.

Electrical heat supply followed Equation 6.3, which really assumed that a net power output from the heat pump should be 5.43 kW, and no constraint were placed on the exact values for heating and cooling from the heat pump. The deviation was due to somewhat different pressures and COP than in design, which are displayed in Figure D.6, but the compressor power was truly close to the targeted value in Figure D.5.

The problem was of course that the resulting cooling of the process air, when the process air became less moist, condensed too much water before adsorption. The heat pump could not supply sufficient heat unless a large amount of heat was rejected from the process. Hence, the only way to avoid the excessive drying seemed to be by supplying more electrical heat,

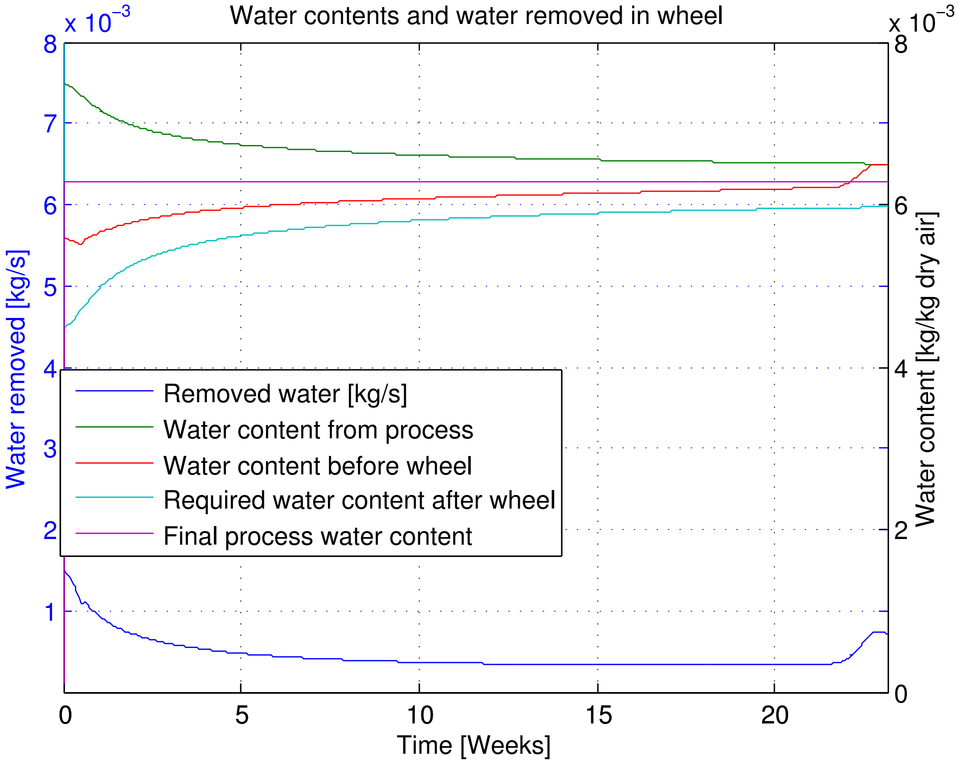

Figure D.3: Amount of water adsorbed in adsorber wheel (left axis) and moisture content in the process air at different places, in addition to the desired water content after adsorption, found from Equation 6.2

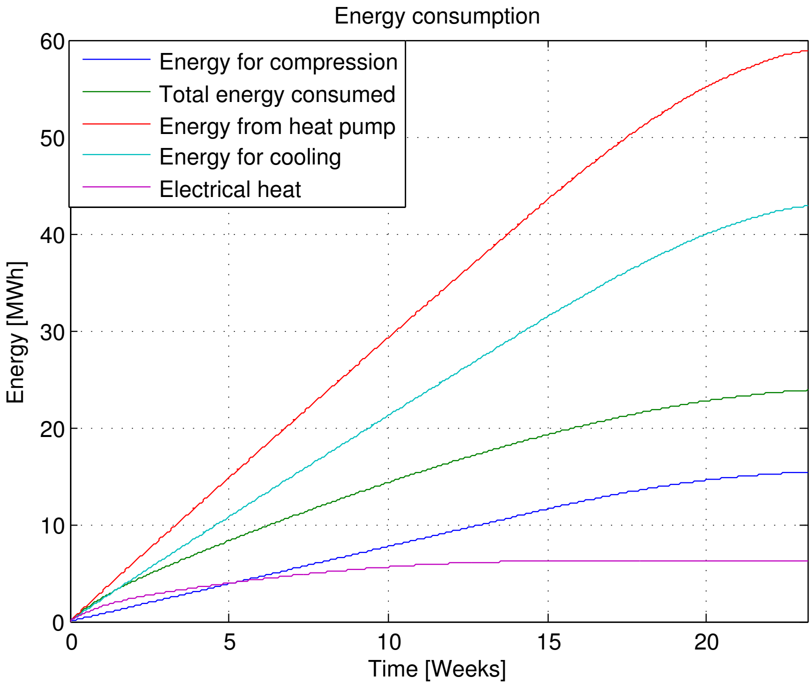

Figure D.4: Energy used in the adsorption system when excessive cooling and condensation resulted: The heat from the heat pump is seen to make up the larger part of the heating demand, and the electrical heat supply stopped after some time, making its accumulated value constant.

which was done in the version of this system presented in Appendix B, making the energy consumption higher than in design. The energy used when the air became too dry is shown in Figure D.4.

If heat for the heat pump could be collected somewhere else, the problem could be better solved. One thought could be to collect it from the exiting regeneration air. At the lowest outdoor temperature, all heat that could be recovered by cooling it to 1 °C was recovered, but at higher outdoor temperatures, the outlet temperature was higher, and more heat could have been recovered. This is seen in Figure B.67. Replacing the heat exchanger by an additional evaporator would give maximum heat recovery and high temperature differences in the gas cooler. The result would be something like heat pump drying of the adsorber wheel.

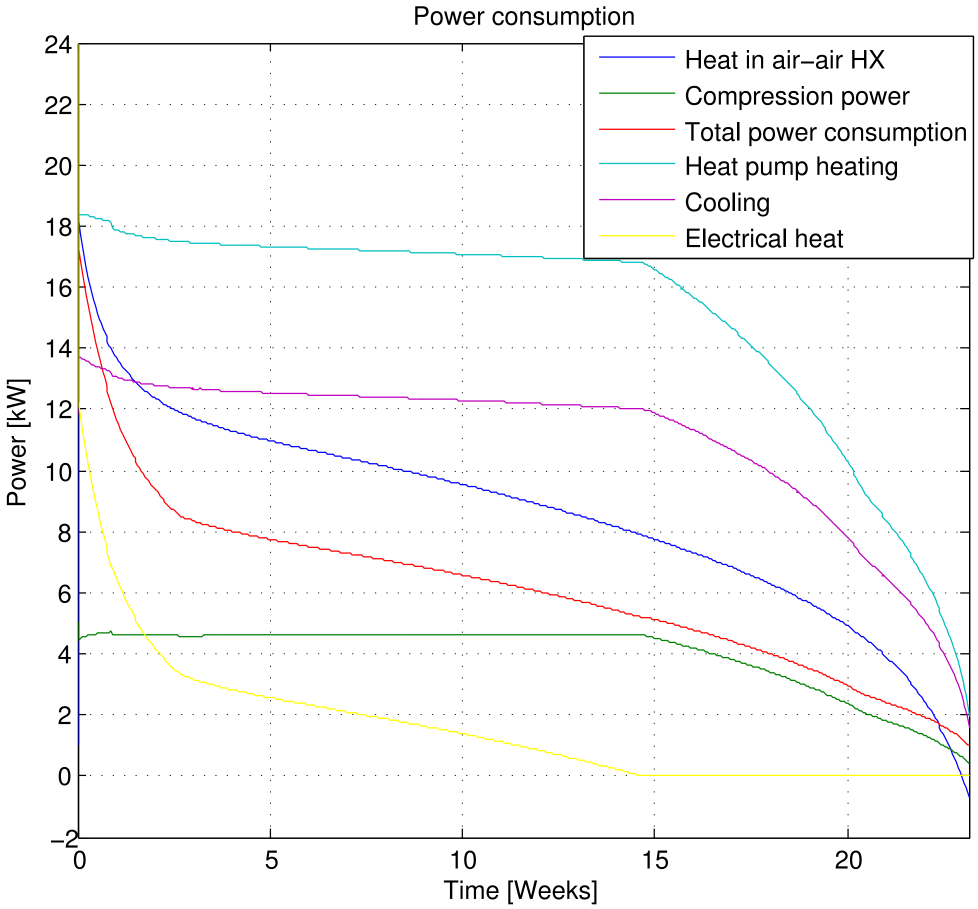

Figure D.5: Power transferred by electrical heating, to and from the heat pump, total power and heat recovered in the heat exchanger in ADS when the system was run as planned and excessive drying resulted are shown. The power from compression was as good as constant, exactly at design point, and decreased at higher outdoor temperature and lower moisture contents. The heating and cooling were quite stable and close to the designed values, deviations are due to pressure variation. The electrical heating made up a smaller part of total supply, because the heat pump supply was large. The recovered heat lowered overall power need substantially, however, it was somewhat negative towards the end of simulation.

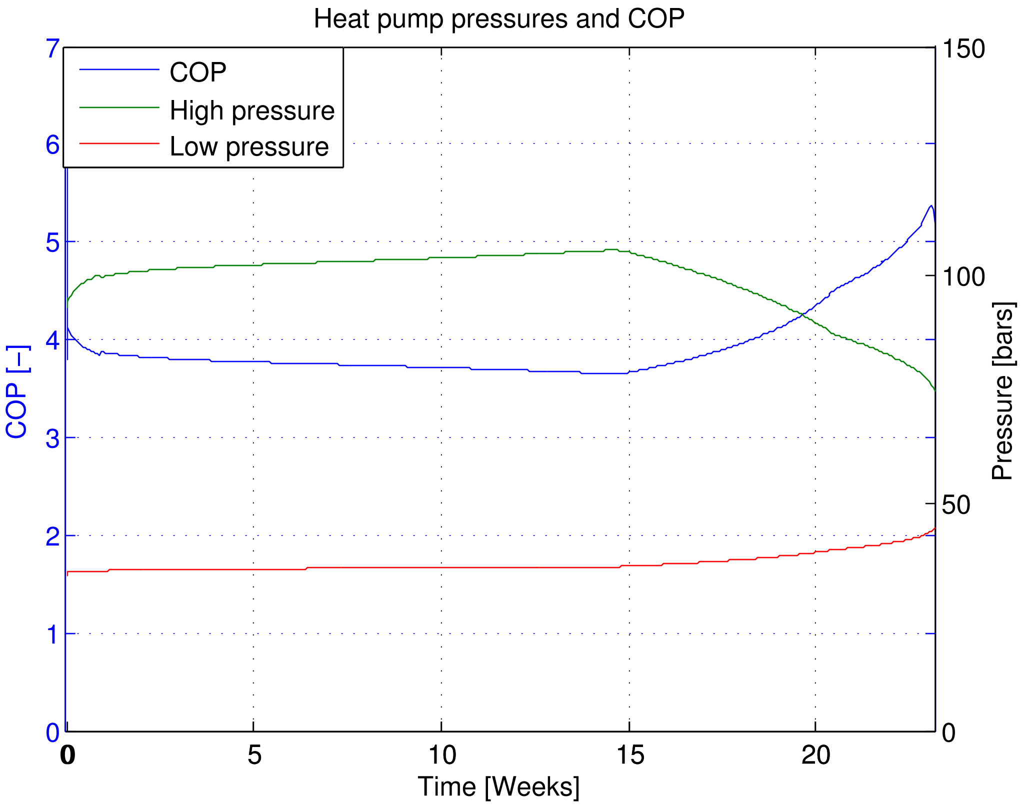

Figure D.6: COP (left axis) and pressures (right) in ADS when excessive drying resulted were fairly constant, close to the designed values, except for the decrease towards the end. The highest pressure should have been kept constant by increasing amount of regeneration air, but implementation of this was unsuccessful.

All power flows decreased towards the end of simulation, and the amount of adsorbed water again became positive. This was because the air moisture content became so low, and the outdoor temperature so high, that the heat pump should hardly supply any heat at all. Hardly any vapour was then condensed before adsorption, and all power flows dropped. The system actually used mainly free outdoor heat to evaporate the adsorbed water.

Early in the simulation, the highest pressure increased a little bit, unlike in the final version of ADS where it decreased, Figure B.65. A larger amount of regeneration air should then have reduced it, as reported by the producer. Because the heat pump was controlled to keep the temperature after adsorption constant, attempts to increase the airflow made the heat pump deliver more heat, and pressure increased instead. It was concluded that this was the wrong control strategy, and another control parameter should be used. Which one is used in real adsorbers is not known. One idea could be to ensure a satisfactory temperature for CO_2 after cooling it, depending on the inlet air temperature. Unfortunately, the author's licence to use DYMOLA expired at this time and the deadline was close, no further attempts to improve the system were made. The COP was generally somewhat better than designed, probably because the pressures and compressor efficiency differed, and superheating was not accounted for in designing, which made it change around the calculated value of 3.76.

It was calculated as heat supply divided by compression power, making it substantially lower than in heat pump systems. Another important reason for this difference was the high temperature lift.

The more heat that was delivered by the heat pump, the better. Naturally, the system would then benefit from moister air. Its performance was very close to design when the air was moist. When the air was drier, the system actually used less energy than when drying the air too much than when obtaining the desired conditions, as presented in Appendix B.

Appendix E

LIST OF PROGRAM FILES

An overview over the files used, their purposes and names, are given in Table E.1. The files for testing of heat exchangers are not listed.

Table E.1: Files used in this work, what they were used for and the name of the file

	Purpose of file	Filename
1	Model of ham and drying tunnel	MediumSaltedHam.mo
2	Calculation of ham diameter	HamDiameter.xlsx
3	Friction factor and pressure drop	FrictionFactor.xlsx
4	Plotting of friction factors	FrictionFactor.m
5	Model of pressure drop	dp0.mo
6	Temperature data fom www.yr.no	TemperatureMeasured.xlsx
7	Plot of temperature profile	TrondheimsClimate.m
8	Modelling outdoor temperature	Outdoor_Temp.mo
9	Modified compressor	Compressor.mo
10	Designing heat exchangers	HXAll.xlsx
11	Calculations on results and costs	EnergyWaterResults.xlsx
12	Removing water after condensation	Demoist.mo
13	Model of BS	BasicSystem22.mo
14	Model of HPS	HeatPumpSystem22.mo
15	Model of HPSX100	HPSX100.mo
16	Model of HPSX37	HPSX37.mo
17	Model of HPSX1	HPSX1.mo
18	Model of CO2S	CO2.mo
19	Model of CS (2.5 bars)	CS2point5bars.mo
20	Model of CS (3.0 bars)	CS3bars.mo
21	Model of CS (3.5 bars)	CS3point5bars.mo
22	Model of ADS	ADS.mo
23	Model of BS heat pump	BS_HP.mo
24	Model of HPS heat pump	HP_GlAir22.mo
25	Model of HPSX100 heat pump	HP100.mo
26	Model of HPSX37 heat pump	HP37.mo
27	Model of HPSX1 heat pump	HP37.mo
28	Model of CO2S heat pump	HPCO2.mo
29	Model of ADS heat pump	AdsHP.mo
30	Model of adsorber wheel	AdsorberWheel.mo

31	DYMOLA results and condtions for BS	BS_res.m
32	DYMOLA results for HPS	HPS_res.m
33	DYMOLA condtions for HPS	HPS_res.m
34	DYMOLA results and condtions forHPSX100	HPSX100_res.m
35	DYMOLA results and condtions for HPSX37 when air flows were mixed before heating	HPSX37mixed_res.m
36	DYMOLA results and condtions for HPSX37 when air flows were mixed after heating	HPSX37unmixed_res.m
37	DYMOLA results and condtions for HPSX1 when air flows were mixed before heating	HPSX1mixed_res.m
38	DYMOLA results and condtions for HPSX1 when air flows were mixed after heating	HPSX1unmixed_res.m
39	Mass flows of ammonia in HPSX and HPS	HPSXMassFlows.m
40	Comparing mixing before or after heating	Comparison.m
41	DYMOLA results and condtions for CO2S	CO2S_res.m
42	DYMOLA results and condtions for CS	CS_res.m
43	DYMOLA results and condtions for ADS	Ads_res.m
44	DYMOLA results and condtions for ADS when final air became too dry	AdsTooDry_res.m

REFERENCES

[AG,] Alfsen og gunderson: Luftavfuktning - avfuktere. `http://ag.no/produkter-og-tjenester/luftavfuktning-avfuktere-1.aspx`. Accessed: 15.12.2014.

[16, 2003] (2003). 1.6. water diffusion in meat. `http://www.tdx.cat/bitstream/handle/10803/6675/16DifusivitatIntroduccio.PDF?sequence=16`. Accessed 20.10.2014.

[Car, 2013] (2013). 30rb/rq modular. `http://www.carrier.co.th/pdcarrier/catalogue/Chiller_Catalog/air_cooled/30RBRQ_Modular.pdf`. Accessed: 30.01.2015.

[Alcazár-Ortega et al., 2011] Alcazár-Ortega, M., Erscrivá-Escrivá, G., Álvarez Bel, C., and Domijan, A. (2011). Active demand response strategies to improve energy efficiency in the meat industry. In *World renewable Energy Congress 2011 - Sweden*.

[Álvarez et al., 2009] Álvarez, D., Garrido, M. D., and Bañón, S. (2009). Influence of pre-slaughter process on pork quality: An overview. *Food Reviews International*, 25(3):233–250.

[Anderson and Williams, 1937] Anderson, W. E. and Williams, H. H. (1937). The rôle of fat in the diet. *Physiological Reviews*, 17(3).

[Anonymous, 1977] Anonymous (1977). Upgrading existing evaporators to reduce energy consumption.

[Arnau et al., 2007] Arnau, J., Serra, X., Comaposada, J., Gou, P., and Garriga, M. (2007). Technologies to shorten the drying period of dry-cured meat products. *Meat Science*, 77(1):81 – 89. 53rd International Congress of Meat Science and Technology (53rd ICoMST).

[Atuonwu et al., 2012a] Atuonwu, J., van Straten, G., van Deventer, H., and van Boxtel, A. (2012a). Improving dryer controllability and amp; energy efficiency. In Bogle, I. D. L. and Fairweather, M., editors, *22nd European Symposium on Computer Aided Process Engineering*, volume 30 of *Computer Aided Chemical Engineering*, pages 847 – 851. Elsevier.

[Atuonwu et al., 2013] Atuonwu, J., van Straten, G., van Deventer, H., and van Boxtel, A. (2013). Improving dryer energy efficiency and controllability simultaneously by process modification. *Computers & Chemical Engineering*, 59(0):138 – 144. Selected papers from ESCAPE-22 (European Symposium on Computer Aided Process Engineering - 22), 17-20 June 2012, London, {UK}.

[Atuonwu et al., 2011a] Atuonwu, J. C., Jin, X., van Straten, G., van Deventer Antonius, H. C., and van Boxtel, J. (2011a). Reducing energy consumption in food drying: Opportunities in desiccant adsorption and other dehumidification strategies. *Procedia Food Science*, 1(0):1799 – 1805. 11th International Congress on Engineering and Food (ICEF11).

[Atuonwu et al., 2011b] Atuonwu, J. C., van Straten, G., van Deventer, H. C., and van Boxtel, A. J. (2011b). Model-based energy efficiency optimization of a low-temperature adsorption dryer. *Chemical Engineering Technology*, 34(10):1723–1732.

[Atuonwu et al., 2012b] Atuonwu, J. C., van Straten, G., van Deventer, H. C., and van Boxtel, A. J. (2012b). On the controllability and energy sensitivity of heat-integrated desiccant adsorption dryers. *Chemical Engineering Science*, 80(0):134 – 147.

[Bantle and Eikevik, 2014] Bantle, M. and Eikevik, T. M. (2014). A study of the energy efficiency of convective drying systems assisted by ultrasound in the production of clipfish. *Journal of Cleaner Production*, 65(0):217 – 223.

[Bantle et al., 2013] Bantle, M., Käfer, T., and Eikevik, T. M. (2013). Model and process simulation of microwave assisted convective drying of clipfish. *Applied Thermal Engineering*, 59(1–2):675 – 682.

[Bantle et al., 2014] Bantle, M., Petrova, I., Raiser, J., and Eikevik, T. M. (2014). Dynamic model and kinetics for convective drying of ham with different salt contents. In *19th International drying Symposium (IDS)*.

[Bantle et al., 2015] Bantle, M., Tolstorebrov, I., Kvalsvik, K., Petrova, I., Nordtvedt, T., and Eikevik, T. M. (2015). Influence of climate conditions on the energy consumption of refrigeration system in the food processing industry. In *24th IIR International Congress of Refrigeration (ICR2015)*. Accepted for publication.

[Bekhit et al., 2014] Bekhit, A. E.-D. A., van de Ven, R., Suwand, V., Fahri, F., and Hopkins, D. L. (2014). Effect of pulsed electric field treatment on cold-boned muscles of different potential tenderness. *Food and Bioprocess Technology*.

[Berger and Pei, 1973] Berger, D. and Pei, D. C. T. (1973). Drying of hydro scopic capillary porous solids-a theoretical approach. *International Journal of Heat and Transfer*, 16:293–302. in [Whitaker, 1977].

[Bergman et al., 2011] Bergman, T. L., DeWitt, D. P., Incropera, F. P., and Lavine, A. S. (2011). *Heat and mass transfer in capillary porous bodies*. Wiley, New York, 7 edition.

[Berlin et al., 1970] Berlin, E., Kliman, P., and Pallansch, M. (1970). Changes in state of water in proteinaceous systems. *Journal of Colloid and Interface Science*, 34(4):488 – 494.

[Besley, 1942] Besley, A. K. (1942). Improved method for determining the distribution of salt and water in cured hams. *Journal of agricultural research*, 64(5):293–306. Key No A-209.

[Cassens, 1995] Cassens, R. G. (1995). Use of sodium nitrite in cured meats today. *Food Technology*, 49:72–81.

[Cassens, 2000] Cassens, R. G. (2000). Historical perspectives and current aspects of pork meat quality in the usa. *Food Chemistry*, (4):357–363.

[Chen and Hernandez, 1997] Chen, C. S. and Hernandez, E. (1997). Design and performance evaluation of evaporation. In Valentas, K., Rotstein, E., and Singh, R., editors, *Handbook of Food Engineering Practice*. CRC Press.

[Chin et al., 1995] Chin, K. B., Keeton, J. T., and Lacey, R. E. (1995). Utilization of vacuumdrying for reduction of pepperoni drying time. In *Proceedings 41st international congress of meat science and technology*, page 501–502.

[Cingi et al., 1992] Cingi, M. I., Cingi, C., and Cingi, E. (1992). Influence of dietary nitrate on nitrite level of human saliva. *Bulletin of Environmental Contamination and Toxicology*, 48(1):83–88.

[Clemente et al., 2011] Clemente, G., Bon, J., Sanjuán, N., and Mulet, A. (2011). Drying modelling of defrosted pork meat under forced convection conditions. *Meat Science*, 88(3):374 – 378.

[Colak and Hepbasli, 2009a] Colak, N. and Hepbasli, A. (2009a). A review of heat-pump drying (hpd): Part 2 – applications and performance assessments. *Energy Conversion and Management*, 50(9):2187 – 2199.

[Colak and Hepbasli, 2009b] Colak, N. and Hepbasli, A. (2009b). A review of heat pump drying: Part 1 – systems, models and studies. *Energy Conversion and Management*, 50(9):2180 – 2186.

[Comaposada et al., 2004] Comaposada, J., Arnau, J., Gou, P., and Monfort, J. M. (2004). Accelerated method for drying and maturing sliced food products. Patent number WO2004IB00661.

[Comaposada et al., 2000] Comaposada, J., Gou, P., and Arnau, J. (2000). The effect of sodium chloride content and temperature on pork meat isotherms. *Meat Science*, 55(3):291 – 295.

[Costa-Corredor et al., 2010] Costa-Corredor, A., Pakowski, Z., Lenczewski, T., and Gou, P. (2010). Simulation of simultaneous water and salt diffusion in dry fermented sausages by the stefan–maxwell equation. *Journal of Food Engineering*, 97(3):311 – 318.

[Cárcel et al., 2007] Cárcel, J., Benedito, J., Bon, J., and Mulet, A. (2007). High intensity ultrasound effects on meat brining. *Meat Science*, 76(4):611 – 619.

[Daigle et al., 2005] Daigle, S., Schilling, M., Marriott, N., Wang, H., Barbeau, W., and Williams, R. (2005). Pse-like turkey breast enhancement through adjunct incorporation in a chunked and formed deli roll. *Meat Science*, 69(2):319 – 324.

[Dubinin, 1960] Dubinin, M. M. (1960). Theory of the physical adsorption of gases and vapors and adsorption properties of adsorbents of various natures and porous structures. *Bulletin of the Academy of Sciences of the USSR, Division of chemical science*, 9(7):1072–1078.

[Çengel and Cimbala, 2010] Çengel, Y. A. and Cimbala, J. M. (2010). *Fluid Mechanics: Fundamentals and Applications*. McGraw-Hill, 1221 Avenue of the americas, New York, 2 edition.

[Fornasieri et al., 2009] Fornasieri, E., Zilio, C., Cecchinato, L., Corradi, M., and Minetto, S. (2009). Natural refrigerant co_2. Technical report, University of Padova. part of Leonard project "NARECO2", edited by Walter Reulens.

[Friedman, 1996] Friedman, M. (1996). Food browning and its prevention: An overview. *J. Agric. Food Chem.*, 44(3):631–653.

[Ghavimi et al., 1986] Ghavimi, B., Rogers, R. W., Althen, T. G., and Ammerman, G. R. (1986). Effects of nonvacuum, vacuum and nitrogen back-flush tumbling on various characteristics of restructured cured beef. *Journal of Food Science*, 51:1166–1168.

[Gou et al., 2002] Gou, P., Comaposada, J., and Arnau, J. (2002). Meat ph and meat fibre direction effects on moisture diffusivity in salted ham muscles dried at 5 ^{o}c. *Meat Science*, 61(1):25 – 31.

[Gou et al., 2003] Gou, P., Comaposada, J., and Arnau, J. (2003). Nacl content and temperature effects on moisture diffusivity in the gluteus medius muscle of pork ham. *Meat Science*, 63(1):29 – 34.

[Gou et al., 2004] Gou, P., Comaposada, J., and Arnau, J. (2004). Moisture diffusivity in the lean tissue of dry-cured ham at different process times. *Meat Science*, 67(2):203 – 209.

[Hankins, 1945] Hankins, O. G. (1945). Quality in meat and meat products. *Ind. Eng. Chem.*, 37(3):220–223.

[Haukås, 2010] Haukås, H. T. (2010). Heat pumps for various applications.

[Hayes et al., 2007] Hayes, J., Kenny, T., Ward, P., and Kerry, J. (2007). Development of a modified dry curing process for beef. *Meat Science*, 77(3):314 – 323.

[Herrmann et al., 2014] Herrmann, S., Duedahl-Olesen, L., and Granby, K. (2014). Simultaneous determination of volatile and non-volatile nitrosamines in processed meat products by liquid chromatography tandem mass spectrometry using atmospheric pressure chemical ionisation and electrospray ionisation. *Journal of Chromatography A*, 1330(0):20 – 29.

[Hui, 2012] Hui, Y. H. (2012). *Handbook of Meat and Meat Processing*. CRC Press, 2 edition.

[Jäger, 2012] Jäger, H. (2012). *Process performance analysis of pulsed electric field (PEF) food applications*. Project work.

[Jäger et al., 2008] Jäger, H., Balasa, A., and Knorr, D. (2008). Food industry applications for pulsed electric fields. pages 181–216.

[Jon and Kiang, 2006] Jon, C. K. and Kiang, C. S. (2006). Heat pump drying systems. In Mujumdar, A. S., editor, *Handbook of Industrial Drying*. CRC Press.

[Kapsalis, 1967] Kapsalis, J. G. (1967). Hygroscopic equilibrium and texture of freeze-dried foods. Technical report, Secretary of the Army Research and Study Fellowship at the Swedish Institute for Food Preservation Research (S.I.K.), Göteborg, Sweden.

[Kapsalis, 1987] Kapsalis, J. G. (1987). Influences of hysterisis and temperature on moisture sorption isotherms. In Rockland, editor, *Water Activity: Theory and Applications to Food*, chapter 9, pages 173–213. CRC Press. Science and advanced Technology directorate, U.S. Army Natick Research, Development & Engineering Center, Natick, Massachusetts.

[Kuprianoff, 1958] Kuprianoff, J. (1958). Fundamental aspects of the dehydration of foodstuffs. In *Conference on Fundamental aspects of the Dehydration of Foodstuffs*, pages 14–23. Society of Chemical Industry. in [Okos et al., 2006].

[Kvalsvik, 2014] Kvalsvik, K. H. (2014). Evaluation of three drying models for dry-cured ham. Project work, NTNU. Available from the Department of Energy and Process Engineering at NTNU.

[Luikov, 1966] Luikov, A. V. (1966). *Fundamentals of heat and mass transfer*. Pergamon, Oxford.

[Lundberg, 1983] Lundberg, P. (1983). Blod och kött, en nmr-studie i rött. Master's thesis, Lunds Universitet. Reference found at `https://www.imh.liu.se/radiologiska-vetenskaper/medarbetarna/peter_lundberg?l=en`.

[Marinos-Kouris and Maroulis, 2006] Marinos-Kouris, D. and Maroulis, Z. B. (2006). Transport properties in the drying of solids. In Mujumdar, A. S., editor, *Handbook of Industrial Drying*. CRC Press.

[Marriott et al., 1987] Marriott, N., Graham, P., Shaffer, C., and Phelps, S. (1987). Accelerated production of dry cured hams. *Meat Science*, 19(1):53 – 64.

[Marriott et al., 1983] Marriott, N., Graham, P., Tracey, J. B., and Kelly, R. (1983). Accelerated processing of boneless hams to dry-cured state. *J. Food Prot*, 46:717–721. in [Toldrà, 2002].

[Marriott et al., 1984] Marriott, N. G., Graham, P. P., Boling, J. W., and Collins, W. F. (1984). Vacuum tumbling of dry-cured hams. *Journal of Animal Science*, 58(6):1376–1381.

[Marriott et al., 1992] Marriott, N. G., Graham, P. P., and Claus, J. R. (1992). Accelarated dry curing of pork legs (hams): a review. *Journal of Muscle Foods*, 3:159–168.

[McBryde, 1911] McBryde, C. N. (1911). *A bacteriological study of ham souring*. Washington D. C. : U.S. Department of Agriculture, Bureau of Animal Industry. in [Besley, 1942].

[McDonnell et al., 2014] McDonnell, C., Lyng, J., and Allen, P. (2014). The use of power ultrasound for accelerating the curing of pork. *Meat Science*, 98(2):142 – 149.

[Milroy, 1917] Milroy (1917). The milroy lectures on meat inspection, with special reference to the developments of recent years. *The Lancet*, 190(4905):335 – 341. Originally published as Volume 2, Issue 4905.

[Montgomery et al., 1976] Montgomery, R. E., Kemp, J. D., and Fox, J. D. (1976). Shrinkage, palatability and chemical characteristics of dry-cured country ham as affected by skinning procedure. *Journal of Food Science*, 41(5):1110–1115.

[Mora et al., 2014] Mora, L., Escudero, E., Fraser, P. D., Aristoy, M.-C., and Toldrá, F. (2014). Proteomic identification of antioxidant peptides from 400 to 2500& #xa0;da generated in spanish dry-cured ham contained in a size-exclusion chromatography fraction. *Food Research International*, 56(0):68 – 76.

[Moran and Shapiro, 2006] Moran, M. J. and Shapiro, H. N. (2006). *Fundamentals of Engineering Thermodynamics*. John Wiley & Sons, 5 edition. SI units.

[Motilva et al., 1994] Motilva, M. J., Toldra, F., Nadal, M., and Flores, J. (1994). Prefreezing hams affects hydrolysis during dry-curing. *Journal of food science*, 59:303–305. in [Toldrà, 2002].

[Mujumdar and Wu, 2007] Mujumdar, A. and Wu, Z. (2007). Thermal drying technologies: New developments and future r&d potential. In *5th International Conference on Heat Transfer, Fluid Mechanics and Thermodynamics, HEFAT2007, Sun City, South Africa*. Paper number: K3.

[Mujumdar, 2006] Mujumdar, A. S. (2006). Superheated steam drying. In Mujumdar, A. S., editor, *Handbook of Industrial Drying*. CRC Press.

[Okos et al., 2006] Okos, M., Narsimhan, G., Singh, R., and Witnauer, A. (2006). Food dehydration. chapter 10. Marcel Dekker/CRC Press, 2 edition.

[Parolari, 1996] Parolari, G. (1996). Review: Achievments, needs and perspectives in dry-cured ham technology: the example of parma ham. *Fod Science Tech. Int.*, 2(2):69–78.

[Petrova, 2015] Petrova, I. (2015). Drying kinetics and modeling of dry-cured ham with different salt concentrations. Nordic drying conference.

[Prevolnik et al., 2011] Prevolnik, M., Škrlep, M., Janeš, L., Velikonja-Bolta, Š., Škorjanc, D., and Čandek-Potokar, M. (2011). Accuracy of near infrared spectroscopy for prediction of chemical composition, salt content and free amino acids in dry-cured ham. *Meat Science*, 88(2):299 – 304.

[Radford, 1976] Radford, R. D. (1976). Water transport in meat. In *Joint meeting of commissions C2, D1, D2, D3 and E1*, number 62, pages 1–8. International Institute of refrigeration. Australian National Committee. in [Trujillo et al., 2007].

[Radford et al., 1976] Radford, R. D., Herbert, C., and Lovett, D. A. (1976). Chilling of meat- a mathematical model for heat and mass transfer. In *Comm. C2 Meeting, IIR Bull. Annex 1976-1*, pages 323–330. in [Trujillo et al., 2007].

[Raiser, 2014] Raiser, J. (2014). Convective drying and sorption characteristics of cured meat slices. Project work, NTNU and SINTEF Energi AS.

[Richard, 1981] Richard, A. H. (1981). Review of the potential hazard from botulism in cured meats. *Canadian Institute of Food Science and Technology Journal*, 14(3):183 – 195.

[Črnivec and Marinšek-Logar, 2010] Črnivec, I. G. O. and Marinšek-Logar, R. (2010). Environmental impact evaluation of innovation in traditional food production lines. part i: Methodological framework. *Acta argiculturae Slovenica*, (1):5–14.

[Rogers et al., 1965] Rogers, R. W., Kemp, J. D., and Varney, W. Y. (1965). Effects of enzyme addition on palatability, tenderness and rancidity development in quick aged country-style hams. *Food Technology*, 19:1509–1513. in [Arnau et al., 2007].

[Ruiz-Cabrera et al., 2004] Ruiz-Cabrera, M. A., Gou, P., Foucat, L., Renou, J. P., and Daudin, J. D. (2004). Water transfer analysis in pork meat supported by nmr imaging. *Meat Science*, 67(1):169–178.

[Schilling et al., 2004] Schilling, M., Marriott, N., Acton, J., Anderson-Cook, C., Alvarado, C., and Wang, H. (2004). Utilization of response surface modeling to evaluate the effects of non-meat adjuncts and combinations of {PSE} and {RFN} pork on water holding capacity and cooked color in the production of boneless cured pork. *Meat Science*, 66(2):371 – 381.

[Siró et al., 2009] Siró, I., Vén, C., Balla, C., Jónás, G., Zeke, I., and Friedrich, L. (2009). Application of an ultrasonic assisted curing technique for improving the diffusion of sodium chloride in porcine meat. *Journal of Food Engineering*, 91(2):353 – 362.

[Song, 1990] Song, X. (1990). *Low temperature, fluidized bed drying with temperature program.* PhD thesis, Norges tekniske høgskole.

[Stollewerk et al., 2012] Stollewerk, K., Jofré, A., Comaposada, J., Arnau, J., and Garriga, M. (2012). The impact of fast drying (qds process®) and high pressure on food safety of nacl-free processed dry fermented sausages. *Innovative Food Science & Emerging Technologies*, 16(0):89 – 95.

[Strømmen, 1980] Strømmen, I. (1980). *Tørking av klippfisk.* PhD thesis, Norges tekniske høgskole.

[Strømmen et al., 2002] Strømmen, I., Eikevik, T. M., Alves-Filho, O., Syverud, K., and Jonassen, O. (2002). Low temperature drying with heat pumps new generations of high quality dried products. In *13th International drying symposium.* In [Colak and Hepbasli, 2009b].

[Strumillo et al., 2006] Strumillo, C., Jones, P. L., and Ẑylla, R. (2006). Energy aspects in drying. In Mujumdar, A. S., editor, *Handbook of Industrial Drying.* CRC Press.

[Su et al., 2014] Su, Y., Zhang, M., and Mujumdar, A. S. (2014). Recent developments in smart drying technology. *Drying Technology*, pages 1–17.

[Theodore, 2008] Theodore, L. (2008). *Adsorbers*, pages 185–246. John Wiley & Sons, Inc.

[Toldrà, 2002] Toldrà, F. (2002). *Dry-Cured Meat Products.* Food & Nutrition press, Trumbull, Connecticut 06611, USA, 1 edition.

[Treharne, 1971] Treharne, T. (1971). Growing interest in meat tumbling. *Food Manufacture*, page 35–39.

[TrønderEnergiAS, 2013] TrønderEnergiAS (2013). Lokal energiutredning i trondheim kommune. Technical report, TrønderEnergi AS.

[Trujillo et al., 2007] Trujillo, F. J., Wiangkaew, C., and Pham, Q. T. (2007). Drying modeling and water diffusivity in beef meat. *Journal of Food Engineering*, 78(1):74 – 85.

[Trujillo et al., 2003] Trujillo, F. J., Yeow, P. C., and Pham, Q. (2003). Moisture sorption isotherm of fresh lean beef and external beef fat. *Journal of Food Engineering*, 60(4):357 – 366.

[Villalobos-Delgado et al., 2014] Villalobos-Delgado, L. H., Caro, I., Blanco, C., Morán, L., Prieto, N., Bodas, R., Giráldez, F. J., and Mateo, J. (2014). Quality characteristics of a dry-cured lamb leg as affected by tumbling after dry-salting and processing time. *Meat Science*, 97(1):115 – 122.

[Waananena et al., 1993] Waananena, K., Litchfieldb, J., and Okos, M. (1993). Classification of drying models for porous solids. *Drying Technology*, 11(1):1–40.

[Wadekar, 2000] Wadekar, V. V. (2000). A che's guide to ches. *Chemical Engineering Progress*, pages 30–49.

[Warner et al., 1997] Warner, R. D., Kauffman, R. G., and Russell, R. L. (1997). Muscle protein changes postmortem in relation to prok quality traits. *Meat Science*, 33:359–372. in [Toldrà, 2002].

[Weiss, 1973] Weiss, J. M. (1973). Ham tumbling and massaging. *Western Meat Industry*, 23.

[Whitaker, 1977] Whitaker, S. (1977). Simultaneous heat, mass, and momentum transfer in porous media: A theory of drying. volume 13 of *Advances in Heat Transfer*, pages 119 – 203. Elsevier.

[Wolf et al., 1972] Wolf, M., Walker, J. E., and Kapsalis, J. G. (1972). Water vapor sorption hysteresis in dehydrated food. *Journal of Agricultural Food Chemistry*, 20(5):1073–1077.